Investigating the interaction of Cigarette Smoke and Alpha-1 Antitrypsin Deficiency in a mouse model of Chronic Obstructive Pulmonary Disease

Angelica Katsifis

School of Life Sciences
Faculty of Science
University of Technology Sydney

Submitted in fulfilment of the requirements for the degree of
Doctor of Philosophy

2025

Certificate of Original Authorship

I, Angelica Katsifis, declare that this thesis is submitted in fulfilment of the requirements for the award of Doctor of Philosophy, in the School of Life Sciences/Faculty of Science at the University of Technology Sydney.

This thesis is wholly my own work unless otherwise referenced or acknowledged. In addition, I certify that all information sources and literature used are indicated in the thesis.

This document has not been submitted for qualifications at any other academic institution.

This research was supported by an Australian Government Research Training Program (RTP) Scholarship doi.org/10.82133/C42F-K220.

Signature:

Production Note:
Signature removed prior to publication.

Date: 10/04/2025

I would like to dedicate this thesis to my parents Andrew and Adriana

Acknowledgements

I would like to acknowledge my supervisors for their guidance throughout my PhD candidature, Prof. Phil Hansbro, Dr Elinor Hortle and Dr Gang Liu.

I would like to acknowledge Dr Caitlin Gillis and Dr Vrushali Chimankar for the donation of mouse samples utilsed in IHC and qPCR in Chapter 3, Aim 1.

For assistance in CS procedures and care of mice I would like to acknowledge Katie Bilson, Dr Bob Lu, Charlotte McEwen, and the casual staff at Centre for Inflammation. I would like to acknowledge lab managers Amy Roman, Sarah Mulvey and Dr Nicole Hansbro, as well as the Centenary Institute Head of Bioresources Tyson Blanch. Special thanks to Danielle Moyes for breeding the A1AT KO mouse colony.

For assistance in the mouse endpoints, which includes organ collection, recording lung function measurements and lung perfusion, I would like to acknowledge Chris Augood, Dr Vrushali Chimankar, Dr Rupa Das, Karl Hegarty, Dr Elinor Hortle, Dr Matt Johansen, Dr Stefan Miemczyk, Dr Christina Nalkurthi, Dr Duc Nguyen, Johann Pai, Nisha Panth, Dr Keshav Raj Paudel, Dr Ashleigh Philp, Dr Vamshi Swaram, Linda Tong and Dr Ridhima Wadhwa. Additionally, for running of the DLCO during the endpoints I would like to acknowledge Dr Jacqueline Marshall. For assistance with flow cytometry, I would like to acknowledge Dr Thomas Ashhurst (assistance with running flow cytometry on Chapter 4, Aim 2), Dr Caitlin Gillis (for teaching flow cytometry and initial panel design), Dr Jacqueline Marshall (assistance with running flow cytometry on Chapter 4, Aim 2), Johann Pai (assistance with running flow cytometry in Chapter 6, Aim 4 and panel design assistance), Ashlea Lorenz (assistance running CBA) and Jinx Moore (assistance in flow pilot model, which was not included in thesis). I would like to acknowledge Dr Bobby Boumelhem for assistance with technical difficulties encountered with the BMG LABTECH POLARstar Omega microplate reader. For assistance with histology, I would like to acknowledge Justin Lee and Caroline Wilson for paraffinizing and sectioning all histology samples.
Special thanks for the support given by Dr Caitlin Gillis, Dr Elinor Hortle, Dr Matt Johansen, Dr Jacqueline Marshall and Johann Pai.

I would like to acknowledge The University of Technology Sydney, The Centenary Institute, and the staff at Centenary Institute Animal House,

ABR Animal Facility and Sydney Cytometry for their equipment, technical support and experimental assistance.

I would like to acknowledge NSW Health for financially supporting this thesis via NSW Health Gene and Cell Therapy PhD Program, as well as TSANZ and NHMRC for additional funding.

I would like to acknowledge my parents, brother Georgio, grandparents, family and friends for their love and support.

Thesis format

This thesis follows the conventional format, encompassing the standard sections of a scholarly work. This includes an abstract summarising the literature and research conducted. This is followed by a general experimental - methodology section. There are four separate results and discussion chapters that encompass the four key aims of this thesis. There is a final section that summarises the thesis and includes future directions. Furthermore, the thesis includes a complete bibliography of all cited sources.

The formatting follows guidelines prescribed by the

University of Technology Sydney, Graduate Research School

Publications that I have contributed to during my thesis

Liu, G.; Jarnicki, A. G.; Paudel, K. R.; Lu, W.; Wadhwa, R.; Philp, A. M.; Van Eeckhoutte, H.; Marshall, J. E.; Malyla, V.; Katsifis, A.; Fricker, M.; Hansbro, N. G.; Dua, K.; Kermani, N. Z.; Eapen, M. S.; Tiotiu, A.; Chung, K. F.; Caramori, G.; Bracke, K.; Adcock, I. M.; Sohal, S. S.; Wark, P. A.; Oliver, B. G.; Hansbro, P. M., Adverse roles of mast cell chymase-1 in chronic obstructive pulmonary disease. Eur Respir J 2022.

Table of Contents

List of Figures and Tables:

Abbreviations

Abbreviation	Description
6FAM	6-carboxyfluorescein
A1AT	alpha-1 antitrypsin
A1AT KO	A1AT knockout (A1AT null)
ABR	Australian BioResources
ADAM	a disintegrin and metalloproteinase
BALF	bronchoalveolar lavage fluid
BHQ1	black hole quencher - 1
BHQ3	black hole quencher - 3
BM	bone marrow
BMDC	bone marrow derived dendritic cells
BMDM	bone marrow derived macrophages
BSA	bovine serum albumen
CBA	cytometric bead array
CCL	chemokine ligand (C-C motif)
CCR	chemokine receptor (C-C motif)
cDC	conventional dendritic cells
cDC1	conventional type 1 DC
cDC2	conventional type 2 DC
cDNA	complementary DNA
CO	carbon monoxide
COPD	chronic obstructive pulmonary disease
CRISPR	clustered regularly interspaced short palindromic repeats
cRPMI	complete RPMI 1640 medium
CS	cigarette smoke
CSE	cigarette smoke extract
CXCL	chemokine ligand (C-X-C motif)
CXCR	chemokine receptor (C-X-C motif)
DAB	3,3'-diaminobenzidine
DC	dendritic cells
DLCO	diffusing capacity of the lungs for carbon monoxide

DNA	deoxyribonucleic acid
ECM	extracellular matrix
EDTA	ethylenediaminetetraacetic acid
ELISA	enzyme-linked immunosorbent assay
ER	endoplasmic reticulum
EtOH	ethanol
FACS	fluorescence-activated cell sorting buffer
FEV1	forced expiratory volume in 1 second
FMO	fluorophore minus one
FRC	functional residual capacity
FVC	forced vital capacity
GFP	green fluorescent protein
GM-CSF	granulocyte-macrophage colony-stimulating factor
GMO	genetically modified organism
IgG	immunoglobulin G
HPRT	Hypoxanthine Phosphoribosyl Transferase
IHC	immunohistochemistry
IL	interleukin
IPF	idiopathic pulmonary fibrosis
IV	intravenous
KC	Mouse CXCL1
LDH	lactate dehydrogenase
LPS	lipopolysaccharide
LTB4	leukotriene B4
M allele (PiM)	normal, non-mutated allele of Serpina1
macs	macrophages
MLI	mean linear intercept
MM	two copies of the M allele
MMP	matrix metalloproteinase
mono	monocytes
MPO	myeloperoxidase
mRNA	messenger RNA
MTT	3-(4,5-dimethylthiazol-2-yl)-2,5-diphenyltetrazolium bromide

MZ	Z heterozygous (one copy of the M allele and one of the Z allele)
NaCl	sodium chloride
NADPH	nicotinamide adenine dinucleotide phosphate
NE	neutrophil elastase
Ne	Neon
nf H2O	nuclease free water
NF-κB	nuclear factor-kappa B
O	Oxygen
pAb	polyclonal antibody
PBS	phosphate buffered saline
PCR	polymerase chain reaction
pDC	plasmacytoid dendritic cells
PFA	paraformaldehyde
PI	protease inhibitor
Pi	protease inhibitor
qPCR	quantitative polymerase chain reaction
RBC	red blood cell
RNA	ribonucleic acid
ROS	reactive oxygen species
RT-qPCR	real time qPCR
RV	residual volume
SEM	standard error of the mean
Serpina1	serine protease inhibitor clade A member 1
sIC	soluble immune complex
SLPI	secretory leukocyte protease inhibitor
TBS	tris-buffered saline
TIMP	tissue inhibitors of metalloproteinase
TLC	total lung capacity
TNF	tumour necrosis factor
WT	wild type mice
Z allele (PiZ)	specific mutated allele of Serpina1
ZZ	Z homozygous (two copies of the Z allele)

Abstract

Chronic obstructive pulmonary disease (COPD) is a progressive lung disease, and the third leading cause of death globally. COPD is characterised by chronic inflammation, small airway remodelling and irreversible lung damage (emphysema) that results in impaired lung function. COPD is predominantly caused by cigarette smoke (CS) however genetic factors such as alpha-1 antitrypsin (A1AT) deficiency also contribute. A1AT protects lung tissues primarily by neutralising proteases, which when uninhibited cause alveolar destruction. This project focuses on two specific A1AT gene mutations: Z and null (which result in the complete absence of A1AT), in PiZ mice (carrying the Z allele) and A1AT knockout (KO) mice.

A1AT deficiency is exacerbated by CS, which increases lung inflammation and disrupts the already impaired A1AT-protease balance accelerating COPD disease progression. This study examined the impact of CS on A1AT deficiency by assessing A1AT gene and protein expression in an experimental model of CS-induced COPD in WT mice. This revealed that CS caused fluctuating increases in A1AT protein in the lung, most likely as a protective response due to CS.

Investigations into the mechanism of A1AT deficiency in CS induced COPD with A1AT KO mice, showed increased inflammation after 2 weeks predominantly driven by neutrophils and IL1β and CXCL15. Furthermore, there was increased alveolar destruction after 8 weeks in A1AT KO CS compared to WT CS mice, highlighting exacerbated lung damage in the absence of A1AT.

Upon investigating the Z mutation, functional, structural and inflammatory changes were observed in PiZ mice, however these were attributed to CS and were not significantly different to WT mice. Although increased alveolar destruction attributed to Z toxicity was found, further experimentation is required to elucidate the mechanism(s) of action.

Investigation of dendric cells (DC) found A1AT specific mechanisms may play a role in the behaviour of DCs. Further studies showed that conventional DCs specifically, accumulated in the lungs of A1AT KO CS mice. Additionally, increased migration was found in A1AT KO compared to WT mice.

These studies have demonstrated novel findings contributing to the field of A1AT deficiency and COPD. This thesis highlights the impact of A1AT, as an antiprotease

and a modulator of inflammation, specifically neutrophils, conventional DCs and certain cytokines. Additionally, an improved mouse model of A1AT deficiency and COPD (A1AT KO CS) was established to test future therapies.

Chapter 1 – Introduction and review of literature

1. COPD and emphysema

1.1 Patient burden

Chronic obstructive pulmonary disease (COPD) is a progressive lung disease, and it is the third leading cause of death globally with 3.23 million deaths in 2019 and 328 million people estimated to have COPD.[1] As of 2017, 55% of the estimated 544.7 million people that had chronic respiratory disease had COPD.[2] In Australia COPD is the 5th leading cause of death with 7,113 people having died directly from COPD in 2018.[3, 4] COPD was an underlying cause or a contributing factor to a further 18,498 deaths in Australia in 2018.[3, 4] COPD accounts for approximately half of the total respiratory disease conditions and is the third leading specific cause of total disease burden with 1 in 7 Australians aged 40 years and over having some form of COPD. Estimates of hospital, non-hospital and pharmaceutical expenses Australia wide value the cost of COPD at approximately $1 billion annually.[4] With NSW representing almost a third of Australia's population, this amounts to a significant community cost from this disease. In the period 2016-17, 75 hospitals across NSW admitted over 44,580 patients with COPD totalling 407,530 bed days with an average length of stay of 9.14 days.[5] In terms of the global cost of COPD, over the next 30 years (2020-2050) the total global cost of COPD has been estimated to be INT$4·326 trillion.[6] Currently, there is no cure for COPD. Existing treatments can reduce exacerbations and improve disease symptoms, however they do not halt or reverse disease progression.

1.2 Cause of COPD

COPD is characterised by chronic inflammation, small airway remodelling, and irreversible lung damage (emphysema) that result in impaired lung function and difficulty breathing. COPD can be caused by environmental, behavioural and genetic factors.

Smoke exposure, particularly cigarette smoke (CS), is the main cause of COPD. This can include active smoking in-utero and early-life exposure to tobacco smoke, passive smoking, vaping or e-cigarette use and smoking cannabis. Environmental exposure related COPD is also a significant risk factor, including bushfire smoke, air pollution, indoor pollutants, and occupational exposures. For example, coal and other fuel sources are common indoor pollutants in low-middle income countries, with exposures contributing to accelerated development and progression of COPD in CS individuals.[7] [8]

Another very important factor in COPD includes genetic factors with about 40% of the variability in airflow limitation and up to 60% of the risk for COPD related to smoking is attributable to genetics.[9] While there are links to many genetic factors the most common one associated with COPD is alpha-1 antitrypsin (A1AT) deficiency. It has also been suggested in the literature that A1AT deficiency is one of the only two monogenetic variants that have been clearly shown to have a causative role in the disease, with telomerase reverse transcriptase mutation being the other.[10]

Another risk factor is lung and systemic infections particularly in low-middle income countries.[11, 12] It has been estimated as high as 42% of people with tuberculosis, HIV or early-life pneumonia develop COPD.[13] Finally, there are also links to childhood asthma and premature birth i.e. impaired lungs early in life.[12, 14]

1.3 Basic Pathogenesis of COPD

COPD is characterised by chronic inflammation, which leads to airway remodelling, emphysema and impaired lung function (Figure 1.1). Chronic inflammation is inflammation lasting for periods of several months to years. It involves accumulation of tissue-infiltrating immune cells, particularly in the lungs and bronchoalveolar space.[15, 16] Chronic inflammation in the pulmonary tissue is also associated with systemic effects ranging from cytokine induced priming of peripheral leukocytes, to muscle wasting induced by cytokines such as tumour necrosis factor (TNF). [15, 16]

Aside from inflammation, COPD pathogenesis is also caused by oxidative stress.[17]

An imbalance between oxidants and antioxidants is a result of increased oxidants, such as from CS and from reactive oxygen and nitrogen species released from inflammatory cells. Oxidative stress can also increase inflammation via complex interactions with NF-kB. NF-kB once activated can increase production of cytokines, chemokines and adhesion molecules, regulate cell functions including proliferation, apoptosis, morphogenesis and differentiation as well as affect innate immune cells and inflammatory T cell recruitment.[18]

Airway remodelling includes any structural changes in the airways due to chronic inflammation, most notably including chronic bronchitis, mucus hypersecretion and changes to the epithelium and the extracellular matrix (ECM). [15, 19]

Emphysema is damage to the acinus, typically described as damage and enlargement of alveoli but also includes the respiratory bronchiole, alveolar sacs, and alveolar ducts.[20, 21] This abnormal permanent dilatation of the airspaces and destruction of their walls results in a decrease in the alveolar and capillary surface area, which decreases the gas exchange.[21]

Finally, impaired lung function results from all these changes to the lung. It is typically measured in humans using FVC (forced vital capacity) or FEV1 the (Forced expiratory volume in 1 second.[22, 23] Interestingly, in mice there is an additional parameter in lung function that is able to be measured - TLC (total lung capacity). TLC is the maximum volume inspired into the lungs and the value is often higher due to air trapping in the lungs.

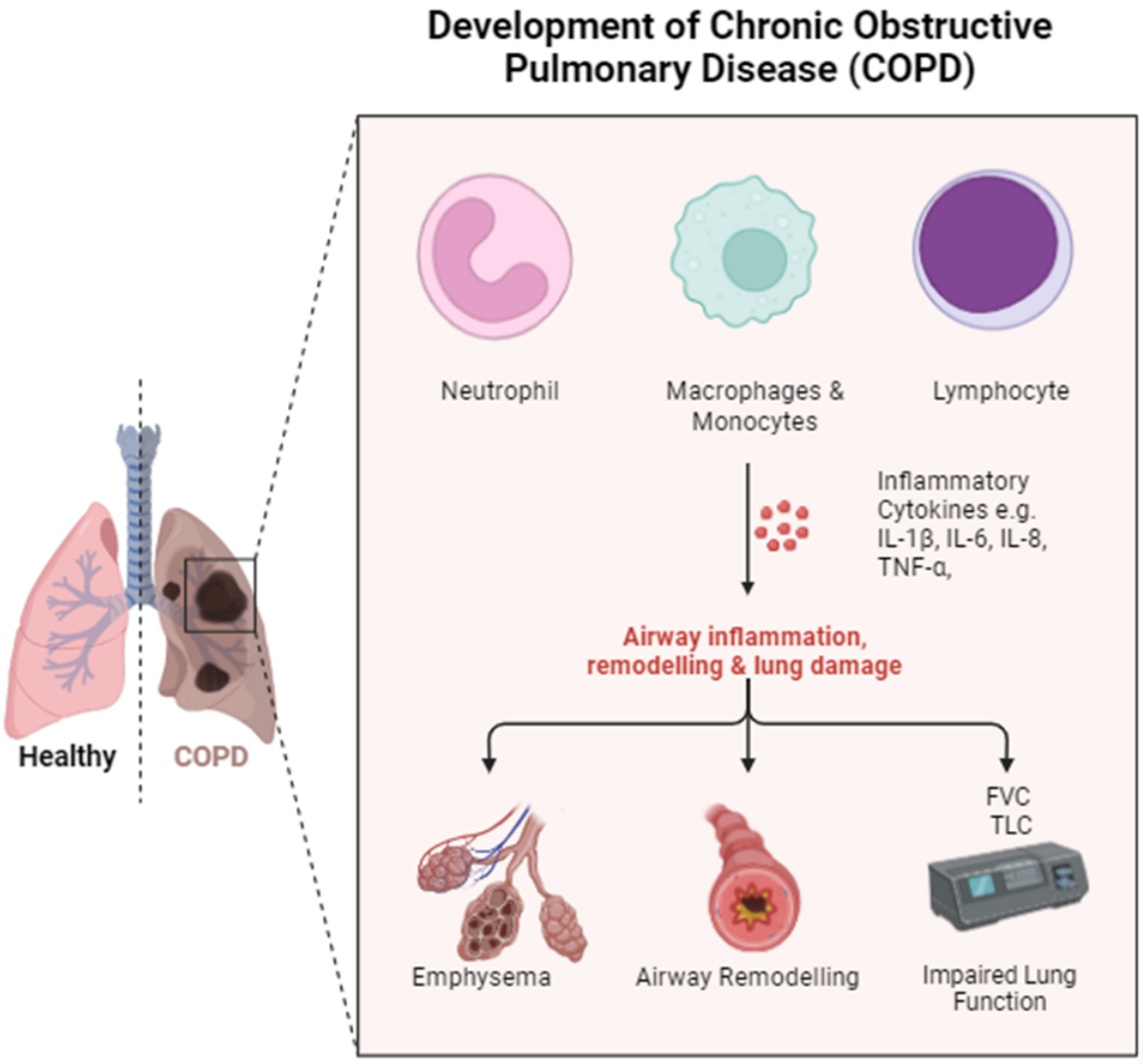

Figure 1.1: Development of COPD.

COPD is caused by chronic inflammation, which involved increased infiltration of immune cells as well as increased inflammatory markers and cytokines. This inflammation causes damage to the lung in the form of emphysema, airway remodelling and impaired lung function (with measures such as FEV1, FVC, and for mice also TLC). In COPD there is also a constant state of inflammation, described as chronic inflammation. These features combined make up the pulmonary disease COPD. Made with BioRender.

1.4 Clinical Features in diagnosis

Diagnosis of COPD involves an awareness of factors that predispose the patient to developing COPD, for example, smoking, working in an environment with increased risk of environmental exposures, or having A1AT deficiency. These risk factors especially in combination with difficulty breathing/shortness of breath, persistent cough or sputum production, recurrent pneumonia, or a family history of COPD are very strong indicators to seek further testing. [24]

Further testing, which leads to eventual diagnosis of COPD involves spirometry and a lung scan (X-ray or CT scan). During chest and lung scans doctors can see evidence of many structural changes to the lung including, emphysema, chronic bronchitis, bronchial wall thickening and even gas trapping. Thus, a valuable and pivotal tool in diagnosis. [24, 25]

Lung function assessments are also crucial to diagnosis, with FEV1 and FVC being two of the most important measures in human diagnosis.[22, 23] In humans, lung function is measured using FVC (forced vital capacity) or the maximum amount of air out of the lungs in a single breath, as well as with FEV1 the (Forced expiratory volume in 1 second, that is the first one second of breathing out). If the FEV1/FVC ratio is less than 70% this indicates airflow limitation and the possibility of COPD.[23] Thus, COPD is associated with an accelerated decline in FEV1.

Hence, COPD diagnosis is based on a combination of risk factor evaluation, symptoms of COPD, and spirometry showing decreased lung function and airflow obstruction. Additionally, CT scans and lung function tests will determine the severity and progression of COPD, which will aid in determining and tailoring specific treatments.

1.5 Current treatments

There is no current cure for COPD, ands as mentioned above, treatments have been developed to reduce exacerbations and improve disease symptoms, however they do not halt or reverse disease progression. The easiest and most effective treatment is to stop smoking and limit environmental exposures, such as pollution and bushfire smoke, that induce exacerbation and worsen symptoms. It is vital to reduce the frequency and severity of exacerbations as they can lead to further decreases in lung function. [26]

Current pharmacological treatments include corticosteroids, bronchodilators, antibiotics, and oxygen therapy. In more serious cases (progressed cases) lung transplantation or reduction surgeries can only reduce exacerbations and improve disease symptoms, however they do not halt or reverse disease progression.[27, 28]

It is important to understand the cause of COPD to explore new therapeutic options for COPD.

2. Inflammation and COPD

Inflammatory cells play a key role in COPD as inflammation in the lung is the first step in developing COPD, and is also the main cause for all resulting damage, including decreased lung function, emphysema and airway remodelling. Inflammation in disease is complex and pathways and mechanisms of disease are constantly being investigated. The cells most implicated in COPD are neutrophils and macrophages as well as certain inflammatory cytokines/markers that are released upon immune cell activation. [29, 30]

2.1. Macrophages

Macrophages play a pivotal, but dual role in chronic inflammation and the development and progression of COPD. Pulmonary macrophages can be divided into two

populations found in anatomically distinct compartments. These are alveolar macrophages (AM), which line the alveolar surface, and interstitial macrophages (IM), which populate the space between the alveolar epithelium and vascular endothelium[31].

Being the most prevalent immune cells in the lungs, macrophages normally play a crucial role in the surveyance and clearance of cellular debris from the airways, immune surveillance, resolving inflammation and maintaining tissue homeostasis in healthy lungs. They achieve this by inducing phenotypic changes in response to environmental stimuli induced in the surrounding tissue, usually described as M1/M2 macrophage polarization. However, these processes become dysfunctional in COPD[31].

As an example, the exposure to CS and particulate matter induces the macrophage release of molecules, driving both innate and adaptive responses. This, in turn, influences local lung inflammation, inducing the development and progression of COPD. In addition, macrophages produce high levels of mediators, such as IL-8 and granulocyte-macrophage stimulating growth factors (GM-CSF), which drive neutrophil recruitment and macrophage maturation[31].

Importantly, macrophage numbers significantly increase in airways and lung tissue, most often linked to disease severity. Macrophage increases in the sputum and lungs of COPD patients have been widely acknowledged as proof of macrophage involvement in COPD. Consequently, the M1/M2 macrophage polarisation shifts towards the M1- proinflammatory phenotype, producing cytokines, chemokines and proteases (such as elastase) attenuating macrophage function, promoting chronic inflammation, tissue remodelling/destruction and damage to the lung tissue, leading to emphysema. [31-33]

Of key note is that a recent study by Takiguchi et al. [34] has shown the classical M1/M2 polarity of macrophages (with CD40 used as the M1 marker and CD163 used as the M2 marker) may not be as applicable to COPD as initially believed due to the complex lung microenvironment and macrophages plasticity. Macrophage M1/M2 double negative cells have been shown to increase in the BALF of COPD patients. Furthermore, the gene signature of these cells was pro-inflammatory and suggested dysfunction in cellular homeostasis, thus leading to disease. The classical M1/M2 polarity of macrophages (even with inclusion of the M1/M2 double positive and double

negative classification) does not sufficiently explain the complexity of macrophages in COPD.

The field of immunology is moving to more complex analysis of macrophages and other immune cells. This is due to classification of these cells by single cell sequencing and omics/multi-omics technologies, that enable classification of macrophages by gene expression levels (i.e. identification of cell-types based on marker gene expression of specific cell clusters). This allows the determination of specific gene increase or decrease in particular subsets of immune cells i.e. neutrophils, macrophages and monocytes, in diseases such as COPD. Thus, single cell sequencing has enabled investigation of immune cells at an even greater complexity and adds another aspect to the immune story in disease beyond cytokines released and cell surface markers.

Takiguchi et al. [34] have identified 13 distinct macrophage/monocyte clusters in BALF fluid of human COPD and healthy control patients and determined that macrophage group 5 termed “monocyte-like” macrophages (characterised by high expression of monocyte-associated genes VCAN and S100A8 together as well as monocyte attractant CCL2 and the late monocyte-to-macrophage differentiation marker CHIT1) and macrophage group 8 termed proliferating macrophages (characterised by proliferation-associated genes MKI67, TOP2A, and NUSAP1, as well as increased expression of histone genes HIST1H4C and HIST1H1D) exhibited the largest relative increase in COPD.

This implies that in COPD it is not just a general increase in the number of macrophages but an active recruitment of specific types of macrophages. Additionally, Sauler et al. [35] have identified 8 macrophage clusters in their research on single cell sequencing on explanted lung tissue from patients with advanced COPD or ‘healthy’ controls. The most notable cluster of macrophages was termed cluster-5 and was characterised by metallothioneins (cysteine-rich metal-binding proteins), with macrophages expressing elevated levels metallothioneins, and increased expression of HMOX1 (Heme oxygenase 1), a target gene of the antioxidant transcription factor NRF2 (Nuclear factor erythroid 2-related factor 2). This finding allows for further investigation not only into metallothioneins, which have also been shown to have protective roles in acute lung injury models, but also more broadly into the various subsets of macrophages and the precise and tailored role these various subtypes or

clusters of macrophages, or even more broadly immune cells, play in the immune response.

All of this is supported by cumulative findings showing the role played by macrophages in the inflammatory process and tissue destruction triggered by COPD. Macrophages can cause damage in a variety of ways, activated by several environmental factors, most notably by CS, macrophages release pro-inflammatory mediators including TNF, CXCL1, CXCL8 (IL-8), LTB4, IL-1β, and ROS which amplify and drive the chronic inflammatory environment, airway remodelling, and tissue destruction leading to functional changes and the structural lung damage seen in COPD.[31-33] Hence, the ability to produce most of the mediators highly expressed in the pulmonary tissue of COPD patients is one of the key speculations about the orchestrating capacity of macrophages in COPD. The damage induced by these proinflammatory factors is amplified by impaired and reduced clearance of irritants (smoke and debris) and pathogens (bacteria, apoptotic cells and inflammatory mediators (phagocytosis), leading to persistent airway inflammation exacerbating lung damage. In addition, metabolic changes such as mitochondrial dysfunction occurs (within the mitochondria) resulting in their impaired function and worsening inflammation. This concomitated release of inflammatory mediators leads to the recruitment of other immune cells like neutrophils thus perpetuating inflammation. [31] Therefore, in parallel with impaired clearance functions like phagocytosis in response to oxidative stress and mitochondrial dysfunction these factors have made them key targets for the development of future therapies.

As mentioned above, macrophage numbers in the lungs are significantly increased in COPD, particularly in the alveolar space, with a 5-10 fold increase in BALF and sputum compared to normal healthy counterparts.[36] Macrophages often accumulate at sites of alveolar wall destruction, where they can also release matrix metalloproteases (MMPs) and proteases (e.g. elastase) which degrade the lung tissue.[36] In human patients, increased macrophages directly correlates to increased emphysema.

Macrophages of COPD patients have been shown to have impairment of phagocytosis and efferocytosis. The diminished phagocytotic ability of macrophages has also been

linked to more frequent COPD exacerbations. In essence the macrophages present in COPD patients are not only increased but are more functionally defective, as cells could not remove apoptotic epithelial cells. This diminished ability of macrophages leads to tissue damage, chronic inflammation and various diseases including microbial infection. This leads to the loss of tissue homeostasis and hence further contributing to the vicious cycle of inflammation and tissue damage.[31, 36]

Aside from the roles of macrophages already discussed, there is also their influence in the larger immune landscape, notably the impact on other immune cells and subtypes, as well as inflammatory cytokines and other mediators, which will be explored later in this study.

2.2. Neutrophils

Neutrophils are one of the other key features of inflammation in COPD, and are responsible for a great deal of damage. Not only are neutrophils increased in the BALF and sputum of COPD (5-10 fold), but so too are various neutrophil chemotactic factors including CXCL1, CXCL5, CXCL8 and LTB4.[36, 37] These chemotactic factors listed cause further damage due to additional recruitment of more inflammatory cells (Figure 1.4).[36, 37] Neutrophils also secrete several proteases including neutrophil elastase, cathepsin G, myeloperoxidase, and MMPs, that can breakdown the ECM and damage the alveolar wall, thus leading emphysema.[38, 39]

Neutrophil elastase (and other mediators) are stored within neutrophil azurophil granules. The area around a degranulating neutrophil has a significantly higher concentration of neutrophil elastase causing the area of a degranulating neutrophil to become significantly damaged.[40] Thus, the more neutrophils degranulating in the lung, the more direct damage from proteases as well as the more inflammatory mediators released, and thus increased neutrophil chemotaxis.[40, 41] Increased infiltration of neutrophils in the lungs occurs in all people with COPD, irrespective of the cause or severity of COPD.[41]

2.3. Other immune cells

Lung structural cells, including airway and alveolar epithelial cells and endothelial cells, as well as fibroblasts are also activated in COPD. They contribute to pathogenesis as upon initial damage they are unable to effectively repair, thus the structure is disrupted and hence, structural integrity lost. They also release inflammatory cytokines, contributing to the high inflammatory environment that leads to further damage. [37, 42]

Other specific inflammatory cells that are increased in COPD and particularly detrimental in COPD including T lymphocytes, dendritic cells (DC) and in some cases eosinophils. Specifically, DCs have been shown to be activated in the lungs of COPD patients, and increased DCs are linked to increased disease severity.[37, 43] This is a pivotal finding as DCs also activate other immune cells including neutrophils, macrophages, T cells and B cells. CD4+ (T helper) and CD8+ (suppressor/cytotoxic) T cells are increased in the airways and lung parenchyma of patients with COPD, with a predominance of CD8+ cells. In smokers who develop COPD there appears to be activation of adaptive immunity, with the infiltration of CD8+ and CD4+ cells in the alveolar walls and small airways. As well in COPD patients with the most severe disease there is the presence of lymphoid follicles that contain a core of B lymphocytes surrounded by T cells.[37, 43, 44]

COPD severity was also found to correlate with increased B cell counts and the number and size of B cell-rich lymphoid follicles in COPD lungs.[45] In addition, increased levels of mediators that promote activation, maturation and overall survival were also found in the lungs of COPD patients. Furthermore, antibodies derived from these B cells, also contribute to lung inflammation of COPD patients by targeting lung cells, fragments of these cells and proteins associated with the extracellular matrix.[45] This was attributed to the formation of various immune complexes which activate complement proteins. Although, studies involving B cell-deficient mice and human COPD patients found a strong correlation to the emphysema phenotype, it should be pointed out the B cells also offer protection during COPD aggravations by promoting various adaptive immune responses that assist the patients defence systems against pathogens.[45]

While eosinophils have been shown to increase in COPD, this finding is not consistent across all patients with COPD,[37] suggesting that there are additional factors and conditions relating to increased eosinophils and hence more research on mechanisms of disease is required. One key finding is that eosinic airway inflammation is strongly linked to patient corticosteroid response.[37, 43]

A key point to remember regarding inflammation is the importance of the interplay between various inflammatory cells, and inflammatory mediators which lead to disease. That is, while some cells and mediators are particularly impactful in disease pathogenesis, the combination of multiple complex inflammatory pathways leading to chronic inflammation and disease, is what makes inflammatory diseases like COPD particularly detrimental as well as difficult to treat, as targeting just one pathway can be insufficient or ineffective in suppressing inflammation. However, treatments have and can still show some improvements.

2.4. Inflammatory mediators

Inflammatory mediators are heavily implicated in COPD pathogenesis. These mediators are small molecules and proteins which are released by both inflammatory and structural cells.

Inflammatory mediators include: lipid mediators such as prostaglandins and leukotrienes (e.g. LTB4), growth factors (e.g. EGF and TGFβ), free radicals/ROS and proteases, inflammasomes (which regulate the expression of proinflammatory cytokines), and most notably cytokines and chemokines.[33, 46]

Cytokines and chemokines are very heavily implicated and studied in COPD, with their main function in COPD to signal and regulate immune cells and immune response. Chemokines are chemotactic cytokines, which attract certain inflammatory cells to move to a chemical gradient.[47, 48] The best example of this in COPD and particularly A1AT deficiency related COPD is neutrophil chemotaxis into the lung. Where specifically IL-8 (CXCL8) and LTB4, have been specifically implicated in neutrophil chemotaxis.[47, 49] One reason this is specifically detrimental to A1AT deficiency is due to the ability of A1AT to regulate human neutrophil chemotaxis induced by soluble immune complexes and IL-8 (via direct binding of A1AT to IL-8).[50] While there are

many cytokines and chemokines implicated in COPD, a few key mediators include IL-8, TNF and LTB4, which are also shown in Figure 1.4.

3. ECM structure and turnover

3.1. Key components of the ECM

Lung ECM is a group of macromolecules including, glycoproteins and proteoglycans, elastin, and collagen, which provide structural support and are essential in maintaining healthy lung function.[51-53] A1AT deficiency in humans leads to excess activity of proteases, such as neutrophil elastase (NE) which induce abnormal deposition of extracellular matrix (ECM) proteins resulting in tissue damage. [54, 55] A1AT deficiency is therefore associated with uncontrolled ECM protein degradation that eventually leads to emphysema in COPD.[28, 55, 56]

In COPD, airway remodelling involves changes in the ECM affecting airway wall thickness, resistance, and elasticity, resulting in the entrapping of gas and limiting airflow. Specifically, ECM remodelling is implicated in alveolar destruction (emphysema), and airway obstruction (airway remodelling) which are key classifications of COPD.[51, 57]

Although collagen and elastin are the main focus of the ECM in lung damage associated with COPD, there are other components of the ECM such as fibronectin, laminin, tenascin, integrins, growth factors and certain matrix metalloproteinases (MMPs) that also contribute but are less explored.[51-53, 57]

Specifically, and of particular importance to COPD is the changes that occur in collagen and in elastin. Elastin is a key component in the ECM giving lungs their elasticity, thus the ability of alveoli to contract i.e. breathe out. In COPD they are a major target of disintegration, damage and thus lung remodelling, with the decomposition of elastin leading to emphysema. Collagens are the main form of structural proteins found in the ECM and are best known for providing tensile strength, however they are also involved in cell adhesion and migration. Collagens are also heavily implicated in remodelling however there are many subtypes of collagen in the lung that serve slightly different roles for example collagen I, II, III, V and XI are arranged into fibrils which provide structural integrity, while collagen IV is the core

component of basement membranes of the ECM providing mechanical strength. [51, 52, 58] Regarding COPD collagen degradation is upregulated and serum fragments of collagen I, III, IV and VI are associated with increased disease severity specifically airflow limitation.[51] Additionally, degradation of certain collagen fragments such as I and IV as well as collagen V formation are increased during COPD exacerbation and decreased to basal levels 4 weeks after exacerbation.[59] Furthermore, collagen IV turnover is predictive of mortality in COPD and affects key pathological processes in COPD.[58, 60] Thus, the importance of collagen, elastin and other ECM turnover products to be used as serum biomarkers, as they are significantly associated with disease severity and clinically relevant outcomes in patients with COPD, as well as their role in disease pathogenesis.[51, 61]

This degradation in elastin and collagen fragments are a direct result of increased inflammation, which for the majority of COPD cases is due to increased inflammation from CS. In addition, with increased chronic inflammation there is also increased fibroblasts and inflammatory cells including neutrophils, macrophages and T cells to the airways. These cells then secrete matrix metalloproteases (MMPs) which degrade the ECM of small airways and parenchyma.[51]

3.2. Protease and anti-protease balance

3.1 outlined the ways in which proteases can degrade lung tissue in COPD patients. In healthy tissue, these proteases are prevented from causing excess damage by the activity of anti-proteases. The major pulmonary anti-proteases and their functions are listed in Table 1.1. These include A1AT, cystatins, which inhibit cysteinyl cathepsins, as well as TIMPS (tissue inhibitors of metalloproteases), which regulate MMPs and ADAMs (a disintegrin and metalloproteinase). [30, 38, 39, 62, 63, 64]

Table 1.1: List outlining common lung proteases, as well as antiproteases that inhibit or regulate them. [30, 38, 39, 62, 63, 64]

Anti-proteases	**Proteases**
A1AT	NE
secretory leukocyte protease inhibitor (SLPI)	Cathepsin G
tissue inhibitors of metalloproteinase (TIMP)	Proteinase 3
Elafin	MMPs (notably MMP-1, -2, -8, -9, -12, -13 and -14)
Alpha-1 antichymotrypsin	ADAM (notably ADAM-17)
Cystains	Dipeptidyl Peptidase IV
	Tryptases
	Chymases
	Cysteine Proteases (e.g. Caspases and Cathepsin S)
	Aspartic Proteases (e.g. Cathepsin D and Cathepsin E)

It is important to note that these proteases and antiproteases do not hold equal weight in their contribution to the destruction of the lung, or in the case of anti-proteases, their protective ability in the lung. For example, while SLPI and Elafin are inhibitors of NE, as well as cathepsin G, chymase, trypsin and proteinase 3 (inhibited by Elafin), they are present in much lower quantities in the lung compared to A1AT. [38, 39] Hence, A1AT is largely considered the primary inhibitor of NE. Additionally, other proteases such as MMPs and ADAMs are largely regulated by TIMP, however there is still significant research on the implication and effect of A1AT/ A1AT deficiency in this regulatory pathway.[38, 39, 63] Thus, the complexity is not just in the protease anti-protease balance, but also in their alternative functions e.g. the ability of A1AT to modulate immune response. This includes, for example, the ability of A1AT to inhibit TNF and MMPs in alveolar macrophages in response to CS extract, as well as to impair LPS-induced monocyte activation and to block apoptosis.[64]

4. A1AT Deficiency

A1AT deficiency is a genetic disorder that has a reduction or complete loss of A1AT protein. A1AT deficiency in humans leads to excess activity of proteases, such as neutrophil elastase (NE) that induces abnormal deposition of extracellular matrix (ECM) proteins and tissue damage.[54, 55] A1AT deficiency is associated with uncontrolled ECM protein degradation that eventually leads to emphysema in COPD.[28, 55, 56] (Figure 1.2).

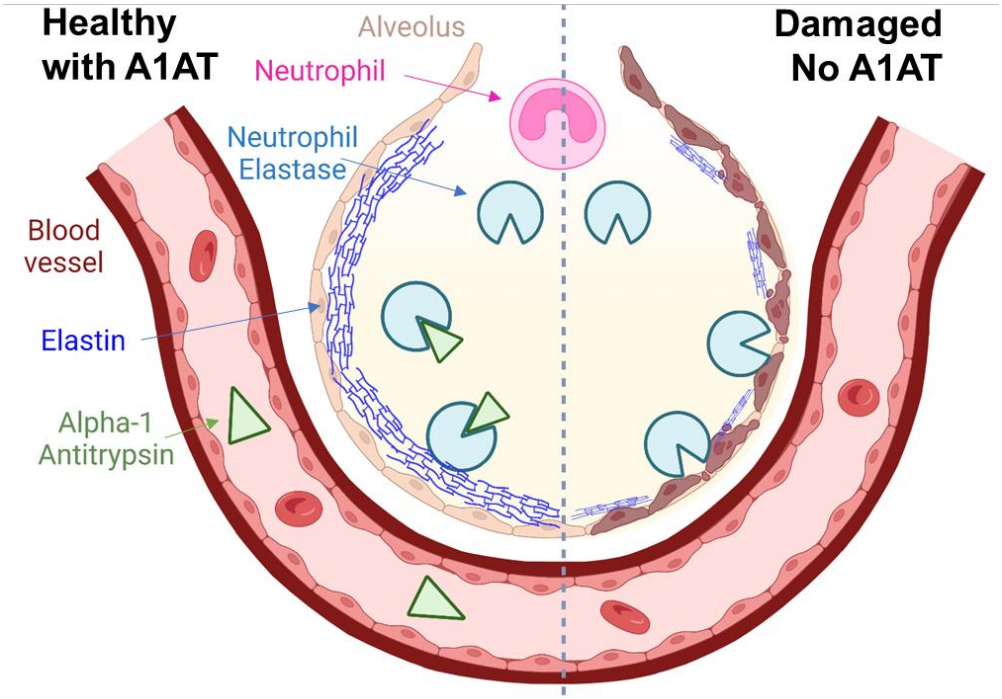

Figure 1.2: Representation of the mechanism of disease in A1AT deficiency compared to normal 'healthy' physiology.

The left 'healthy' side of this figure shows a system with healthy alveoli with functional A1AT and inhibition of proteases such as neutrophil elastase. In contrast, the side with no A1AT shows uninhibited proteases (neutrophil elastase) which degrade ECM lung structures leading to damage. Thus, highlighting a main mechanism in how A1AT protein is protective in the lung, specifically against damage to the ECM and alveoli. Made with BioRender.

4.1. Prevalence of disease

A1AT deficiency is one of the world's most prevalent and serious hereditary disorders and the most common genetic factor contributing to COPD. Approximately 1 in 9 Australians carry a faulty A1AT gene.[65] Furthermore, 90% of diseased individuals are undiagnosed i.e. they don't know they have A1AT deficiency. [66]

Laboratory testing, such as testing genotyping and phenotyping (pathology) is the most common way of A1AT deficiency diagnosis, however lack of diagnostic tools remains a major issue of A1AT deficiency. A recent study by Nakanishi *et al.* (2020)[67] showed that only 9 out of 140 individuals with PiZZ genotype were diagnosed with A1AT deficiency. Studies also showed that even among A1AT deficient (PiZZ) individuals already diagnosed with COPD, 77% were not diagnosed with A1AT deficiency.[67] Diagnosis is often very slow, with an average of 5 to 8 years from first symptom onset to diagnosis of A1AT deficiency. [67] This is particularly detrimental due to the significant irreparable damage occurring over this time, and since there is no cure for A1AT or COPD this damage is permanent.

This suggests that A1AT is not a rare disease but a rarely diagnosed disease. Hence, there is an unmet need for more research into A1AT deficiency and potential treatments and cures for patients with A1AT deficiency and COPD.

4.2. A1AT Gene and Mutations

Alpha-1 antitrypsin (A1AT) is a 52 kDa serine protease inhibitor (clade A member 1 encoded by the SERPINA1 gene located on chromosome 14. A1AT is primarily produced by parenchymal cells in liver and is transported to the plasma where it is circulated to the lungs.[68, 69] It is also produced in many other cells, including bronchial epithelial cells, neutrophils, monocytes, macrophages – including alveolar macrophages, and epithelial cells[70, 71]. The A1AT gene has two separate promotors, one liver specific and the other monocyte specific. [72]

To date, well over 100 mutant alleles of A1AT have been identified, with some mutations resulting in an absence of A1AT protein.[73] The M allele is the normal, non-mutated allele. Individuals with two copies of this allele, termed PiMM (protease inhibitor MM), have 100% normal circulating A1AT protein with serum concentration values of 20-53 μM. A1AT concentrations below a minimum serum A1AT threshold of 11 μM, are under the 'protective threshold'. have a severe deficiency, and greatly increased risk of lung disease. Intermediate A1AT deficiency ranges between 11-20 μM with serum ranges from 20-60% of the normal. A decreased A1AT serum concentration or impaired, less functioning A1AT protein is dependent on the genotype.[69, 74-76] This means depending on the severity of the mutated allele and if it is homozygous or heterozygous, will influence how increased the risk of disease is, which is supported by the correlation between different A1AT genotypes and increased risk of COPD development. [76-78] Some of these alleles are described in Table 1.2.

Table 1.2: Characteristics of selected A1AT genes/alleles.

This shows the type of mutation, cellular defect, mutation, and effect of mutation. The types of alleles are normal (M), deficiency (Z and S), null (alleles with no protein or no mRNA) and dysfunctional alleles (Z and F).[73, 78, 79]

Allele	Mutation	Cellular defect	Effect of mutation	Disease association
M	None	None	None	Normal (None)
Z	Glu342Lys	Intracellular accumulation	Polymerisation and low A1AT serum levels (10-20%)	Lung, Liver
S	Glu264Val	Intracellular degradation	Quantitatively and functionally deficient A1AT (~50%) of	Lung

			normal serum levels	
F	Arg223Cys	Defective neutrophil elastase inhibition	Protein is functionally impaired in binding and inhibiting neutrophil elastase (quantitatively normal)	Lung
I	Arg39Cys		mild quantitative deficiency	Lung
Null (numerous alleles)	Numerous	No mRNA, or no protein	No functional protein	Lung

The most common mutation is the Z mutation, accounting for >95% of clinical A1AT deficiency cases.[80] The Z mutation contains an amino acid substitution of lysine for glutamic acid at position 342 i.e. (E342K) or (Glu342Lys mutation). The mutated Z-A1AT protein is prone to self-aggregation and polymerisation, causing it to misfold and accumulate in the endoplasmic reticulum of hepatocytes.[81, 82] This results in a gain-of-toxic function leading to inflammation, fibrosis, cirrhosis, and increased risk of hepatocellular carcinoma.[83] Since the protein is accumulated in the liver it cannot travel to the serum and lungs, hence a lower concentration is measured in the serum of Z heterozygous (MZ) and homozygous (ZZ) individuals, and less is present in the lungs where it is protective.[81, 82]

Individuals with one normal copy (M) and one mutated Z copy are PiMZ and have on average 60% circulating A1AT gene, however the PiZ genotype is present in up to 5% of the general population. Additionally, those with 2 mutated Z alleles have been reported at between 10-20% circulating A1AT.[69, 74, 77, 80] Z allele homozygosity has

severe A1AT deficiency and hence a high risk of disease, however those with genotypes with intermediate A1AT deficiency, although at a greater risk compared to healthy individuals, may not ever develop COPD if their environmental risk factors are low.[77] Individuals with A1AT deficiency who inhale cigarette smoke, increase their chances of developing COPD. Cigarette smoke and other occupational and environmental inhalants can further disrupt the protease-anti-protease imbalance in A1AT deficiency patients and further increase the risk of COPD, as depicted in Figure 1.3.[76, 77, 84]

4.3. A1AT deficiency and COPD

The current paradigm for the association between A1AT deficiency and COPD risk is represented graphically outlined in Figure 1.3, this shows the protease – antiprotease balance as A1AT presence vs neutrophil elastase burden.

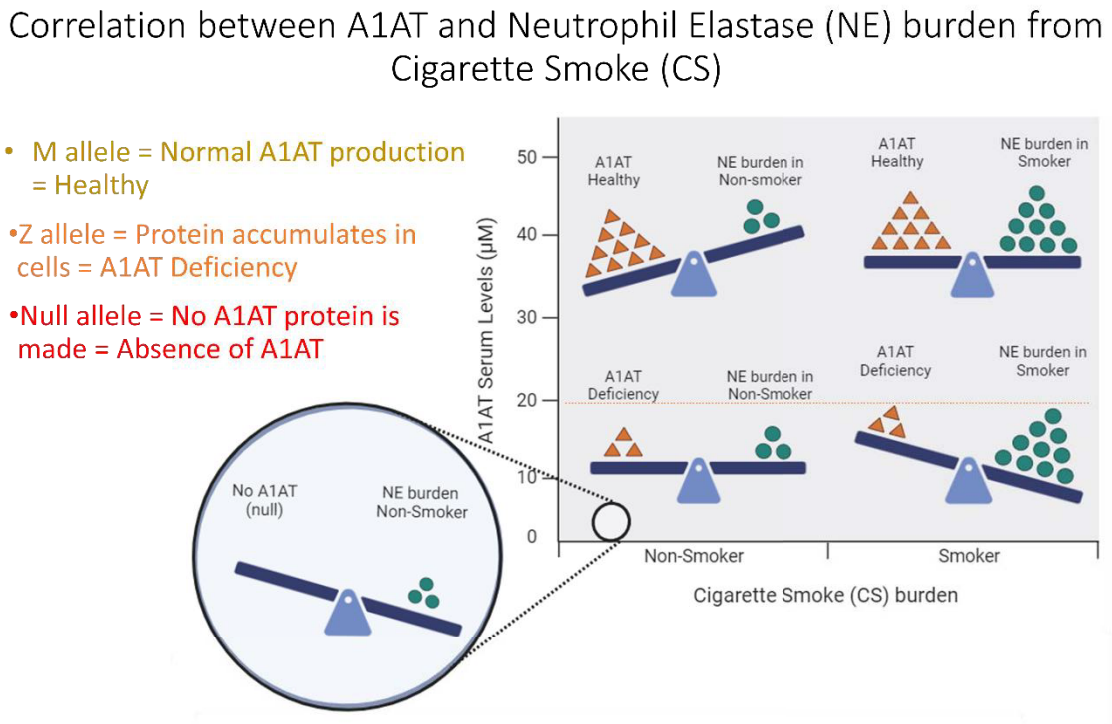

Figure 1.3: Conceptual model showing the correlation between alpha-1 antitrypsin (A1AT) concentrations (levels) and neutrophil elastase, by genotype.

This shows the protease anti-protease balance as A1AT protection vs neutrophil elastase. This figure shows the detriment of a lack of A1AT e.g. A1AT deficiency or severe A1AT deficiency 'no A1AT' from null genotype individuals. The figure also

shows how increased NE burden can also be a detriment, leading to an imbalance and thus disease, as well as how A1AT deficiency further increases this imbalance. Made with BioRender.

While neutrophil elastase burden can be increased due to many factors including cigarette smoke, influenza, COVID-19 etc. this graph assumes a healthy environment and the increased burden of neutrophil elastase from CS. In the top left (of Figure 1.3) we have healthy individuals, who have lots of protective A1AT that can inhibit neutrophil elastase and no disease. If these healthy individuals are exposed to cigarette smoke however the neutrophil elastase burden is increased. This can still lead to disease progression but since there are high levels of A1AT there is still some protection from the A1AT as it will inhibit the neutrophil elastase.

With A1AT deficiency however, the A1AT level is already quite low and so the impact of cigarette smoke is more severe as the neutrophil elastase is uninhibited and can damage the lung. Furthermore, in patients with no A1AT, null individuals, as well as very severe deficiencies (which can even include PiZZ) there is very little to no protective A1AT and the neutrophil elastase impact is severe. This means that patients with A1AT deficiency the neutrophil elastase burden from CS is even higher, and they are at increased risk of developing COPD. In some cases, patients with A1AT deficiency develop COPD without ever having smoked.[85]

Those with genotypes with intermediate A1AT deficiency, although at a greater risk compared to healthy individuals, may not ever develop COPD if their environmental factors are low. Individuals with A1AT deficiency who inhale cigarette smoke, increase their chances of developing COPD. Cigarette smoke and other occupational and environmental inhalants can further throw off the protease-anti-protease imbalance in A1AT deficiency patients and further increase risk of COPD.[86]

4.4. A1AT deficiency and macrophage function in COPD pathogenesis

A second critical role of A1AT is its anti-inflammatory properties attributed to A1AT's ability to suppress macrophage activation. Therefore, in systems without A1AT there is increased inflammation, less ability to clear apoptotic cells and control infections resulting in more damage to lung tissue.[32]

Macrophages typically produce/secrete A1AT, and this is a key source of A1AT excluding the main source which is liver hepatocytes.[72] In A1AT deficiency this production is reduced, dysfunctional, or non-existent depending on the specific mutated variant of the gene.[78] Thus, in A1AT deficiency, the macrophages are already inherently different in that there is less protective A1AT, even in the presence of macrophages. Both, peripheral lung macrophages isolated from bronchoalveolar lavage and monocyte-derived macrophages (MDM) transcribe the A1AT gene, and secrete A1AT. Monocyte differentiation to macrophages increases the level of gene expression 3-fold, though still 70 times less than hepatocytes,[32] suggesting that macrophages contribute a greater component of local A1AT in the lungs than monocytes. However, monocytes still contribute to the local pool of A1AT in the lungs and the overall anti-inflammatory system, but to a lesser extent than when differentiated into macrophages.

A1AT has several other effects on macrophages unrelated to its direct anti-protease activity. Neutrophil elastase binding to macrophages induces the release of LTB4, a major neutrophil chemoattractant, but this pathway is inhibited by A1AT, leading to reduced LTB4 release in vitro and in vivo. This includes the ability of A1AT to abrogate IL-8 and LTB4 mediated neutrophil chemotaxis by up to 40%, as well as inhibition of TNF secretion by A1AT induced inhibition of the TNF converting enzyme (TACE) on the membrane surface. Thus, reducing neutrophils chemotaxis, and neutrophil degranulation which leads to further protease release and further lung damage (Figure 1.4).[87]

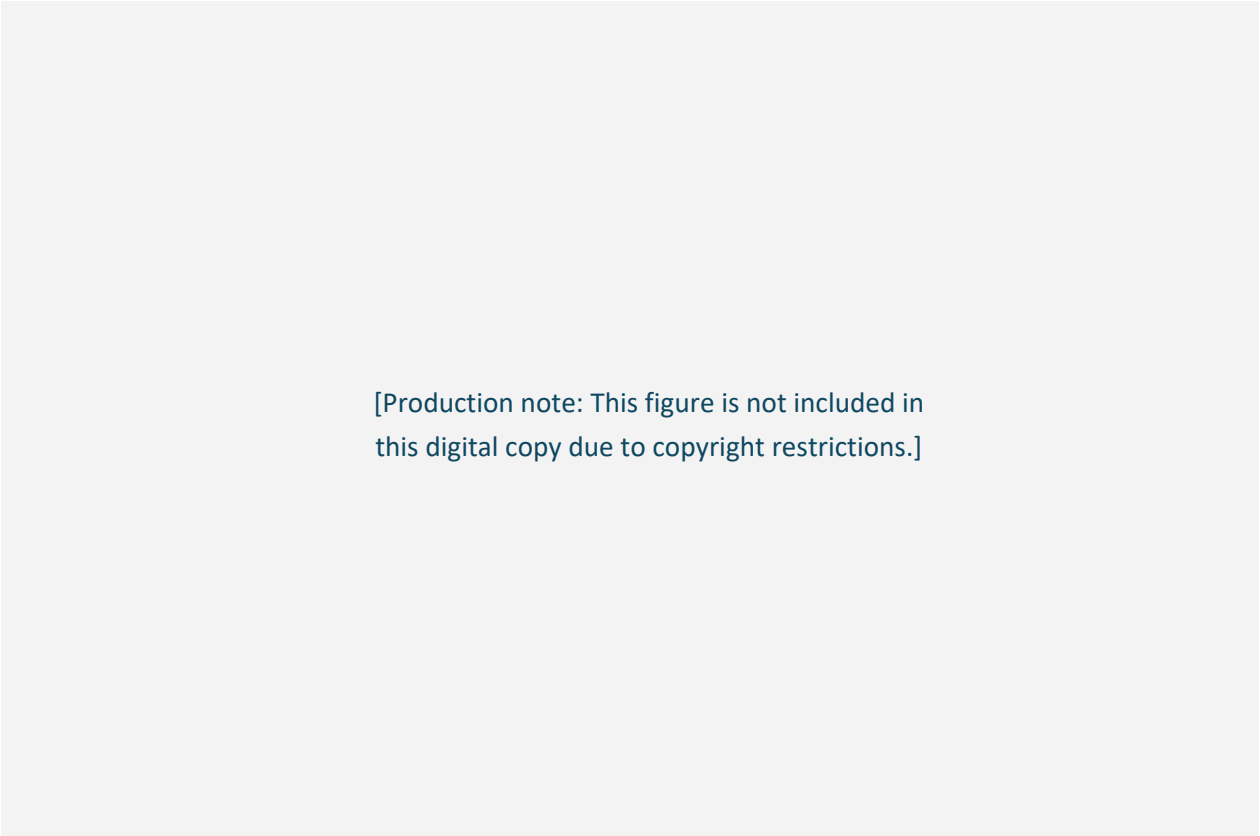

Figure 1.4: Main effects of A1AT on inflammatory pathways.

This shows the impact of key cytokines on neutrophil migration, degranulation and neutrophil elastase release, as well the subsequent pathways and resulting damage to the lungs. Reproduced from Smith D. J. et al [87].

4.5. Other diseases associated with A1AT deficiency

While this project primarily focuses on A1AT and COPD it must be noted that A1AT is implicated in many other conditions.

Mutated A1AT can misfold in the liver and cause cirrhosis of the liver with further complications leading to liver failure and liver cancer. Additionally, greater than 20% of adult individuals with ZZ homozygous genotype have significant liver fibrosis and 10% have advanced fibrosis. [88] Lung fibrosis has also been loosely linked to a very rare A1AT deficient variant, however this variant is not well studied or explored in this thesis[89].

A1AT can influence the immune system in multiple ways, many of which are still being uncovered and require further exploration and investigation. For example, A1AT deficiency can cause infectious lung diseases to be more severe, such as influenza, pneumococcal disease, and COVID-19.[90, 91] Similarly, A1AT has been shown to be protective in various autoimmune disease such as Type 1 Diabetes, Rheumatoid Arthritis, Systemic Lupus Erythematosus.[92, 93] A recent study showed that neutrophils from A1AT deficient patients had increased chemotaxis towards IL-8 ex vivo.[50] This finding suggests that A1AT deficiency leads to inherent differences in immune cell behaviour.

Typical pulmonary manifestations associated with A1AT deficiency include emphysema and bronchiectasis, however other lung conditions are also implicated including asthma.[89] The link between A1AT deficiency and asthma is associated with the protease antiprotease imbalance mechanism of disease as well as the lack of A1AT anti-inflammatory and immunomodulatory properties[94].

Also of note is the link between A1AT deficiency and lung cancer, specifically squamous and adenocarcinoma types – for which an increased risk of development of lung cancer was increased with A1AT deficiency, but survival rate was not impacted[95].

The vast range of diseases associated with A1AT deficiency emphasises the importance for the creation of A1AT based therapeutics and also suggests that the importance of A1AT is not limited to the protease anti-protease balance which is highlighted as a main cause of COPD in A1AT deficient patients. Hence, the importance of understanding the depth of the role that A1AT plays in inflammatory response to CS and in disease.

4.6. Current Treatments

The only current treatment for A1AT deficiency is augmentation therapy. The patient receives weekly to monthly intravenous (IV) infusions of A1AT protein, obtained from blood donors, to raise levels of the protein in the serum.[75, 80] This therapy aids slightly

to slow down lung damage however the treatment is very transient and has risks of allergic reaction and viral contamination. Gene therapy has been considered in the treatment of A1AT deficiency patients. The benefit of gene therapy is the potential of a single dose treatment or a longer time frame between treatments, stable A1AT levels in the body as the body will be able to self-produce A1AT protein, and hence, A1AT deficiency therapy will no longer be reliant on human blood donations.[75, 80] There are two major considerations for gene therapies: the vector used to deliver the gene and the target site. Methods investigated for A1AT gene treatment include gene editing techniques, including clustered regularly interspaced short palindromic repeats (CRISPR) and zinc-finger nucleases, as well as methods of gene delivery including retrovirus, adenovirus, adeno associated virus, plasmid and liposomal vectors, with typical target sites including the lung, liver and muscle.[80] However, most of gene therapy has severe side effects or limited ability to deliver gene to target cells.[96]

It is important to note that much of the field of genomic editing regarding the A1AT gene and increasing A1AT production involves either using some version of viral vector to deliver functional A1AT gene or by specifically targeting and manipulating the A1AT regulatory region including the promoter and enhancer region. Thus targeting or inserting specific DNA regions in the A1AT gene structure that when activated leads to increased A1AT production[72].

5. Mouse models of COPD/A1AT deficiency

Many experimental mouse models have been established both for understanding the mechanisms of A1AT deficiency and for testing potential treatments and therapies. Like with most animal models there is some variation between the animal model and the human disease. For A1AT deficiency something to note is that the Serpina1 gene present in humans varies to that in mice. In humans A1AT protein is expressed by a single gene (SERPINA1) however mice have 3-5 distinct protease-inhibiting genes (Serpina1a-e) depending on the strain, with C57BL/6 mice possessing genes Serpina1a-e.[84, 97, 98]

These genes are quite similar however only Serpina1a and Serpina1b were found to inhibit neutrophil elastase, which as mentioned earlier, is the major physiological target

of human A1AT and hence, will be the main targets and focus of this study.[99] Interestingly, Serpina1c-e, have specificity for proteases other than neutrophil elastase.[99] Additionally, upon deletion of Serpina1a in mice there was resultant embryonic lethality, although this is not the case when Serpina1a-e genes were deleted. Serpina1a and Serpina1b are present in all mice that have been investigated, however, much is still unknown about murine Serpina1 genes, and some have been investigated less than others.[84, 97, 98, 100]

Three major mouse models of A1AT deficiency are studied in the literature.

PiZ mice: The PiZ mice carry an insert of expressed sequence of the human A1AT mutant Z gene on a C57BL/6 background. These mice present with the liver phenotype of A1AT deficiency disease with reductions in circulating levels of A1AT protein.[82] Previous studies have shown that these mice develop increased pulmonary inflammation after acute (5 days) CS exposure.[70]

A1AT KO mice: The A1AT KO mice have knock out of genes Serpina1a-e on a C57BL/6 background.[98] They have undetectable levels of A1AT in serum and an absence of A1AT in liver tissue. These mice spontaneously develop emphysema by the time they reach ~1 year old.[98]

Pallid mice: these mice possess a partial A1AT serum deficiency. Symptoms of lung disease do not manifest until age 8-10 months.[101]

To date most of the experimental work with these models has looked at either acute smoke exposure (which can only replicate CS induced inflammation) or the effects of A1AT deficiency in isolation. Our lab has established an experimental model of cigarette smoke (CS) induced COPD. The mice develop all characteristics of COPD, including chronic inflammation, small airway remodelling, emphysema and impaired lung function in 8 weeks.[102] Of particular note regarding this CS model is the use of a custom apparatus that allows nose only inhalation of CS as opposed to full body CS exposure which is present in most of the CS exposure models in the literature. This model will allow me to investigate the intersection of A1AT deficiency and CS induced disease in a true COPD model.

In this thesis I will be investigating the connection between cigarette smoke induced emphysema and A1AT deficiency using two previously developed transgenic models

of A1AT deficiency; PiZ mice and A1AT KO mice. This work will aid in creating a suitable mouse model in order to test future therapies, particularly novel genomic editing based therapies. By combining existing CS exposure mouse models with A1AT deficient GMO mice and create a model that has both CS damage and A1AT related damage as well as potentially a worsened model in A1AT deficiency compared to control (non-A1AT deficient). Thus, these models not only allow investigation into the many complex mechanisms leading to disease but also elucidate how these models are similar or vary to human disease, and to existing models.

6. Aims and Hypotheses

Thesis Goal: To gain a greater understanding of the interaction between A1AT deficiency and CS exposure.

Hypothesis: That the role of A1AT is pivotal as a key immunomodulator, as A1AT is known to impact certain key inflammatory pathways, contributing to COPD.

Aim 1: To assess the gene and protein expression of A1AT in an experimental model of CS-induced COPD in mice.

Hypothesis: We hypothesise that A1AT expression changes upon exposure to CS and COPD.

Aim 2: To investigate the mechanisms of A1AT deficiency in CS induced COPD

Hypothesis: That A1AT KO mice will experience worsened COPD due to CS when compared with WT controls.

Aim 3: To investigate the mechanism of human Z mutated A1AT toxicity in CS induced COPD.

Hypothesis: That PiZ mice will experience more severe COPD due to CS when compared to WT controls, as well as liver damage due to A1AT accumulation in the liver.

Aim 4: To elucidate the biology of dendritic cells in an A1AT deficient, CS-induced COPD model.

Hypothesis: That there is a potential DC involvement in priming the immune system in COPD that could lead to worsened disease outcomes.

Chapter 2 – Methods

This chapter contains all the methods used throughout this thesis. This is due to significant overlap in protocols across some chapters, for example all chapters involve the use of CS exposed mice.

Mice

A1AT KO (C57BL/6J-Serpina1em3Chmu/J) mice used in this study were acquired (breeder pairs) from The Jackson Laboratory (Harbor, Maine, United States). Mice were created by using CRISPR/Cas9 to delete all of the mouse *Serpina1* genes[98]. Imported mice were subsequently bred homozygous KO x homozygous KO at the Centenary Institute. These mice have a C57BL/6 background and hence C57BL/6 is used as the experimental control.

PiZ (B6.Cg-Tg(SERPINA1*E342K)Z11.03Slcw/ChmuJ) mice used in this study were acquired (breeder pairs) from The Jackson Laboratory (Harbor, Maine, United States). Mice express mutant human SERPINA1, from a knock in for the human Z mutation which carries a glutamic acid to lysine substitution at residue 342 (E342K). These PiZ mice accumulate α1-antitrypsin in hepatocytes and develop liver damage, and have a C57BL/6 background with functional mouse A1AT. Imported mice were subsequently bred at Australian BioResources (ABR), and imported as required to the Centenary Institute.

Wild-type (WT) C57BL/6 mice were imported from ABR, Ozgene ARC, and WEHI. Imported mice were acclimatised in the facility for a minimum of 7 days prior to experimentation. All mice at Centenary were kept in 12h light/dark cycle and fed standard irradiated chow. All experimental work was approved by the Sydney Local Health District Animal Welfare Committee. Protocol numbers 2022-002 and 2022-009.

Genotyping – A1AT KO mice

Homozygous A1AT KO breeder mice were obtained from The Jackson Laboratory.[103] Ear clippings were taken from A1AT KO breeder parents and F1 generation. DNA was extracted from the ear clippings using MyTaq Extract-PCR Kit (BIO-21127, Bioline) as per manufacturer's instructions (heat at 75°C for 5 mins, then 95°C for 10 mins).

PCR product was made by adding a master mix (9.5µl) to the extracted DNA from mouse ear clippings (0.5µl) and thermocycling based on specifications from the Jackson Laboratory (Table 1)[104]. The master mix included 10 µM forward primer (0.5µl, A1AT KO sequence: 5'-TCA GAC TAT ACA GGG AGC TGG TC-3'), 10 µM reverse primer (0.5 µl; A1AT KO sequence: 5'-CAC CAG CTT CAG GTC ATT GTT-3'), My Taq HS Red Mix (2x, BIO-25047, Bioline) and dH2O (3.5 µl).

Table 2.1: Cycling conditions for creating PCR product.

The thermocycling protocol is based off specifications from Jackson Laboratory, for genotyping A1AT KO mice.[104]

Step	Temperature (°C)	Time	Note
1	94	5 mins	
2	94	30s	
3	65	30s	-0.5 C per cycle decrease
4	68	30s	
5			repeat steps 2-4 for 10 cycles
6	94	30s	
7	60	30s	
8	72	30s	
9			repeat steps 6-8 for 28 cycles
10	72	5s	
11	10	∞	hold

PCR product or ladder (Bioline HyperLadder 50bp, BIO-33039, 1µL), GelRed (BIO-41009 6X GelRed, 1µL) and H_2O (4µL) was pipetted into the well of 2.2% agarose gel in 1x TAE buffer (pH8). Gel was run at 90V, for 40 mins and imaged on a BioRad ChemiDoc^{TM}MP Imaging System. Mice were confirmed to be A1AT KO mice by the presence of characteristic KO band (at 200bp) compared to WT band (300bp).

Genotyping–PiZ mice

Hemizygous PiZ breeder mice were obtained from The Jackson Laboratory.[105] Ear clippings were taken from all mice. DNA was extracted from the ear clippings using MyTaq Extract-PCR Kit (BIO-21127, Bioline) as per manufacturer's instructions (heat at 75^{o}C for 5 mins, then 95^{o}C for 10 mins).

qPCR product was made by adding a master mix (9.5µl) to the extracted DNA from mouse ear clippings (0.5µl) and thermocycling based on specifications from the Jackson Laboratory (Table 1).

The master mix included 5µl of KAPA PROBE FAST One-Step qRT-PCR Master Mix (2X) Universal (Roche), 0.4µl of 10µM forward primer (transgene sequence: 5'- AGA AAA GGG ACT GAA GCT GC -3'), 0.4 µl of 10µM reverse primer (transgene sequence: 5'- ACC ACT TTT CCC ATG AAG AGG -3'), 0.4µl of 10 µM forward primer (internal positive control sequence: 5'- CAC GTG GGC TCC AGC ATT -3'), 0.4µl of 10 µM reverse primer (internal positive control sequence: 5'- TCA CCA GTC ATT TCT GCC TTT G -3'), 0.15µl of 10 µM Tg probe ([6FAM] CCC CCC GAG GTC AAG TTC AAC AA [BHQ1]) for the transgene primers, and 0.15µl of 10 µM IC probe ([Cyanine5] CCA ATG GTC GGG CAC TGC TCA A [BHQ3]) for the internal control primers, as well as nuclease free (nf) H_2O (3.5 µl) for each well/ mouse sample.

As the volume of ear clipping DNA required is only 0.5µl, and the required volume of nf H_2O 2.6µl to make up the volume of 10µl, a mix of DNA and nf H_2O was made to reduce pipetting error. This involved adding 3µl of DNA, and 15.6µl of H_2O, and pipetting 3.1µl of this mix into each well, for each mouse sample. The master mix of primers, probes and KAPA probe fast, was then pipetted into the well (6.9µl), for a total volume of 10µl.

Table 2.2: Cycling conditions for genotyping PiZ mice.

The thermocycling protocol is based off specifications from Jackson Laboratory, for genotyping PiZ mice.[106]

Step	Temperature (°C)	Time	Note
1	95	3 mins	
2	95	3s	
3	60	20s	Repeat steps 2-3 for 40 cycles

Smoke model

Mice were simultaneously exposed to cigarette smoke (twelve 3R4F reference cigarettes [University of Kentucky, Lexington, Ky] twice per day and 5 times per week for 1 to 12 weeks Figure 1). Cigarette smoke was delivered by using a custom-designed and purpose-built nose-only, directed-flow inhalation and smoke-exposure system (CH Technologies, Westwood, NJ) housed in a fume and laminar flow hood with each exposure lasting 75 minutes. To achieve nose-only smoke exposure, mice were placed in specialised containment tubes where smoke could only enter directly to the nose of the mouse. Mice were exposed to increasing amounts of CS to allow for acclimatisation, exposure is as follows, first day 1 session of 6 cigarettes, second day 2 sessions of 6 cigarettes, third day 2 sessions of 9 cigarettes and from then on 2 sessions of 12 cigarettes. Smoke was delivered in 2-second puffs, with 30 seconds of normal air between each puff, each cigarette has 12 puffs. Following the 75 minutes of smoke exposure mice are monitored for 10 minutes (or longer if required). Age-matched control mice were exposed to room air.

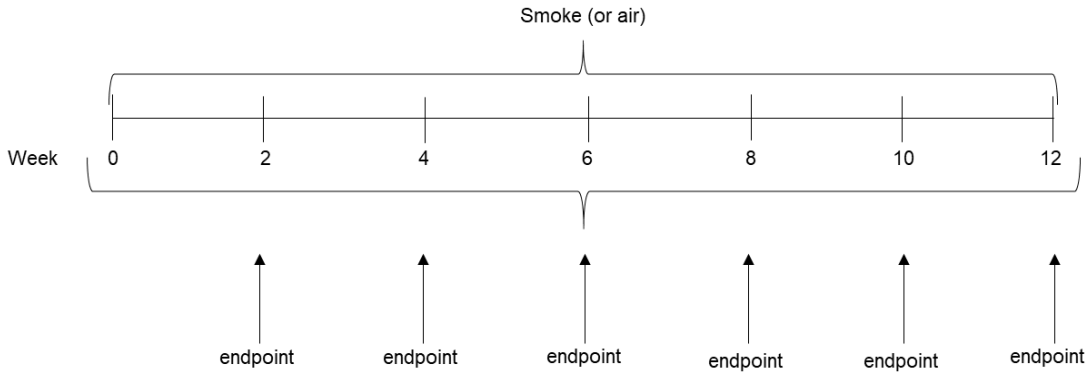

Figure 2.1: Experimental model of cigarette smoke (CS)-induced COPD.

Mice were exposed to air/CS for a variety of timepoints, i.e. 2, 4, 6, 8, 10 and 12 weeks. Endpoint refers to the end of each timepoint, that is the conclusion of the model and collection of samples for experiments.

For Chapter 3, Aim 1 (the COPD time course) WT mice samples were taken from mice that were exposed to air/CS for 2, 4, 6, 8, 10 and 12 weeks.

For Chapter 4, Aim 2 (the A1AT KO model) A1AT KO and WT mice were exposed to air/CS for 2, 4, 8, and 12 weeks.

For Chapter 5, Aim 3 (the PiZ model) PiZ and WT mice were exposed to air/CS for 8 weeks.

For Chapter 6, Aim 4 (Dendritic cells/BMDC model) A1AT KO and WT mice were exposed to air/CS for 8 weeks.

DLCO (Diffusing capacity of the lungs for carbon monoxide)

DLCO is a measurement of the uptake of carbon monoxide (CO) measured as CO/s/mm of Hg, with Neon as the control gas. DLCO is a parameter that determines the lungs ability to transfer inspired gas throughout the bloodstream. Mice were anesthetised with ketamine and xylazine made up in PBS. Tracheostomy was then performed, followed by cannulation and ligation to secure. Three separate mixes were created to give to the mix as various stages across the procedure, these are as follows: mix 1 given prior to DLCO mice receive 130mg/kg of ketamine and 16mg/kg of xylazine; mix 2 given after DLCO mice receive 300mg/kg of ketamine and 15mg/kg of xylazine; mix 3 given during lung function 20mg/kg of xylazine.

Mice receive 1ml of gas (0.299% CO, 0.499% Ne, 20.76% O, Nitrogen balance), left for 9 seconds in the mouse, collected and diluted 1:1 with room air and measured in the DLCO (Inficon Micro GC Fusion^{TM} Gas Analyser). DLCO will record the output of each gas component i.e. the peaks due to CO and Ne. Using equation 5.1 we determined the DLCO of each mouse expressed as a value between 0 and 1; where complete uptake of CO = 1, and no uptake =0.

$$1 - \left[\frac{\left(\frac{CO\ sample}{CO\ calibration}\right)}{\left(\frac{Ne\ sample}{Ne\ calibration}\right)}\right] \quad (2.1)$$

Equation 2.1: Calculation of DLCO, where CO calibration is the value of CO gas during the machine calibration, Ne calibration is the value of Ne gas during the machine calibration, CO sample is the value of CO gas output from the mouse and Ne sample is the value of Ne gas output from the mouse.

Lung function

Mice were anesthetized (as per DLCO methods, with ketamine and xylazine) and cannulated (tracheostomy with ligation) before being attached to the flexivent apparatus. The flexiVent apparatus (Legacy System; SCIREQ, Montreal, Canada) assesses a variety of parameters using various forced breathing manoeuvres or scripts, including: inspiratory capacity (measured by deep inflation-35), lung resistance, elastance and compliance (measured with Snapshot-150), Newtonian (airway) resistance, tissue elastance and dampening (measured with Quick prime-3), Area/Hysteresis (measured by PVs-P-35), forced expiratory volume (FEV) and forced vital capacity (FVC) (measured by NPFE) and various lung volume parameters such as total lung capacity (TLC), residual volume and functional residual capacity (measured by lung volume scan). Ventilation of these mice is set to 450 breaths/min, with tidal volume set to 10mg/kg.

Note the order of these programs is vital as some manoeuvres are more taxing on the lungs and can cause issues in recording values and data. This order is deep inflation-35, snapshot-150, quick prime-3 and PVs-P-35 (run 4 times, last 3 values accepted

and averaged), NPFE (4 times, last 3 accepted and averaged), lung volume scan (1 value per mouse).

Blood Collection

Blood was collected immediately upon death via cardiac puncture and collected in an EDTA coated tube. The blood was centrifuged at 2000 rpm at room temperature (21 ^{o}C) for 10 mins after which plasma, was collected and stored at -80 ^{o}C for later use. This applied to all mouse models unless otherwise specified.

Bronchoalveolar Lavage Fluid (BALF)

BALF was collected by inflating the single lobe with 0.5 mL of Hanks buffer via the trachea, and collecting the resulting fluid. The other four lung lobes were tied off to prevent fluid entering. This procedure was repeated twice with a typical yield of 1-0.8 mL of BALF collected. BALF was collected differently in the third flow cytometry experiment (Chapter 6, Aim 4, endpoint), for this experiment to have enough BALF for flow cytometry, all lung lobes were washed with Hanks buffer, thus two lots of 1ml (2ml total) were used to inflate the lung lobes.

Airway inflammation was assessed by counting total leukocytes (x10^4 mL^{-1} BALF) using trypan blue stain (0.4%) and a hemocytometer, as well as differential enumeration of inflammatory cells in bronchoalveolar lavage fluid (BALF).

For differential enumeration of inflammatory cells, BALF was performed and cells affixed onto the slide by cytospin. BALF (70 µL) was set on a glass slide (Livingstone 76.2 × 25.4 mm, thickness 1.0-1.2 mm) using Thermo Scientific Cytospin 4, run at 300 rpm for 7 mins and dried overnight. Slides were stained with May Grunwald's solution (5 min) wash (distilled water, 1 min) Giemsa's solution (1:20 Giemsa: pH 6.4 Buffer, 20 min) wash (distilled water, 5 min) twice and dried overnight and cover slipped. Differential count was conducted on a Zeiss Microscope (Zen software) - 200 cells were counted and differentiated morphologically as macrophages, neutrophils, eosinophils, lymphocytes. Macrophages were differentiated from epithelial cells by the position of the nucleus, lack of adherence to other cells, and lack of apical brush border.

Organ Collection

Lungs lobes (excluding the left lung lobe which was taken for histology) did not undergo the BALF procedure, and were tied off, collected, and immediately snapfrozen in liquid nitrogen. The liver was collected and snapfrozen in liquid nitrogen and the spleen was collected, placed on ice, weighed, and snapfrozen in liquid nitrogen. This applied to all mouse models unless otherwise specified.

Protein Quantification (Detergent Compatible Protein Assay)

Detergent Compatible protein assay was used to quantify protein of homogenised lung samples (for both A1AT ELISA and Elastase Activity Assay). Lung samples were further diluted 1/10 in nf H_2O (2 µL in 20 µL total).

Bovine Serum Albumen (BSA) stock was made of 4.0 mg/mL (20 mg in 5 mL nf H_2O), was completely dissolved and filtered, and was further serially diluted (1/2 dilution i.e. 100 µL + 100 µL) to create standard curve of 4.0, 2.0, 1.0, 0.5, 0.25, 0.125, 0.0625 mg/mL as well as a blank of 0 mg/mL.

In a 96-well clear round bottom plate 5 µL of standards and sample was added to each well, with standards run in triplicates and samples in duplicates. To each well, 25 µL of mixed Protein Assay Reagent A (an alkaline copper tartrate solution from BIORAD 5000113) and Protein Assay Reagent S (a surfactant solution from BIORAD 5000115) was added in a ratio of 1:50, S:A, (20 µL of S per 1000 µL of A). Following this 200 µL of Protein Assay Reagent B (dilute Folin reagent for colorimetric assays from BIORAD 5000114) was added to each well and incubated in the dark for 15 mins. The absorbance was then measured at 750 nm in a BMG LABTECH POLARstar Omega plate reader, with shaking at 500 rpm for 5 seconds.

The data was analysed as a linear trend was plotted with standards and the protein concentration of the unknown samples calculated in mg/mL.

Elastase Activity Assay

Elastase activity assay was completed using the Thermofisher, Invitrogen™, EnzChek kit. Kit components were first rehydrated and made to appropriate concentrations.

First 1X reaction buffer was prepared but diluting 10X in 1/10 with dH_2O. Then DQ elastin substrate 1.0 mg/mL solution was made by rehydrating with 1ml of 2 mM sodium azide in PBS. DQ elastin working solution 100 ug/mL, was then prepared by diluting 1/10 in 1X reaction buffer. Our final kit component was made up by reconstituting porcine pancreatic elastase with 0.5 mL of dH_2O to make a 100 U/mL.

Standards of porcine pancreatic elastase was made at concentration 0.2 U/mL and serially diluted for concentrations 0.1, 0.05, 0.025, 0.0125, 0.0065, and 0 U/mL with 1X reaction buffer.

To a 96 well black clear bottom plate the following was added, 50 µL of 1X reaction buffer, followed by 50 µL of 100 µg/mL DQ elastin working solution (final concentration of 25 µg/mL) and then mixed. To sample wells 10 µL of lung homogenate was added with 90 µL of 1X reaction buffer (100 µL total). Note that lungs were homogenised in 200 µL of PBS with a 5mm stainless steel bead in a Qiagen TissueLyser LT at 50 oscillations per second, for 3 mins, twice. To standard wells 100 µL of porcine elastase working solution was added, concentrations of 0.2, 0.1, 0.05, 0.025, 0.0125, 0.0065, and 0 U/mL. Fluorescence intensity was measured with excitation at 485-12 nm and emission 510-10 nm over time every 10 mins for 2 h on the BMG LABTECH POLARstar Omega microplate reader.

For each time point measured, background fluorescence was accounted for and removed by subtracting the value derived from the no-enzyme control) i.e. 0 U/mL. Fluorescence was plotted over time (fluorescence vs time graph), and change in fluorescence between two timepoints (taken from linear portion of fluorescence vs time plot) was also calculated.

A1AT ELISA

A1AT ELISA colorimetric kit was used (Mouse Alpha-1 Antitrypsin ELISA Kit ab205088) to measure the quantity of A1AT protein. This kit was used on blood plasma samples and homogenised lung samples. To prepare lung tissue samples for the ELISA they were first homogenised. Samples were homogenised in 150 µL of PBS with a 5 mm stainless steel bead (Qiagen) and homogenised in a Qiagen TissueLyser

LT at 50 oscillations per second, for 3 mins with a 5 min break and then another 3 mins of homogenisation.

Samples were then diluted in 1x diluent as per manufactures instructions, that is a dilution of 1/80,000 for plasma samples (2 µL of sample diluted in 200 µL (1/100 dilution), then further diluted as 10 µL in a total of 200 µL, (1/20 dilution) then finally 5 µL in 200 µL (1/40 dilution) that is 1/80,000 from the stock. Lung tissue samples were further diluted in 1X diluent as 1/2000 from the stock. To achieve this there was first a 1/100 dilution (2 µL lung homogenate sample in 200 µL) and then 1/20 dilution (10 µL in 200 µL total).

Standards (prepared as per manufacturer's instructions using mouse A1AT calibrator at 0, 6.25, 12.5, 25, 50, 100, 200 ng/mL) and samples were added (100 µL) to the pre-coated anti-mouse A1AT ELISA microplate and incubated at room temperature for 60 mins. Following this the wells were aspirated and then washed four times with 1X wash buffer (200 µL, that is empty wells, add wash, aspirate, and repeat). After the final wash, 1X Enzyme-Antibody Conjugate (100 µL) was added to each well and incubated for 60 mins in the dark. Again, after this the wells were aspirated, and washed four times with wash buffer. TMB Substrate Solution (100 µL) was added into each well and incubate in the dark at room temperature for precisely 10 mins before adding Stop Solution (100 µL) to each well and immediately measuring the absorbance on the BMG LABTECH POLARstar Omega microplate reader at 450 nm.

Data analysis was done on GraphPad Prism 9, but first the background absorbance was removed from all standards and samples. A standard curve was then created and plotted exponentially and the unknown values interpolated. For the blood samples the dilution factor was applied and a concentration of A1AT obtained in mg/ml

For the A1AT protein in the lung this value was divided by the total protein to account for any protein loading discrepancies from slight variation in lung size and total protein quantity, hence lung was measured as mg/ml of A1AT per mg of protein.

RNA extraction

RNA extraction was performed on one lung multilobe (superior lobe) and a portion of one liver lobe, using TRI Reagent® (T9424 Sigma-Aldrich) as per manufacturer's instructions. For homogenisation of samples, 1 mL of TRI Reagent was added to each sample with a 5 mm stainless steel bead (Qiagen) and homogenised in a Qiagen TissueLyser LT at 50 oscillations per second, for 3 mins with a 5 min break and then another 3 mins of homogenisation. Samples were then centrifuged (12,000 g for 10 mins at 3ºC). To purify, the supernatant was transferred to fresh tubes and 250 µL of chloroform added, then vortexed (8 s), incubated (10 mins at room temperature) and centrifuged (12,000 g for 15 mins at 3ºC). Post centrifugation 3 distinct layers were visible, the top clear layer collected to which 500 µL isopropyl alcohol (4ºC) was added. Samples were vortexed (8 s), incubated (room temp for 10 mins), vortex again (8 s) and centrifuged (12,000 g for 10 mins at 3ºC). The resulting supernatant was discarded to leave behind pellet. The pellet was then washed with 75% EtOH (1 mL), vortexed to mix (8 s), centrifuge (8,000 g for 5 mins at 3ºC) and the supernatant removed. This was repeated one more time and the resultant pellet rehydrated with 30 µL of H_2O.

The purity and concentration of the RNA samples was measured on a Thermo Scientific Nanodrop One with samples accepted with the condition that there is only one peak, A260/A280 must be above 1.8 and A260/A230 must be above 2.

cDNA synthesis

Nanodrop readings (ng/µL) were used to prepare total RNA in nuclease-free (nf)-H_2O at a concentration of 100 ng/ µL which allowed consistent loading of 1000 ng of total RNA (with a total volume of 8 µL of RNA and H_2O per well). To the RNA, 10X DNAse Reaction Buffer (1 µL) and DNase I 'amplification grade' (1 µL) (Sigma-Aldrich), mixed and incubated at room temperature (15 mins). Following this DNAse I STOP Solution (1 µL, 25 mM EDTA, from Sigma-Aldrich) was added and gently mixed (chemical inactivation of DNAse I) followed by incubation (65°C, 10 mins using thermal cycler (Bio-Rad T100™). Random Primers (1µl, hexamers at 50 ng/µL) and 10 mM dNTPs (1 µL, 2.5 mM for each A, T, C, G) (Meridian Bioscience) was added, spun down and incubated (65°C, 5 mins). The reaction was put on ice and 5X Reaction Buffer (4 µL, MMLV reaction buffer, 1st strand buffer, Invitrogen/Thermo Fisher), 100 mM DTT (2

µL, Sigma-Aldrich) and nf-H_2O (1 µL) was added, then mixed, spun down and incubated (37°C, 2 mins). Finally, MMLV reverse transcriptase (1 µL, 200U, Invitrogen/Thermo Fisher) was added, mixed spun down and incubated at 25°C for 10 mins, then 37°C for 50 mins and finally at 70°C for 15 mins. Nf H_2O was then added (79 µL) to make a total 100 µL of cDNA.

CDNA was also synthesised with a different kit, the Applied Biosystems™ High-Capacity cDNA Reverse Transcription Kit by Thermo Fisher Scientific. The kit components were first thawed on ice and to each sample (10 µL) an equal amount (10 µL) of reaction mix was added. The reaction master mix was 10X RT buffer (2 µL), 25X dNTP mix (100 µM, 0.8 µL), 10X RT Random Primers (2 µL), MultiScribeTMReverse Transcriptase (1 µL), and RNase Inhibitor (1 µL) and nf H_2O (3.2 µL). The plate was then sealed, spun down, and incubated for 10 mins at 25°C, then 120 mins at 37°C, and finally 85°C for 5 mins before being held at 4°C till removed (using thermal cycler Bio-Rad T100™). The samples were made up to volume with nf H_2O (100 µL total hence 100 µL total of cDNA).

Quantitative Polymerase Chain Reaction (qPCR)

The gene levels of Serpina1, IL1β, IL-13, KC (CXCL1), CXCL15, TNF, Marco and YM-1 were assessed by qPCR, with the primers described in Table 2, and Hprt as a housekeeper gene. The intercalating dye used was Kapa SYBR, for 40 cycles on the Bio-Rad CFX96™ and CFX384™ Real-Time PCR Detection Systems (C1000 Touch™ thermo cycler). Plate running temperature 50°C for 2 mins, 95°C for 2 mins, then 40 cycles of 95°C for 15 s, annealing temperature (60°C unless otherwise specified) for 30 s, followed by 95°C for 10 s, and then slowly increase temperature 0.5°C every 5 s starting from 60°C to 95°C after which the plate is read.

Table 2.3: Mouse RT-qPCR primers for transcript analyses. Primer sequences of each gene are included, 5'-3'.

Gene	Forward sequence	Reverse sequence
IL1β	TGGGATCCTCTCCAGCCAAGC	AGCCCTTCATCTTTTGGGGTCCG
KC (CXCL1)	GCT GGG ATT CAC CTC AAG AA	CTT GGG GAC ACC TTT TAG CA
CXCL15	AAGGAAGTGATAGCAGTCCCAAA	GCCAACAGTAGCCTTCACCC
TNF	TCTGTCTACTGAACTTCGGGGTGA	TTGTCTTTGAGATCCATGCCGTT
Marco	GCACTGCTGCTGATTCAAGTTC	AGTTGCTCCTGGCTGGTATG
Hprt	AGGCCAGACTTTGTTGGATTTGAA	CAACTTGCGCTCATCTTAGGCTTT
Serpina1A	GTGGTCGAAGCGCAGGATA	CTCCACCAGCTTCAGGTCAT
Serpina1B	CCTGAAGCTCAGCCAGGCT	CTCCACCAGCTTCAGGTCAT
Serpina1A-E	CCCTGAAGCTCAGCAAGGC	CTCCACCAGCTTCAGGTCAT

Histology

The lung lobe used in histology was first perfused via heart puncture with needle/syringe (5 mL syringe, injected very slowly at a constant rate, with no greater than 5 mL of solution, until lung lobe turned pale white) with 0.9% NaCl solution. Formalin, 0.5 mL 10% Formalin, was then supplied to the lung lobe via injection from the hole in trachea, to inflate the lung. The trachea was then tied off to ensure the lung lobe remained inflated, and both lung lobe and trachea were removed. This lung lobe along with a liver lobe sample were collected fresh and stored in 10% Formalin for 2 days, after which the trachea and connecting tissue was removed and discarded, and the inflated lung lobe and liver lobe were stored in 70% ethanol (EtOH). Samples are then paraffinized in wax, that is lung and liver sections were placed in a cassette in 75% ethanol and placed into the processor (Leica HistoCore PEARL) and washed with 70% EtOH (x3), 80% EtOH, 95% EtOH, 100% EtOH (x3), xylene (x3) and paraffin (x3). The sample was then embedded (using Leica HistoCore ArcadiaH). To section, the samples are first cooled on the HistoCore Arcadia C cold plate, then sections of 3.5 microns were cut using the Leica RM2125 RTS microtome and placed on a glass slide (Livingstone 76.2 x 25.4 mm, thickness 1.0-1.2 mm).

Immunohistochemistry (IHC)

Sections were deparaffinised and rehydrated (heat (15 mins) then xylene (x2), then gradient of 100-50% ethanol (EtOH) i.e. 100% EtOH (x2), 95% EtOH, 75% EtOH, 50% EtOH with each wash 3 mins long).

Slides then underwent antigen retrieval where they were submerged in sodium citrate buffer (ph-6.0) in a steamer (95-100^{o}C, 20 mins). Slide wash step (all wash steps in Tris-buffered saline (TBS) plus 0.025% Triton X-100 with gentle agitation) twice followed by blocking step (5% BSA, 1h, room temperature) and primary antibody staining (4^{o}C overnight). Primary antibody used was A1AT Antibody (ab231093) stained 1:2000 and secondary antibody used was goat pAb to Rb IgG (ab205718) stained 1:4000 which were both obtained from abcam and made up in 5% BSA in TBS. Slides underwent wash step twice then stained with secondary antibody (1h room temperature) after which a further 3 wash steps with TBS were performed before staining with DAB stain as per kit instructions (40 µL, 5 mins). Slides were rinsed with water (2 x 3 mins) and stained with haematoxylin (3 mins) then rinsed (2 x 3 mins water) and dehydrated (gradient of 50-100% ethanol – 50, 75, 90, 100%, then xylene, 3 mins each). Slides were mounted with Entellan®new (Millipore) mounting medium and cover slipped (Series 1 No.1 Coverslips Trajan 24 mm x 50 mm). Images were taken on Zeiss AXIO Microscope (using Zen pro software) at 40x magnification with 20.769 ms exposure time and exported as tiff images. Image analysis was conducted on ImageJ. For IHC, the specifications for analysis were: colour deconvolution 1, threshold 150, channel 2 (brown H DAB stain), to calculate the area of A1AT which was then converted to % A1AT by equation 2.2.

$$\frac{Area\ A1AT}{Total\ Area} \times 100 = \%\ A1AT \qquad (2.2)$$

Equation 2.2: Area A1AT is the total stained area from DAB stain measured in pixels on a single image and total area is the total number of pixels present in the image (6076416 pixels).

Sirius Red Staining

The Sirius Red Staining used throughout this thesis was a picro-sirius stain with the addition of 0.1% fast green FCF to the solution and was made with Sirius Red F3B (CI35782) (0.5g), fast green FCF (0.5g) (F7252-5G, Sigma Aldrich) and saturated aqueous picric acid (500ml) (P6744-1GA, Sigma Aldrich (Merck)).

Weigerts Haematoxolyin was made and used on the day and was made by mixing equal parts of two solutions, solution A (150ml) and solution B (150ml) to make up a total of 300ml. Solution A is made with Haematoxylin dye (1g) (ADH.100G, Australian Biostain) dissolved in absolute alcohol (100ml). Solution B is made with 29% ferric chloride (29g in 100ml dH2O, 4ml) (157740-1KG, Sigma Aldrich (Merck)), dH_2O (95ml) and 32%M HCl (1ml).

Following standard histology preparation, the sections were deparaffinised and rehydrated with heat (20 mins) then xylene (x2), 100% EtOH (x2), and H_2O (x1), with each wash 5 mins long. The sections were then stained with Weigerts Haematoxolyin (8 mins) followed by a wash in H_2O (10 mins) and then stained in Picro Sirius (1 h). Following the Picro Sirius stain the samples are dipped 4 times in each, acidified water (10ml glacial acetic acid made up to 2 L in MilliQ H_2O) (x2), tap water (x1). Samples were left to dry completely (1 h) and mounted with Entellan®new (Millipore) mounting medium and cover slipped (Series 1 No.1 Coverslips Trajan 24 mm x 50 mm).

Collagen Deposition Around Small Airways

Collagen deposition was measured by histological analysis of Sirius Red stained lung sections. Images (6-8 images of small airways) were taken on Zeiss AXIO Microscope (using Zen pro software) at 40x magnification with 20 ms exposure time and exported as tiff images. Image analysis was conducted on ImageJ. For collagen deposition, the inner and outer perimeter of the red stained collagen around the airway was traced with the polygonal tool and copied to the colour deconvoluted image: Sirius red + fast green, and measured at threshold 180, channel 1 (red channel). Collagen was measured using equation 2.3.

$$\frac{Outer\ Area\ (\mu m) - Inner\ Area\ (\mu m)}{Inner\ Perimeter\ (\mu m^2)} = Collagen\ (\mu m) \quad (2.3)$$

Equation 2.3: Calculation of Collagen deposition in the airway measured in µm where inner perimeter was obtained by tracing the inner side of the collagen (the visible red stain around the airway). The inner area was measured as per the inner perimeter and the outer area was obtained by tracing the outer side of the collagen.

Epithelial Thickness

Epithelial thickness was measured by histological analysis of Sirius Red stained lung sections. Images (6-8 images of small airways) were taken of Sirius Red stained slides on Zeiss AXIO Microscope (using Zen pro software) at 40x magnification with 20 ms exposure time and exported as tiff images. Image analysis was conducted on ImageJ. Epithelial thickness was calculated using equation 2.4, by measuring the inner and outer perimeter of the green stained airway epithelium (with the polygonal tool), to find the perimeters and areas.

$$\frac{Outer\ Area\ (\mu m) - Inner\ Area\ (\mu m)}{Inner\ Perimeter\ (\mu m^2)} = Epithelial\ Thickness\ (\mu m) \quad (2.4)$$

Equation 2.4: Calculation of Epithelial Thickness measured in µm where inner perimeter was obtained by tracing the inner side of the epithelium (the visible green stain of the airway). The inner area was measured as per the inner perimeter and the outer area was obtained by tracing the outer side of the epithelium (near the visible red stain of the collagen).

Haematoxylin and Eosin

First stock and working solutions of Gill's haematoxylin and of eosin were made. Gill's haematoxylin No. 3 was made by first dissolving 4g of haematoxylin (anhydrous certified haematoxylin) and 110g of aluminium sulphate.16H_2O (aluminium sulphate 16 hydrate hexadecahydrate, CAS No.16828-11-8, FSBA/2520/61, Thermo Fisher) in 500 mL of hot H_2O. 750 mL of ethylene glycol was added and then made up to volume of 2 L with H_2O, and then 50 mL of glacial acetic acid was then added and mixed well. Separately, 1 g of sodium iodate was dissolved in 450 mL of H_2O, vortexed on high, and added down the side of the of the container and mixed well. After at least 2 days, the solution was filtered and strained.

Eosin stock was made, per 100 mL of stock, 1 g of Eosin Y Certified (eosin gelblich) (ADEY.100GM, Australian Biostain) dissolved in 20 mL of dH_2O after which 80 mL of 95% EtOH is added. For working stock, 50 mL of Eosin stock solution, 120 mL of absolute alcohol, 30 mL dH_2O and 1 mL glacial acetic acid are combined.

Following standard histology preparation, the sections were deparaffinised and rehydrated with heat (20 mins) then xylene (x2), 100% EtOH (x2), and H_2O (x1), with each wash 5 mins long. Sections were then stained in Gill's Haematoxylin (1 min), wash in dH_2O (3 mins), Eosin (4 mins), then 100% Ethanol (x3) for 1 s each and finally in xylene (4 mins). Before being left to dry completely (1 h) and mounted with Entellan®new (Millipore) mounting medium and cover slipped (Series 1 No.1 Coverslips Trajan 24 mm x 50 mm).

Mean Linear Intercept (MLI)

Images were taken on haemotoxolin and eosin stained slides using a Zeiss AXIO Microscope (using Zen pro software) at 40x magnification with 20 ms exposure time and exported as jpeg images. 90-110 images were taken at random (randomised on Zen pro software) and images of the parenchyma were selected while images with blood vessels, excessive blood cells, airways, or images that were cut off were

immediately excluded. From the remaining images, 10 were selected and image analysis then conducted.

A standard grid (of 11 lines running horizontally across with a total length of 3435.85 µm) was then burnt/overlayed over the selected images, and the number of intercepts of the parenchyma with the grid were counted on imageJ. To obtain the mean linear intercept (MLI) equation 2.5 was used and an average of these 10 images is taken.

$$\frac{\#\ Intercepts}{Total\ length\ of\ grid\ lines\ (\mu m)} = MLI\ (\mu m) \tag{2.5}$$

Equation 2.5: Calculation of MLI measured in µm where # intercepts is the number of times the standard grid and the lung parenchyma intercepted, and the total length of grid lines is the total length (horizontally) of the 11 lines of the standard grid, which totals to 3435.85 µm.

Parenchymal inflammation

The images used for MLI analysis were further analysed for parenchymal inflammation. All visible leukocytes (identified by morphology) were counted in each image. The average count of 10 images was used to calculate the score for each individual mouse. The count is presented as cells/field of view, where the field of view is 78,278 μm^2.

Flow cytometry

Lung Collection

Flow cytometry was run on lung tissue and blood. At the time of mouse endpoint, blood was first collected by cardiac puncture and left in EDTA coated tube till the time for processing. BALF was then collected from lungs, as per BALF methods section for flow cytometry (Chapter 6, Aim 4), and then the whole lung was perfused via cardiac puncture with a continuous steady state flow of PBS, till lung appeared white (as white as possible), and PBS leaving the mouse did not visibly show blood. The multilobes were cut off and superior, middle and inferior lung lobes were collected and placed into a C tube containing 4.7 mL of HEPES buffer and kept on ice till processing.

Isolation of Lung Immune Cells (lung processing)

To the lungs (in the C tube) Collagenase D (100 µL of 100 mg/ µL) and DNase I (50 µL of 20,000 U/mL) were added and homogenised in the GentleMACS™ Octo Dissociator (MACS Miltenyi Biotec) for 7 seconds at 297 rpr. Samples were then incubated for 30 mins at room temperature (21-23°C) on a larger rocker at 150 rpm. Samples were again homogenised in the GentleMACS™ Octo Dissociator for 37 s at 2079 rpr and then centrifuged for 3 mins at 300g. They were then filtered (70 µm filter) then rinsed with 5 mL HEPES buffer, and filtered again, and finally centrifuged at 4°C for 5 mins at 300 g. The supernatant was then discarded and the sample placed on ice and 1 mL of eBioscience™ 1X RBC Lysis Buffer added, then 4 mL FACs buffer (FACs buffer is made up of 1% BSA, 2 mM EDTA in PBS) added 5 mins later to neutralise the reaction, before centrifuged (4°C for 5 mins at 300 g). The supernatant was again discarded and 500 µL FACS buffer added to the remaining cells.

The lung cells were then counted on a haemocytometer. An aliquot (10 µL) was taken from each sample and diluted 1:20 in FACS buffer (190 µL), and then diluted a further 1:10 in FACS (90 µL). An aliquot of 10 µL was taken and diluted with 10 µL of trypan blue. Live cells were counted on a haemocytometer (10 µL), and additional FACS buffer added to ensure that the number of cells per sample were relatively consistent. That is in 200 µL of sample there were 4 million cells, for the 4 week model, and 1.8 million cells, for the 8 week model.

Isolation of Blood Immune Cells

From the blood collected, 100 µL is taken and placed on ice, to which 7 mL of eBioscience™ 1X RBC Lysis Buffer added and then neutralised after 7 mins with 7.5 mL of FACS buffer. The samples are centrifuged for 7 mins at 350 g before the supernatant is discarded and then blood cells resuspended in 200 µL of FACS buffer.

Isolation of Bronchoalveolar Immune Cells

BALF was collected and centrifuged at 300 g at 4°C for 5 mins and the supernatant was collected and stored at -80°C. To the remaining sample (pellet), 250 µL RBC lysis buffer was added and left on ice for 5 mins, after which 1 mL of cRPMI (complete RPMI) medium was added to neutralise the reaction. cRPMI medium was made with

RPMI 1640 supplemented with 10% foetal bovine serum (FBS), 100 U/ml β-mercaptoethanol (2ME), 100 U/ml penicillin and 100 µg/ml streptomycin. The sample was centrifuged at 300 g at 4°C for 5 mins and the supernatant discarded. The cells were then resuspended with 220 µL cRPMI. From this 200 µL was used for flow cytometry and 10 µL for cell counting.

Staining for Fluorophore-conjugated Cell Markers

Table 2.4: Fluorophore-conjugated Cell Markers used in flow cytometry in Chapter 4, Aim 2, (WT and KO mice received 4 and 8 weeks of Air/CS).

Table shows, the Cell marker, and fluorophore used with dilutions of each fluorophore.

Cell marker	**Fluorochrome/ Fluorophore**	**Dilution factor**
Live Dead	Near infra-red	1/800
CD45	BV786	1/400
F4/80	BV605	1/200
CD11b	BUV395	1/200
CD11c	BV480	1/200
Ly6G	APC	1/200
Ly6C	PerCP-Ly5.5	1/200
CD4	BV711	1/400
CD8a	PE-Cy7	1/200
CD19	FITC	1/400
SiglecF	BV421	1/400
MHCII	AF700	1/400
CD115	PE	1/200

Table 2.5: Fluorophore-conjugated Cell Markers used in flow cytometry in Chapter 6, Aim 4, for lung, blood and BALF cells.

Table shows, the Cell marker, and fluorophore used with dilutions of each fluorophore.

Cell marker	**Fluorochrome/ Fluorophore**	**Dilution factor**
Live Dead	Blue UV	1/800
CD45	BUV395	1/400
TCRb	BUV661	1/200
CD4	PerCP	1/200
CD8a	BUV805	1/200
CD19	APC/Fire750	1/200
F4/80	BUV737	1/100
CD11b	BV650	1/400
CD11c	FITC	1/200
Ly6G	BV711	1/200
Ly6C	PE-Cy7	1/200
SiglecF	AF647	1/400
MHCII	AF700	1/400

Table 2.6: Fluorophore-conjugated cell markers used in flow cytometry in Chapter 6, Aim 4, for BMDCs.

Table shows, the Cell marker, and fluorophore used with dilutions of each fluorophore.

Cell marker	**Fluorochrome/ Fluorophore**	**Dilution factor**
Live Dead	Blue UV	1/800
CD45	BUV395	1/400
CD11c	FITC	1/200
MHCII	AF700	1/400
Ly6C	PE-Cy7	1/200
CD103	BV786	1/200
F4/80	BUV737	1/100
CD172	PerCP Cy5.5	1/200
XCR1	Spark Blue 574	1/200
CCR7	RB780	1/200

The following samples (lung, blood, BALF and BMDC) and control stains were: sample, unstained sample, single stained (that is with just one fluorescent antibody), FMOs (Fluorophore minus one, for lung, blood, and BALF), single stain on beads, and unstained beads.

To some samples additional FACs was added to aid processing. The plate was spun at 300g for 5 mins and supernatant removed. The cells were resuspended in 100 µL of either live dead and Fc block (BD Pharmingen ™ – Purified Rat Anti-Mouse CD16/CD32, Mouse BD Fc Block ™) or just Fc block, before being incubated in the dark for 20 mins, after which 50 µL FACS is added and the plate centrifuged at 300g for 5 mins and supernatant removed.

For the single stain on beads BD™ CompBeads negative control and BD™ CompBeads Anti-Rat and Anti-Hamster Ig κ, were combined in equal parts and 100

µL and added to each well. To each well 50 µL FACS was added and the plate centrifuged at 300 g for 5 mins and supernatant removed.

Both cells and beads were then resuspended in 100 µL in their appropriate stains that is FMOs, single stain, unstained, etc. The plate was again incubated in the dark for 20 mins and 50 µL of FACS was added to each sample. The plate was centrifuged for 5 mins at 300 g and the supernatant removed, and then the samples were fixed in 150 µL of 4% PFA, and incubated in the dark for 15 mins. The plate was centrifuged again (300g for 5 mins), the supernatant removed and the cells resuspended in FACS.

Flow Cytometric Analysis

The experiment was run on a Cytek™ Aurora 5L (5 laser). The controls used were the single stain on the beads and this was set as a positive control for each fluorophore. Flow cytometry results were analysed as per Figure 2.2.

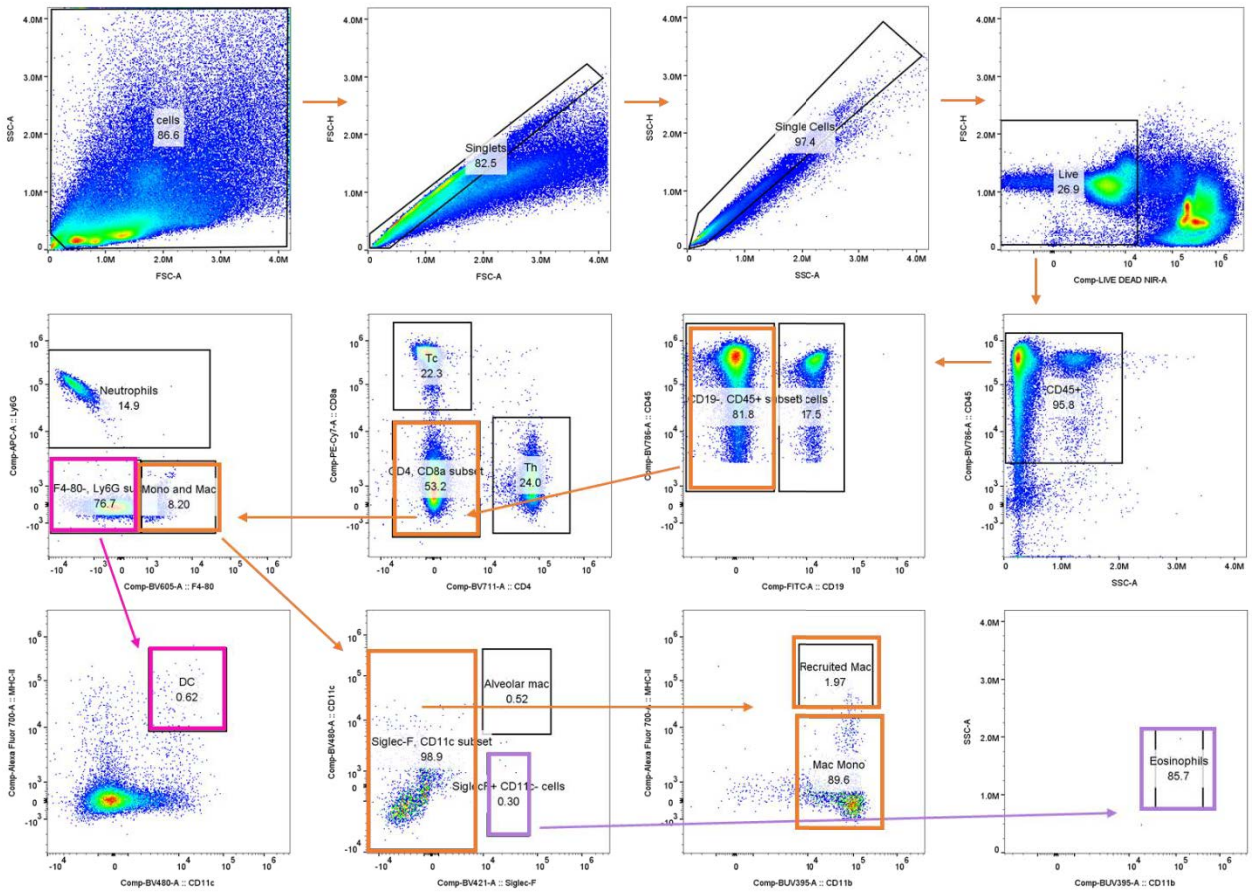

Figure 2.2: Gating strategy of flow cytometry samples for Chapter 4 Aim 2.

Both A1AT KO and WT mice were exposed to air/CS for 4 and 8 weeks. Both lung and blood samples from this model were analysed using this gating strategy. N=5-6 for each sample.

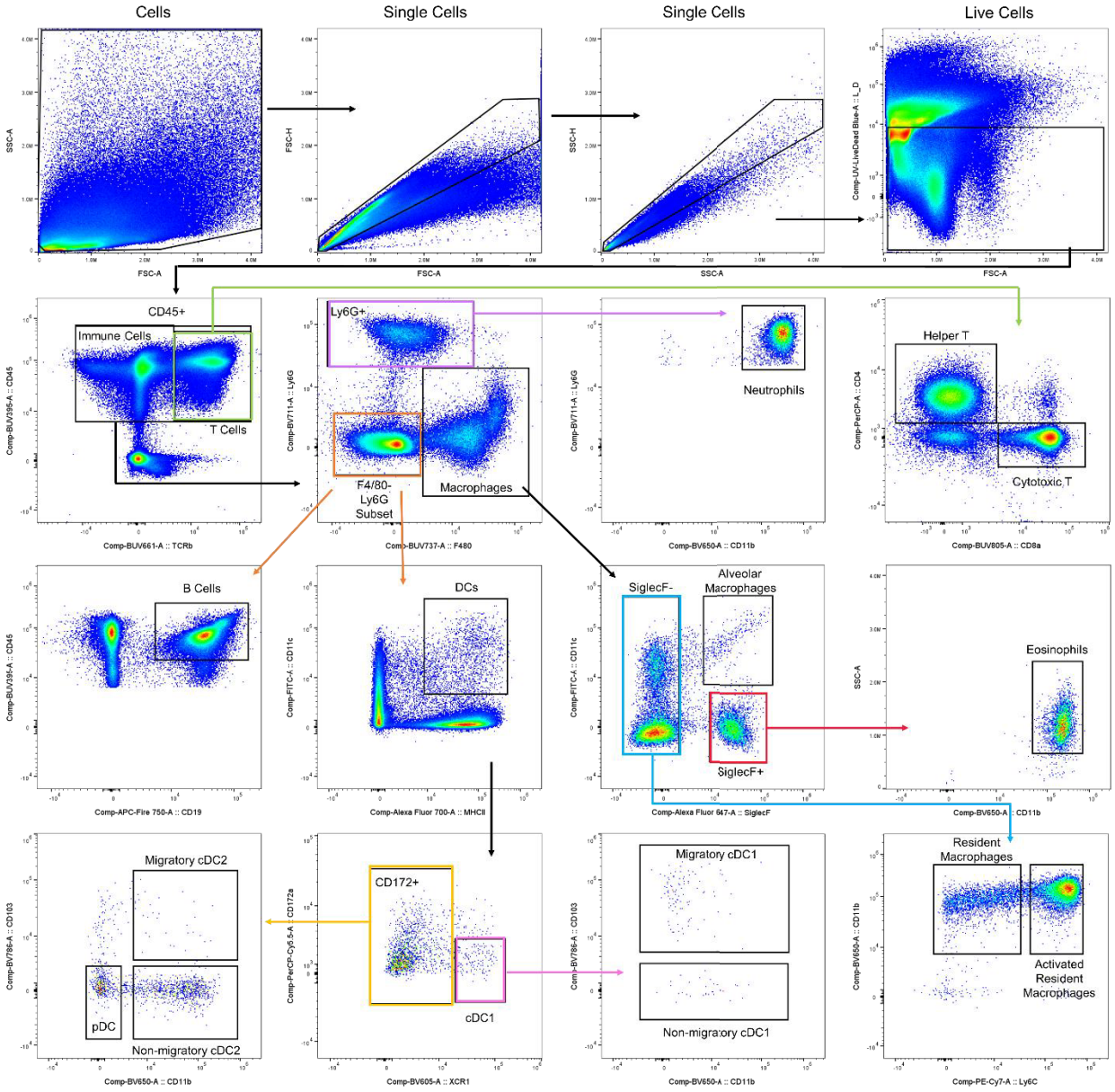

Figure 2.3: Gating strategy of flow cytometry samples for Chapter 6, Aim 4.

A1AT KO and WT mice were exposed to air/CS for 8 weeks, after which mice were end pointed. Lung, BALF and blood were collected and processed for flow cytometry were analysed using this gating strategy. Note: blood and BALF do not have as many

Macrophage and DC gates, and blood samples have a circulating macrophages gate (not resident macrophages). N=8 for each sample.

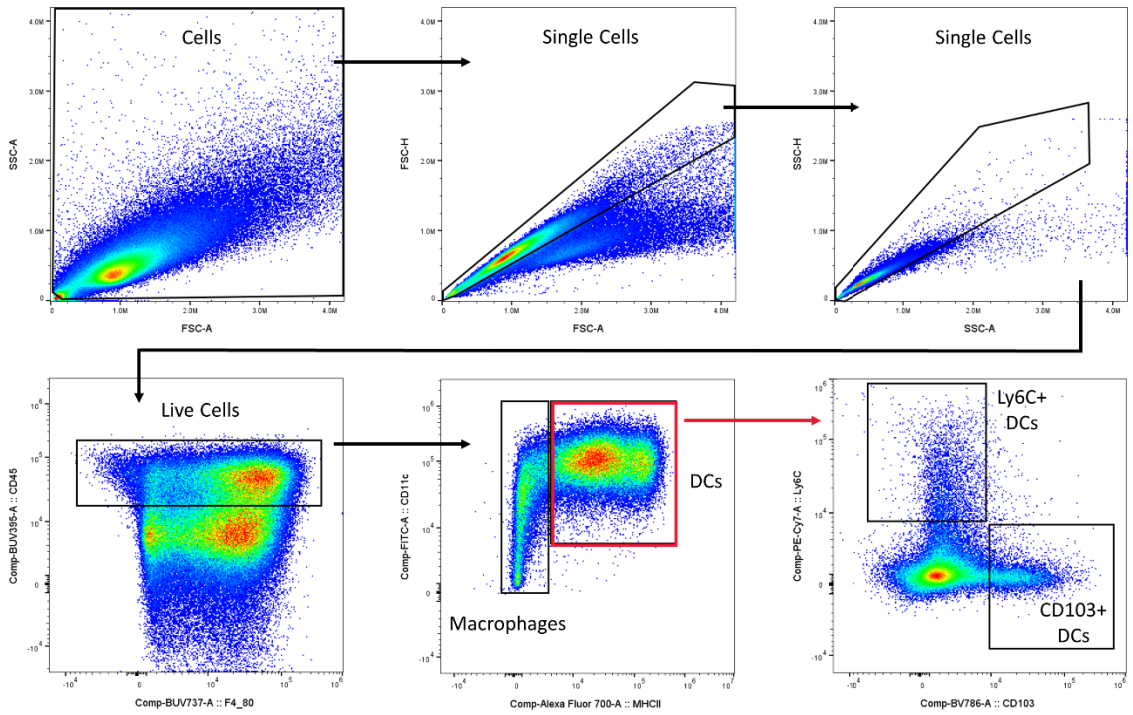

Figure 2.4: Gating strategy of flow cytometry samples for Chapter 6, Aim 4, BMDC experiment, cells are pre stimulation and pre migration assay.

BMDCs were analysed using this gating strategy. N=8 for each sample.

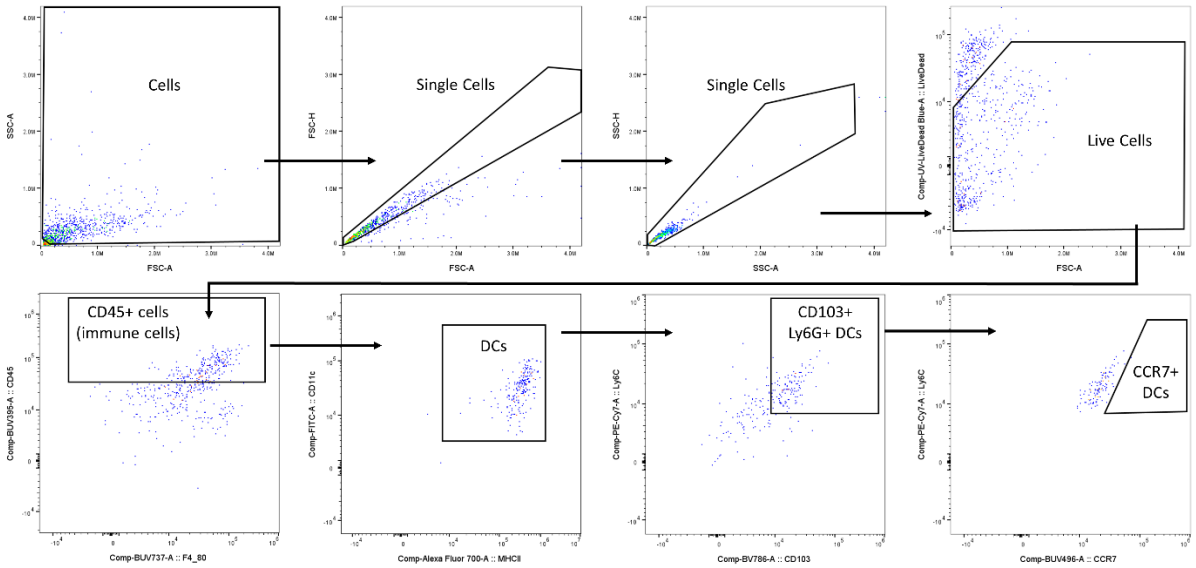

Figure 2.5: Gating strategy of flow cytometry samples for Chapter 6, Aim 4, BMDC experiment, cells are post stimulation and post migration.

BMDCs were analysed using this gating strategy. N=3-4 for each sample.

Bone marrow derived dendritic cells (BMDC)

BMDC methods were based off of two main protocols, Abcam[107] and STAR protocols[108] BMDC isolation protocols.

Bone Marrow Harvest

For each mouse, four leg bones, two tibias and two femurs were collected into a 50 mL falcon tube containing 20 mL hanks buffer. Leg muscle and tissue was carefully removed from the bone and both ends of the bone cut to expose the bone marrow. The bone marrow was flushed out into a clean 50 mL falcon tube using a 26G needle and 10 mL of Hanks buffer. All four bones of the same mouse were flushed into the same 50 mL tube, which were agitated by pipetting up and down gently, to minimise clumps. The cells were filtered into a clean 50 mL falcon tube using a 70 µm strainer, with an additional 10 mL of Hanks buffer added from rinsing the previous falcon tube. The cells were centrifuges at 300 g for 5 mins at room temperature, after which the supernatant was removed. The cells then underwent RBC lysis where they were resuspended in 2 mL RBC lysis buffer, incubated on ice for 5 mins, and quenched by adding 10 mL cRPMI. The cells were again centrifuged at room temperature at 300 g for 5 mins. The supernatant was again removed, and the pellet resuspended in 1 mL cRPMI. From this 10 µL was used for cell counting and the rest was plated.

Cells were counted on a haemocytometer using trypan blue in order to plate 2.4×10^6 cells seeded per well of a 6 well plate. Each mouse had a slightly different total cell yield and hence 1-2 6 well plates were used per mouse. To each well, 2-3 mL of cRPMI + GM-CSF (20 ng/mL) was added. Plates were then placed in an incubator at 37^{o}C with 5% CO_2 environment.

The medium was changed on days 2, 4 and 6 by first gently aspirating the old medium and removing it, then gently washing the cells with 2 mL of warmed (approximately 37ºC) PBS, then removing the PBS and adding 2 mL of fresh, warmed cRPMI + GM-CSF (20 ng/mL) to each well. On days 2 and 4, the old medium was centrifuged for 5 mins at 300 g, the supernatant removed, the cells rehydrated in 200 µL and divided equally among the wells for that mouse.

On day 7 the cells were collected. The old medium was very gently swirled in the plate and removed from the well (to collect dead non adherent cells). To collect the bone marrow derived dendritic cells (BMDC), and avoid collecting bone marrow derived macrophages (BMDM), the following steps were done gently to remove loosely adherent BMDCs and leave behind the majority of BMDMs on the plate. cRPMI (1 mL) was gently washed over the cells on the well, collected and re-washed over the cells, an additional 1 mL of cRPMI was added and again collected and pipetted over the cells, twice. The medium containing DCs was transferred to a 50 mL falcon tube, with one tube per mouse. The cells were centrifuged at room temperature at 300 g for 5 mins, and the supernatant discarded. The cells were resuspended in 1 mL of cRPMI and 10 µL was taken for cell counting using a haemocytometer (cells stained with trypan blue). For each mouse $5x10^5$ cells were taken for flow plating and staining and $6x10^5$ was taken for stimulation and migration assay ($6x10^5$ cells/well).

BMDC stimulation and migration (day 8)

Trans wells size 5 µm, were washed by adding 100 µL of PBS and removing after 5 mins. The following stocks of stimulation were then made: cRPMI medium (no stimulation), cRPMI medium with 1% CSE (100% CSE was made by smoking one 3R4F cigarette in 10 mL RPMI), and cRPMI medium with 100 ng LPS. Cells were placed in the upper compartment and relevant medium with stimulation added (500 µL to the lower compartment and 100 µL to the upper compartment. The trans wells were placed for 18h in an incubator at 37ºC with 5% CO_2 environment.

After 18h, the medium in the lower compartment was removed, and medium from the top compartment (50-100 µL) was collected and stored (-80ºC) for CBA. To the lower chamber 600 µL one of the following was added: RPMI, RPMI with 200 ng/mL of

CXCL19, or RPMI with 200 ng/mL of CXCL21. The trans wells/plate was incubated for 2 h at 37°C with 5% CO_2 environment. After 2 h, the cells in the upper chamber underwent LDH assay, and the cells in the lower compartment were plated and stained for flow cytometry using markers from Table 2.6.

For flow cytometry $6x10^5$ cells were seeded per well with plating and staining conducted as previously described using markers from Table 2.6.

LDH cytotoxicity assay

Promega CytoTox 96® Non-Radioactive Cytotoxic Assay was used to measure cell viability in the upper compartment of transwell post stimulation and migration.

To the upper compartment 10 µL of 10x lysis buffer was added to yield maximal LDH release and hence inferring 100% mortality. The plate was incubated at 37.5°C for 45 mins after which 50 µL media/supernatant was collected from the upper compartment and transferred to a fresh 96 well flat bottom plate. To the plate, 50 µL was added of kit negative controls (50 µL media) and positive controls (1 µL positive control in 5 mL 1%BSA in PBS). Finally, 50 µL of reagent buffer was added to each well followed by 15 mins incubation and absorbance was read at 490 nm on the BMG LABTECH POLARstar Omega microplate reader.

Cytometric Bead Array (CBA)

10 µL of either lung homogenate (1 lobe in 200 µL of PBS described previously) or cell supernatant was used. And the Cytometric Bead Array kit from BD Biosciences was used.

The stock standards were made by rehydrating with 400 µL of diluent buffer. The top standard was made by mixing 30 µL of each analyte and making up to volume (300 µL) with assay diluent. The top standard (2500 pg/mL) was then serially diluted, ½ dilution factor, 7 times to make standards.

To prep a 96-round bottom plate, 100 µL of wash buffer was added and removed. Capture bead stock was mixed by pipetting up and down at least 20 times, with 10 µL diluted beads added per well i.e. 0.2 µL of each analyte bead, made to volume with

capture bead dilution. Standards and sample were then added to the appropriate wells, and the plate incubated at room temperature, in the dark for 1 h. After which 10 µL of the mixed diluted PE detection reagent was added, made by thoroughly mixing the stock of each analyte, and taking 0.2 µL of each analyte used, and making up to 10 µL volume with diluent. The plate was then incubated at room temperature, in the dark for 2 h, after which 100 µL of 4% PFA was added to fix the cells. Samples were then run on the BD Bioscience FACSCanto-II flow cytometer.

Chapter 3 – Aim 1

Introduction

The prevalence, pathogenesis, and severity of COPD in humans and the importance and limitations of animal studies have been previously discussed in Chapter 1. Furthermore, the availability of in vivo models enables the evaluation of the entire complex living system including inflammation, targeted organs and off target effects. They are also a good indicator in assessing drug candidates, efficacy of treatments, toxicity and safety.

The importance of understanding and elucidating the complex mechanisms of how A1AT deficiency related disease develops in humans has previously been highlighted. To aid in this research, many experimental models have been established for understanding the mechanisms and for evaluating potential treatments and therapies. However, as with most animal models there are variations between the animal models and the human disease. In A1AT deficiency the Serpina1 gene present in humans varies to that in mice, which is expected. In humans, A1AT protein is expressed by a single gene (SERPINA1), however, mice have 3-5 distinct proteinase-inhibiting genes (*Serpina1a-e*) depending on the strain.[84, 97, 98]
These genes are quite similar however, only *Serpina1a* and *Serpina1b* were found to inhibit elastase, particularly neutrophil elastase, which, as mentioned earlier, is the major physiological target of human A1AT and hence will be a main target and focus of this study. Additionally, upon deletion of *Serpina1a* in mice there was a resultant embryonic lethality. *Serpina1a* and *Serpina1b* are present in all mice that have been investigated, however, much is still unknown about the mouse Serpina1 genes, and some have been investigated less than others.[84, 97, 98, 100]

There is an established experimental model of cigarette smoke (CS) induced COPD, which will be utilised in this chapter. These mice develop many characteristics of COPD, including chronic inflammation, small airway remodelling, emphysema and impaired lung function in 8 weeks[102].

This chapter aims to describe the changes, or lack thereof, that occur to the Serpina1 gene, or subsequent encoded A1AT protein, upon disease i.e. in a mouse model of COPD. Specifically, a model that exposes mice to CS via the nose and mouth only and causes changes and damage from increased inflammation, decreased lung function, and increased lung damage. These specific indicators of lung damage and COPD will be discussed in detail and will explore how A1AT is affected or effects these models. This will provide a basis for future chapters, most notably, should A1AT change upon CS exposure, would mice with less or no A1AT be expected to show different or increased indicators of disease and disease progression.

This model utilises a previously established cigarette smoke model, which mimics key hallmarks of human COPD, including increased number of leukocytes in the bronchoalveolar lavage fluid (BALF); collagen deposition around the small airways; alveolar destruction; and changes to lung volume and compliance[102].

Therefore, the aim of this chapter is to investigate how A1AT expression changes in CS-induced COPD mouse model.

Results

Serpina1 expression decreased in CS mice

To understand the effect of CS exposure in C57BL/6 (WT) mice, *Serpina1* expression was analysed after 4, 6, 8, 10 and 12 weeks of CS exposure. Gene expression was measured by qPCR of whole lung and liver homogenates from WT CS exposed mice and air controls. Specific primers for *Serpina1a, Serpina1b* were used alongside a pan-Serpina primer that amplified *Serpina1a-e* simultaneously. Expression was calculated relative to the housekeeper HPRT. CS exposure did not induce any significant differences in *Serpina1* expression in the liver at 4, 6, or 12 weeks (Figure 3.1 A-C). A slight but significant decrease in *Serpina1a* and *Serpina1b* was observed in the liver after 8 weeks of CS exposure (Figures 3.1A and3.1B respectively). In the lungs, *Serpina1* expression decreased with progressive smoke exposure. For *Serpina1a*, a significant decrease in expression was observed at both 6 and 12 weeks of CS compared to air (Figure 3.1D). For *Serpina1b*, a significant decrease in

expression was observed at 8 and 12 weeks (Figure 3.1E) and for *Serpina1a-e* a significant decrease in expression was observed at 12 weeks (Figure 3.1F).

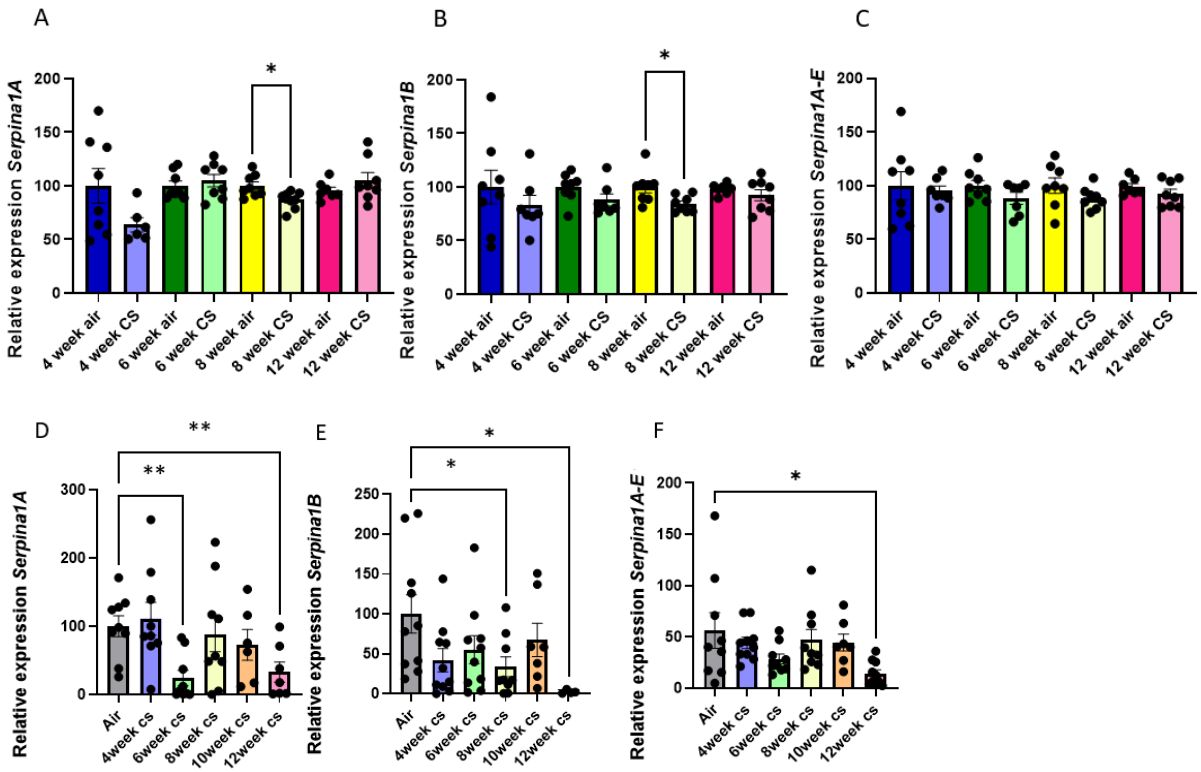

Figure 3.1: Serpina1 gene expression in mouse livers and lungs in experimental model of cigarette smoke induced COPD.

*Wild type (WT) mice were exposed to CS for up to 12 weeks, and mouse liver and lungs were collected at different time points (4, 6, 8 and 12 weeks) post CS exposure. Serpina1a (A), Serpina1b (B) and Serpina1a-e (C) in mouse livers were measured by qPCR. Serpina1a (D), Serpina1b (E) and Serpina1a-e (F) in mouse lungs were measured by qPCR. Relative expression to HPRT (housekeeping gene). N=6-9. Results are means ± SEM. * p<0.05, ** p<0.01 compared to air controls. Statistical difference was determined with unpaired two tailed t test, (95% confidence interval).*

A1AT protein increased in the lungs of CS exposed mice

To determine whether the CS induced reduction in *Serpina1* expression resulted in reduced A1AT, blood, lung and liver samples from CS mice were analysed.

A1AT ELISA was used to determine quantity of circulating A1AT from blood plasma, and from lung homogenate. Abundance of circulating A1AT was lower in CS mice and this was significant at 2 and 12 weeks of CS exposure (Figure 3.2 A-D).

Additionally, A1AT protein in blood plasma was measured, as this can indicate the amount of protein that is leaving from the liver and entering the blood stream to circulate in the body and hence to get to the lungs. This is where the lungs get the majority of A1AT protein from, however some is produced locally (in the lungs).

Analysis of lung homogenate by ELISA showed a trend of increased A1AT in WT CS mice after 8 weeks, but this was only statistically significant at 12 weeks of CS (Figure 3.2 E-H). The samples of lung homogenate were taken from lung samples that did not have BALF taken or had been perfused, hence the A1AT is a measure of lung tissue and A1AT found in the bronchoalveolar space, that includes any A1AT from inflammatory cells (e.g. macrophages). Hence, A1AT protein in lungs that have had BALF taken was also measured, removing most of these inflammatory cells. For this lung and liver histology sections were taken and stained by IHC using an antibody against A1AT (representative images in Figure 3.4). No significant differences in A1AT abundance were observed between air and CS exposed mice in the liver (Figure 3.3 A-C), matching the qPCR data on Serpina1 expression. In the lungs however, CS exposed mice had significantly increased A1AT at weeks 2, 4 and 12 (Figure 3.3 E-I).

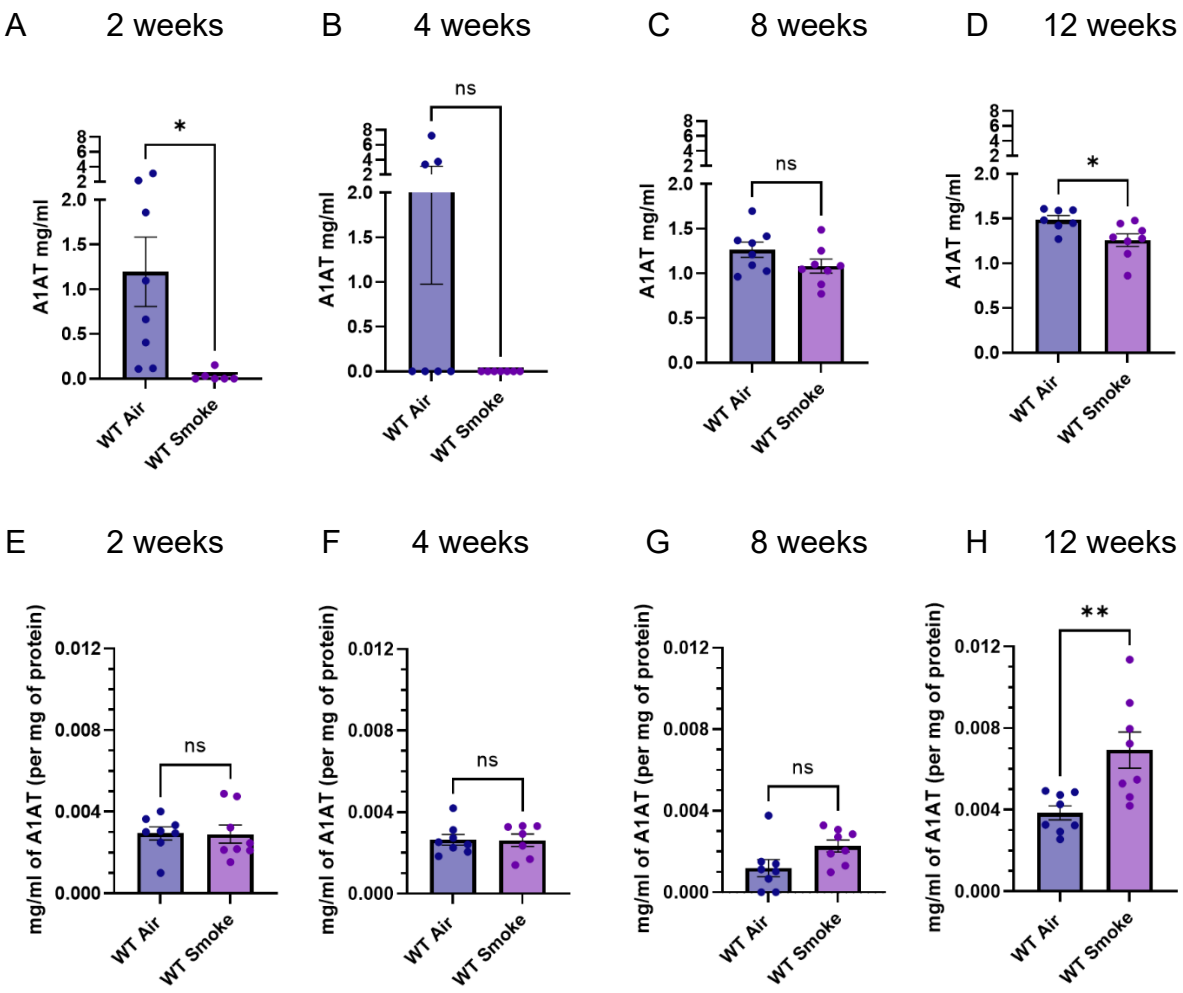

Figure 3.2: A1AT protein levels in mouse blood plasma and lung homogenates in experimental model of CS induced COPD (measured by ELISA).

*WT mice were exposed to CS up to 12 weeks, and mouse liver and lungs were collected at different time points after CS exposure. Mouse plasma A1AT protein was measured at 2 weeks (A), 4 weeks (B) 8 weeks (C) and 12 weeks (D) by A1AT ELISA assay. Similarly, mouse lung protein was measured at 2 weeks (E), 4 weeks (F) 8 weeks (G) 12 weeks (H) by A1AT ELISA assay. N=8. Results are means ± SEM. ns = p>0.05, * p<0.05, ** p<0.01, **** p<0.0001 compared to air controls. Statistical difference was determined with unpaired two tailed t test, (95% confidence interval).*

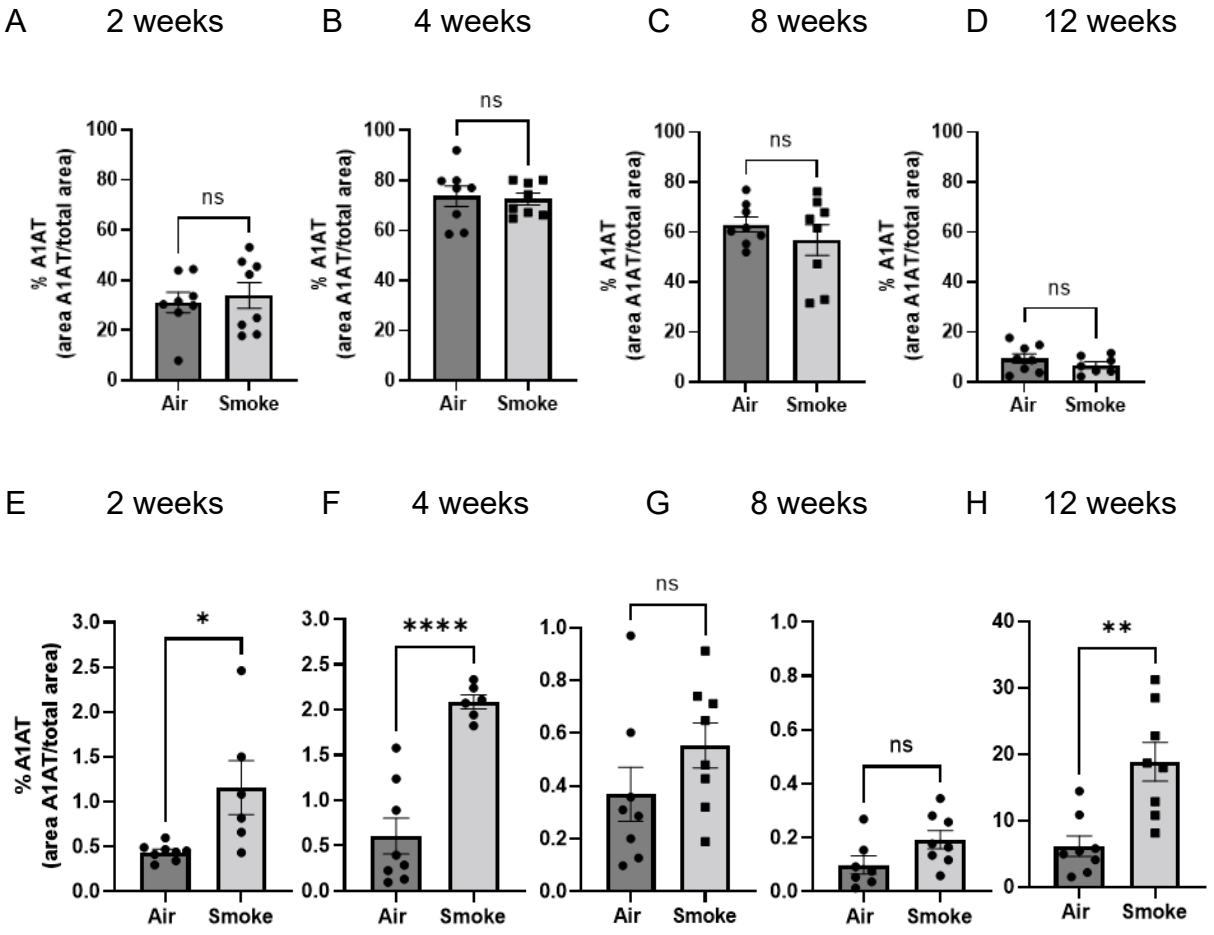

Figure 3.3: A1AT protein levels in mouse livers and lungs in experimental model of CS induced COPD (measured by IHC).

*WT mice were exposed to CS up to 12 weeks, and mouse liver and lungs were collected at different time points after CS exposure. Mouse liver A1AT protein was measured at 4 weeks (A), 6 weeks (B) 8 weeks (C) and 12 weeks (D) by IHC. Similarly, mouse lung protein was measured at 2 weeks (E), 4 weeks (F) 6 weeks (G) 8 weeks (H) and 12 weeks (I) by IHC. N=6-8. Results are means ± SEM. ns = p>0.05, * p<0.05, ** p<0.01, **** p<0.0001 compared to air controls. Statistical difference was determined with unpaired two tailed t test, (95% confidence interval).*

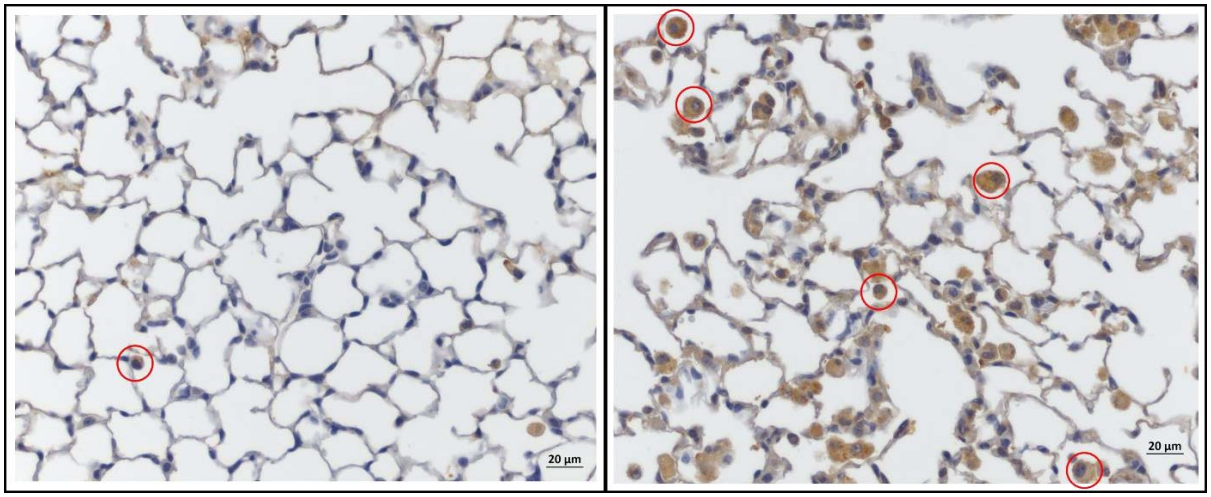

Figure 3.4: Representative image of DAB (brown) stain for A1AT protein in mouse lungs in experimental model of CS induced COPD.

WT mice were exposed to CS up to 12 weeks, and mouse lungs were collected at different time points after CS exposure. This is a representative image taken from the 4 week timepoint, and shows the WT Air sample (A) compared to the WT CS sample (B). Additionally, representative DAB stained macrophages have been highlighted (clearly shown circled in red) for easier identification showing presence of A1AT protein. It must be noted that the WT CS sample (B) had substantially more macrophages and thus only a few have been circled in red, not all of them.

Discussion

This chapter aimed to determine how cigarette smoke exposure affects A1AT expression and localisation in C57BL/6 mice. A1AT is predominantly produced in the liver to be transported around the body via the bloodstream.[71] In humans, the liver produces 70-80% of the body's A1AT.[71] It is also produced in many other cells, including bronchial epithelial cells, neutrophils, monocytes, macrophages – including alveolar macrophages, and epithelial cells[70, 71]. Additionally, in response to inflammation, neutrophils will release A1AT[109]. Therefore, the liver, lungs and blood of mice exposed to 2-12 weeks of cigarette smoke were examined. Analysis of these organs gave a representation of the following: the site at which the majority of the

protein is produced i.e. the liver; the circulation of A1AT in the blood plasma; and the site of damage i.e. the lung.

Overall, analysis of gene and protein expression in the liver indicated that there were no significant changes between air and CS, aside from the minor gene change at 8 weeks (Figure 3.1 and 3.3). A possible explanation is that exposing mice to CS via inhalation predominately affects the lung and not the liver. Alternatively, as A1AT is predominately produced in the liver[71], A1AT protein production may be increasing in the liver as a result of increased CS, but that protein is immediately exported to the lung as a protective response and hence, constant levels of A1AT protein are observed in the liver. It is also possible that the CS challenge to the mice is not sufficiently intense to activate changes in the liver.

Changes to A1AT expression in the mouse lung occurred both in gene expression and in protein levels. Gene expression, as measured via qPCR (Figure 3.1) and while some timepoints did not vary between the air and CS groups, others showed a significant decrease in CS samples. There was a significant decrease in *Serpina1a* gene expression at 6 weeks and at 12 weeks in CS compared to air. Similarly, a significant decrease was found in *Serpina1b* at 8 weeks and at 12 weeks. Mice have 3-5 distinct protease-inhibiting genes, and elastase inhibitory activity appears to be limited to *Serpina1a* and *Serpina1b*[98]. Hence, the significant decrease in *Serpina1a* or *Serpina1b* at time points 6, 8 and 12 weeks show there is a decrease in the local expression of the antiprotease gene that is shown to be protective against damage in the lung[110].

In contrast to the reduction in gene expression, the amount of A1AT protein in the lung (measured by ELISA, Figure 3.2) was significantly increased with CS exposure at 12 weeks. At first glance the lung protein amount and gene expression seem to contradict, however The Serpina1 gene has been shown in the literature to self-regulate, for example Serpina1 expression is downregulated in human hepatocytes upon treatment with A1AT[72, 92, 111].In mice exposed to smoke the circulating protein was decreased suggesting liver-produced A1AT is being taken up in the lung to act protectively due to the presence of smoke and increased inflammation and damage from the smoke. Therefore, a possible explanation for the discrepancy between the

mRNA and protein responses, as more liver-produced protein enters the lung due to increased inflammation and irritants from CS, there is less need for A1AT to be produced locally in the lung.

Interestingly, the literature has shown that the A1AT production from the monocyte specific A1AT promoter is heavily controlled by IL-6, but also by LPS, IL-1β and TNF which cause 2-3 fold increase in A1AT production by peripheral blood monocytes[72] [112]. LPS and elastase have also been shown to increase Serpina1 expression, specifically bronchoalveolar macrophages and peripheral blood monocytes[113,114].
Since increased inflammatory cells infiltration, including from monocytes and macrophages, are increased in the lungs of COPD/CS, it is highly likely that the increased A1AT protein observed in the lung results from A1AT in monocytes and macrophages. This is also highlighted visually in Figure 3.4 where significantly more A1AT positive (brown) macrophages and monocytes are depicted.

Serpina1 gene expression and regulation is affected by inflammation and the presence of A1AT. In humans it has also been shown that there are liver specific and monocyte specific promoters for A1AT.[72, 92] Additionally, in mice (including C57Bl/6 mice) there is the *Serpina1f* homologue that is liver specific, as mice can have *Serpina1a-f* genes compared to human SERPINA1 gene[98]. Hence, there may be changes in some organs but not others.
Additionally, Serpina1 gene regulation is also affected by gene transcription enhancers and repressors.[72, 92] Furthermore, regarding A1AT enhancers, promoters and gene self-regulation, there are hepatocyte (liver) and monocyte specific promoters, as well as a tissue specific enhancer, which is a specific DNA region in the A1AT gene structure that when activated leads to increased A1AT production.[72] Hence both hepatocytes and monocytes are critical cell types for A1AT production and changes in these specific regions would impact A1AT production in the liver and blood (circulation) respectively.

Interestingly, a significant increase in A1AT protein was observed at early timepoints when using IHC, but not ELISA. IHC showed a significant increase in smoke exposed mice at 2, 4 and 12 weeks, whereas ELISA only showed a significant increase at 12 weeks. The ELISA was carried out on lung homogenate of the post caval lobe, which

was not perfused, and which was not rinsed with Hanks buffer to collect BALF. In contrast IHC was carried out on a sample that had BALF collected and were perfused. This means that quantification by ELISA contains mixed results that may be confounded by the drop in blood A1AT levels, as well as any infiltrating immune cells.

The fact that A1AT is significantly increased in the lung at both early and late timepoints (2, 4, 12 weeks), but not at middle timepoints (6 and 8 weeks), suggests that the A1AT response fluctuates over the course of chronic exposure.
A1AT function works on a feedback system, such that in acute inflammation, the A1AT gene upregulates in response to inflammatory mediators, and A1AT protein works to suppress inflammatory cytokine gene expression. As a consequence, this system works quite effectively at controlling inflammation. However, in chronic inflammation and autoimmune disease this may not be the case as the upregulated A1AT can be exhausted due to chronic inflammation, while cytokines and other inflammatory molecules further increase expression of inflammatory genes, thus offsetting the effect of A1AT to inhibit cytokines.

In summary, as there were no changes in A1AT due to CS in the liver, this suggests it is still produced and present in the liver at approximately the same amounts. At first glance the protein amount and gene expression seem to contradict in the lungs, however the A1AT protein may be self-regulating. That is, as more protein enters the lung due to increased inflammation and irritants from CS, there is less need for A1AT to be produced locally in the lung. Additionally, A1AT protein in blood plasma was measured as this typically shows what protein is leaving from the liver into the blood stream where it circulates the body to get to the lung where it is protective.

In mice exposed to smoke the circulating protein was decreased, one possible explanation could be because it is being taken up in the lung to act protectively due to the presence of smoke and increased inflammation and damage from the smoke.

Conclusion

In this chapter it was shown that chronic CS exposure leads to changes in *Serpina1* expression, and fluctuating increases in A1AT in the lung. However, this does not provide an accurate account of the capability of A1AT to bind and inhibit elastases that are causing damage in the lung. The A1AT protein may be increasing as a protective response due to the increased inflammation to the lung, however in order to be protective it must be active A1AT. A1AT protein may be inactivated by the environment produced from cigarette smoke, and the relevant disease pathways. It has been suggested in the literature that A1AT is inactivated by cigarette smoke, in particular, the oxidation of methionine 358, 351, and potentially others in A1AT which decrease A1AT.[115] In order to fully understand the impact of this increased protein expression, future experiments will measure the activity of A1AT and/or elastase in these samples to confirm whether the increased A1AT in the lung is able to inhibit elastin, or otherwise change the protease/anti-protease balance. Further analysis of the activity and protectiveness of A1AT is conducted in chapters 2 and 3.

Chapter 4 – Aim 2

Introduction

Alpha-1 Antitrypsin (A1AT) deficiency is a genetic disease with at least 100 mutated alleles of A1AT (SERPINA) identified.[73] These alleles belong to one of 4 main subcategories that are characterised by function; normal, deficient, null, and dysfunctional.[90, 116] This chapter focuses on the null category, where there is an absence of detectable A1AT protein in the plasma.

Null mutations represent the extreme end of A1AT deficiency and while these alleles only encompass a small proportion of A1AT deficient patients, their impact is severe. To date there are at least 26 different null variants discovered,[117] and patients with Null mutations are considered a subgroup at particularly high risk of emphysema within the spectrum of A1AT deficiency. [90, 116] Null alleles result from different molecular mechanisms, including large gene deletions, intron mutations, nonsense mutations, frameshift mutations due to small insertions or deletions, and missense mutations associated with amino acid substitutions in potentially critical structural elements. Of the 26 known null alleles, 2 have large deletions, 5 have intron mutations, 6 have nonsense mutations, 9 have frameshift mutations, and 4 have missense mutations. [117] The one common trait considered in all null mutations is the complete absence of circulating A1AT in the blood serum. [90, 116]

Patients suspected of having an A1AT null mutation will undergo an initial evaluation which can include an evaluation of the patient's medical history and a physical examination, a liver function test, complete pulmonary function tests – spirometry and diffusing capacity of the lungs for carbon monoxide (DLCO), chest radiography (chest x-ray), and a blood serum test of circulating A1AT protein levels. If low serum levels of A1AT are detected there must be further testing not only for the severity of the deficiency but also to conclude if there are additional risks associated with that genotype[90, 116].

Smoking is an important risk factor in COPD development, particularly in A1AT null individuals.[118] For these patients, lung damage is believed to result from protease anti-protease imbalance, where the lack of A1AT to inactivate neutrophil elastase, leads to high quantities of active neutrophil elastase which along with other elastases, breaks down elastin in the lungs and causes alveolar damage and emphysema.[39] This is exacerbated when cigarette smoke induces neutrophil recruitment to the lung, increasing the total burden of neutrophil elastase. Studies on people with severe A1AT deficiency showed that even passive smoking and various occupational inhalants were found to negatively impact respiratory health, but in moderate A1AT deficiency cases this finding was not always statistically significant.[118] This highlights the severity of these more severe mutations such as the null mutation.

Interestingly, there is great variability in A1AT disease progression. Some of this variation can be explained by the severity of specific genotypes, for example a person with two copies of the null allele (Pinull/null) is more susceptible to lung damage than a person with one copy (PiMnull), or even two copies of a less severe mutation like the S mutation. Even when considering just genotype for example PiZZ (two copies of the Z mutated allele), there is still significant variation in disease progression and severity in individuals. Some patients with the exact same genotype suffer from a significantly more severe lung disease than others, even when environmental and smoking habits are consistent. This suggest that there may be other mechanisms of disease progression that are not being accounted for at this stage. [90, 116]

In addition to its role as an antiprotease, A1AT has other functions which may contribute to the pathogenesis of COPD. It can reduce free radical production and associated damage, can bind to IL-8 and LTB4 and thus reducing neutrophil migration towards inflammation, and can reduce cytokine release by neutrophils, macrophages and monocytes.[30] Finally, A1AT also affects B and T cell function as A1AT has anti-viral and anti-microbial properties. Even though the impact of neutrophils is severe in A1AT deficiency, so too are other inflammatory cells, suggesting unexplored effects and a need for further study on all inflammatory cells.[30]

It has been shown that an increased neutrophilic environment negatively correlated to baseline FEV1.[119] As COPD is characterised by chronic inflammation, airway remodelling, emphysema and impaired lung function, FEV1 is one of the most important measures in human diagnosis.[22, 23] In humans, lung function is measured using FVC (forced vital capacity) or the maximum amount of air out of the lungs in a single breath, as well as with FEV1 the (Forced expiratory volume in 1 second, that is the first one second of breathing out). If the FEV1/FVC ratio is less than 70% this indicates airflow limitation and the possibility of COPD.[23] Thus, COPD is associated with an accelerated decline in FEV1, and hence a negative correlation of baseline FEV1 with significant increases in cytokine levels, neutrophil counts and neutrophil elastase levels suggesting early instances of a neutrophil led inflammatory environment. In most instances this is a long-lasting environment that will lead to the development of lung injury prior to A1ATD lung function impairment.[119] This is not the only paper that suggests the implication of neutrophils is more than just the proposed neutrophil elastase vs A1AT, protease anti protease balance.

The overall aim of this chapter is to understand the interaction of A1AT deficiency and cigarette smoke (CS) exposure using an animal model equivalent to the human A1AT null allele, with mice that have a knock out (KO) of the A1AT gene. These A1AT KO mice have no detectable A1AT and also progress to develop emphysema at 50 weeks of age. Mice will be exposed to CS as per the established cigarette smoke model, which reflects key hallmarks of human COPD, including increased number of leukocytes in the bronchoalveolar lavage fluid (BALF); collagen deposition around the small airways; alveolar destruction; and changes to lung volume and compliance.[120]

The primary objective of this chapter is to investigate the inflammatory, structural and functional changes in A1AT KO mice across a time course of cigarette smoke exposure from early (stage 1) to very severe (stage 4) COPD. It is hypothesised that A1AT KO mice will experience accelerated and deteriorated COPD due to CS when compared with WT controls.

The secondary objective is to establish this combined A1AT null and cigarette smoke exposure model as a platform that can be used in future to test therapies for A1AT null patients.

Results

Cigarette smoke induces more severe inflammation in A1AT KO mice

A crucial hallmark of CS induced COPD is chronic inflammation. Therefore, to determine whether A1AT KO mice responded differently to cigarette smoke than WT mice, first lung inflammation was measured in both the BALF and the lung tissue with 2, 4, 8 and 12 weeks of smoke exposure.

Enumeration of leukocytes in the bronchoalveolar lavage fluid (BALF) showed that cigarette smoke exposure caused a significant increase in total leukocyte number in all groups and at all timepoints (Figure 4.1A-D). For WT mice this inflammation peaked at just below 10 x 10^4 cells/mL at 4 weeks of smoke exposure (Figure 5.3B), and reduced to 5 x 10^4 cells/mL by 12 weeks of exposure (Figure 4.1D). Interestingly, A1AT KO mice had a similar peak of inflammation (10 x 10^4 cells/mL), but this peak was delayed compared to WT mice. This resulted in significantly fewer cells that WT mice at 4 weeks (Figure 4.1B), and significantly more cells that WT at both 8 and 12 weeks (Figure 4.1C-D).

Interestingly, total leukocytes were also increased in A1AT KO CS compared to WT CS with both 8 and 12 weeks of smoke exposure (Figure 4.1C and 2D). Additionally, at the 4 week timepoint, there was an increase in total leukocytes in the WT CS mice when compared to the A1AT KO CS (Figure 4.1B).

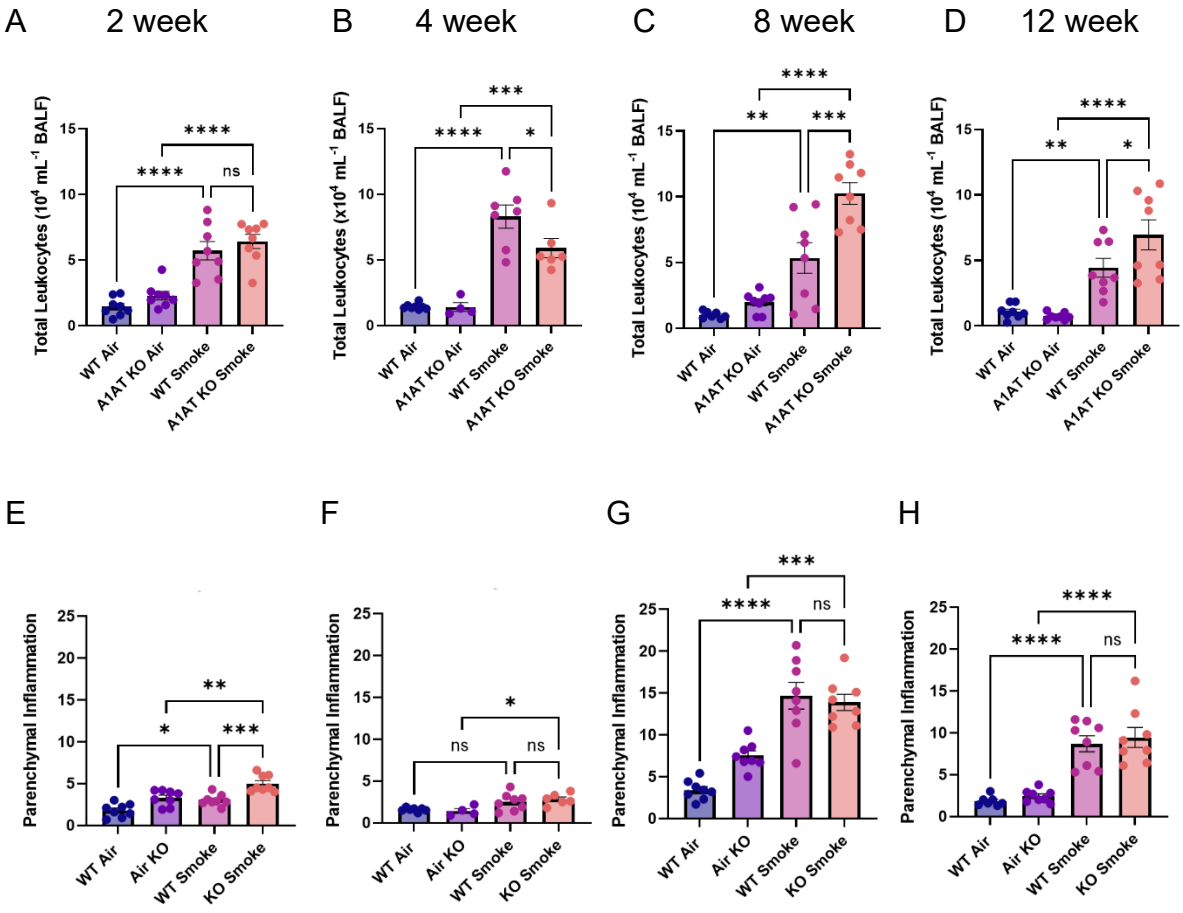

Figure 4.1: Cigarette smoke induces increased airways inflammation in A1AT KO mice.

*Measure of airway inflammation from BALF of WT and KO mice in a 12 week experimental model of CS induced COPD. Changes were observed in total leukocytes at 2 weeks (A), 4 weeks (B), 8 weeks (C) and 12 weeks (D). Parenchymal inflammation measured the number of inflammatory cells in the parenchymal space, where the field of view is 78,278 μm², measured as cells per field of view. Parenchymal inflammation was measured at 2 week (E), 4 week (F), 8 week and (G) 12 week (H) mouse model. N=8. Results are means ± SEM. ns = p>0.05, * p<0.05, ** p<0.01, *** p<0.001, **** p<0.0001. Statistical significance was determined with Ordinary One-Way ANOVA with Bonferroni's multiple comparisons.*

Parenchymal inflammation is a measure of total leukocytes in the parenchyma of the lung. Parenchymal inflammation increased due to CS in the KO mice at all four timepoints measured, for the WT mice this was significant at 2, 8, and 12 weeks

(Figure 4.1E-H). With 2 weeks of exposure, KO mice had significantly more inflammatory cells in the lung than WT (Figure 4.1E), however at all other timepoints, there was no difference between WT and KO mice. Together these results suggest that A1AT primarily affects inflammatory cell migration into the alveolar space. Thus, A1AT increases leukocyte migration into the bronchoalveolar space in the early phase of disease, and reduces migration in the chronic phase of disease.

To determine whether A1AT affects specific cell types migrating into the alveolar space, BALF cell types were enumerated by morphological analysis. A peak in inflammatory cells was observed in A1AT KO mice at 8 weeks, which was primarily driven by a significant increase in neutrophils (Figure 4.2G and H). Regarding the peak in inflammatory cells observed in WT mice at 4 weeks, macrophages are the predominant driving factor (Figure 4.2B) and neutrophils are only a small contributor to the inflammation but also not significantly different to the A1AT KO mice (Figure 4.2F).

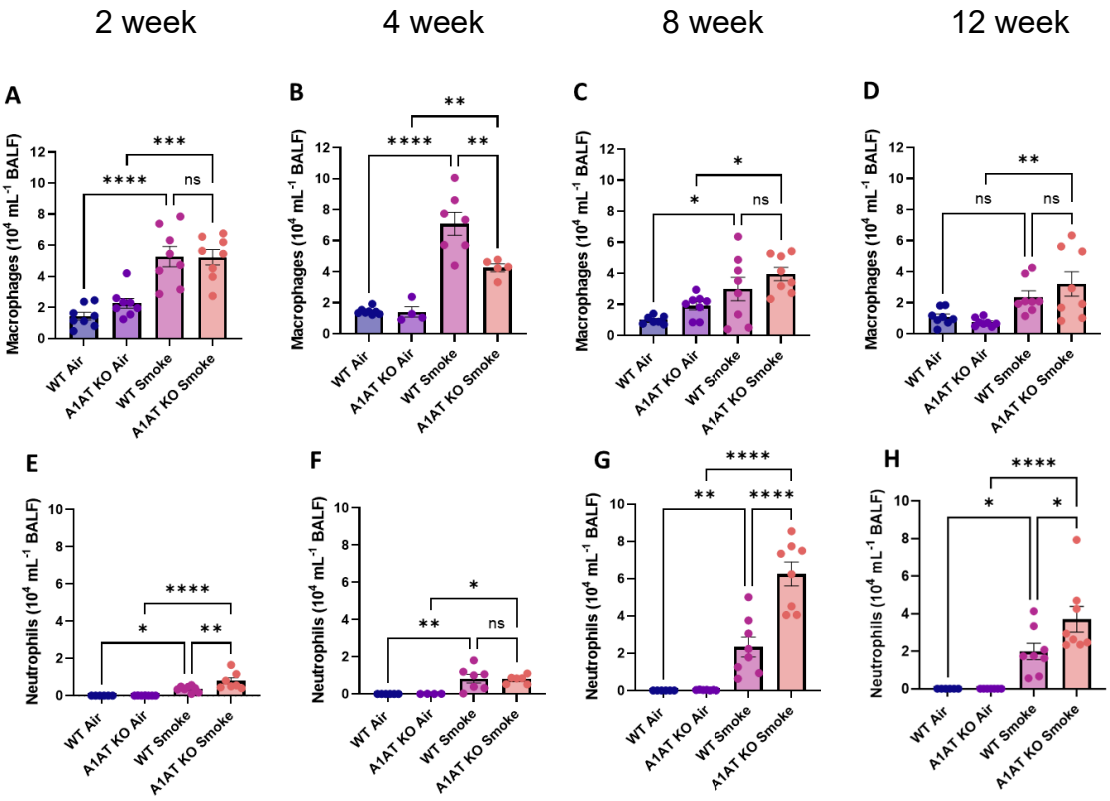

Figure 4.2: Cigarette smoke induced increased total leukocytes was primarily driven by neutrophils in A1AT KO mice. Cells differentiated from total leukocytes in the BALF of WT and KO mice in an 8 week experimental model of CS induced COPD. Changes

*were observed in macrophages (A-D), and neutrophils (E-H). Results are means ± SEM. ns = p>0.05, * p<0.05, ** p<0.01, *** p<0.001, **** p<0.0001. Statistical difference was determined with Ordinary One-Way ANOVA with Bonferroni's multiple comparisons.*

To investigate if a significant increase in neutrophils in A1AT KO mice at 8 weeks in the BALF was also reflected in the lung or in circulation, lung tissue and blood samples were analysed by flow cytometry. There was an increased proportion of neutrophils in circulation in A1AT KO mice at 4 weeks (Figure 4.3B), but interestingly no significant increase in the lung, at 4 or 8 weeks (Figure 4.3A and C).

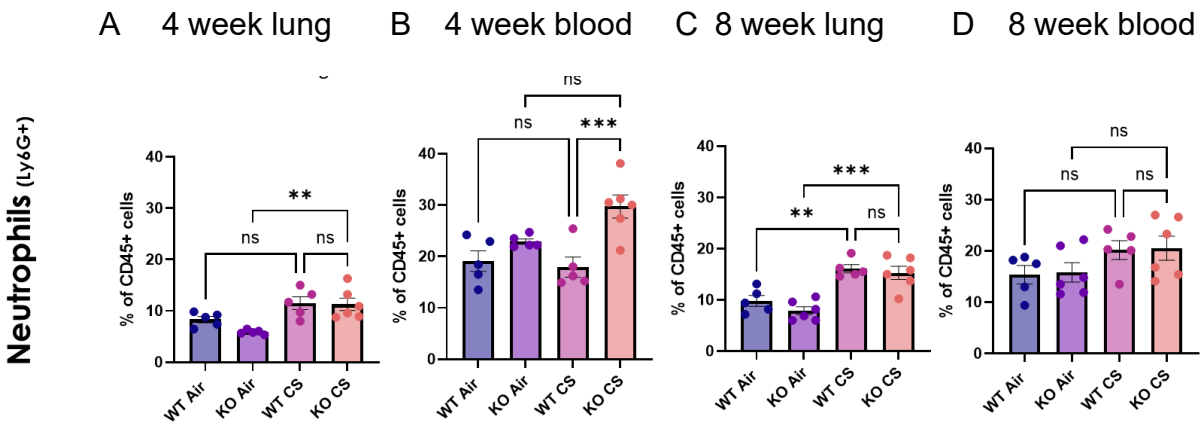

Figure 4.3: A1AT KO mice have increased Neutrophils compared to WT mice.

*Analysis of neutrophils showed an increased proportion against all CD45+ cells, in A1AT KO CS mice compared to WT CS mice. At 4 weeks in the lung (A) and blood (B), and 8 weeks in the lung (C) and blood (D). N=6 Results are mean ± SEM. ns = p>0.05, * p<0.05, ** p<0.01, *** p<0.001, **** p<0.0001. Statistical difference was determined with Ordinary One-Way ANOVA with Bonferroni's multiple comparisons.*

Another interesting finding from our initial airway inflammation findings in our BALF, was increased total alveolar macrophages in WT CS mice when compared to A1AT KO mice. Hence, it was pivotal to look at the 4 week timepoint in particular. From the

analysis of the flow cytometry findings there was an increase in recruited macrophages (both MHCII high and MHCII low) in the lung at 4 weeks (Figure 4.4 A and E) due to CS, particularly WT mice. Interestingly this same increase was also observed at 8 weeks (Figure 4.4 C and G). This is consistent with the previous findings in the BALF and suggests increased macrophages to be a driving factor in CS inflammation in WT at 4 weeks. From the flow cytometry analysis, an increase in dendritic cells due to CS was also observed in the lung at 8 weeks, and in the blood at 4 weeks (Figure 4.5).

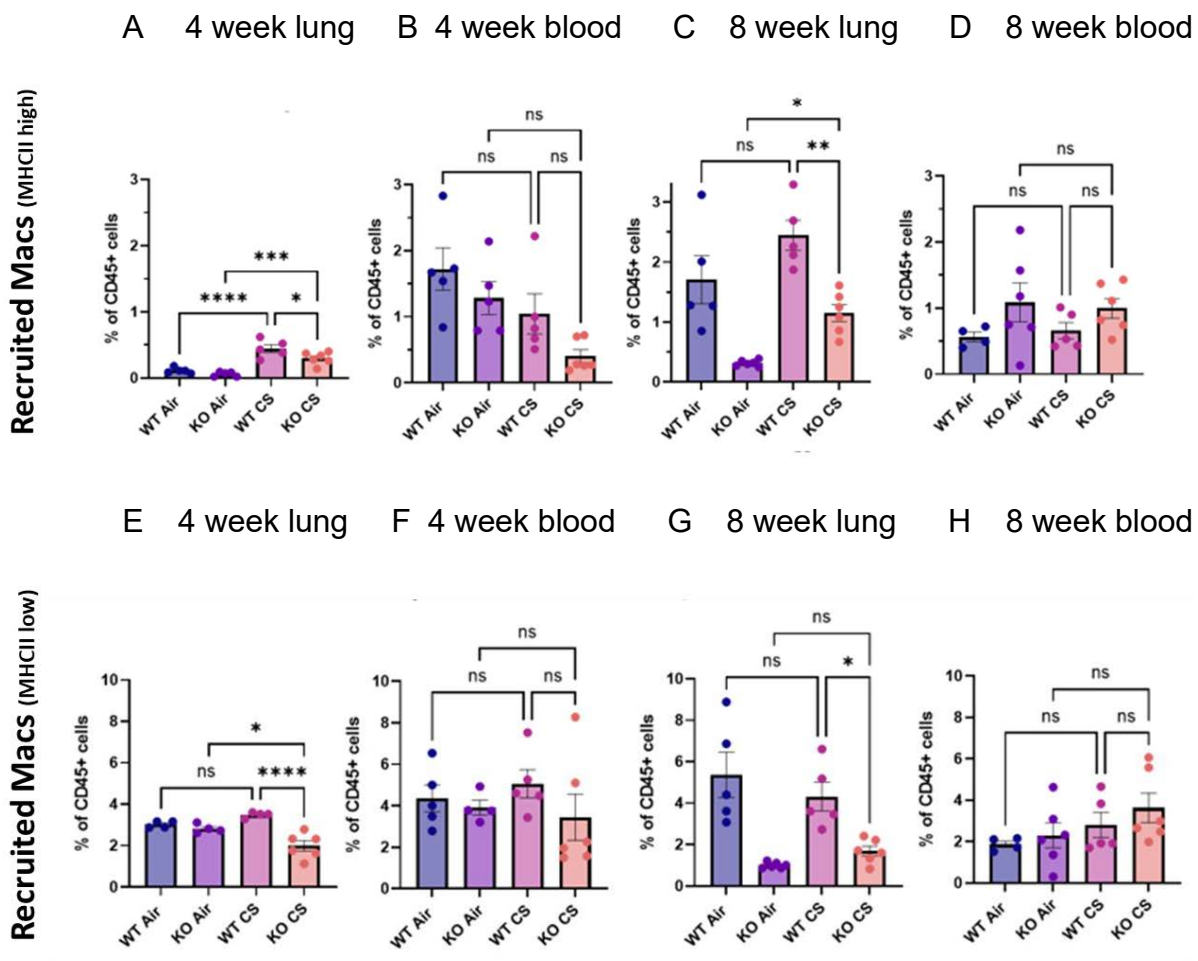

Figure 4.4: WT mice have increased Macrophages compared to A1AT KO mice.

There was an increased proportion of recruited macrophages against all CD45+ cells, in WT CS mice compared to A1AT KO CS mice. Recruited (macs) macrophages (MHCII high) at 4 weeks in the lung (A) and blood (B), and 8 weeks in the lung (C) and blood (D). Recruited (macs) macrophages (MHCII low) at 4 weeks in the lung (E) and blood (F), and 8 weeks in the lung (G) and blood (H). N=6. Results are mean ± SEM.

*ns = p>0.05, * p<0.05, ** p<0.01, *** p<0.001, **** p<0.0001. Statistical difference was determined with Ordinary One-Way ANOVA with Bonferroni's multiple comparisons.*

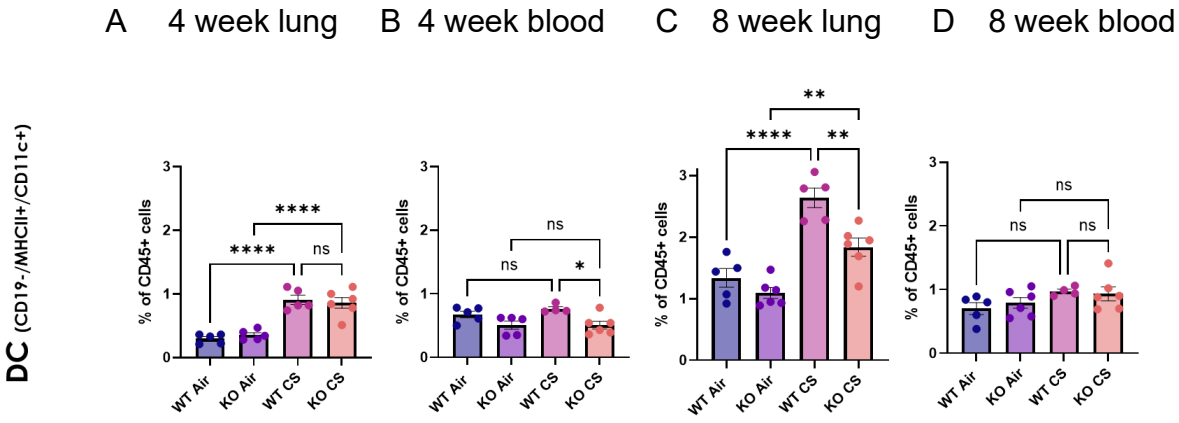

Figure 4.5: WT mice have increased Dendritic Cells compared to A1AT KO mice.

*Dendritic cells showed an increased proportion of dendritic cells against all CD45+ cells, in WT CS mice compared to A1AT KO CS mice. At 4 weeks in the lung (A) and blood (B), and 8 weeks in the lung (C) and blood (D). N=6. Results are mean ± SEM. ns = p>0.05, * p<0.05, ** p<0.01, *** p<0.001, **** p<0.0001. Statistical difference was determined with Ordinary One-Way ANOVA with Bonferroni's multiple comparisons.*

Cigarette smoke induces more severe alveolar destruction in A1AT KO mice

To investigate whether the observed increase in neutrophils in A1AT KO mice correlated with an increase in alveolar destruction, histological analysis of the lung was performed. To determine if there was alveolar damage present in this model, mean linear intercept (MLI) analysis was conducted on lung sections. In this analysis, a low number of intersections between the grid (shown in Figure 4.6) and alveolar walls, indicates fewer, larger alveolar spaces, which is consistent with alveolar destruction and emphysema. That is the distance between the alveolar walls are larger, larger 'gaps'. Conversely, if there are more intersections, it would indicate more smaller alveoli, and a smaller distance between alveoli, consistent with normal, healthy tissue. It is evident that exposure to CS significantly increased MLI in both WT and KO mice, but alveolar damage was exacerbated in KO mice, highlighting the impact of A1AT absence on damage to the lung in mice exposed to smoke (Figure 4.6).

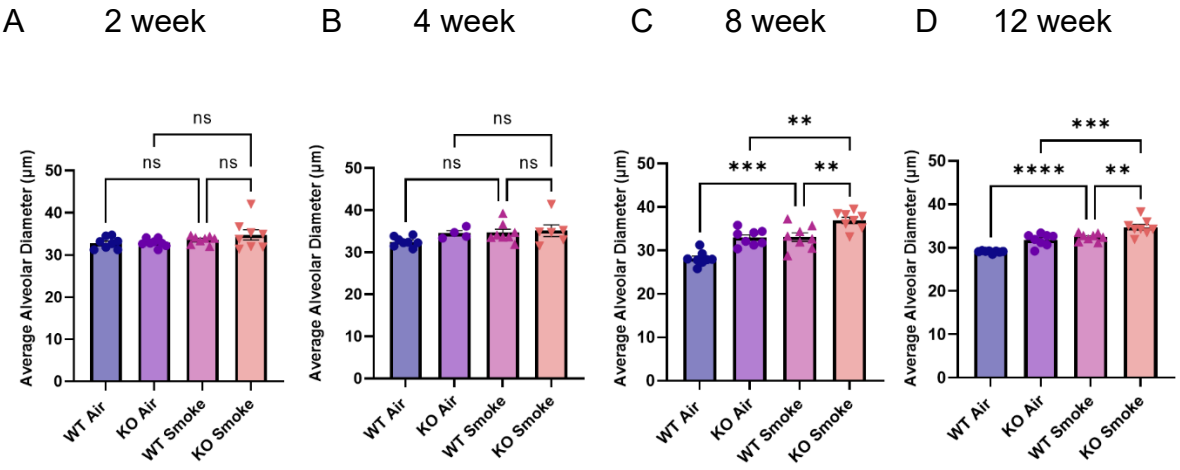

*Figure 4.6: Cigarette smoke induces increased alveolar destruction in A1AT KO mice. Increased alveolar damage in A1AT KO mice is evident by increased mean linear intercept (MLI) at 8 weeks (C) and 12 weeks (D), but not in 2 weeks (A) and 4 weeks (B). N=8. Results are means ± SEM. ns = p>0.05, * p<0.05, ** p<0.01, *** p<0.001, **** p<0.0001. Statistical difference was determined with Ordinary One-Way ANOVA with Bonferroni's multiple comparisons.*

A1AT KO does not exacerbate CS induced changes to lung function

To determine whether the increased inflammation and alveolar destruction in A1AT KO smoke mice caused more significant lung damage, lung function was assessed by plethysmography, using a Flexivent system. Additionally, with increased alveolar destruction observed in the MLI results, it is expected this would translate to increased lung volume. Lung function measures a variety of parameters pertaining to damage of the lung. Two measures of lung volume are total lung capacity (TLC) and forced vital capacity (FVC). TLC and FVC both show increased lung volume in mice exposed to smoke (Figure 4.7), hence increased damage. However, they did not show an increase in lung volume in A1AT KO mice compared to WT (Figure 4.7). This shows that there are structural changes in A1AT KO mice, however this did not translate into deteriorated lung function.

There are additional lung function parameters that are measured, in particular changes to lung compliance. Measures of compliance include dynamic compliance, resistance and elastance. Changes to dynamic compliance, resistance, and elastance remained unchanged in WT and in A1AT KO mice until the 12 week timepoint (Figure 4.8 H). At

12 weeks of CS dynamic compliance was lower in the A1AT KO CS mice compared to the A1AT KO air mice (Figure 4.8 L). In addition, elastance, which is considered the reciprocal of compliance, was significantly higher in the KO CS mice at this time (Figure 4.8). Resistance, a measure of the level of constriction in the lungs increased in KO mice upon CS exposure after 12 weeks, both when compared to air and interestingly, also compared to WT CS mice.

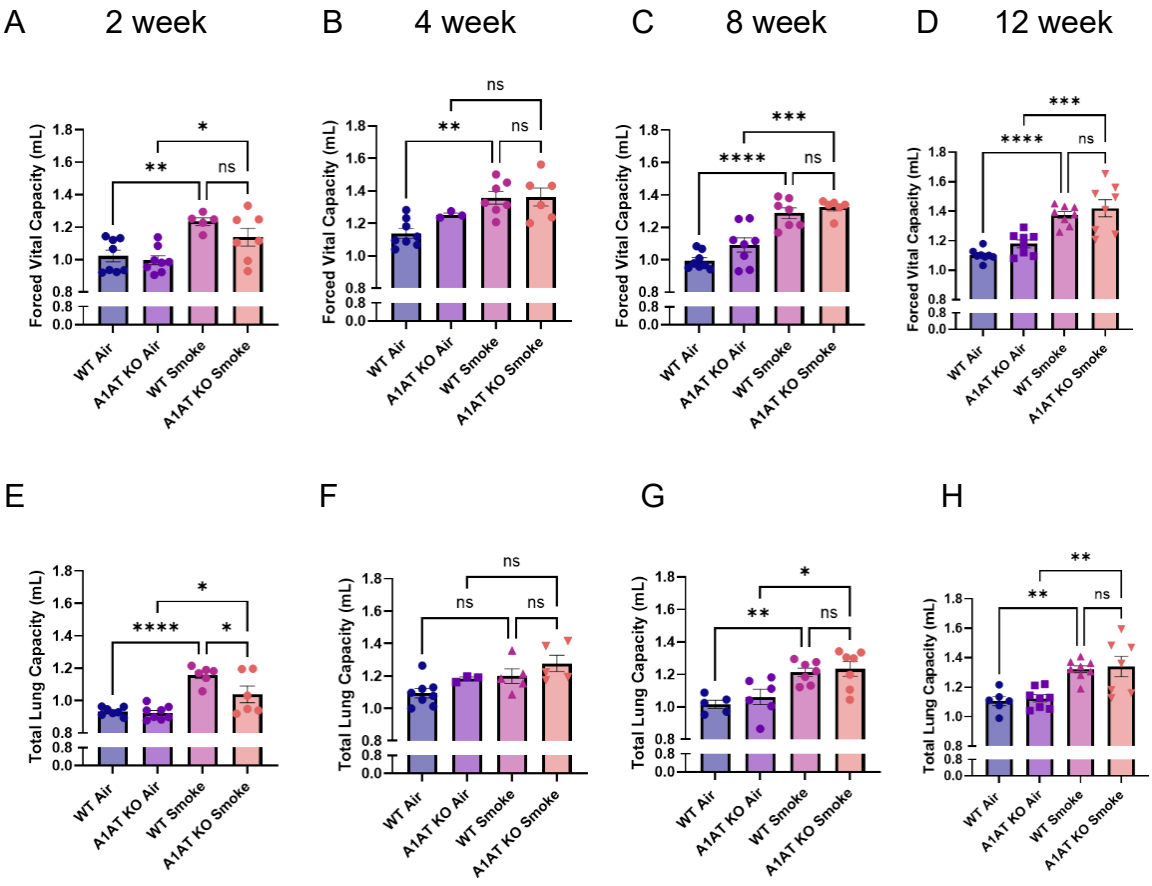

Figure 4.7: A1AT KO mice do not have increased lung volume and worsened lung function compared to WT mice.

*WT and KO mice were exposed to CS with lung function performed and lung volume assessed by forced vital capacity (FVC) (A-D), and total lung capacity (TLC) (E-H). N=8. Results are mean ± SEM. ns = p>0.05, * p<0.05, ** p<0.01, *** p<0.001, **** p<0.0001. Statistical difference was determined with Ordinary One-Way ANOVA with Bonferroni's multiple comparisons.*

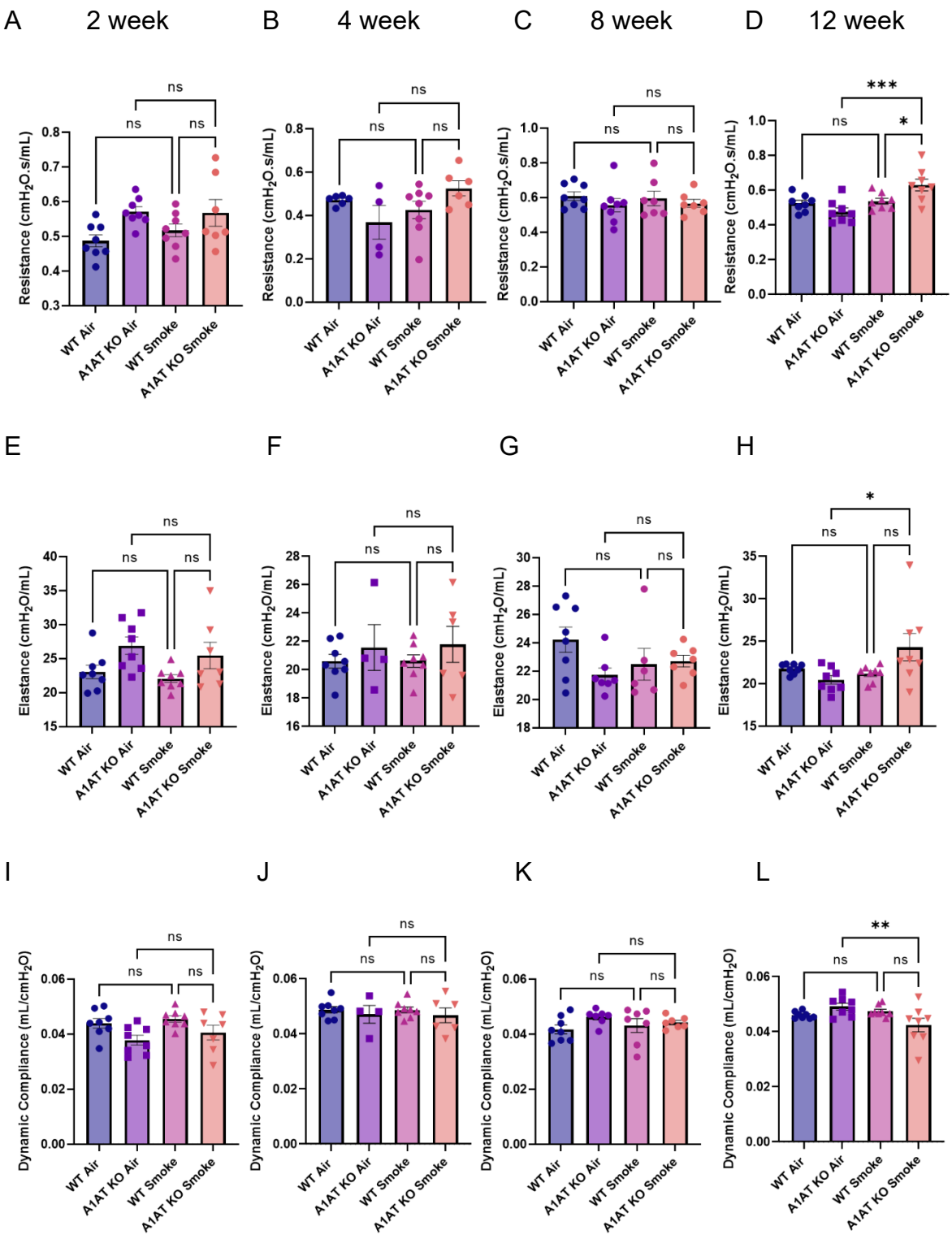

Figure 4.8: A1AT KO mice do not have worsened increased compliance and decreased resistance compared to WT mice.

WT and KO mice were exposed to CS and lung function was performed, with resistance, elastance and compliance assessed. N=8. Results are mean ± SEM. ns =

*p>0.05, * p<0.05, ** p<0.01, *** p<0.001, **** p<0.0001. Statistical difference was determined with Ordinary One-Way ANOVA with Bonferroni's multiple comparisons.*

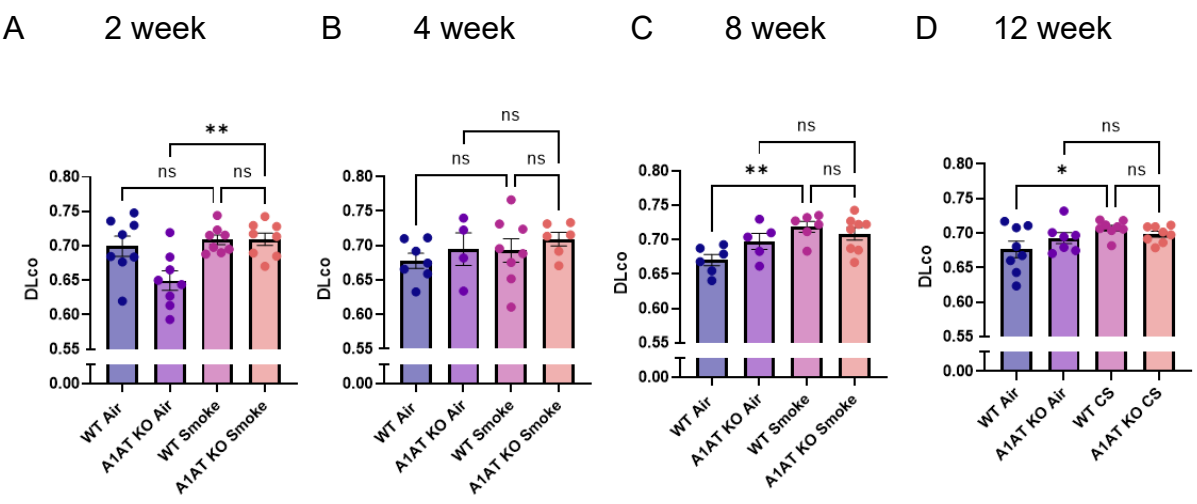

Figure 4.9: A1AT KO mice do not have decreased DLCO.

WT and KO mice were exposed to CS and DLCO was performed (A-D). N=8. Results are mean ± SEM. ns = p>0.05, * p<0.05, ** p<0.01, *** p<0.001, **** p<0.0001. Statistical difference was determined with Ordinary One-Way ANOVA with Bonferroni's multiple comparisons.

Deteriorated disease is not associated with elastase activity

An important mechanism of structural damage in the lung is due to increased elastase/protease activity. There is no A1AT present in the A1AT KO mice, evident in Figure 5.12 A-H) where there is no circulating A1AT protein and no A1AT lung protein. As there is no A1AT present to inhibit elastase activity, investigation of elastase activity in lung homogenates was undertaken to determine if there would be increased elastase activity in the lung. Interestingly there were no changes in elastase activity between any groups (Figure 5.12 I-L). Thus, there was no change in elastase activity upon CS exposure or in A1AT deficiency.

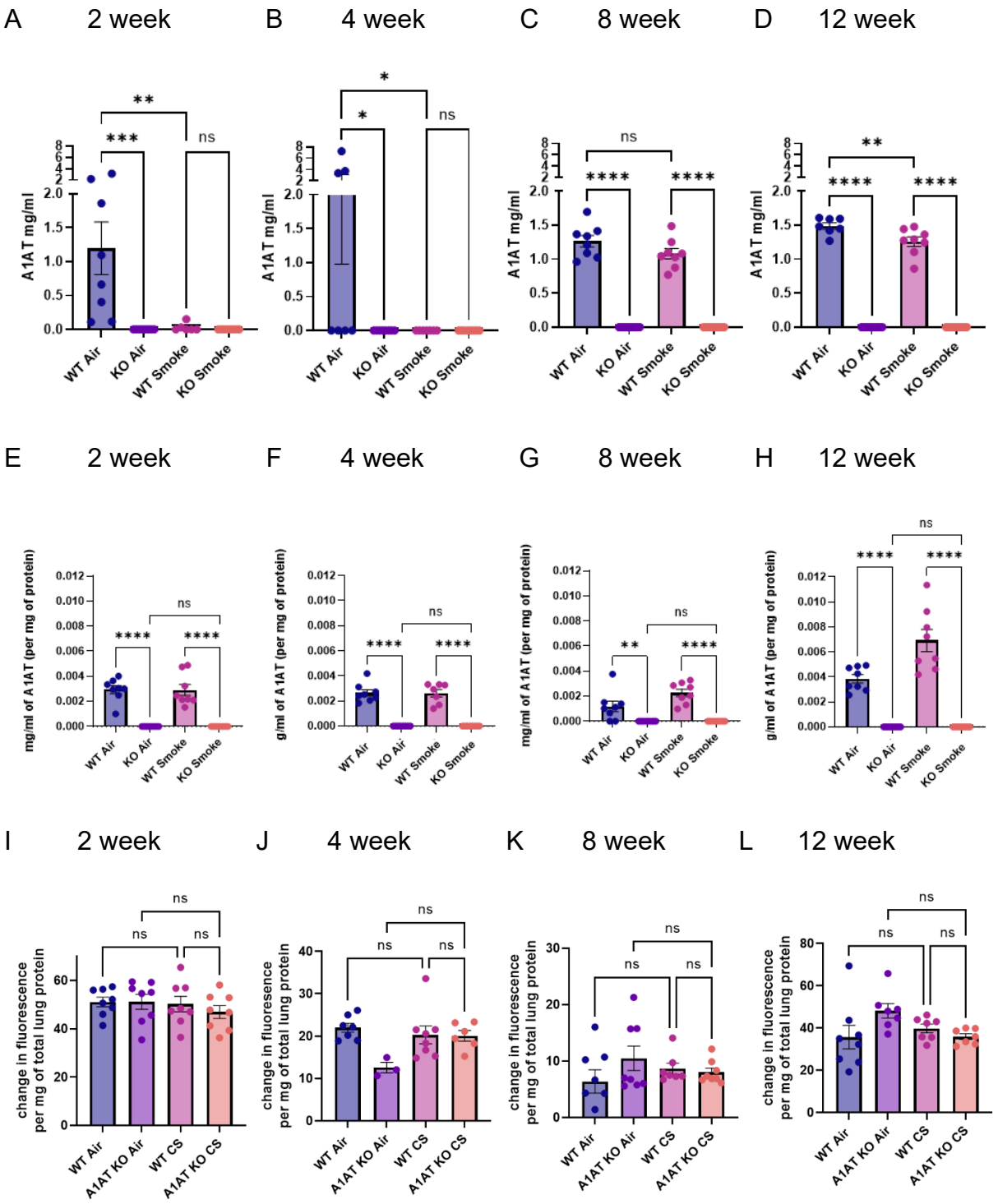

Figure 4.10: A1AT KO mice don't have increased lung elastase activity

A1AT KO mice contain no detectable circulating A1AT (A-D), no detectable A1AT in lung homogenates (E-H), and elastase activity in lung homogenates measured as change in fluorescence (I-L). Results are mean ± SEM. ns = $p>0.05$, * $p<0.05$, ** $p<0.01$, *** $p<0.001$, **** $p<0.0001$. Statistical difference was determined with Ordinary One-Way ANOVA with Bonferroni's multiple comparisons.

Elastases/proteases are typically linked to structural damage. To investigate any changes to the structure of the airways and epithelium, collagen deposition around the small airways and epithelial thickness were measured (Figure 4.11).

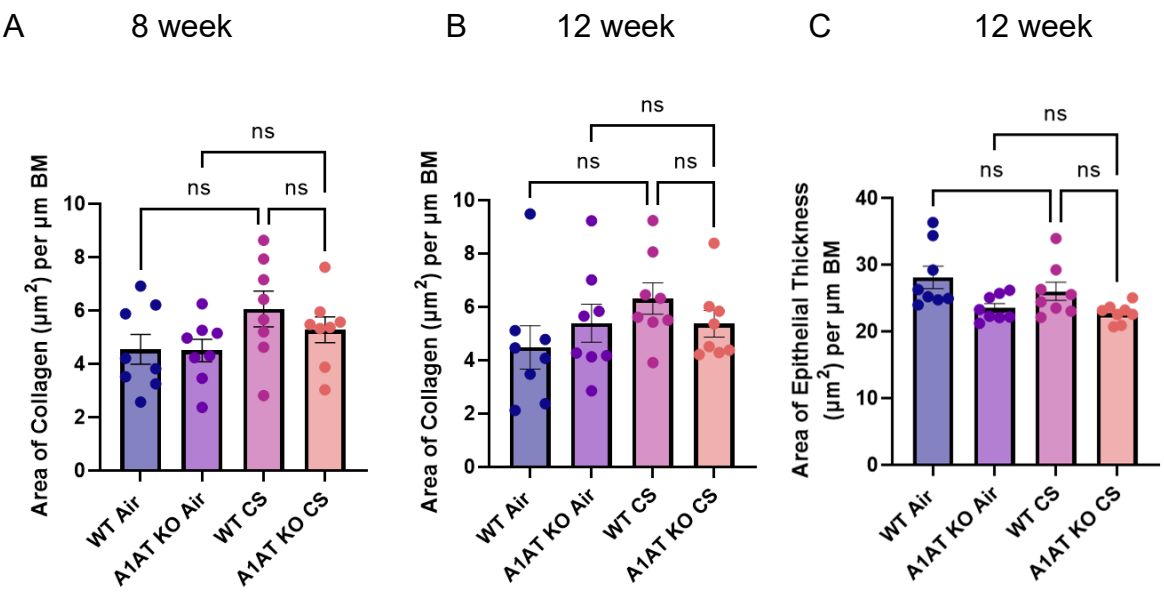

Figure 4.11: A1AT KO mice shown no signs of structural changes to small airways.

*Small airways of mice exposed to 8 and 12 weeks of CS were analysed histologically for additional lung structural changes. Collagen deposition (area of collagen) around the small airways were measured for 8 week (A) and 12 week (B) mouse models. Additionally, epithelial thickness was analysed after 12 weeks of CS (C). Results are mean ± SEM. ns = p>0.05, * p<0.05, ** p<0.01, *** p<0.001, **** p<0.0001. Statistical difference was determined with Ordinary One-Way ANOVA with Bonferroni's multiple comparisons.*

Worsened disease is associated with increased gene expression of inflammatory mediators

To determine whether the increase in neutrophil infiltrate in A1AT KO mice was associated with any inflammatory changes within the lung tissue, the expression of several key cytokines was assessed by qPCR of lung homogenates. A significant increase expression of IL1β, CXCL15 in A1AT KO CS mice compared to WT CS mice

was observed (Figure 4.12). IL1β, CXCL15, and KC are all cytokines that are strongly associated with neutrophilic inflammation. There is no change in KC in A1AT KO CS mice compared to WT CS mice (Figure 4.12 and 15). There was also a significant increase in KC, Marco and TNF due to cigarette smoke, suggesting increased inflammation and increased cytokines due to CS. Interestingly, there was also an observed increase in TNF and Marco at 4 weeks of CS in WT mice compared to A1AT KO mice. (Figure 4.13).

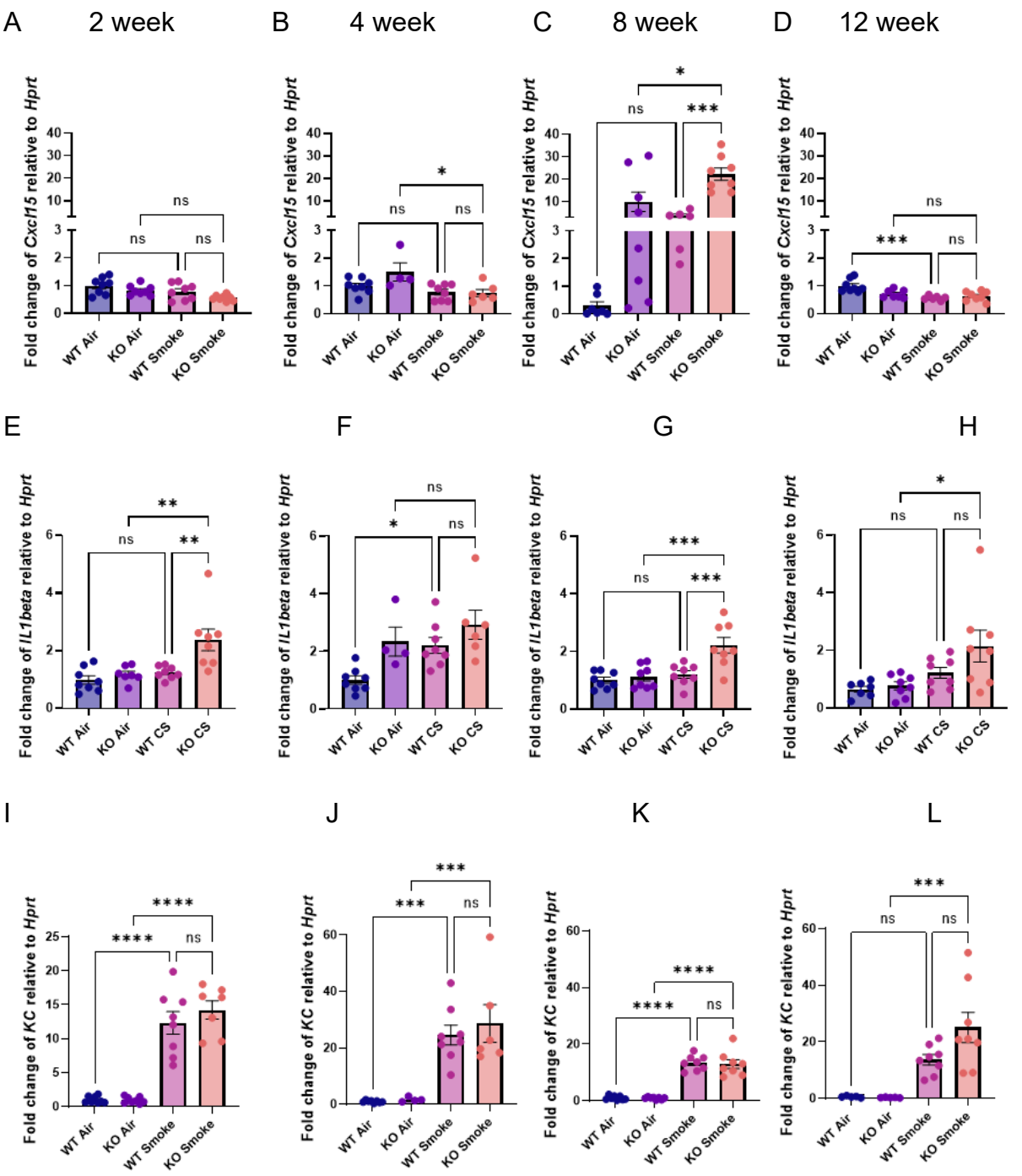

Figure 4.12: A1AT KO mice have increased gene expression of IL1β and CXCL15.

*Gene expression by qpcr of lung homogenates of various neutrophil associated markers including Cxcl15 (A-D), IL1β (E-H), and KC (I-L). Gene expression relative to housekeeping gene HPRT. N=4-8. Results are mean ± SEM. ns = p>0.05, * p<0.05, ** p<0.01, *** p<0.001, **** p<0.0001. Statistical difference was determined with Ordinary One-Way ANOVA with Bonferroni's multiple comparisons.*

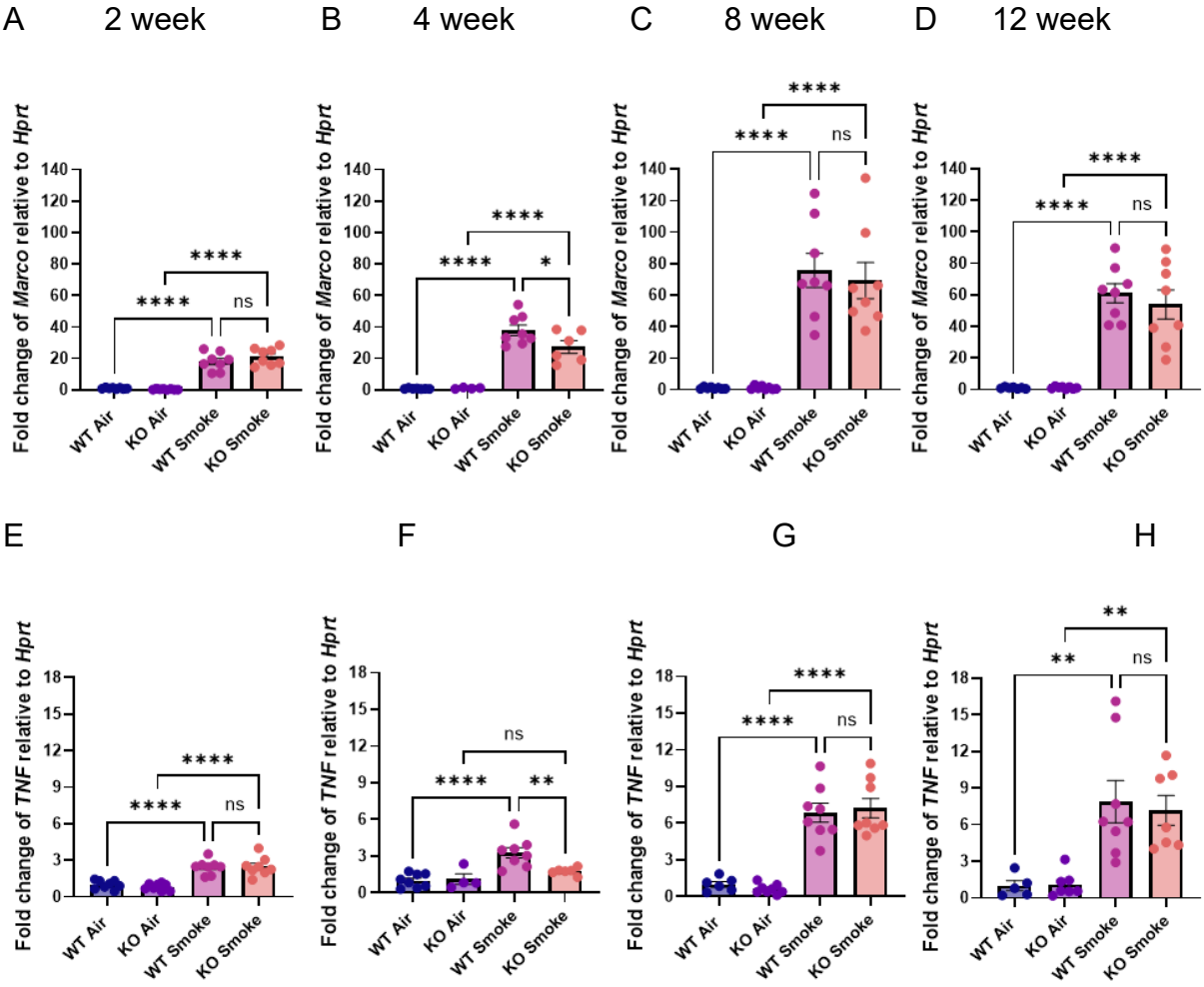

Figure 4.13: WT mice have increased gene expression of Marco and TNF compared to A1AT KO mice.

*Gene expression by qpcr of lung homogenates of macrophage marker Marco (A-D), and TNF (E-H). Gene expression relative to housekeeping gene HPRT. N=4-8. Results are mean ± SEM. ns = p>0.05, * p<0.05, ** p<0.01, *** p<0.001, **** p<0.0001. Statistical difference was determined with Ordinary One-Way ANOVA with Bonferroni's multiple comparisons.*

Additionally, protein quantity of inflammatory markers was also quantified, most notably KC, which was increased in CS in both A1AT KO and WT mice (Figure 5.16).

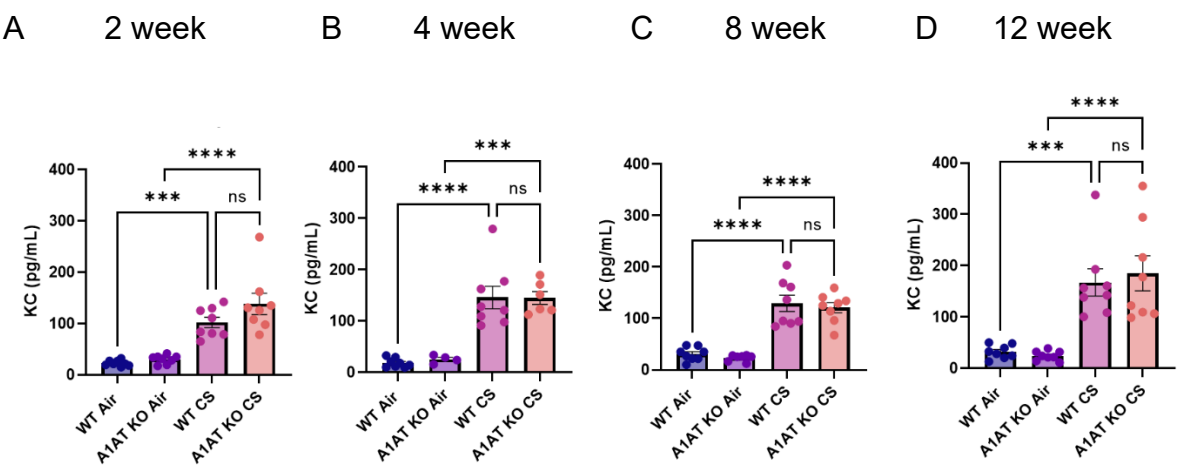

Figure 4.14: CS mice have increased protein quantity of KC.

*Protein quantity of lung homogenates by CBA of KC (A-D). N=4-8. Results are mean ± SEM. ns = p>0.05, * p<0.05, ** p<0.01, *** p<0.001, **** p<0.0001. Statistical difference was determined with Ordinary One-Way ANOVA with Bonferroni's multiple comparisons.*

Discussion

Cigarette smoke induces more severe inflammation in A1AT KO mice

A1AT knockout (KO)/WT mice were exposed to CS for 2, 4, 8 and 12 weeks. An important outcome of this is the observed changes in inflammation in A1AT KO mice over time and over disease progression. Through this method, coincident changes can be observed in time.

An increase in infiltration of total leukocytes, was observed in A1AT KO CS as compared to WT CS mice at 8 and 12 weeks, that is the two later timepoints that were analysed.

An observed increase in neutrophils was observed in A1AT KO CS compared to WT CS mice at this same time, at 8 and 12 weeks, suggesting this increase in airway inflammation is predominantly driven by neutrophils.

In addition to the increase in the BALF, there is also increased parenchymal inflammation in the A1AT KO mice when compared to WT mice, at 2 and 12 weeks of CS. Interestingly this neutrophil increase in the BALF after 8 weeks, which peaked at 8 weeks of CS, did not translate to increased proportion of neutrophils in lung homogenates at 8 weeks or at 4 weeks in the flow cytometry analysis. There was however an increased proportion of neutrophils relative to $CD45^{+}$ cells in the blood, in circulation, at 4 weeks. Since this model was repeated for flow cytometric analysis, it is possible that neutrophils are increased in the lung homogenates, but the timepoint was missed from the previous run of the mouse model. There may be an overall increase in the total number of neutrophils rather than in proportion to CD45+, however this has not been calculated. This is possible as there was an increased proportion in circulating neutrophils at 4 weeks and hence it is expected to see the neutrophils travel to the lung.

Correlating this to human disease, neutrophil mobilisation from the bone marrow is tightly controlled with neutrophil CXCL4 and bone marrow stromal cell (CXCL12) interactions causing cell retention or cell return to the bone marrow and increasing surface expression of neutrophil CXCR2 causing neutrophil release into the circulation.[30] Once in the circulation, neutrophils are able to navigate towards the source of inflammation using only small gradients in inflammatory cytokines. [30] To enable migration through dense extracellular matrices, neutrophils utilize granules containing high concentrations of proteinases such as NE and proteinase 3. Once at the site of inflammation, which regarding COPD is the lung, these neutrophils cause damage, recruit more neutrophils, and produce more proteases (such as neutrophil elastase), myeloperoxidase, defensins, and nicotinamide adenine dinucleotide phosphate (NADPH) oxidase which form ROS, which all leads to further damage.[30]

The role of A1AT in inhibiting neutrophil elastase activity in the lung and protecting the lung against elastolytic activity which is caused by elastase, in particular that released by neutrophils, has been described.[121] However, neutrophils have been further implicated in A1AT deficiency pathogenesis. There has always been an observed increase in neutrophils in A1AT deficiency. This is even true for individuals with normal

lung function, without COPD. One such study shows a 3 fold higher neutrophil count, 2 fold increase in protease levels, and 2–4 fold higher levels of IL-8, IL-6, IL-1β and LTB4 in the lung epithelial lining fluid compared to controls, as well as increased neutrophil elastase.[119]

While increased neutrophils have been implicated in disease burden, so to has the function of these neutrophils. Initially, it was thought that neutrophil function was normal in A1AT deficient patients (i.e. comparable to non A1AT deficient patients), however there is increasing evidence to suggest otherwise, which can also be suggested from the results of this chapter. Specifically, regarding the observed increase in neutrophils, which can be attributed to two main reasons.

The first is that the neutrophils themselves are inherently different in A1AT deficiency (A1AT KO mice) to non-deficient (WT mice). This excessive mobilisation of neutrophils in the lungs is consistent with what is observed in human COPD patients[50]. A study by Bergin et al.[50] found a link between A1AT and neutrophil chemotaxis. They found that A1ATD human patients showed increased inflammation and increased neutrophil chemotaxis ex vivo, particularly from IL-8. It has been shown that neutrophils isolated from A1AT deficient patients had increased chemotaxis in response to IL-8 and soluble immune complex (sIC) receptor (which was shown to mediate chemotaxis by divergent pathways). Interestingly, upon A1AT augmentation therapy the A1AT deficient patients had increased A1AT binding to IL-8, and increased A1AT binding to the neutrophil membrane, resulting in normalisation of chemotaxis. [50] It was found that A1AT modulated neutrophil chemotaxis in response to sIC by controlling membrane expression of the glycosylphosphatidylinositol-anchored (GPI-anchored) Fc receptor FcγRIIIb. This process was mediated through inhibition of ADAM-17 enzymatic activity. Neutrophils isolated from clinically stable A1AT-deficient patients were characterized by low membrane expression of FcγRIIIb and increased chemotaxis in response to IL-8 and sIC.[50] Additionally, a study from Murphy et al. showed that isolated neutrophils from A1AT deficient individuals have increased activity and increased number of neutrophil primary granule proteins in the membrane proteome when compared to control COPD. Upon stimulation these neutrophils had greater ROS and neutrophil elastase response when compared to the COPD controls. Also, these controls were matched regarding lung function damage, that is they had similar FEV1.[87, 122] Furthermore, while further investigation is required, one cannot discount

the studies that have observed accelerated neutrophil apoptosis and reduced phagocytic ability of neutrophils in A1AT deficiency.[30] This suggests two things of particular relevance to the findings of this chapter, first that neutrophil turnover may be higher in A1AT deficiency, and this may make it harder to consistently detect neutrophils, and second, that the neutrophils are inherently different. To compliment these findings and see if the neutrophils in A1AT KO mice are inherently different, future directions should include in-vitro studies exposed to smoke, to determine if these neutrophils respond differently to those taken from WT mice. Thus, neutrophil viability and metabolic activity can be determined with an LHD or MTT assay.

The second reason that can be attributed to the increased neutrophils is due to increased signalling of neutrophils. It is suggested that A1AT regulates neutrophil chemotaxis via more than one pathway, [50] however an important consistent finding is the implication of IL8 as one of the main neutrophilic chemoattractants. One mechanism that has been briefly discussed is that the neutrophils in A1AT deficiency have increased migratory ability to the sputum (compared to BALF in these mice studies) which not only reflects the increased chemoattractant burden but is amplified by the deficiency of functional A1AT. A1AT can bind directly to IL8 deterring neutrophil recruitment. By doing this, it prevents binding of IL8 to neutrophil CXCR1 and ADAM17. Where ADAM17 binding leads to the process previously described, that is, Fc receptor FcγRIIIb interactions (neutrophil surface), thus usually leading to downstream chemotaxis signalling.[30, 50] There is also the implication of increased LTB4 which increases swarming of neutrophils in inflamed tissues. Furthermore, LTB4 and IL-8 are significantly higher in COPD exacerbations of A1AT deficient patients than non A1AT deficient COPD patients. It has also, been suggested that A1AT abrogates IL8 and LTB4 mediated neutrophil chemotaxis by up to 40% via direct binding and inhibition. This is independent of A1ATs antiprotease activity.[87]

Since mice do not have IL8, changes in KC (CXCL1) and CXCL15 were investigated, which are both mouse homologues of IL8. Inflammatory cytokine CXCL15 significantly increased in KO mice compared to WT at 8, 12 and also 2 weeks (Figure 4.12 A-D). Hence a mechanism similar to those described could also be occurring in mice, as the increased CXCL15 could be a contributing factor to the increased neutrophil burden in A1AT KO mice observed in the airways from BALF cell enumeration i.e. mice without

A1AT have increased neutrophil burden which may be due to increased chemotaxis in response to CXCL15. KC significantly increased in CS compared to air but not between WT and A1AT KO mice (Figure 4.12 I-L). Additionally, KC protein quantity was also assessed (Figure 4.13), and similar to gene expression, increased due to CS. This suggests that A1AT reduces CS induced neutrophilic infiltration via CXCL15 but KC does not, thus the mechanism may be specific to CXCL15. To gain a better understanding of the mechanisms, additional experiments are required targeting in-vivo or in-vitro studies on neutrophil burden in the lung.

There is also the implication of pro inflammatory cytokines TNF and IL1β. Studies have shown that A1AT inhibits TNF and IL1β release from activated neutrophils.[123] A1AT modulates the release of TNF, and TNF facilitates neutrophil migration to the bronchial mucosa, stimulates degranulation of neutrophils and also upregulates IL8 release, which then leads to more inflammation and more damage. Active TNF is a principle driver of inflammation in COPD, and this is reflected by increased TNF in the sputum.[87] Results showed increased TNF with the presence of CS (Figure 4.13 E-H) as would be expected from the literature. Of even greater interest is the observed increase in TNF in WT mice at 4 weeks compared to A1AT KO mice which will be discussed later.

IL1β, is a potent activator of alveolar macrophages[124] and also stimulates the production of neutrophilic chemoattractants[125], therefore increased neutrophilic inflammation. The results showed a significant increase in expression of IL1β in the lung (Figure 4.12 E-H), which is increased due to smoke but in particular increased in A1AT KO mice compared to WT at 2 and 8 weeks, which as described, plays an important role in initiating and maintaining airway inflammation.

As IL1β and CXCL15 increased in A1AT KO compared to WT mice, this shows that the increase in these particular inflammatory markers may play a crucial role in A1AT deficiency induced COPD. Furthermore, this increased signalling and production of inflammatory cytokines not only leads to increased neutrophil chemotaxis but also to increased damage from increased inflammatory cells, and also increased cytokines, which lead to further damage and destruction.

Impact of other inflammatory cells, differences in A1AT KO and WT mice

While neutrophils are the main inflammatory cells implicated in A1AT deficiency, they are not the only ones implicated. In COPD, macrophages are heavily implicated in disease, specifically in inflammatory response, oxidative stress and tissue destruction associated with COPD.[126]

In the BALF results there was an increase in total leukocytes at 4 weeks in the WT mice compared to the A1AT KO mice and an increase in macrophages was the main contributor. There was also increased macrophages and total leukocytes in WT CS mice compared to A1AT KO. At this timepoint neutrophils are only a small contributor to inflammation, i.e. to total leukocytes. Additionally, this is the only timepoint that neutrophils were not significantly different between WT and A1AT KO mice.

Macrophage associated inflammatory markers have been shown to increase upon exposure to CS. This was reflected in Figure 4.12, which showed increase in TNF and Marco expression in mRNA. Additionally, TNF also plays a crucial role in inflammatory cell recruitment and tissue remodelling in COPD reflected by increased TNF mRNA and protein levels present in COPD patients. [120] Increased Marco suggests increased recruitment of macrophages to the airways as well as increased inflammation. Marco belongs to a class A scavenger receptor family which are known for their ability to bind and internalise a variety of molecules including particles like CS, thus important in phagocytosis in CS.[127] Interestingly, both TNF and Marco increased in 4 week WT CS lung samples when compared to A1AT KO mice. This seems to complement the increased macrophage finding in the BALF.

In COPD, although macrophages are essential in pulmonary protective mechanisms, they also promote a dysregulated inflammatory response which contributes to lung damage and the pathogenesis of COPD. It is hence pivotal to explore this observed inflammatory profile in greater depth, particularly at 4 and 8 weeks, which was done with flow cytometry. However recruited macrophages (both MHCII high and MHCII low) were examined in lung homogenates, not the BALF. The macrophages in WT CS mice increased due to smoke in the lung at 4 weeks, which was consistent with the

previous findings in the BALF and suggests increased macrophages to be a driving factor in CS induced damage at 4 weeks.

Analysis of flow cytometry showed an increase in dendritic cells due to CS in the lung at 4 and 8 weeks. Interestingly, A1AT KO mice had a significantly reduced proportion of DCs at 4 weeks in the blood, and 8 weeks in the lung. While dendritic cells have previously been shown to increase in COPD,[128] this is the first data to suggest that A1AT helps facilitate this recruitment. While no other studies were found linking DCs and A1AT in COPD, there have been studies that showed human A1AT is able to inhibit DC activation and function in models of lupus.[92] Hence, the hypothesis that A1AT may increase DC migration. In order to investigate this hypothesis, DC migration towards the lung and accumulation in the lung and bronchoalveolar space needs to be investigated as a future direction (investigated in Chapter 6 Aim 4).

Dendritic cells serve as innate lung sentinels and as orchestrators of adaptive immunity and are well equipped to drive pathological processes from the earliest stages of COPD pathogenesis to end-stage disease.[128] Additionally, dendritic cells (DC) can be further categorised into three main subtypes: type 1 classical or conventional DC, type 2 classical or conventional DC and plasmacytoid DC.[128, 129] As a future direction it would be helpful to further classify the dendritic cells analysed into these subtypes, as for example, type 2 conventional DCs are major producers of proinflammatory cytokines, thus promoting further recruitment of inflammatory cells.[128] It would be interesting to conduct further research to see which of the 3 main subtypes of DCs is driving this change and if this finding is reproducible in humans, i.e. does this finding also translate to human research.[130]

Furthermore, studies have suggested the effects of A1AT on other cell types, including neutrophils and macrophages, are important for therapeutic benefits, and that there may be cross-talk among the aforementioned findings and mechanisms. One example is the blocking of TNF signalling by the interaction of A1AT with TNF receptors, which leads to the inhibition of downstream gene expression in DCs.[92]

As this particular finding in COPD has not been previously shown or explored, future studies would be beneficial, and it would be pivotal to see if these same findings are present in human studies or human samples.

Cigarette smoke induces more severe alveolar destruction in A1AT KO mice and yet does not worsen CS induced changes to lung function

Analysis of histologically apparent changes to the lung and to lung function were conducted to see if they accompanied the increased inflammation observed in A1AT KO mice. To achieve this, MLI analysis was performed on lung sections to measure alveolar destruction. In this analysis, the bigger the alveolar space, the larger distance between intersections on the grid, correlates to greater alveolar destruction and emphysema. This increased MLI was observed in CS mice after 8 weeks when compared to those exposed to air. Air mice had smaller distances between alveoli, indicating a larger number of smaller alveoli, consistent with normal, healthy tissue. MLI was also increased in the absence of A1AT, thus alveolar damage was exacerbated in A1AT KO mice, evident from a significantly greater MLI in A1AT KO mice at 8 and 12 weeks compared to WT mice (Figure 4.6). This finding highlights the impact of A1AT absence on damage to the lung in mice exposed to smoke. To place this in the context of human COPD, smoking, regardless of A1AT gene status, causes lung damage, but in those deficient in A1AT, smoking-related damage is exacerbated.

Increased alveolar destruction was observed, and hence it was expected that there would be increased lung volume, as alveolar destruction leads to loss of elastic recoil and air trapping and thus lung hyperinflation, i.e. emphysema. Lung function measures a variety of parameters pertaining to the damage of the lung. Two measures of lung volume are TLC (total lung capacity) and FVC (forced vital capacity). TLC and FVC both show increased lung volume in mice exposed to smoke, hence increased damage. However, they did not show an increase in lung volume in A1AT KO mice compared to WT. This shows that although there are structural changes in KO mice, this did not translate into functional changes at this time point. This is actually not all that inconsistent with literature, as some moderate A1AT deficiency cases that have been exposed to passive smoking and various occupational inhalants, did not always

have significantly decreased respiratory health. However, in severe A1AT deficiency cases there was significant decreased respiratory health[118]. Additionally, in humans with A1AT deficiency, there is an environment of high inflammation, that is increased cytokine levels, neutrophil counts and neutrophil elastase levels, even before any development of lung injury or lung function impairment.[119] Considering this, and that these mice are still young compared to other studies that have used A1AT KO mice [98] where mice are aged to almost a year old, lung function differences between A1AT KO mice and WT mice may not be seen at this earlier timepoint, only the worsening of lung function from CS.

As previously mentioned, lung function can measure a variety of parameters. Of particular interest are parameters that measure the effects from A1AT deficiency, i.e. the loss of elastin. While CS alone will cause some loss of elastin, which gives lungs their elasticity and strength, this impact is expected to be more severe in systems with no A1AT as there is no A1AT to inhibit neutrophil elastase. The loss of elastase in lungs makes them more compliant, which interestingly was not observed. Similar measures of resistance and elastance are affected by decreased elastin in the lung. Resistance specifically measures the level of constriction in the lungs while elastance measures the elastic stiffness of the respiratory system at the ventilation frequency, and is considered the reciprocal of compliance and vice versa. After 12 weeks however, there is a slight yet significant change in these parameters in the A1AT KO mice, and this shows the converse of what is expected. There is a decrease in lung compliance and an increase in lung elastance. With more damage, it is expected that there would be less elastase in the lung, therefore decreased elastance and increased compliance as there is less elasticity and resistance, making the lungs more compliant. There is, however, also more resistance in A1AT KO CS compared to A1AT KO air, and to WT CS, which is unexpected in this model. While this could suggest increased fibrosis of the lung, since there were no significant changes to gas exchange in DLCO, and nothing yet indicative of fibrotic changes, this is unlikely. It would also be beneficial to measure elastin in A1AT KO and WT mice as this may be indicative of why there is no difference in compliance. To see if this may be the case, elastase activity and elastin protein in the lung need to be investigated.

Deteriorated disease is not associated with elastase activity

In this chapter the impact of CS in mice with no A1AT was explored. The absence of A1AT is evident from Figure 4.9. This allows exploration of the protease anti protease balance in a system of no A1AT where it is expected that there would be increased neutrophil elastase and thus increased lung damage.

There were no significant changes in elastase activity (Figure 4.10 I-L). This was an unexpected finding as increased presence and activity of elastases and other proteases have been considered in the literature to be a main mechanism of damage to the lung. Damage from neutrophil elastase is caused by multiple mechanisms. It is the main, but not the only protease related to lung damage, there is also protease 3, cathepsin G as well as metalloproteinases. [131] However, neutrophil elastase is the main contributor, particularly in the small airways. Typically, when neutrophil elastase is implicated in A1AT deficiency related damage, much emphasis is placed on its role in protease activity which is associated with almost all facets of COPD, that is, emphysema, airway remodelling – particularly destruction and damage to the small airway, as well as chronic bronchitis, and even bacterial infections and colonisation.[30] Neutrophil elastase degrades key features of the extracellular matrix. Neutrophil elastase is responsible for degradation and key cleavage of many features of the extracellular matrix, such as elastin, collagen, fibronectin and many others, which provide structural support, strength, elasticity, cell adhesion, cell migration, cell differentiation, among other things.[30]

Additionally, analysis of both collagen deposition around the small airways and epithelial thickness were unchanged in A1AT KO mice compared to WT mice (Figure 4.11). Thus, there were no remodelling changes other than alveolar destruction, and this may be due to the lack of change in elastase activity. A1AT is not the only inhibitor of elastases, such as neutrophil elastase, as SLPI and elafin also inhibit neutrophil elastase. These other antiproteases may be the reason for the lack of change in elastase activity. A more comprehensive list of proteases and antiproteases is described in Table 1.2. To confirm this, it would be beneficial to investigate the individual effects of key proteases including NE, proteinase 3, cathepsin G, ADAM-17

and MMPs, perhaps by immunofluorescent staining or proteomics. Neutrophil elastase also activates matrix metalloproteinases (2, 3, and 9) and cathepsin B, which are heavily implicated in disease progression in COPD in humans and in mice. (MMP-9 is abundant in asthma, IPF, and COPD). [132]

In this particular model, these findings suggest that the main cause of damage is from the high inflammatory environment and related mechanisms of increased inflammatory cells, increased cytokines and possibly increased chemotaxis. There is also the implication of the absence of A1AT in these pathways, mainly A1AT anti-inflammatory and immunomodulatory effects (e.g. the ability of A1AT to regulate cytokine production), as opposed to the protease antiproteases balance.

The ability of neutrophils to modulate inflammation has been discussed previously, however neutrophil elastase also has immunomodulatory effects. Neutrophil elastase enhances endothelial and epithelial cell secretion of inflammatory mediators (such as IL 8), and enhances macrophage secretion of pro-inflammatory cytokines. Additionally, it plays a role in cell death by increasing cell apoptosis (epithelial and endothelial cells), and cell function, in particular cellular oxidative stress, and neutrophil/A1AT complexes are chemotactic for neutrophils.

Conclusion

This chapter sought to understand the interaction of A1AT deficiency and cigarette smoke exposure in an animal model equivalent to the human A1AT null allele with mice that have a knock out (KO) of the A1AT gene.

Investigation of inflammatory, structural and functional changes in A1AT KO mice across a time course of cigarette smoke exposure found increased inflammation at 2, 8 and 12 weeks of cigarette smoke which was predominantly driven by neutrophils, and increased cytokines related to neutrophil chemotaxis (IL1β and CXCL15). There were interesting inflammatory profiles of both A1AT KO mice but also WT mice, which showed increased macrophages and dendritic cells, particularly at 4 weeks of smoke.

The inflammatory profile fluctuates over time and the increased inflammatory markers also compliment this change. This highlights that the inflammatory story is pivotal to A1AT deficiency related damage and should be investigated further. There was increased alveolar destruction in A1AT KO mice compared to WT mice after 8 weeks (8 and 12 week timepoint) and decreased lung function due to CS.

These changes led to the second goal, which was to establish a combined A1AT null and cigarette smoke exposure model as a platform that can be used in future to test therapies for A1AT null patients. Since this model has shown increased airway inflammation, alveolar damage, and decreased lung function compared to air mice, this mouse model can now be used as a basis for further treatments. In particular, the 8 week model, which is the earliest timepoint where alveolar damage was detected.

Chapter 5 – Aim 3

Introduction

The aim of this chapter was to understand the interaction of A1AT toxicity and cigarette smoke (CS) exposure. This chapter utlises an animal model that can be considered equivalent to the human PiZ allele, as the mice have a knock in of the human mutated Z allele. These PiZ mice develop liver damage due to the accumulation of A1AT in hepatocytes.[82, 105]

As discussed in the previous chapter, this established cigarette smoke model exhibits key hallmarks of human COPD, including increased number of leukocytes in the bronchoalveolar lavage fluid (BALF), alveolar destruction, and changes to lung volume and compliance.[120]

This chapter has two primary aims; the first is to investigate the changes in PiZ mice due to CS which anticipates that PiZ mice will experience deteriorated COPD due to CS compared to WT controls. This hypothesis is not due to A1AT deficiency in mice, as these mice retain functional mouse A1AT, but instead due to the presence of toxic Z A1AT accumulation in mice which has been previously reported in the literature to cause liver damage.[82] The second aim is to establish an experimental model of CS induced A1AT deficiency/toxicity related lung damage. Hence, to investigate if these PiZ mice have Z toxicity related damage, and also if this is a suitable model for testing future therapies.

Results

Cigarette smoke induces inflammation and increases inflammatory cell counts in PiZ mice

Chronic inflammation specifically increased infiltration of inflammatory cells into the airways and lung parenchyma, is a significant hallmark of CS induced COPD. Hence, to elucidate changes to the inflammatory environment of PiZ mice due to CS, BALF was collected and enumeration of leukocytes was conducted.

Results showed increased total leukocytes due to CS, reflected in both the PiZ mice and the WT control mice (Figure 5.1A). Differentiation of inflammatory cells showed that the predominate cell contributor in PiZ mice was neutrophils (Figure 5.1C), while in WT mice both macrophages and neutrophils were significantly increased in CS (Figure 5.1B-C).

Furthermore, there was an increase in parenchymal inflammatory counts due to CS, evident in both WT and PiZ mice (Figure 5.1D). This shows that overall there were increased inflammatory cells in the lung due to CS. However, there was an absence of changes in total leukocytes, macrophages or neutrophils between PiZ and WT mice. Hence, the contributor to inflammation is most likely due to CS, even if inflammation in PiZ mice appears to be neutrophil driven (evident from increased neutrophils in BALF of PiZ CS mice compared to air).

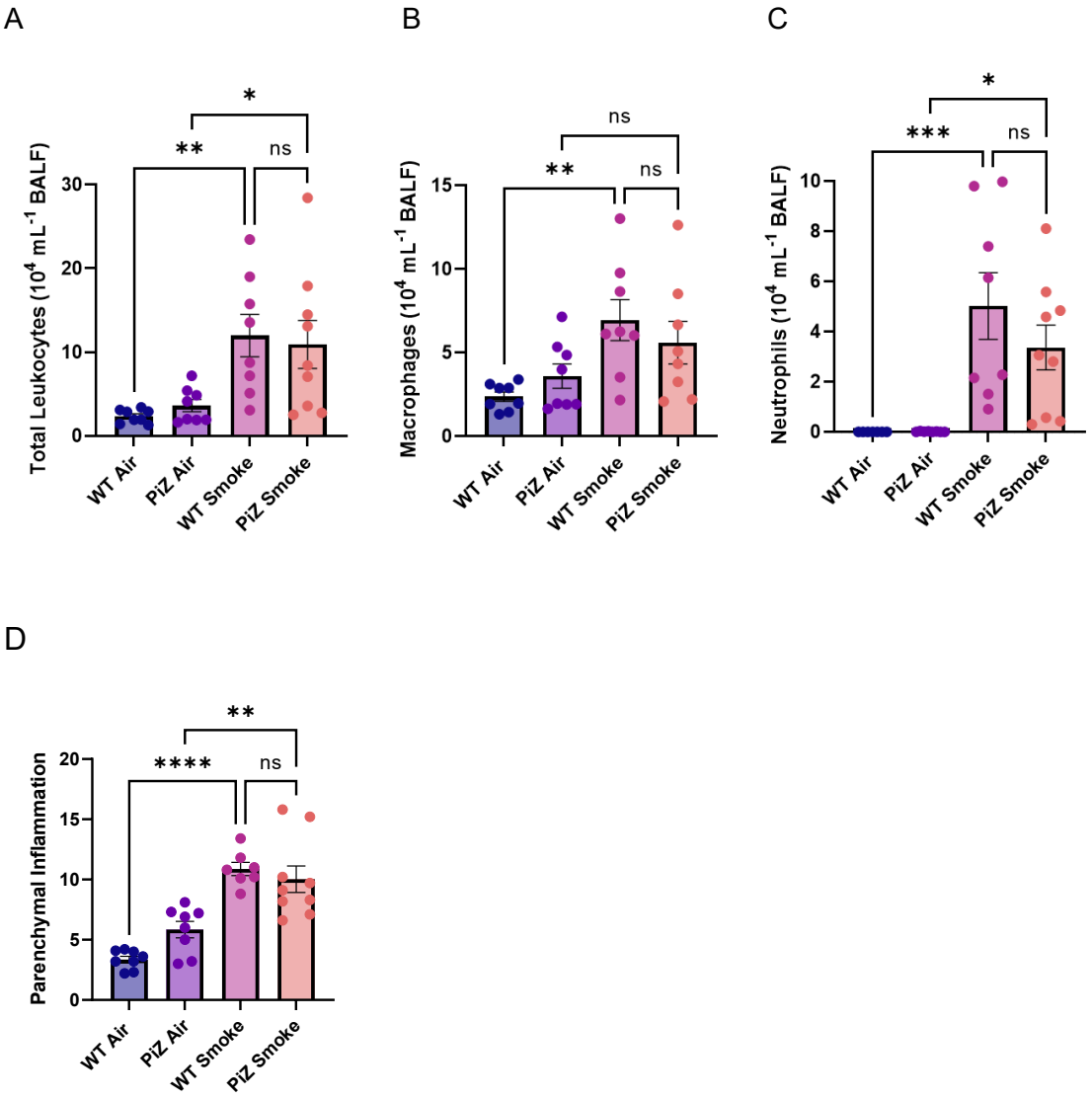

Figure 5.1: Cigarette smoke induces increased airway inflammation in PiZ and WT mice.

*Measure of airway inflammation from BALF of WT and PiZ mice in an 8 week experimental model of CS induced COPD. Inflammatory changes in BALF were observed in total leukocytes (A), macrophages (B), and neutrophils (C). Parenchymal inflammation was also measured as the number of inflammatory cells in the parenchymal space, where the field of view is 78,278 μm², measured as cells per field of view (D). N=8. Results are means ± SEM. ns = p>0.05, * p<0.05, ** p<0.01, *** p<0.001, **** p<0.0001. Ordinary One-Way ANOVA determined statistical significance with Bonferroni's multiple comparisons.*

Cigarette smoke induces more severe alveolar destruction in PiZ mice

Alveolar destruction was measured to determine if there was structural damage to the lung, specifically the alveoli. For this the mean linear intercept (MLI) was calculated. This quantifies damage by measuring the distance between alveolar walls, where an increased distance corresponds to fewer and larger alveolar spaces consistent with emphysema. Figure 5.2 shows increased distance and hence damage due to CS, as well as increased damage in PiZ mice compared to WT mice. Hence, alveolar destruction is exacerbated in PiZ mice compared to WT.

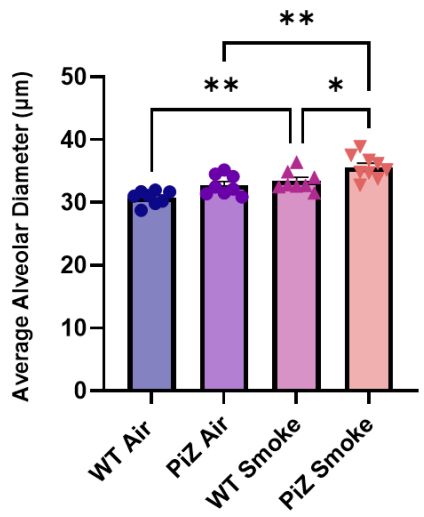

Figure 5.2: Cigarette smoke induces increased alveolar destruction in PiZ mice. Increased alveolar damage in PiZ mice is evident by increased mean linear intercept (MLI) at 8 weeks. N=8. Results are means ± SEM. ns = p>0.05, * p<0.05, ** p<0.01, *** p<0.001, **** p<0.0001. Statistical difference was determined with Ordinary One-Way ANOVA with Bonferroni's multiple comparisons.

CS does not cause deteriorated lung function in PiZ mice compared to WT

Lung function was also measured to elucidate any functional changes to the lung volume, elasticity and strength. There was an increase in lung volume shown as increased total lung capacity (TLC, Figure 5.3A) and forced vital capacity (FVC, Figure 5.3B) due to CS. Interestingly, measures of resistance, compliance, and elastance

showed no change between PiZ and control or between CS and air control (Figure 5.3C-E).

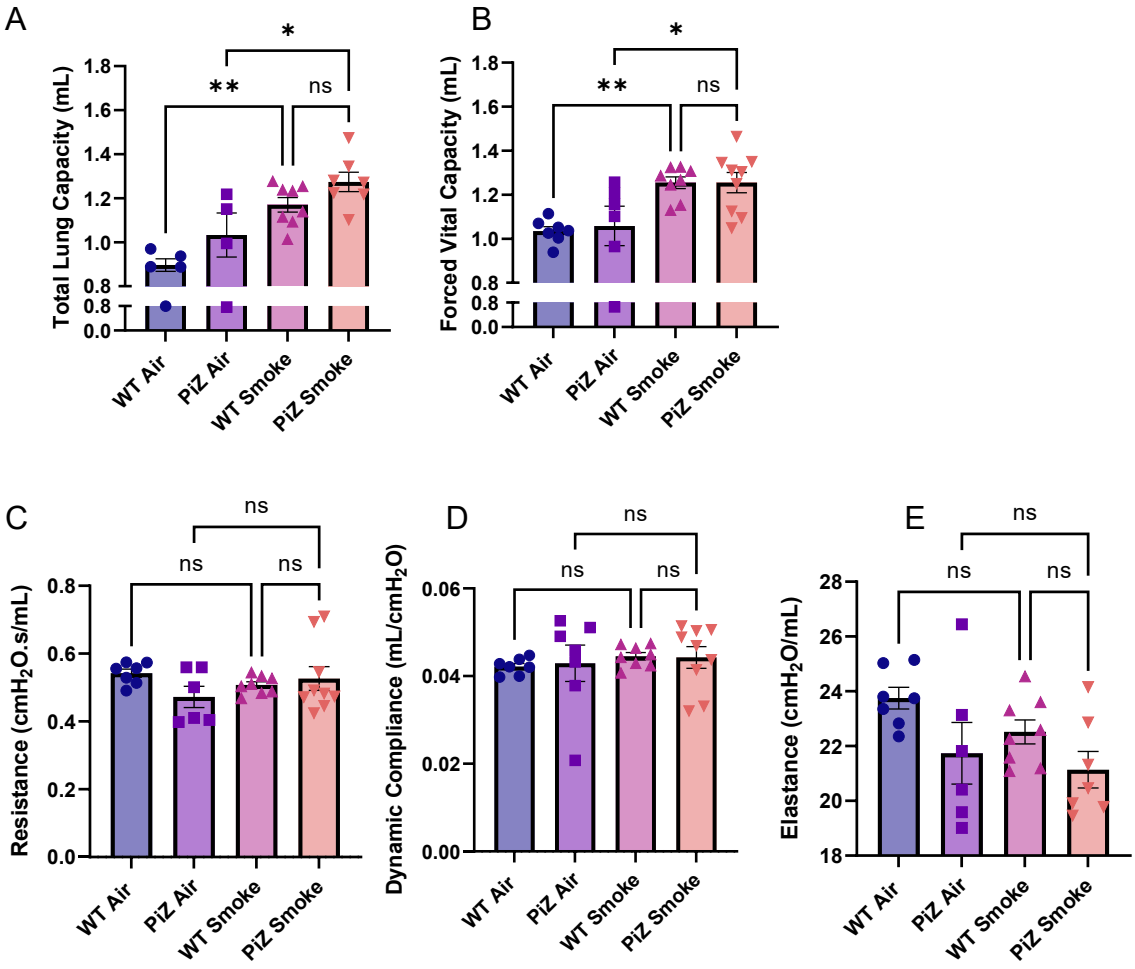

Figure 5.3: PiZ mice do not have worsened lung function compared to WT mice.

*WT and PiZ mice were exposed to CS. Lung function was performed and lung volume assessed by forced vital capacity (FVC) (A), and total lung capacity (TLC) (B). Resistance (C), Dynamic compliance (D) and Elastance (E), were also measured. N=8. Results are mean ± SEM. ns = p>0.05, * p<0.05, ** p<0.01, *** p<0.001, **** p<0.0001. Statistical difference was determined with Ordinary One-Way ANOVA with Bonferroni's multiple comparisons.*

Aggravated disease is not associated with elastase activity

PiZ mice do not have the mouse Serpina1 genes knocked out and hence would be expected to be able to produce A1AT. Hence it was pivotal to measure A1AT. A1AT quantity in blood plasma showed a decrease in A1AT protein in PiZ CS compared to PiZ air mice as well as to WT CS mice (Figure 5.4A). Lung protein however, shows an increase in A1AT in CS mice in both PiZ and WT (Figure 5.4B).

A1AT is an inhibitor of elastase, and hence elastase activity was measured. Interestingly, elastase activity was decreased in all groups compared to the control, WT air (Figure 5.4). This initially seemed counterintuitive to literature reports, as increased elastase activity would suggest an increased presence or availability of elastase, or less active A1AT present for it to bind.

A A1AT circulating B A1AT lung

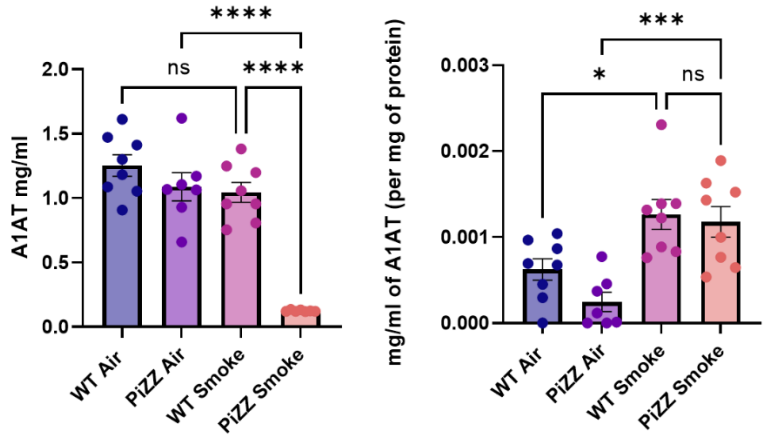

C Fluorescence vs Time – Lung samples

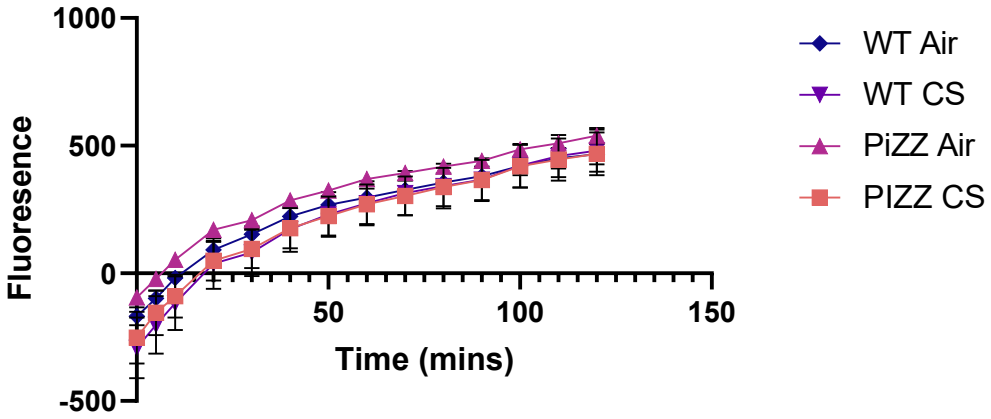

D Fluorescence vs Time – Purified Elastase Standards

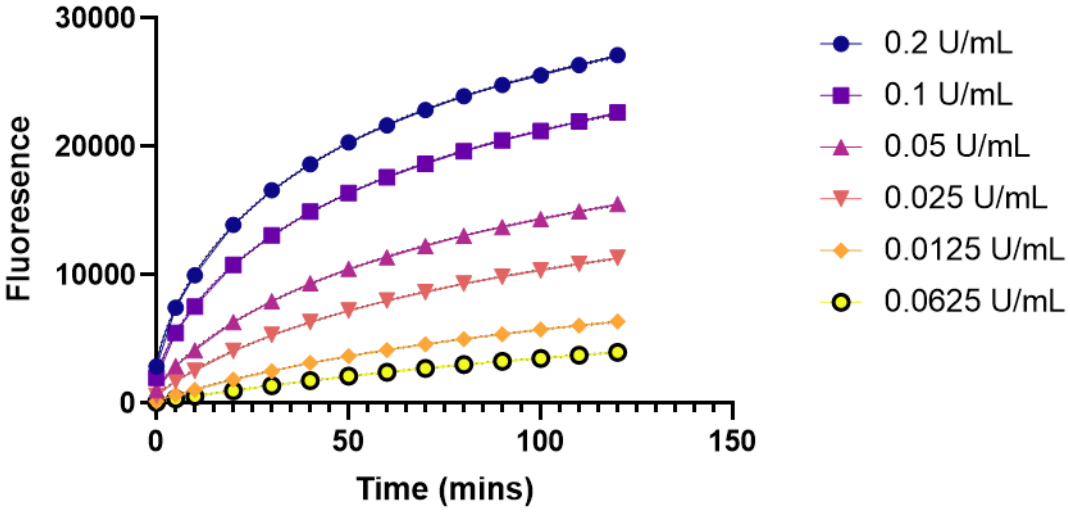

E Elastase activity

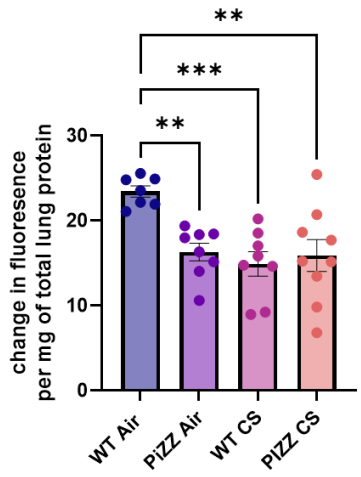

Figure 5.4: A1AT KO mice relationship between A1AT protein and elastase activity.

*WT and PiZ mice were exposed to CS. A1AT protein was measured in blood plasma (A) and lung sample homogenates (B). Elastase activity was also measured in lung homogenate samples with multiple measurements of fluorescence over time (Fluorescence vs Time) (C) as well as standards of purified porcine pancreatic elastase (0.2, 0.1, 0.05, 0.025, 0.0125, 0.0625 and 0) were measured as appropriate controls (D). Lung samples were calculated as change in fluorescence over time (measured in AU) which equates to elastase activity (E). This was achieved by selecting the values of graph C which are positive and the slope linear, which was between t=20 to t=100. N=8. Results are mean ± SEM. ns = p>0.05, * p<0.05, ** p<0.01, *** p<0.001, **** p<0.0001. Statistical difference was determined with Ordinary One-Way ANOVA with Bonferroni's multiple comparisons.*

Aggravated disease due to CS is associated with increased inflammatory markers

To determine whether the increased inflammatory cell infiltrate in the lung of CS PIZ mice was associated with any increases in inflammatory markers within the lung tissue, the gene expression of several key cytokines (and inflammatory markers) by qPCR of lung homogenates was assessed. There was a significant increase in gene expression of markers *IL1*β, *KC* and *TNF* in PIZ and WT CS mice compared to Air mice (Figure 5.5B-D), hence, increased inflammation and increased cytokines due to

CS. There were no changes in *Cxcl15* (Figure 5.5A). *Marco* was also increased due to CS in PiZ and WT mice (Figure 5.5E). The protein quantity of various cytokine markers was also measured by CBA, namely *IL1*β and *TNF*. While it showed increased RNA expression due to CS, it did not show an increase in protein quantity in the lungs at this time (Figure 5.6A and C). KC and Mcp1 were increased in CS mice, however there were no change between WT and PiZ mice (Figure 5.6B and D).

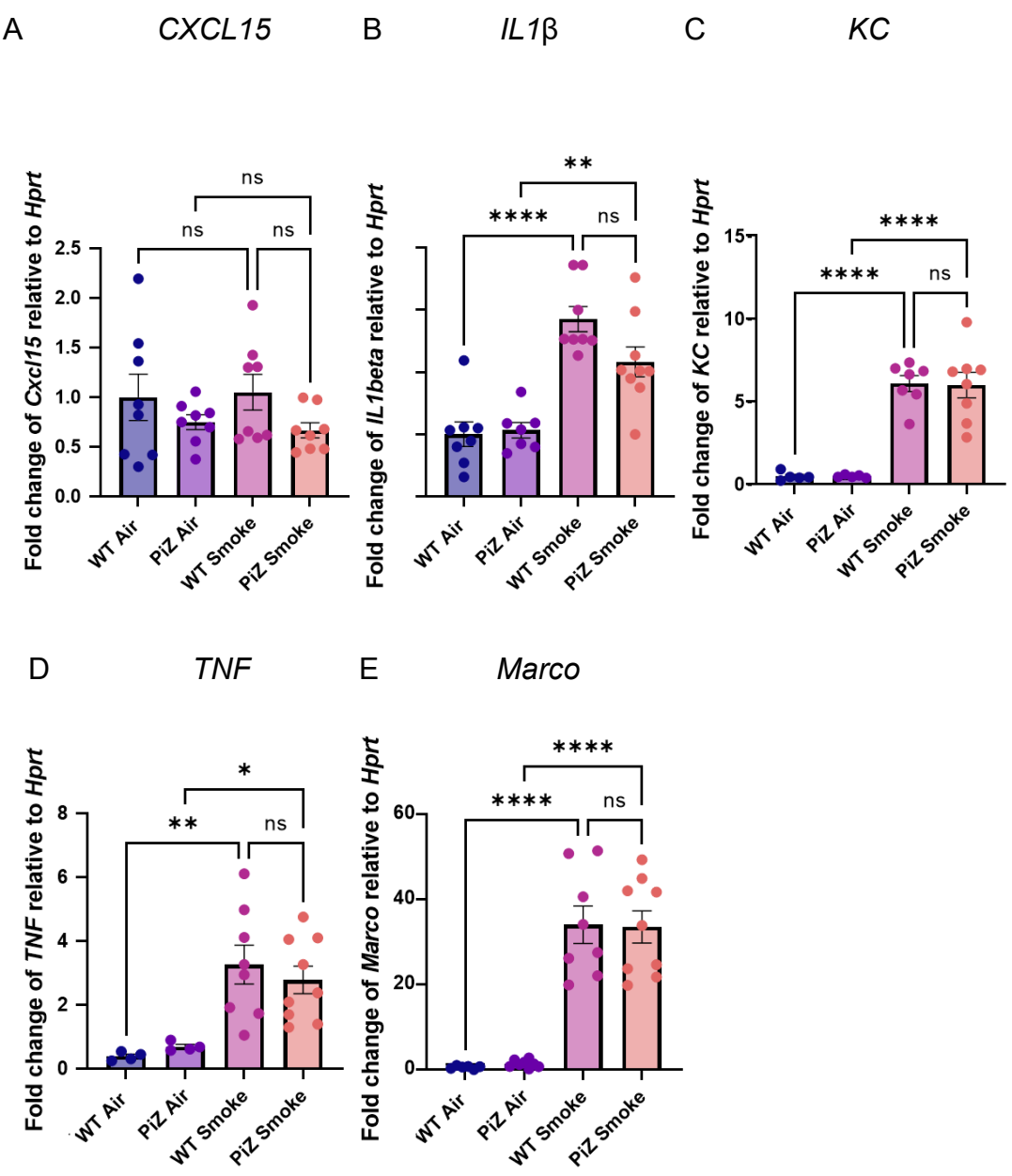

Figure 5.5: CS PiZ mice have increased mRNA expression of inflammatory markers compared to Air.

*Gene expression by qpcr of lung homogenates of various inflammatory markers including Cxcl15 (A), IL1β (B), and KC (C), TNF (D) and Marco (E). N=8. Results are mean ± SEM. ns = p>0.05, * p<0.05, ** p<0.01, *** p<0.001, **** p<0.0001. Statistical difference was determined with Ordinary One-Way ANOVA with Bonferroni's multiple comparisons.*

A *IL1β* B KC C TNF D Mcp1

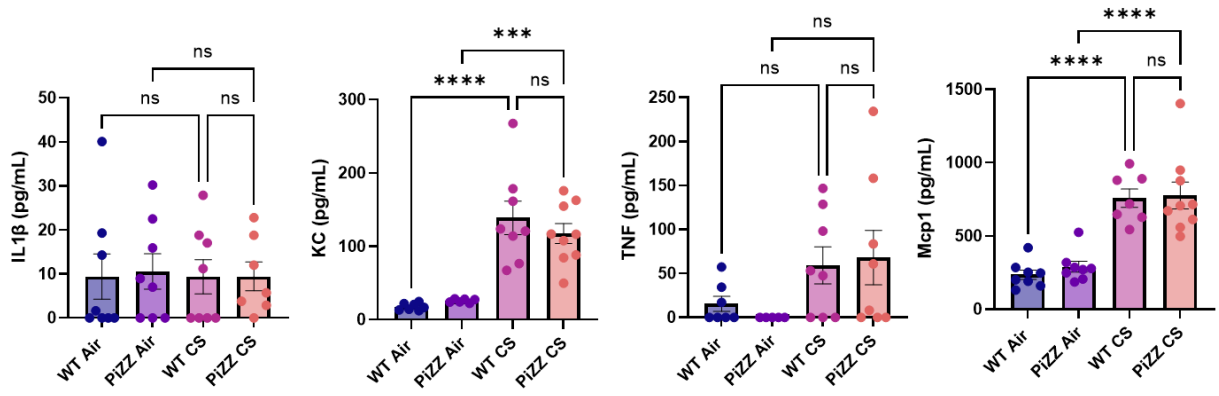

Figure 5.6: PiZ and WT CS mice have increased protein quantity of KC and Mcp1 compared to Air mice.

*Presence and quantity of inflammatory markers were measured by Cytometric bead array (CBA) of lung homogenates. Lung homogenate was tested and key cytokines IL1β (A), KC (B), TNF (C) and Mcp1 (D) measured. N=8. Results are mean ± SEM. ns = p>0.05, * p<0.05, ** p<0.01, *** p<0.001, **** p<0.0001. Statistical difference was determined with Ordinary One-Way ANOVA with Bonferroni's multiple comparisons.*

Discussion

This chapter aimed to investigate the relationship between Z mutated A1AT toxicity in CS induced COPD. Mice expressing human Z misfolded A1AT proteins were exposed to CS for 8 weeks. Results after CS showed firstly a similar degree of chronic inflammation in bronchoalveolar space, and functional pulmonary parameters between PiZ and WT mice post CS exposure. Secondly, increased structural damage in PiZ mice. Thirdly, further analysis showed a significant low level of mouse A1AT protein observed in PiZ CS mice compared to PiZ air mice or WT CS mice.

PiZ and WT mice displayed similar disease presentation for COPD

Inflammatory cell infiltrate into the bronchoalveolar space is a key feature in COPD and was assessed in PiZ mice. There was an increase in total leukocytes and neutrophils in the BALF and an increase in parenchymal inflammation due to CS (Figure 5.1-5.2). Additionally, gene expression and protein quantity were determined in lung homogenates to determine if there was an increase in inflammatory markers to support the increased cell infiltrate in the lung due to CS. Inflammatory mediators *IL1*β, *TNF*, *KC and Marco* showed increased gene expression in PiZ and WT CS mice compared to Air mice (Figure 5.5). Additionally, there was increased levels of Mcp-1 and KC protein in PiZ and WT mice exposed to CS (Figure 5.6). There were no increases observed between PiZ and WT mice regarding these specific inflammatory cells and inflammatory markers, thus implying these changes are all a result of CS.

The chronic inflammatory environment characteristic of COPD was however present in both PiZ and WT mice, and thus it was also key to investigate if this led to any differences in lung function between PiZ and WT mice. Regarding lung function changes, the main focus was to show any changes in lung volume, and of lung resistance and compliance. Two such measures of lung volume measured, include total lung capacity (TLC) and forced vital capacity (FVC) which both increased in PiZ and WT mice due to CS (Figure 5.3A-B). While there was no increase in TLC or FVC in CS PiZ compared to CS WT mice, this finding does still show that PiZ mice are

susceptible to lung damage due to CS, and that this does translate to functional changes.

Included are measurements that show dynamic compliance, resistance and elastance (Figure 5.3 C-E). While these parameters are useful in describing overall the potential deterioration of various lung function parameters in mice, these are of particular interest as they represent and describe the ease at which the lungs can expand and contract, which is particularly useful considering the importance of elastin in the lungs and the relationship between A1AT deficiency and increased elastase, which leads to decreased elastin and increased damage. Since elastin in the lung would be the key reason for any differences in these measurements, it is pivotal that elastase activity as well as A1AT quantity are measured.

With respect to lung function translation to humans, while there is a significant link between A1AT deficiency and COPD, differences may not be statistically significant between all versions or severities of A1AT deficiency, particularly when CS is also a contributing factor. There have been numerous studies that have reported patients with PiMZ (one of the less severe forms of A1AT deficiency as only one gene produced mutated less functional A1AT while the other is fully functional) genotype and PiMM genotype, and there are some varying results. When CS is removed from the equation, comparing PiMM and PiMZ individuals, there is evidence that shows that there is a steeper lung function decline in non-smoking PiMZ patients than in non-smoking PiMM subjects[133].While some measures of spirometry varied in significance between publications, one that was relatively consistent was the decline of the FEV1/FVC ratio. It was also found that the PiMZ genotype was associated with lower FEV1/FVC ratio which correlates in humans with decreased lung function, confirmed in patients by chest CT as having exacerbated emphysema[134]. Hence, the importance of the FEV1/FVC ratio, and thus the importance of measuring FEV1 and FVC. Hence, when discussing these COPD models, it was pivotal to look into FVC. In mice TLC was also measured, which is not possible in humans. It should also be noted that measurements in mice sometimes oppose that in human disease. This is due to differences in spirometry and forced breathing manoeuvres. While there are differences in lung volume and thus deteriorated lung function due to CS, based on the lack of consistent statistic differences in humans with both functional (M) and

dysfunctional (Z) gene, it is not surprising to see no changes in lung function between our Z and WT mice, especially considering our Z mice have some functional mouse A1AT to be protective.

Z A1AT gene resulted in exacerbated emphysema

Canonically in the literature, PiZ mice have been shown to not develop pulmonary pathology owing to the intact functional mouse *Serpina1* genes.[135] However, particularly due to CS, there is a development of some pulmonary pathology.

To analyse alveolar destruction MLI analysis was performed on lung sections. In 8 week PiZ mice there was a significant visual increase in alveolar space. This was quantified by MLI where the bigger the alveolar space, the larger distance between intersections on the grid, correlates to greater alveolar destruction and emphysema. MLI was statistically increased due to CS in PiZ and WT mice, however, there was also a significant increase in PiZ CS mice compared to WT CS mice (Figure 5.2). MLI was pivotal to quantify in this study, as measures of lung structure, particularly alveolar destruction have not been investigated in the CS models in the literature. There has been a study that investigated collagen deposition, in particular collagen I, deposition throughout the lungs, including alveolar septal walls and around airways. There was an increase in collagen deposition in PiZ (PiZ x GFP-LC3 mice) compared to control (GFP-LC3).[136] In our previous chapter collagen deposition around the small airways was analysed, using collagen IV (collagen 4) with no changes found. However, it would be beneficial in future to determine if collagen IV is increased in PiZ mice, as well as collagen I as shown in the literature.

Since increased alveolar destruction was observed in PiZ CS mice, this suggests that the model exhibits increased lung damage in PiZ mice compared to WT. Thus, it can be used as a potential model of A1AT toxicity and CS induced COPD. Hence, it has been shown that alveolar damage is worsened due to the presence of the Z mutation. However, the mechanism of action as to why there is increased emphysema in PiZ mice is somewhat unknown as analysis of certain inflammatory cells, inflammatory markers or lung function parameters were not worsened in PiZ. To confirm this in

future it would be beneficial to conduct a more in depth study on inflammation i.e. flow cytometry panel of basic inflammatory cells e.g. macrophages, neutrophils, B and T cells, DC, eosinophils etc. as well as investigating other inflammatory markers.

PiZ and WT mice showed comparable level of inflammasomes

Regarding inflammatory markers, *IL1*β and *TNF* showed increased gene expression in PIZ and WT CS mice compared to air mice (Figure 5.5 B and D), hence, increased inflammation and increased cytokines due to CS. While the protein quantity of these same markers was analysed, there was no increase in these mice (Figure 5.6A and C). This could be due to some samples fitting below the standard curve, hence readings of zero. It would be beneficial to repeat these findings with high sensitivity CBA kits for these two markers in the future, particularly due to the lack of lung inflammatory data in PiZ mice in the literature. Additionally, there was an increase in both KC quantity (Fig 5.6B) as well as gene expression (Figure 5.5C) in the lungs of PiZ and WT CS mice compared to air. This increase due to CS, highlights KC as a key inflammatory cytokine in CS disease. Interestingly, CXCL15 showed no changes due to CS or PiZ genotype (Figure 5.5A), which was different to the A1AT KO model. This difference between PiZ and A1AT KO cytokine expression was particularly interesting to note. While CXCL15 and KC have both been associated and linked to human IL-8, which is strongly associated with A1AT increased disease pathology via increasing neutrophil chemotaxis, it is interesting to see the potential for a slightly different mechanism being hinted at in this study. There is also a significant increase in mcpt-1 protein in CS mice (Figure 5.6D). The increase in TNF, mcpt-1 shown in our model, seem to be linked to the same mechanism, which also involves IL-6 and NF-κB. However, these increases were present in both PiZ and WT mice exposed to CS, compared to air, and this is not a change specific to the Z genotype. Hence, further investigation into the mechanisms of action are required.

The increase in mcpt-1 is also of particular interest. There was increased mcpt-1 protein due to CS in PiZ and WT mice, however this was not significantly more increased in PiZ compared to WT. It has previously been shown that there was

increased gene expression of mcpt-1 in WT mice after 8 weeks of CS.[120] The literature has shown that this increase in mcpt-1 and TNF could be indicative of the damage caused by Z-A1AT, as the toxic gain-of-function effect of intracellular Z-A1AT not only in hepatocytes, but also in the endoplasmic reticulum of monocytes, as well as neutrophils and alveolar macrophages[137-139], thus activating endoplasmic reticulum (ER) stress, has been previously described[140]. This results in increased levels of inflammatory cytokines and activation of NF-κB signalling[138] as well as a cascade of issues resulting in increased inflammation particularly due to TNF, mcp-1 and IL-6.[70] Additionally, increased Z-A1AT accumulation in neutrophils leads to increased ER stress marker CHOP and TNF, which is responsible for enhanced neutrophil apoptosis[137]. This could even play a role in the neutrophil cell counts (Figure 5.1C), as increased neutrophil apoptosis could explain the less than expected neutrophil infiltration detected in lungs of PiZ mice i.e. less neutrophils to count due to increased death.

PiZ mice show unexpected A1AT protein levels compared to WT mice

Having shown increased alveolar destruction in PiZ mice, the next step was to determine whether this was associated with a difference in elastase activity, as well as a difference in A1AT quantity.

Initially, the observed decrease in elastase activity in all groups except WT air was surprising, as it was expected there would be increased elastase in mice with no or less A1AT as well as in mice with CS. This is because mice with less total A1AT in the lung would have less A1AT to inhibit elastase. It could be due to the increased A1AT present in the lungs that there is no increase in elastase activity. Since this A1AT is most likely to be functional mouse A1AT that is inhibiting the elastase. While a great portion of the study has assumed and described damage as a result of increased neutrophil elastase, all elastase activity was measured, and specific kits or proteomics may shed more light on the behaviour of neutrophil elastase and other specific elastases individually. Based on this finding this may explain the lack of changes in lung function, specifically, elastance, resistance and compliance. While the PiZ mice had increased inflammation and decreased lung function due to CS, the only change

worsened by the presence of the Z genotype was increased alveolar destruction (structural histology changes). This suggests a strong possibility that there are additional mechanisms of action (specific to Z toxicity).

In Chapter 4, it was discussed how no A1AT (A1AT KO) affected elastase. There was a dramatic decrease in A1AT protein in blood samples in PiZ smoke mice comparative to PiZ air mice and also to WT smoke mice (Figure 5.4 A). This shows that in PiZ mice only, there is a significant effect due to smoke but also due to genotype, this result could be due to a combination of both factors. In the lung however (Figure 5.4 B), an increase in A1AT quantity in CS mice was observed. Additional analysis was done to compare the baseline quantity of A1AT in WT and PiZ (air) mice, as a difference to this could be a direct influence of the genetic modification of these mice. It was found there was a significant decrease ($p<0.05$, comparison not shown) in A1AT in the lungs of Air PiZ mice, compared to Air WT mice. Hence, at a baseline at approximately 16 weeks of age, there is less A1AT found in PiZ mice. In CS mice there was no significant difference in A1AT between PiZ and WT mice in the lung, however the circulating A1AT was significantly decreased in PiZ mice, which may link to our initial hypothesis in aim 1, where again it was found that less A1AT in circulation in the blood/blood plasma may result from a greater need for protective A1AT in the lung and hence increased transportation of A1AT to the lungs. Active A1AT readily inhibits elastases in the lung, which cause damage. WT CS, PiZ Air and PiZ CS all had less elastase activity compared to WT Air control group (Figure 5.4 F). Studies have previously shown that exposure to CS decreases A1AT activity in the lungs[141].

Future directions and considerations

While there are not many other published studies on these mice, and even less that include exposure to CS, there are some key findings that shed light to inflammatory changes in the lung. First it is pivotal to compare base differences between the mice. Here, it is important to note that these studies use PiM mice (where PiM mice are genetically modified mice containing a ‘knock in’ of the human M gene – which has human functional A1AT) as a control and not C57BL/6 WT. Regarding studies that describe these significant increases inflammation in PiZ mice comparative to PiM

mice, these findings are comparing a different control group and some discrepancies are expected, as these mice have human A1AT as well as mouse A1AT. They may have other differences, particularly due to genetic modification in the creation of the line, have not been explored, and are beyond the scope of this study, however should not be discounted.

One study showed at baseline intracellular accumulation of misfolded α1-antitrypsin Z in respiratory epithelial cells of the PiZ model resulted in activation of autophagy, and increased leukocyte infiltration compared to WT mice.[136] It must be noted that this was done by measuring CD45+ cells infiltrating the lungs. Additionally, macrophages ($F4/80^{+}$) were not increased, hence the increased infiltration is likely to be from neutrophils, lymphocytes, or other inflammatory cells.[136]

Interestingly, models of smoking regarding PiZ mice do seem somewhat inconsistent, however there are differences in the models, particularly mouse backgrounds, length of time the mice are exposed to CS and methods for analysis. One study where mice received 2 cigarettes/day, 6 days/week over 6 months showed PiZ (heterozygous) mice were not susceptible to emphysema by histological examination.[142] However, PiZ mice (C57Bl/6 background) exposed to just four 1R3F cigarettes daily for 5 days showed lungs exposed to cigarette smoke had a greater influx of pulmonary cytokines, total cells, neutrophils, and macrophages, increased in neutrophil elastase and an exaggerated ER stress compared to PiM mice.[142] Previous studies from this same group showed increased leukocytes in the BALF of both PiZ and PiM (heterozygous) mice (CBA background) exposed to CS, compared to non-smoked controls, which is consistent with our findings. Where this study deviates from our findings is the significant increase in neutrophils in BALF of CS PiZ mice compared with CS PiM mice.[70] This suggests a similar mechanisms to that explored in Chapter 4 on A1AT KO mice, as neutrophil elastase released by degranulated neutrophils is believed to be a main contributor to the pathogenesis of alveolar destruction and emphysema. Hence, it does seem unusual that while there was no statistically significant increase in neutrophil infiltration in the BALF (Figure 5.1), it can still be confidently inferred that findings regarding increased infiltration due to CS, are not only clearly evident in Figure 5.1, but consistent with literature.[70, 136, 142]

The final possibility as to the increased alveolar destruction in PiZ mice in the absence of increase in inflammation in PiZ relative to WT controls, is that 8 weeks of CS may

be too long a time period to see inflammatory changes. Previous studies used mice of comparable age to those used in this study, and yet only smoked mice for 5 days, using significantly less cigarettes (4 cigarettes per day, compared to 24/day). This leads us to hypothesise that perhaps this was too long of an exposure, as A1AT deficiency related COPD is suggested to cause a more rapid decline of the lungs (than systems with A1AT). This suggests that PiZ mice may have experienced an early 'peak' in inflammation, e.g. an earlier timepoint of 1 or 2 weeks, and that WT mice may have less inflammation than PiZ mice at this earlier timepoint. This would not be too unusual as in Chapter 4, where A1AT KO and WT C57Bl/6 mice were studied it was noted that inflammation varied between timepoints. Specifically, total leukocytes in the BALF peaked at 8 weeks for A1AT KO mice exposed to CS, compared to a somewhat delayed peak observed in WT control mice exposed to CS, which peaked at 4 weeks. Hence, it may be beneficial to run a shorter 1 or 2 week model in the future.

It should also be noted that while the changes observed in this model while quite interesting, the disease progression of A1AT KO mice (Chapter 4) was more consistent and hence those mice were analysed further and deemed a better model overall to investigate A1AT deficiency and CS for this thesis. It was also deemed that the A1AT KO mice were the optimum for any future drug or genetic treatments, particularly due to the fact that the PiZ mice seemed more complex, and more appropriate in studies of A1AT toxicity. However, it is pivotal not to discount the usefulness of the PiZ mice, given more time and resources, it would be beneficial to continue to study these mice as explored in future directions.

Conclusion

The aim of this chapter was to understand the behaviours of the Z mutation of A1AT deficiency as well as cigarette smoke exposure. To achieve this, an animal model was utilised. While PiZ mice and short term models of CS exposure have previously been conducted, this model sought to use PiZ mice (two copies of the Z mutation) as well as a longer term model of 8 weeks of exposure to CS.

The aim was to describe inflammatory, functional and structural changes after 8 weeks of CS. It was discovered that while there were functional, structural and inflammatory changes to the PiZ mice, this was due to the CS and not significantly different to WT mice, aside from increased alveolar destruction by MLI.

Additional changes were recorded to A1AT protein and elastase activity, which showed PiZ CS mice had decreased circulating A1AT and increased lung A1AT, suggesting increased migration of A1AT to the lung. Elastase over-activity and lack of inhibition by A1AT has been shown to be relevant to disease progression, i.e. emphysema, particularly in A1AT deficiency. Interestingly, this was not seen in this project, and elastase is not responsible for the damage observed in this model. At this timepoint at least, elastase damage was a minimal contributor to lung damage in this model, and this may be confirmed by the lack of lung function changes in measures of resistance, compliance and elastance, as these are linked to lung elastin.

Additionally, another goal of this chapter and the previous on A1AT KO mice, was to establish a combined A1AT deficiency PiZ model and cigarette smoke exposure model as a platform that can be used in future to test therapies that included the most common mutation in human patients, being the Z mutation. While the Z mice alone show liver issues indicative of that occurring in humans, the lung issues were non-existent until CS exposure to these mice. While it was initially hoped that prolonged exposure would lead to more damage with time, this was unfortunately not the case, compared to the literature. This in itself is an interesting if slightly unexpected finding, and led to the suggestion that while the PiZ mice may get worsened disease with prolonged CS, this is not significantly different to WT mice that are exposed to CS, most likely due to the still active mouse A1AT the mice still produce, as while A1AT quantity varied between PiZ air and PiZ CS mice, interestingly elastase activity did not.

However, as a mouse model for the lung phenotype it is still considered somewhat effective. While there is only increased alveolar destruction due to the Z genotype, with the addition of CS exposure, PiZ mice had increased inflammation and decreased lung function compared to PiZ air, or WT air.

Chapter 6 – Aim 4

Introduction

Chronic inflammation is an important characteristic of COPD that causes lung damage and impaired lung function in patients. Increased number of dendritic cells (DCs) is a critical factor contributing to the development of COPD. While this increase in DCs could initially be thought of as beneficial, they actually initiate and contribute to the chronic inflammatory state of COPD by activating other inflammatory cells including macrophages, neutrophils, and T and B lymphocytes, as well as cytokines, leading to damage. [43, 143]

Details of the A1AT KO mice were previously reported in chapter 4, Aim 2, which provided an additional rationale for this chapter. One such finding was that involving inflammation and DCs (summarised in this paragraph). Previous investigations and characterisation of the inflammatory profile in A1AT KO mice exposed to CS highlighted a dynamic inflammatory profile over time. While A1AT KO inflammation was determined to be predominantly neutrophil driven, there was an interesting and unexpected finding involving DCs. When exposed to CS, DCs increased WT mice compared to A1AT KO mice, specifically, increased circulating DCs after 4 weeks, and increased DCs in the lung at 8 weeks of CS exposure. Of particular interest however was the increase in WT CS mice compared to A1AT KO CS mice. This suggests a potential mechanism involving A1AT, i.e. A1AT specific effect of DCs.

DCs are antigen-presenting cells that are pivotal to the detection of pathogens and initiating and regulating the immune response. While DCs are typically associated with T lymphocytes, due to their ability to capture, process and present antigens to lymphocytes, and thus initiating their adaptive immune response, their immune regulating role is not only limited to T cells.[144] Airway and lung DCs can activate a number of inflammatory and immune cells such as neutrophils, macrophages, and T and B lymphocytes, in response to inhaled irritants.[37]

DCs are not well understood as their development and maturation is complex. When studying and discussing DCs, it is essential to understand the subcategories of DCs. Conventional dendritic cells (cDC) are antigen presenting cells located in the lymph nodes and the majority of tissues where they regulate the innate and adaptive immune response.[145] Within this category are cDC1 and cDC2 dendritic cells, with cDC1 expressing XCR1 and cDC2 expressing CD11b and CD172a (as less specific defining markers).[129, 145] Additionally, cDC1 are predominantly associated with priming NK cells and cytotoxic T cells, and regulating immune response, whereas cDC2 is predominantly associated with priming helper T cells.[145-147] Plasmacytoid dendritic cells (pDC) secrete type 1 interferons (IFNs) and are important in the immune response. They can also become antigen presenting cells, as they promote an immune response due to viruses.[145, 148] Finally, there are also the DC3 subset of DC which show a phenotypic relation to monocytes and cDC2s but are developmentally different.[149] cDCs have been more commonly linked to COPD and are hence the focus of this study.

There are also various states of cDC referring to their different phenotypic activation i.e. mature (activated) or immature (resting/non activated) DC states. DC maturation is different but often confused (or used synonymously) with DC differentiation. While differentiation refers to the developmental transition from DC progenitors (common DC precursor, pre-DC) to fully differentiated immature DC in the periphery, that reside in lungs, brain, etc., or in the lymph nodes as resident immature DC.[129] DC maturation is an activation process that happens after differentiation. During this process fully developed yet immature DC switches from an antigen sampling sentinel mode to antigen presenting and transmitting.[129]

Of particularly interest, is the increase in DCs in WT CS mice compared to A1AT KO CS mice, which suggests a potential effect of A1AT specific to DCs. While there have been some studies regarding the impact of A1AT on DC function and activation, the change in DC population pertaining to A1AT deficiency and COPD is severely under investigated. Hence, the need for a basic characterisation of DCs regarding changes in DC concentration in circulation, lung and BALF, as well as changes in differentiation, mortality and migration.

In order to achieve this, both in vivo and in vitro (ex vivo) methods were utilised to allow to directly link the findings of DCs in the cell culture to in vivo immune responses. An 8 week CS mouse experiment was repeated using WT and A1AT KO mice. Inflammatory cells retrieved in BALF, isolated lung cells, and blood cells were analysed in flow cytometry. From this model, bone marrow was collected and BMDCs cultured, and subsequently tested to investigate differentiation, mortality and migration.

Results

Increased inflammatory response was observed in BALF following CS exposure

In this chapter, A1AT KO mice and WT controls were again exposed to air/CS for 8 weeks in an experimental model of A1AT deficiency and CS induced COPD. Inflammation was assessed in BALF, lung and blood. To assess inflammation in the bronchoalveolar space, BALF was once again collected and total leukocytes enumerated. Figure 6.1 shows enumeration by hemocytometer (Figure 6.1 A) and by flow cytometry using live dead stain to determine total live cells (Figure 6.1B).

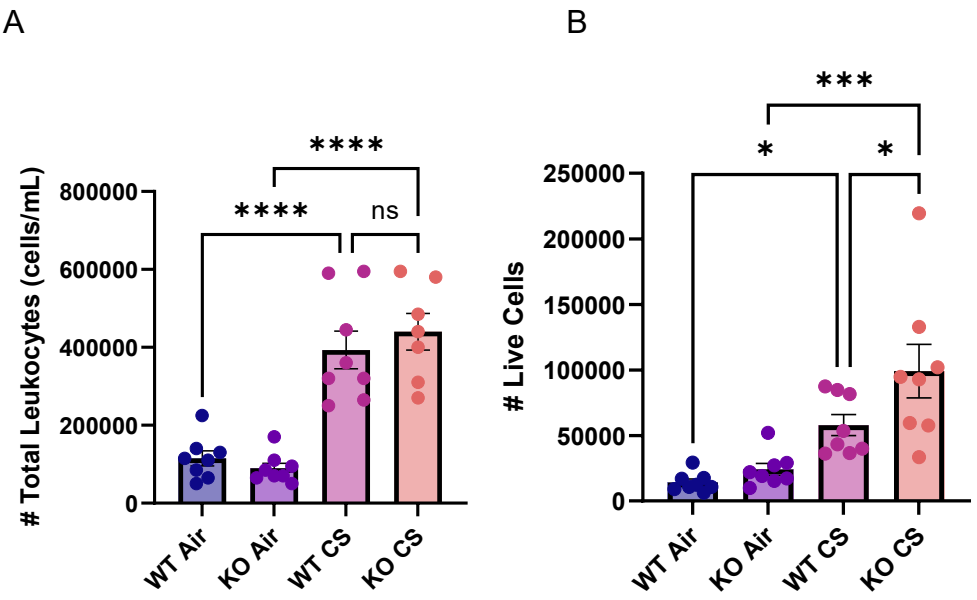

Figure 6.1: Enumeration of total leukocytes in the BALF.

*BALF was collected from WT and A1AT KO mice exposed to CS/Air for 8 weeks. Total Leukocytes were enumerated using a hemocytometer and displayed as A) Total leukocytes in the BALF in cells/mL and as B) Total leukocytes were also measured using flow cytometry, as a measure of total live cells. N=8. Results are mean ± SEM. ns = p>0.05, * p<0.05, ** p<0.01, *** p<0.001, **** p<0.0001. Statistical difference was determined with Ordinary One-Way ANOVA with Bonferroni's multiple comparisons.*

Inflammatory cell infiltrate into the lung bronchoalveolar space is a key indicator of inflammation in COPD. This increase in total leukocytes was also shown previously (Chapter 4, Aim 2) in that inflammatory cells increased in the BALF i.e. increased total leukocytes due to CS exposure in WT and A1AT KO mice as well as increased total leukocytes in A1AT KO CS mice compared to WT CS mice at 8 weeks. This was reproduced in this model, evident in Figure 6.1 A-B which showed increased total leukocytes due to CS, in both WT and A1AT KO mice. Interestingly, when cells were enumerated using flow cytometry, an increase in A1AT KO smoke mice was observed compared to WT smoke mice (Figure 6.1B).

In addition to this increase in total leukocytes in response to CS, there were also increased neutrophils, eosinophils, cytotoxic T cells and helper T cells (Figure 6.2).

Interestingly, and potentially contradictory to previous findings (chapter 4 Aim 2), alveolar macrophages were decreased in both A1AT KO and WT CS samples.

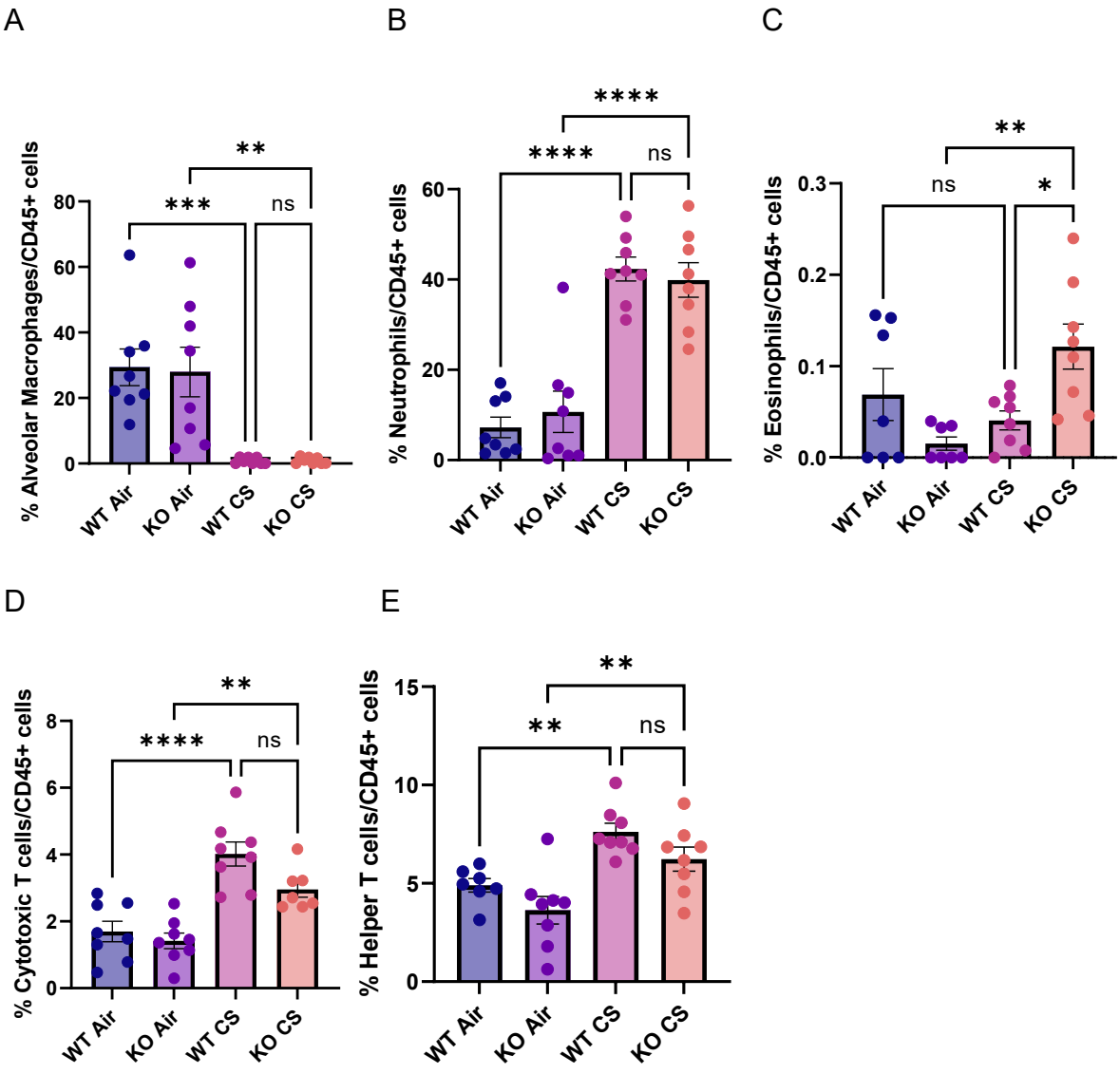

Figure 6.2: Percentage of inflammatory cells increased in BALF due to CS.

*BALF was collected from WT and A1AT KO mice exposed to CS/Air for 8 weeks. Inflammatory cells were assessed by flow cytometry and plotted as percentages of total CD45+ cells. A) Alveolar macrophages were decreased in CS samples. However, all other key inflammatory cells increased in A1AT KO CS samples, notably: B) Neutrophils, C) Eosinophils, D) Cytotoxic T cells and E) Helper T cells. N=8. Results are mean ± SEM. ns = p>0.05, * p<0.05, ** p<0.01, *** p<0.001, **** p<0.0001. Statistical difference was determined with Ordinary One-Way ANOVA with Bonferroni's multiple comparisons.*

DC increased in BALF and lung following CS exposure

DCs were characterised, including circulating, lung and BALF infiltration. Circulating DC (in the blood) were for the most part, unchanged due to CS, with both A1AT KO and WT CS mice comparable to air. The only increases in DCs was due to CS, and were in the percentage of cDC1 (in both A1AT KO and WT) and cDC2 increase in WT CS (Figure 6.3 B-C). On the other hand, changes due to CS in the lung and BALF were much more significant. Dendritic cells were increased in the lungs and BALF of CS mice, specifically, cDC1 and cDC2 (Figure 6.4 and 6.5). There was also a visible increase in cDC1 and cDC2 migratory ($CD103^{+}$) cells in the lungs of CS mice. The most interesting and elucidating finding however, was the increase in cDC1 and migratory cDC1 cells in response to A1AT KO CS mice comparative to WT CS mice. This finding is of particular interest as cDC1 cells are associated with cytotoxic T cells and regulating immune response.

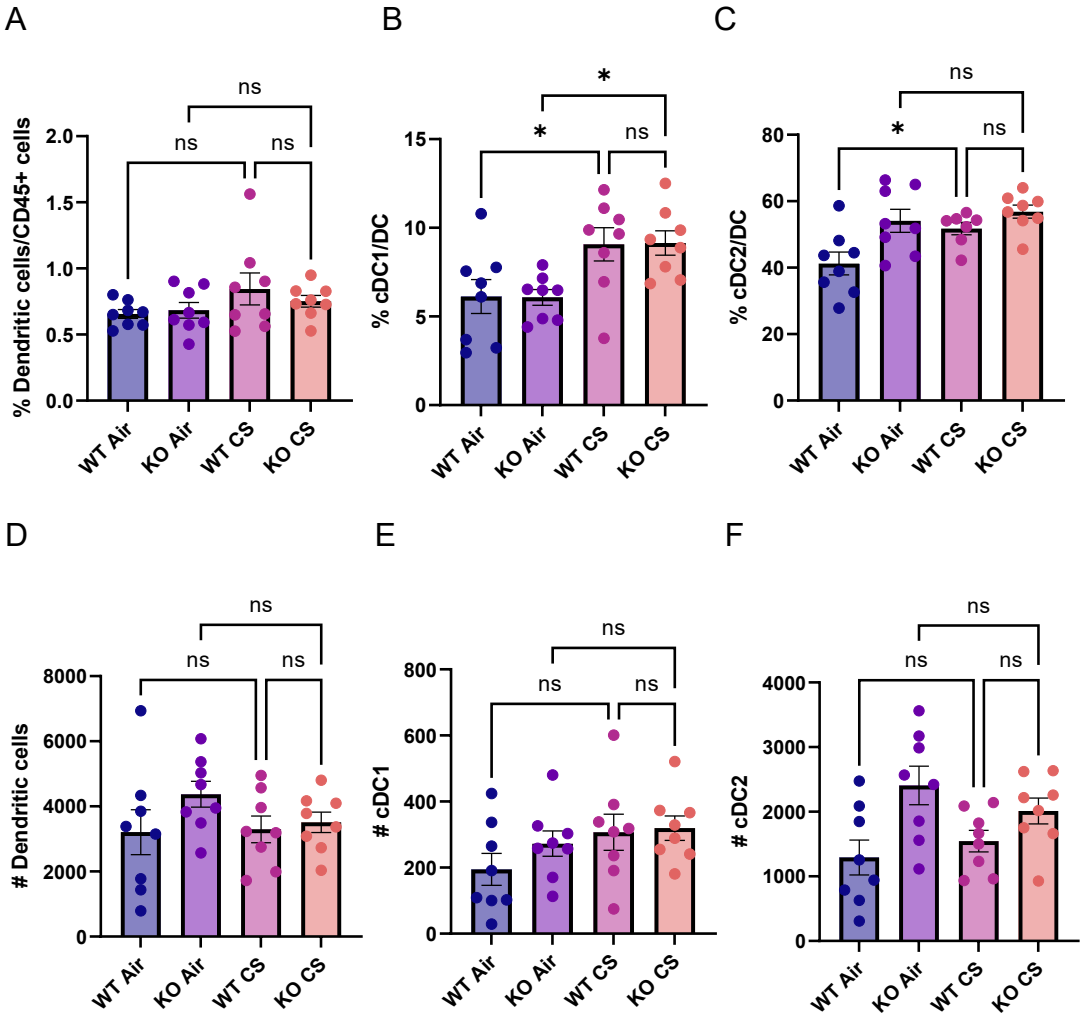

Figure 6.3: No change in circulating DCs in the blood following eight weeks of cigarette smoke.

*DC were measured in blood samples collected from WT and A1AT KO mice exposed to CS/Air for 8 weeks. A) DC were assessed by flow cytometry and plotted as percentages of total CD45+ cells. B) cDC1, and C) cDC2 were also assessed and plotted as a percentage of total DCs. D) The number of DC (#DC), E) cDC1, and F) cDC2 calculated and graphed. N=8. Results are mean ± SEM. ns = p>0.05, * p<0.05, ** p<0.01, *** p<0.001, **** p<0.0001. Statistical difference was determined with Ordinary One-Way ANOVA with Bonferroni's multiple comparisons.*

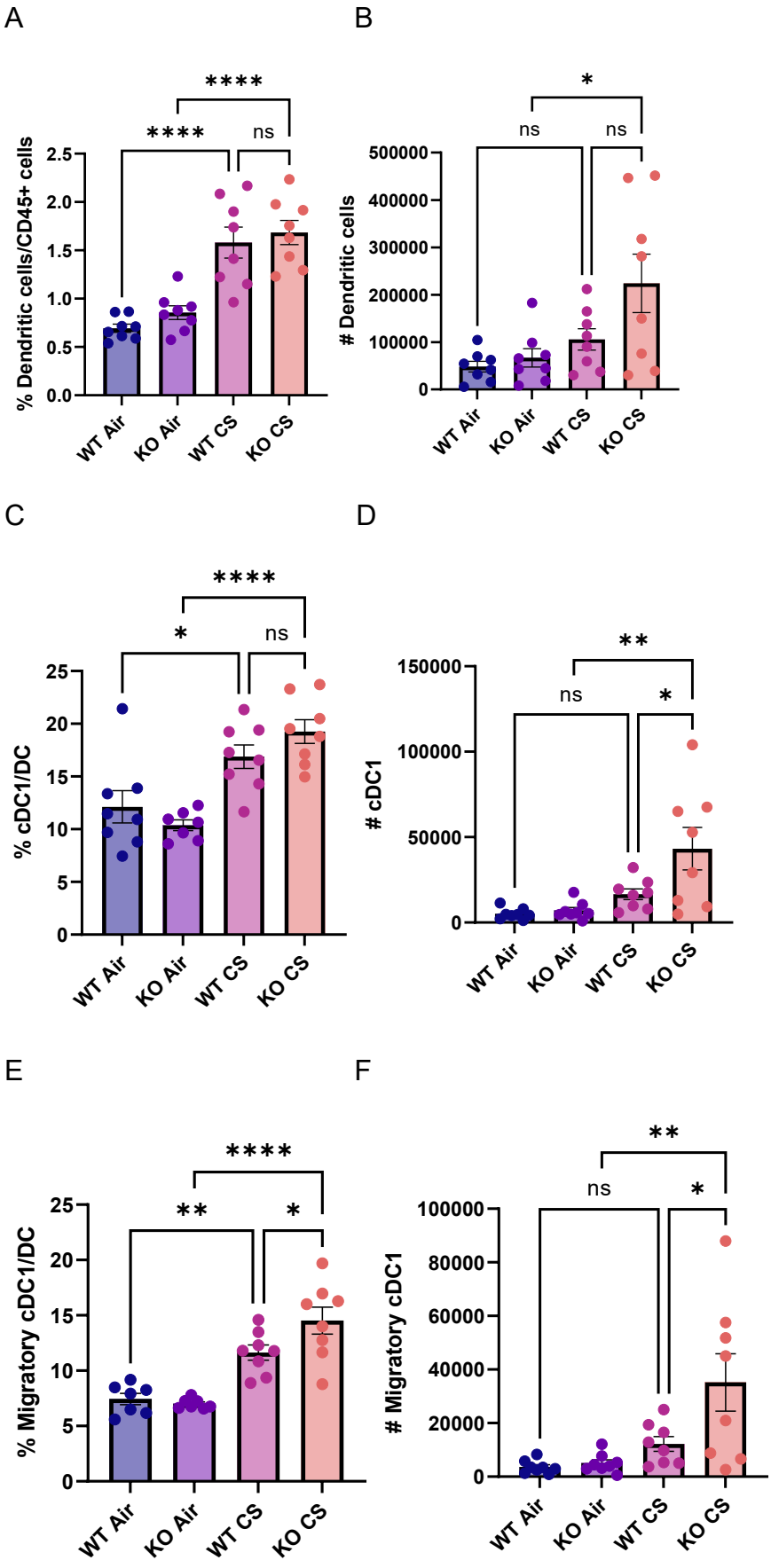
A
B
C
D
E
F
% Dendritic cells/CD45+ cells
# Dendritic cells
% cDC1/DC
# cDC1
% Migratory cDC1/DC
# Migratory cDC1
WT Air
KO Air
WT CS
KO CS
****
ns
*
**

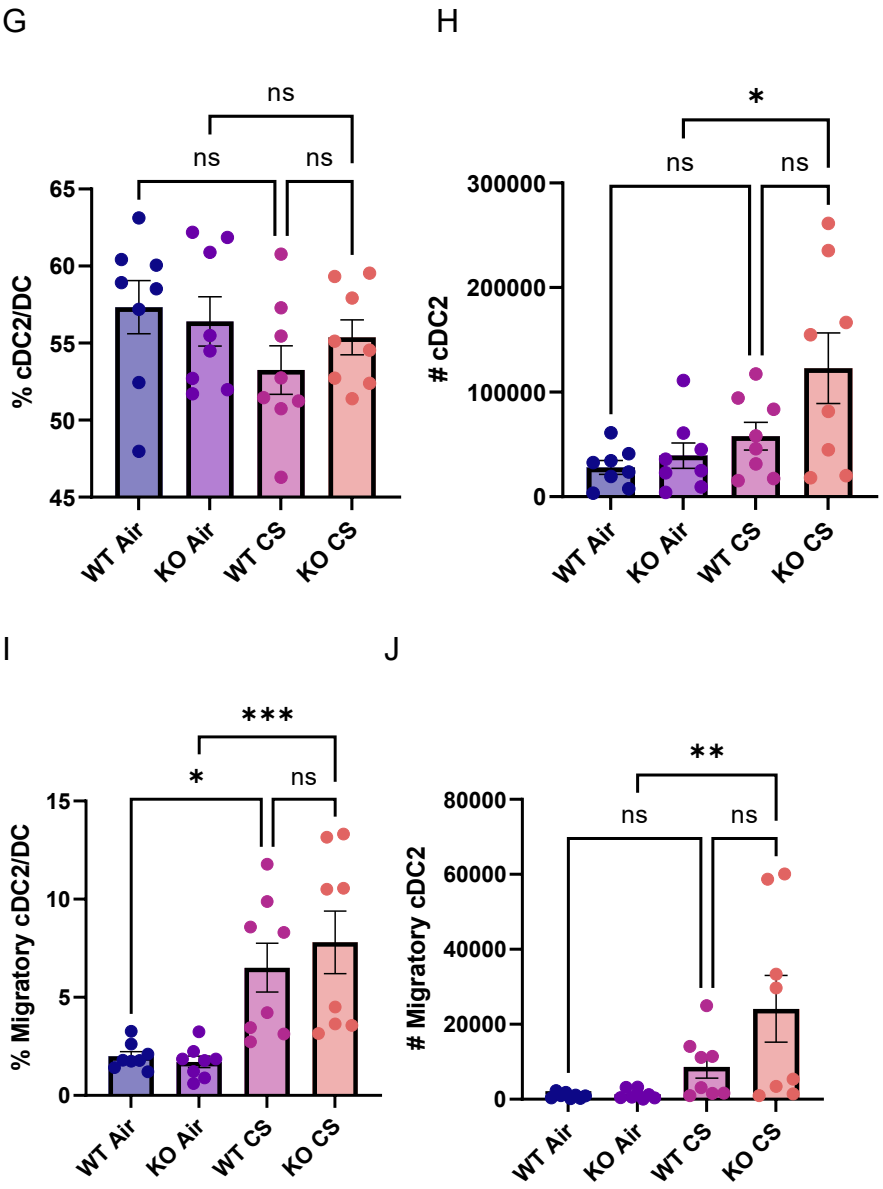

Figure 6.4: Increase of DCs in the lung tissue following eight weeks of cigarette smoke.

*DC were measured in lung tissue collected from WT and A1AT KO mice exposed to CS/Air for 8 weeks. A) DC were assessed by flow cytometry and plotted as percentages of total CD45+ cells, B) and as total number. Additionally, C-D) cDC1, E-F) Migratory cDC1, G-H) cDC2, I-J) Migratory cDC2. N=8. Results are mean ± SEM. ns = p>0.05, * p<0.05, ** p<0.01, *** p<0.001, **** p<0.0001. Statistical difference was determined with Ordinary One-Way ANOVA with Bonferroni's multiple comparisons.*

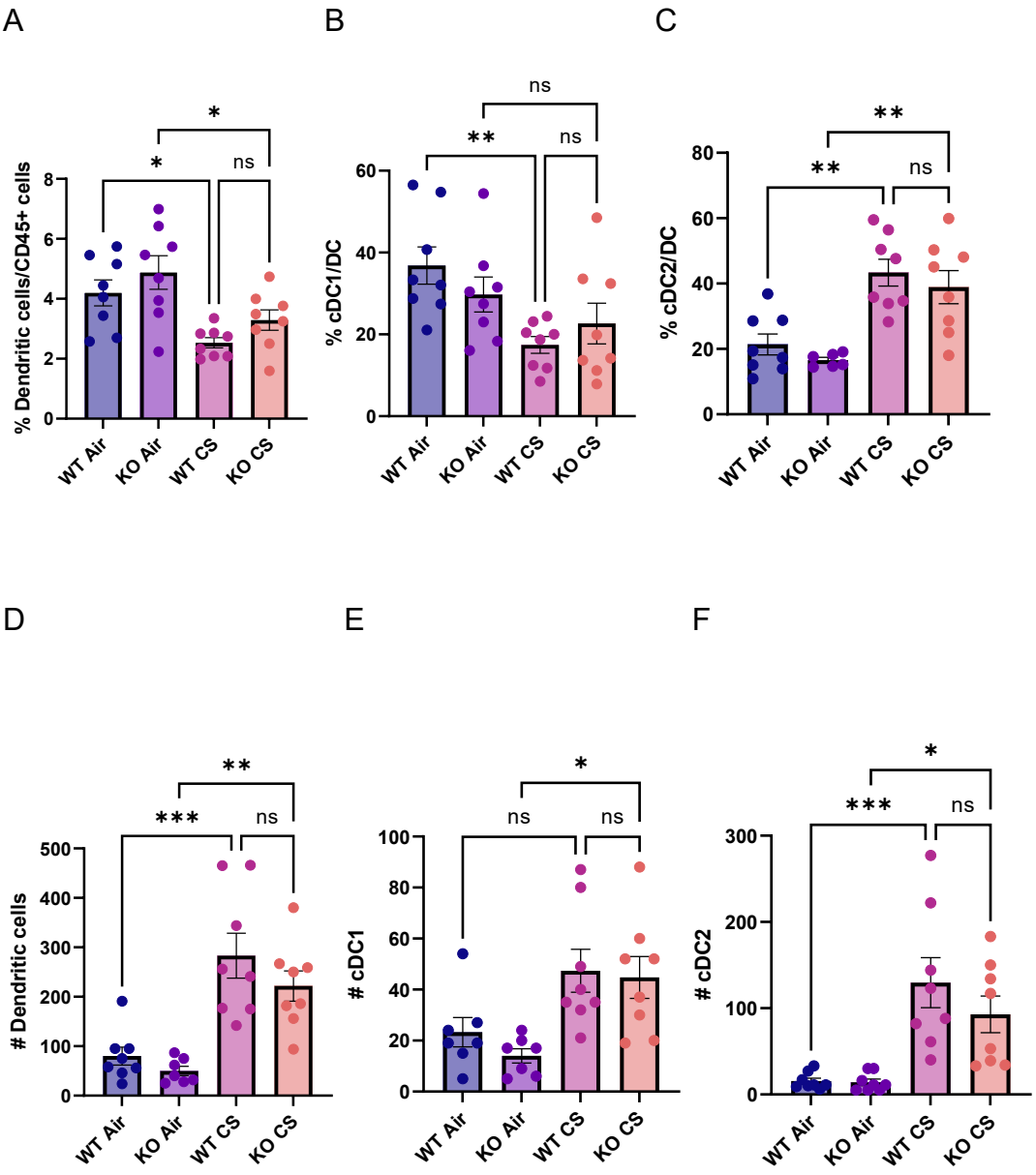

Figure 6.5: Increase of DCs in bronchoalveolar space following eight weeks of cigarette smoke.

*DC were measured in BALF collected from WT and A1AT KO mice exposed to CS/Air for 8 weeks. A) DC were assessed by flow cytometry and plotted as percentages of total CD45+ cells. B) cDC1, and C) cDC2 were also assessed and plotted as percentages of total DCs. E) Calculated and graphed number of DC (#DC), F) cDC1 and G) cDC2 . N=8. Results are mean ± SEM. ns = p>0.05, * p<0.05, ** p<0.01, *** p<0.001, **** p<0.0001. Statistical difference was determined with Ordinary One-Way ANOVA with Bonferroni's multiple comparisons.*

BMDCs derived from A1AT KO CS mice showed similar ability to differentiate compared to controls

To better explore the changes in DC, bone marrow was collected, processed and supplied with GM-CSF for differentiation into DC, i.e. bone marrow derived dendritic cells. Bone marrow cells were harvested from all four mouse groups, WT Air, A1AT KO Air, WT Smoke and A1AT KO Smoke. This was done to determine if bone marrow derived dendritic cells from the four mouse groups demonstrated similar ability to differentiate and/or develop.

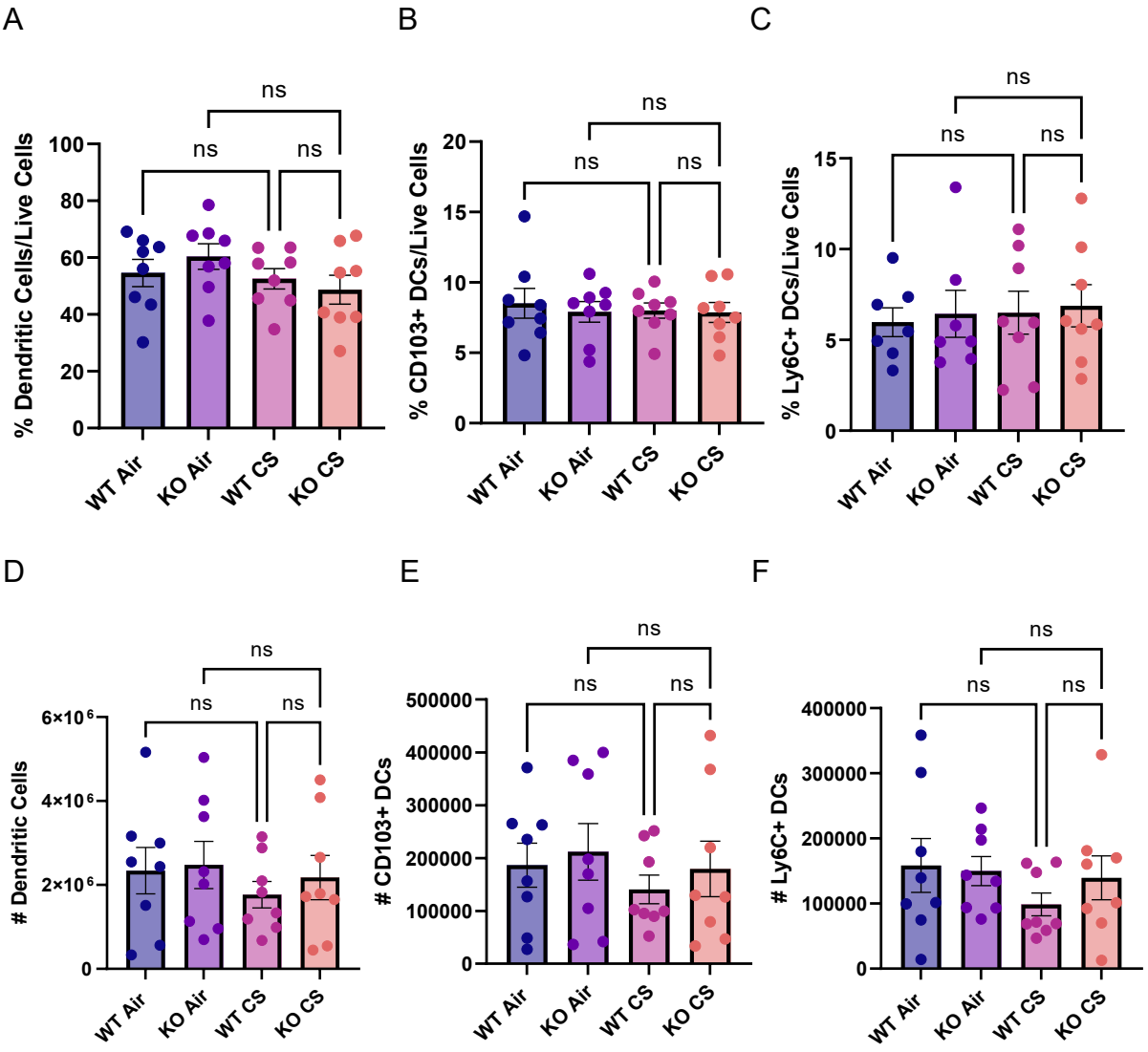

Figure 6.6: Differentiation of DC, ex vivo i.e. BMDC differentiation following eight weeks of cigarette smoke.

*Bone marrow was collected from WT and A1AT KO mice exposed to CS/Air for 8 weeks, and differentiated ex vivo with GM-CSF. A) DC, B) CD103+ DC and C) Ly6C+ DC, were assessed by flow cytometry and plotted as percentages of total Live cells. D) Calculated and graphed number of DC, E) CD103+ DC and F) Ly6C+ DC were also. N=8. Results are mean ± SEM. ns = p>0.05, * p<0.05, ** p<0.01, *** p<0.001, **** p<0.0001. Statistical difference was determined with Ordinary One-Way ANOVA with Bonferroni's multiple comparisons.*

The abundance of DCs, after 8 days of GM-CSF stimulated culture from bone marrow cells, remained constant across all groups. There were no changes to DC across genotype or CS exposure. This was also observed in $CD103^+$ and $Ly6C^+$ subsets of DC.

BMDCs showed similar viability in response to LPS or CSE treatment but increased migration following LPS.

BMDC mortality in response to LPS and CSE exposure was also investigated using a lactate dehydrogenase (LDH) assay. There were no statistically significant changes in mortality due to CSE or LPS evident in Figure 6.7.

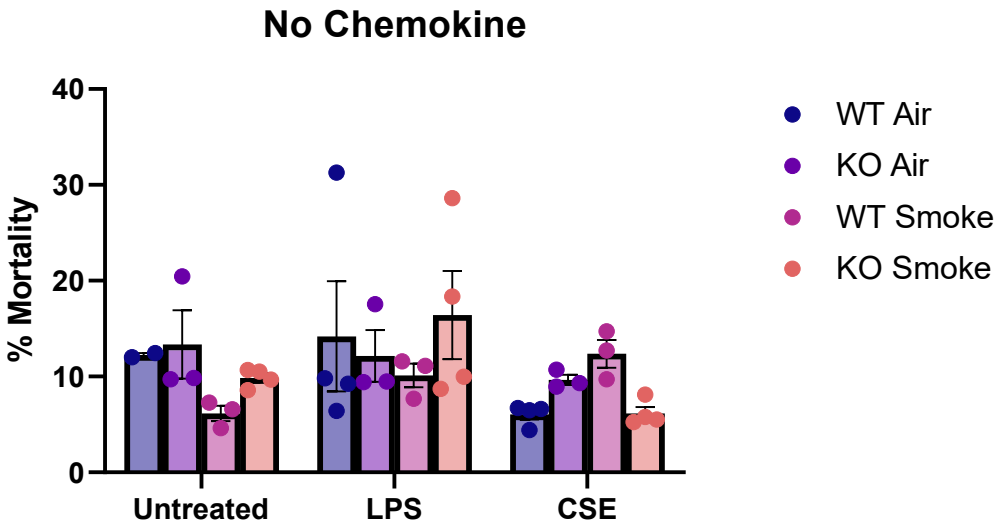

Figure 6.7: Mortality of BMDC upon exposure to LPS and CSE.

Post 18h stimulation with CSE or LPS, and migration assay with relevant chemokine (in this case with no chemokine in the lower compartment), the cells remaining in the upper compartment were used to calculate mortality. There were no significant changes due to stimulation or mouse group. N=3-4. Results are mean ± SEM. ns = p>0.05, Statistical difference was determined by Ordinary two-way ANOVA, full model.

BMDC were also used to determine differences in the migration of DCs due to the mouse group (WT/A1AT KO and Air/CS) as well as those due to treatment that BMDCs were exposed to prior to the migration assay (untreated, LPS, CSE). LPS is used as a positive control as it has been consistently shown in the literature to stimulate immune cells thus triggering an inflammatory response.

In LPS stimulated cells there was a significant variation due to the chemokine and mouse BM donor group. Specifically, when Ccl19 was used as the chemokine to induce migration to the lower chamber there was a visible decrease compared to the Ccl21 and even to the migration with no chemokine (Figure 6.8 A-C)

To show this more clearly, these values were also plotted by chemokine. In all three Chemokine graphs, i.e. no chemokine, Ccl19, and Ccl21 (Figure 6.8 D, E and F

respectively) there is a significant variation due to stimulation, specifically significant increases in LPS relative to untreated and CSE treated samples.

Interestingly, in the no chemokine samples, there was also significant variance attributed to mouse group, as there was increased migration in cells of smoke mice exposed to LPS compared to air mice exposed to LPS.

A

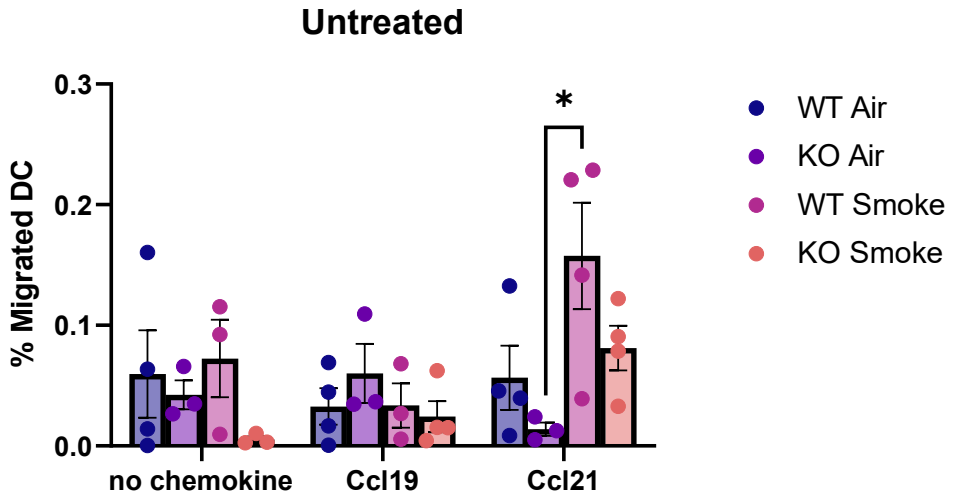

B

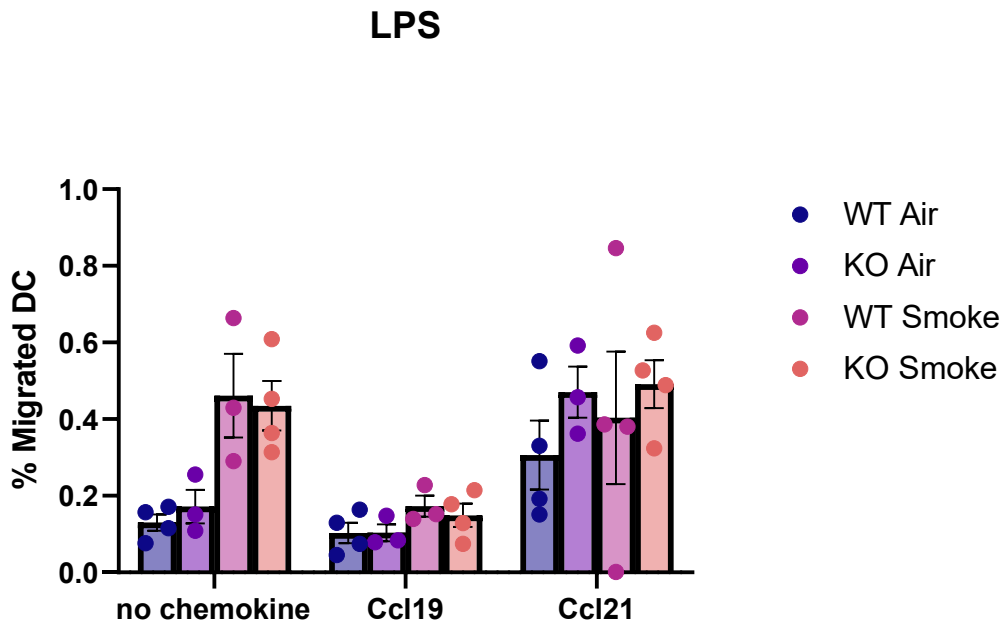

C

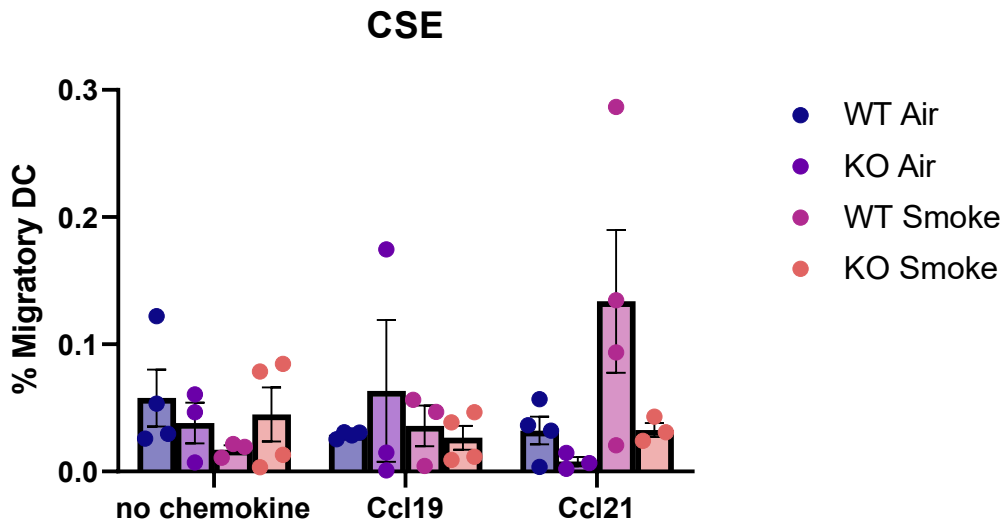
CSE
% Migratory DC
0.3
0.2
0.1
0.0
no chemokine
Ccl19
Ccl21
WT Air
KO Air
WT Smoke
KO Smoke

D

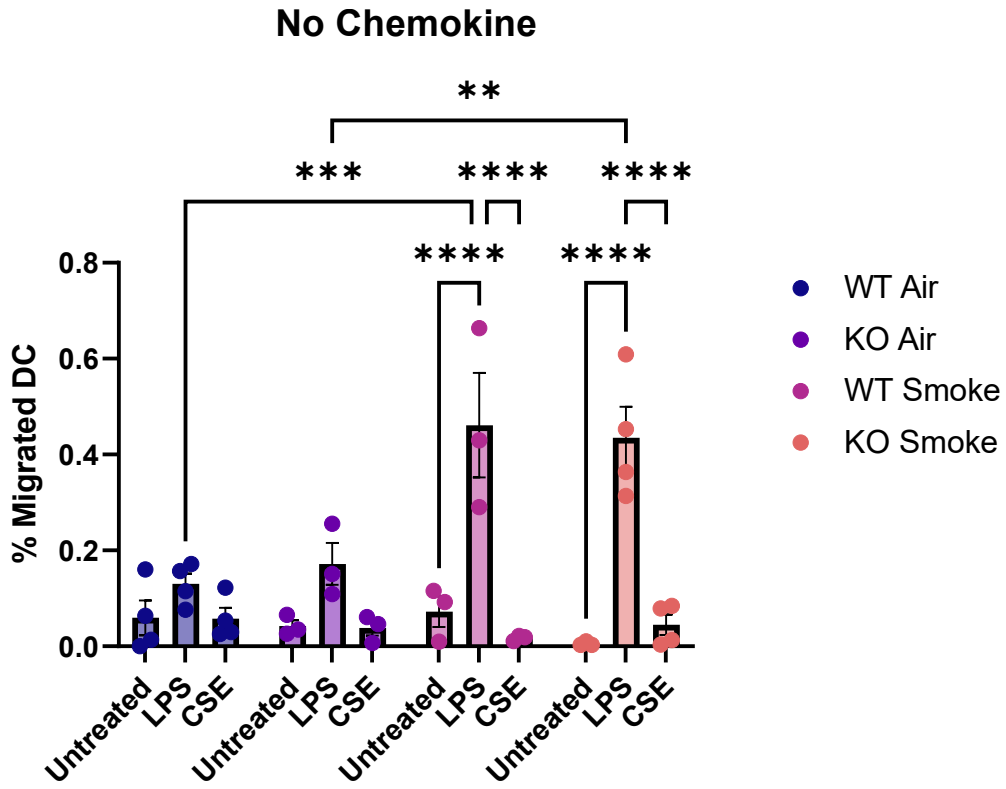
No Chemokine
**
***
****
****
****
****
% Migrated DC
0.8
0.6
0.4
0.2
0.0
Untreated
LPS
CSE
Untreated
LPS
CSE
Untreated
LPS
CSE
Untreated
LPS
CSE
WT Air
KO Air
WT Smoke
KO Smoke

E

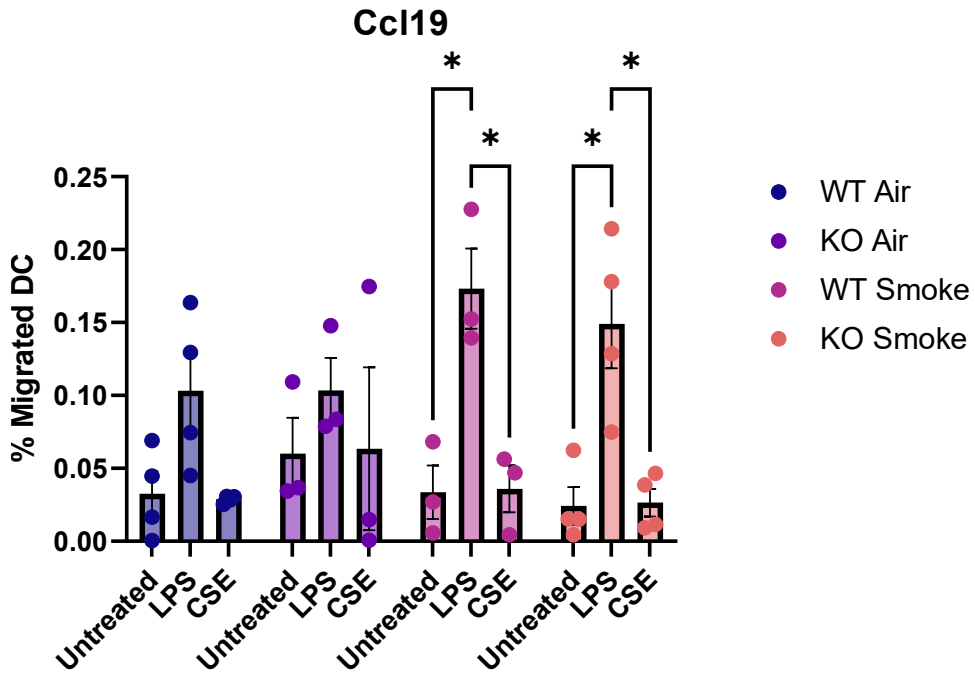
Ccl19
% Migrated DC
0.25
0.20
0.15
0.10
0.05
0.00
*
*
*
*
Untreated
LPS
CSE
WT Air
KO Air
WT Smoke
KO Smoke

F

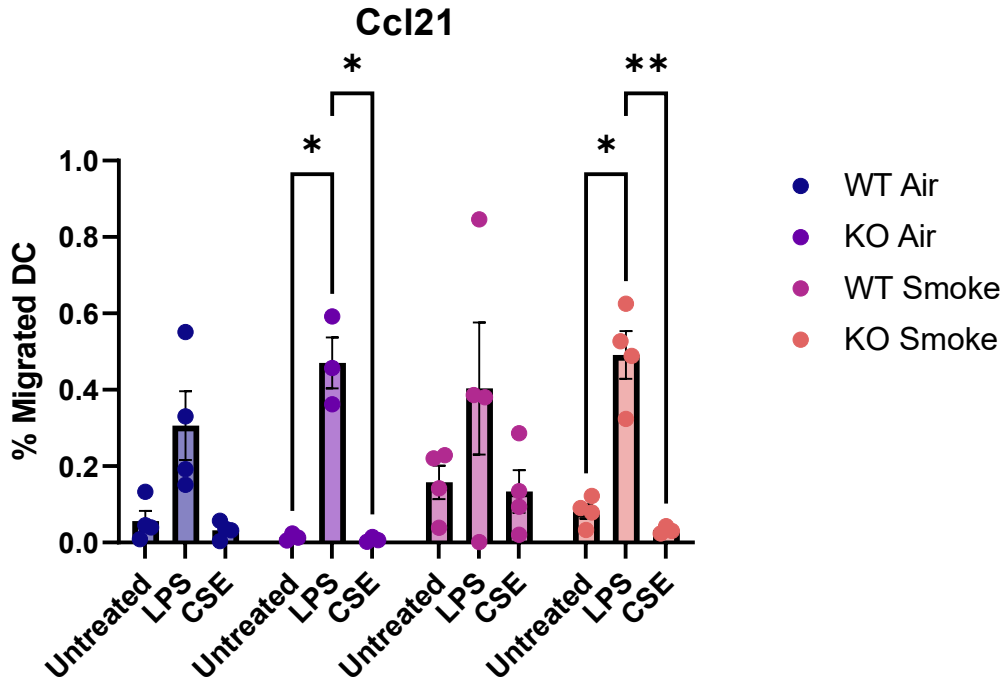
Ccl21
% Migrated DC
1.0
0.8
0.6
0.4
0.2
0.0
*
*
*
**
Untreated
LPS
CSE
WT Air
KO Air
WT Smoke
KO Smoke

Figure 6.8: Migratory ability of BMDC, specifically DC upon exposure to LPS and CSE.

Post 18h stimulation with no treatment (untreated), CSE or LPS, and migration assay with relevant chemokine, the cells that migrated to the lower compartment were collected, stained, and analysed by flow cytometry.

Percent migrated DC. To clearly outline the source of significant variation in groups as a response to Chemokine and donor mouse i.e. genotype and presence or absence of CS, values were plotted with A)Non stimulated cells, which showed no source variation B) LPS stimulated cells which showed Significant variation attributed to Chemokine (34.38% of total variation p <0.0001), and by Mouse Group (14.36% of total variation p=0.0232), C) and CSE stimulated cells, which showed no source variation by Ordinary two-way ANOVA, full model.

To clearly see and compare any changes due to stimulation, and donor mouse, values were also graphed by chemokine. D) Shows the migrated DC from non- chemokine samples, in order to clearly see and compare any changes due to stimulation, and donor mouse group. There was significant variation between groups due to Stimulation (responsible for 54.58% of total variation p <0.0001) by mouse group (responsible for 7.518% of total variation p=0.0098) as well as due to the combined interaction of Stimulation and mouse group (21.77% of total variation p=0.0002), E) Ccl19, where the only significant source of variation was from the different Stimulations (50.72% of the total variation p<0.0001), and F) Ccl21 where again the only significant source of variation was attributed to Stimulation (62.58% p<0.0001). N=3-4. Results are mean ± SEM. Statistical difference was determined by Ordinary two-way ANOVA, full model, with Bonferroni's multiple comparisons.

BMDCs showed increased inflammatory markers in response to LPS

Investigation of inflammatory cytokines showed an increase in TNF, IL1β, KC, and IL6 due to LPS (Figure 6.9). There were also changes in mouse group, notably, an increase in TNF in LPS CS mice particularly in A1AT KO which was significantly higher than WT.

A

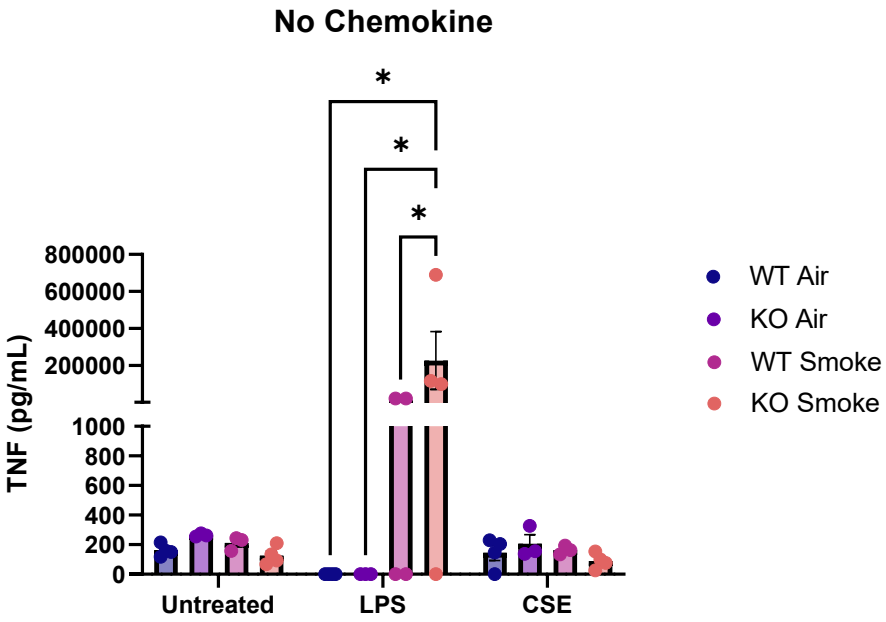
No Chemokine
TNF (pg/mL)
800000
600000
400000
200000
1000
800
600
400
200
0
Untreated
LPS
CSE
*
*
*
WT Air
KO Air
WT Smoke
KO Smoke

B

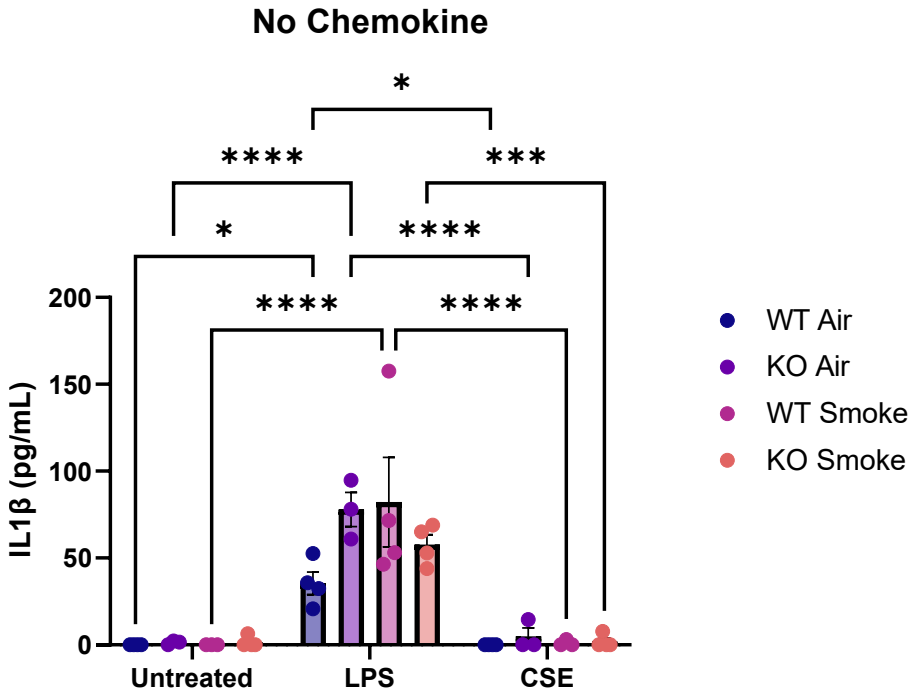
No Chemokine
IL1β (pg/mL)
200
150
100
50
0
Untreated
LPS
CSE
*
****
***
*
****
****
****
WT Air
KO Air
WT Smoke
KO Smoke

C

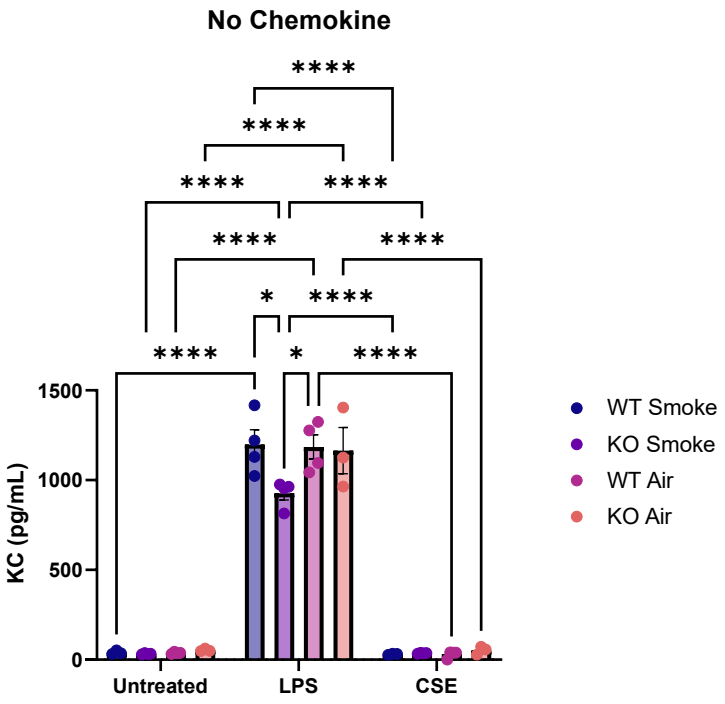
No Chemokine
****
****
****
****
****
****
*
****
****
*
****
1500
1000
500
0
KC (pg/mL)
Untreated
LPS
CSE
WT Smoke
KO Smoke
WT Air
KO Air

D

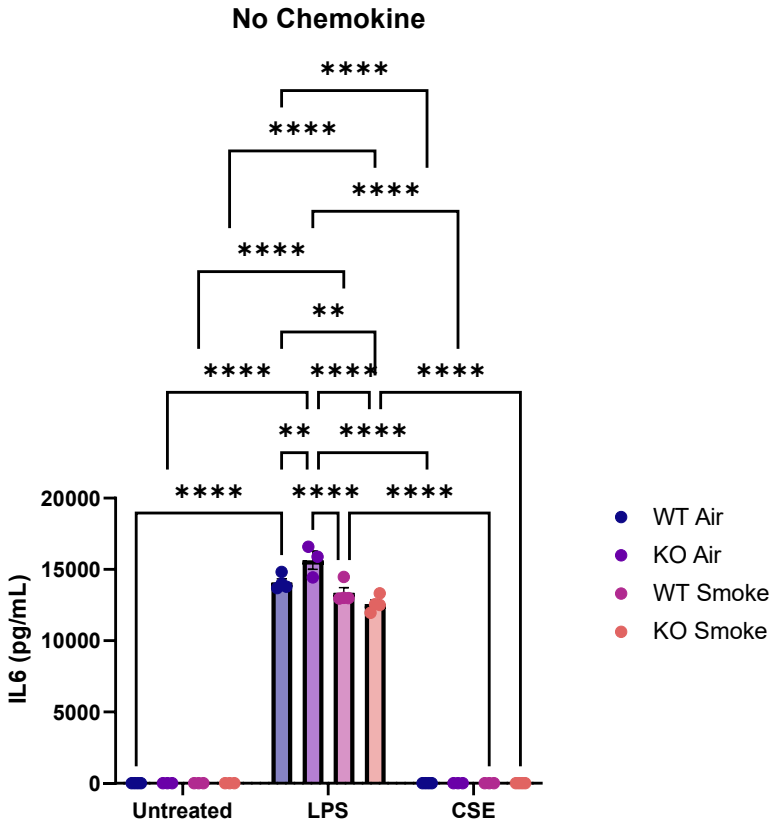
No Chemokine
****
****
****
****
**
****
****
**
****
****
****
****
20000
15000
10000
5000
0
IL6 (pg/mL)
Untreated
LPS
CSE
WT Air
KO Air
WT Smoke
KO Smoke

Figure 6.9: Migratory ability of BMDC, specifically DC upon exposure to LPS and CSE.

Post 18 h stimulation with no treatment (untreated), CSE or LPS, and migration assay with relevant chemokine, the cells that migrated to the lower compartment were collected, stained, and analysed by flow cytometry. Protein quantities of A) TNF, B) IL1β, C) KC and D) IL6 were assessed by CBA. N=3-4. Results are mean ± SEM. Statistical difference was determined by Ordinary two-way ANOVA, full model, with Bonferroni's multiple comparisons.

Discussion

Increased inflammatory response was observed in BALF following CS exposure

While the immune cell profile of A1AT KO mice exposed to air/CS compared to WT mice has previously been discussed and investigated (notably in Chapter 4, Aim 2), in this chapter additional immune cells in the BALF were investigated. It was discovered that generally, these findings are consistent with the literature, however, there are some interesting differences.

One such finding that is consistent with the literature is the increased, total leukocytes in the BALF. From enumeration by both haemocytometer (Figure 6.1 A-B) and by flow cytometry (Figure 6.1 C), there was an increase in total leukocytes due to CS. Furthermore, by flow cytometry, there was a significant increase in total leukocytes in A1AT KO CS mice compared to WT CS, thus, showing increased inflammatory cells due to CS and due to A1AT KO. This is consistent with previous findings, where increased total leukocytes was observed in A1AT KO mice after 8 weeks of CS compared to WT CS mice. This was also observed previously at 2 and 12 weeks of CS. Additionally, increases in total leukocytes in BALF of CS has been well reported. However, increases in A1AT KO mice in response to CS is not as well documented regarding total leukocytes whereas increased neutrophils in BALF has been reported previously in A1AT KO CS mice compared to WT CS. [150]

Neutrophilic increase in the BALF was observed in samples exposed to CS (Figure 6.2A), which is a crucial hallmark of increased inflammation in CS and feature in COPD, as well as a cause of lung damage. Regarding A1AT deficiency, it is arguably of even greater importance as neutrophilic inflammation is reportedly higher in A1AT deficiency due to a number of factors. A1AT deficiency predisposes the lung to unchecked proteolytic activity due to the absence or decreased A1AT that can bind and inhibit predominantly neutrophil-derived proteases, most notably neutrophil elastase. There is also an inherently different ability of neutrophils from A1AT deficient subjects, which have been shown to have increased neutrophil chemotaxis. There is also increased neutrophils, increased neutrophil driven inflammation and thus increased inflammation, driven by A1AT related mechanisms.[29, 50] It is interesting to note however, that while previously, increased neutrophils in the BALF of A1AT KO CS mice were observed compared to WT CS mice at this timepoint, this was not observed by flow cytometric analysis at this time.

One unexpected finding, was the substantial and significant decrease in alveolar macrophages following CS, observed in A1AT KO and WT mice (Figure 6.2F).

According to the literature, immune cells typically increase in the BALF by 3-5 fold, which is mostly driven by alveolar macrophage cellularity. Additionally, this increased cellularity is typically attributed to chemotactic factors generated in the lung. [151]

The observed decrease in alveolar macrophages is hence unexpected, as typically a decrease in the airway of the lung is an immediate response shortly after infection.[152]

It is a possibility this decrease in alveolar macrophages is attributed to the methodology and processing, specifically the flow cytometry processing of BALF. This is a consideration as the results of this thesis has previously consistently shown macrophages to increase in the alveolar space (BALF) in immune cell differential counts in five different mouse models of CS (over multiple timepoints 2, 4, 8 and 12 weeks of CS, including WT and A1AT KO mice). The other possibility for this observed decrease in alveolar macrophages may be attributed to peripheral blood monocytes replenishing the lung macrophages[153] that are being depleted upon increased phagocytosis caused by CS. This would support the increase in total monocytes that have previously been observed in the BALF as these macrophages are not classified

by expression of surface markers, as alveolar macrophages have been classified in mice as Siglec F^+, $CD11c^+$, $CD64^+$, $F4/80^+$, and $CD11b^-$. While this is an interesting observation, and possible basis for future experiments, specifically including the involvement of A1AT deficiency, the focus of this chapter is on dendritic cells and possible exploration into bone marrow derived macrophages would be outside the scope of this current project, particularly as DCs are much less explored in A1AT deficiency and COPD than macrophages.[154]

Eosinophils are also implicated in COPD however markedly less so then in asthma, and their role in COPD is much less certain. There was an increase in eosinophils in BALF due to CS in A1AT KO mice which did not occur in WT mice. Additionally, there was an increase in eosinophils in A1AT KO CS mice compared to WT CS mice (Figure 6.2 E). Thus, eosinophils were increased due to the absence of A1AT (A1AT KO) and due to CS. This is of particular interest, as eosinophils are not consistently increased in COPD, as some studies have shown, suggesting additional conditions and factors in eosinophilic increase. Furthermore, eosinophilic airway inflammation is associated with worsened COPD outcomes and differences in eosinophil counts may determine patient response to corticosteroid therapy. Regardless of this, the increase in eosinophils suggests increased inflammation.

T-lymphocytes play a pivotal role in the mechanism of COPD. As described earlier, DCs play a key role in initiating immune response, including activating T-cells. There was a significant increase in helper T and cytotoxic T cells in the BALF due to CS (Figure 6.2 C-D). This is consistent with the literature, which shows an increased total number of T cells in the lung parenchyma and peripheral and central airways of COPD patients, in particular with increases in CD8+, namely cytotoxic T cells.[155]

DC increased in BALF and lung following CS exposure

DC were characterised by flow cytometry. In the blood, there were no changes to DC and thus a steady level of DCs circulating in the body following eight weeks of cigarette

smoke exposure (Figure 6.3). When this was broken down into DC subcategories, a slight increase in the percentage of cDC1 cells, relative to total DC, in CS exposed mice was observed. However, the total number of cDC1 cells did not increase upon CS exposure.

There was also an observed increased in DC in the lung following CS. That is the percentage of DC increased in CS samples, additionally there was an increased quantity of DC in A1AT KO CS mice compared to air, but this was not statistically significant in WT. There was also an observed increase in A1AT KO CS compared to WT CS, however this was also not statistically significant (p= 0.0677).

Previous findings (chapter 4, aim 2) showed increased DCs in WT CS mice compared to A1AT KO CS mice, specifically circulating (blood) at 4 weeks, and lung at 8 weeks. Thus, A1AT KO CS mice had slightly less total DCs. This is contrasting to the current inflammatory condition in the lung at 8 weeks, as total DCs are consistent between A1AT KO and WT. This is most likely due to the dynamic inflammatory environment, which has been observed in date described in previous chapters. While there were no differences in the lung regarding total DCs in this current experiment, specific subsets of DCs were gated in order to gain additional knowledge on the specific differences in subsets between A1AT KO and WT mice, as well as due to CS, and thus which subset is specifically responsible for changes in DCs and thus the inflammatory environment as a whole. This will also help elucidate which function the DCs are serving as various DC subsets have different functions.

Regarding the specific subtypes of DC investigated, an increased percentage of cDC1 due to CS and interestingly, also increased number of cDC1 in A1AT KO CS mice was observed, compared to A1AT KO air and also to WT CS, thus A1AT KO CS mice showing the greatest increase in cDC1 cells (Figure 6.4). Additionally, cDC2 cell numbers were also increased in A1AT KO CS mice compared to air (Figure 6.4).

This finding is of particular interest as cDC1 play a pivotal role in COPD, in a process specific to cDC1 and not mediated by cDC2, which is priming natural killer (NK) cells. This process results in increased cytotoxicity of NK cells towards lung epithelial cells (in vitro).[146 156]

This is particularly interesting as NK cells have been shown in the literature to be modulated by A1AT. Specifically, A1AT can inhibit the proteases (such as granzyme B – a key protein released by NK cells) and thus dampen NK cytotoxic function. Hence, A1AT can also modulate NK cell function, and decrease tissue damage, thus A1AT deficient individuals can also experience lung damage due to protease activity via this mechanism also.[146, 156] This would hence be interesting to include additional flow cytometry markers in future to gate out NK cells and enumerate possible changes between A1AT KO and WT mice. Additionally, this mechanism could also be a reason for the previously observed increase in emphysema in the histology by MLI in A1AT KO mice, as since there were previously no evidence of increased proteases or decreased lung function, the main cause of damage and structural change specific to this model is most likely due to specific inflammatory changes between A1AT KO and WT mice.

Migratory DC were also investigated. From the literature, it has been found that CD103+ DC are the primary migratory DC subset present in the lung, however there is a smaller subpopulation of $CD11b^{hi}$ DC that also possesses migratory ability.[157] Thus, for this chapter, DC103+ cells were used as the classification of migratory DCs. There was an observed increase in the percentage of migratory cDC1 cells due to CS, and an increased number of migratory cDC1 in A1AT KO CS mice compared to A1AT KO air and to WT CS (Figure 6.4 E-F). Migratory cDC2 show a slightly different story in that migratory cDC2 are increased in CS (increased percentage for A1AT KO and WT, and increased number in A1AT KO samples, Figure 6.4 I-J).

The data shows increased DCs in the lung, specifically increased cDCs of A1AT KO CS mice compared to any other group i.e. WT CS and A1AT KO air. This alone suggests increased accumulation of cDCs in the lungs of A1AT KO CS mice. This is further highlighted by the lack of change/increase in circulating DCs (DCs in the blood). This shows that there is a constant presence and supply of DCs to be supplied to the lung, implying a constant signal for DCs to be produced. Finally, there is also an increase in $CD103^{+}$ cDCs also termed migratory cDCs due to this population being the most implicated in migration. Hence, overall, strong evidence to support increased accumulation of DCs and also their implication in damage.

This is also consistent with the literature, which suggests an accumulation of DC in COPD pathogenesis, specifically, increased DCs accumulating within the lung after continuous recruitment from the bone marrow.[128] Additionally, the most common chemokine receptors implicated in DC recruitment and migration are CCR6 and CCR7. It has been shown that in mice exposed to CS, CCR6 attenuated recruitment of DCs and also partially protected against emphysema (lower MLI and destructive index). Thus, a strong correlation between DCs and emphysema, specifically implicating DC recruitment (CCR6). Additionally, Ccl21 is the ligand that binds to CCR6 and mRNA has been shown to be significantly higher in COPD patients compared to both smoker and non-smoker individuals that did not have COPD.[128]

Changes to DC in BALF was also observed upon CS, notably a decreased percentage of total DC, however, increase number of DC (Figure 6.5 A and D). Regarding subcategories, the percentage of cDC2 (Figure 6.5 C) was the only percentage increase while cDC1 (Figure 6.5 B) and other DC subsets, namely pDC (not shown) were decreased relative to total DC. Of greater interest however is the increase in the number of DC, cDC1, and cDC2 with CS, evident in both A1AT KO and WT mice. This suggests increased infiltration of DC into bronchoalveolar space following eight weeks of cigarette smoke. DC have been shown to play an important role in COPD pathogenesis, and accumulation has previously been reported in the bronchial mucosa of CS patients and COPD patients.[43]

BMDCs derived from A1AT KO CS mice showed similar ability to differentiate compared to controls

Certain cell types notably neutrophils and macrophages, have been suggested in the literature to behave inherently different in A1AT deficiency and in CS. Hence, it was decided to investigate DCs and determine if DCs are inherently different due to A1AT deficiency and also CS. To test if DCs were inherently different in their ability to differentiate, BMDCs from WT and A1AT KO mice exposed to Air and CS, were cultured and evaluated by flow cytometry. The bone marrow from each mouse was differentiated ex vivo with GM-CSF. Here, there was no differences in either the

percentage of dendritic cells relative to live cells, or in the total number of dendritic cells (Figure 6.6 A and D). CD103+ and Ly6C+ DC were also consistent across mouse groups (Figure 6.6 B,C,E and F). Thus, bone marrow derived dendritic cells from four mouse groups demonstrated similar ability to differentiate/develop. The smoked mice did not show any differences in the ability to generate immature DC in the bone marrow, however, it may also be useful in the future to expose immature DC to CS alongside GM-CSF which is used to differentiate DC, thus exposing immature DC to CS during differentiation. Previous studies have shown that short term (18-24 h, consistent with the timeframe of exposure) coculture with CSE stimulated immature DCs towards more mature cells as evident due to upregulation of DC activation markers (MHCII, CD83, CD86, CD40) as well as increased inflammatory markers (IL-12, IL-6 and TNF) which are released upon DC activation. It was also stipulated that CSE may drive DCs towards full maturation.[158] While DC maturation was not tested experimentally through specific activation markers in this chapter, literature reports the effect of CS on dendritic cells, and its importance in COPD.

The lack of changes in DC differentiation across genotype is somewhat surprising however, as in mouse models of lupus, treatment of BMDCs with human A1AT significantly reduced BM-derived DC differentiation.[93] This in addition to the ability of A1AT to inhibit DC (specifically cDC maturation and cytokine production led us to think there may be changes due to the absence of A1AT (A1AT KO). However, lupus is a disease that is heavily implicated by DCs where they have profound alterations that contribute to damage. While cDCs in A1AT KO mice are increased (Figure 6.4) compared to WT mice which possess circulating functional A1AT and there is strong scientific merit to the impact of A1AT on DC function, this does not seem to be true for differentiation of DCs. That is the converse of this finding that A1AT reduced BMDC differentiation does not have to be true i.e. that no A1AT will impact DC differentiation.

The in vitro finding is particularly interesting when examined alongside the in vivo DC findings for each mouse group. In vivo, mice across all groups showed comparable levels of DC circulating the body, following 8 weeks of air/CS irrespective of genotype (Figure 6.3). This suggests that any changes that may be seen later in DCs are most

likely not occurring as a result of differentiation or of increased generation of DCs in the bone marrow, and thus circulating, as the recorded levels of circulation are consistent across mouse groups. This is however based on the possibly incorrect assumption that the number of DCs are consistent, or at least consistent across mouse groups over time and not just after eight weeks of air/CS. Based on the fluctuation in inflammatory cells discussed in Chapter 4 Aim 2, total leukocytes, neutrophils and macrophages change over the time course of CS (2, 4, 8 and 12 weeks of CS), the assumption that DCs do not fluctuate over time may not hold true.

Hence, we will amend it as following eight weeks of CS exposure there is no change in blood DCs or differentiation across mouse groups and due to CS exposure, and hence at this time, any increases in DCs in the lung are most likely due to accumulation of DCs in the lung.

BMDCs derived from A1AT KO CS mice showed similar viability compared to controls, in response to LPS or CSE treatment.

Viability of the BMDC in response to LPS and CSE was also investigated by lactate dehydrogenase (LDH) assay. LDH is an enzyme in the cell membrane, that upon cells death is released after the cell membrane becomes permeable. Regarding these samples, this was plotted as percentage mortality. In the non-chemokine samples, the effect of treatment, mouse group, and a combination of the two variables were measured. Within all groups and across all variables there were no statistically significant changes in mortality observed (Figure 6.7). As mentioned earlier, it was previously observed (data not shown) that there was significant cell death in culture of lung epithelial type II cell line when exposed to 5% CSE, and thus a lower dose of 1% was used in this study as it was important that a yield/survival number large enough for sufficient cells to conduct a migration assay. While others have used 5% CSE for longer periods of time (72h) without triggering LDH release from cells, other studies have shown doses of 1% to be sufficient for some effects, whilst doses of 10% to led to significant cell death. [159]

Hence, in this experiment a conservative dose of CSE was given to cells to ensure there were sufficient cells to run migration assays. Hence a limitation of this study is

that the dose of CSE given may have been too low for any significant changes to occur, and LPS was used as a positive control to attempt to gauge this.

Viability was pivotal to record in this experiment as it could also be a contributing factor to any changes in the migration assay. Increased death in some samples may result in decreased migration as there are less live cells to migrate or less live cells detected by flow cytometry. Since BMDC taken from the four mouse groups demonstrated similar viability following LPS and CSE exposure, it can be inferred that any changes reported in BMDC are not a result of changes in cell death.

To place this in the context of in vivo studies, when the mice were exposed to CS there was an increase in the number of DC in the BALF of CS mice compared to air (Figure 6.5 D), and thus exposure to CS increases infiltration of DC in the bronchoalveolar space. Additionally, DC were also increased in the lung of A1AT KO CS mice compared to air (Figure 6.4 B). DC infiltration in BALF, accumulation in the lung, and no increases in circulating DC were observed in vivo after eight weeks of CS. When combined with the ex vivo findings from BMDCs, which show no significant change in cell survival/mortality due to CS, this suggests that increased DC apoptosis due to CS is not likely.

BMDCs showed increased migration following LPS exposure.

Migration of DCs was also assessed. BMDC from four mouse groups were exposed to three different treatments, and chemokines were placed in the lower compartment of transwells to encourage migration of DC. There were two main points for this experiment, the first was to determine if there were any migratory changes in response to CSE exposure. To determine the effect of the CSE treatment, it was also decided to compare this to an LPS treated group, as LPS is known to activate BMDC, as well as to determine the ability of DC to mature in response to inflammatory stimuli.[160]

The second point was to see if there were any changes in migration in the presence of chemokine added to the lower compartment, as well as the type of chemokine used. Some previously reported chemokines of particular interest to this study include Ccl19

and Ccl21. DC migration is a tightly regulated process controlled by a large variety of chemotactic factors, of which chemokines play an important role.

The migration of DCs to the lymph nodes is a complex process that relies on two main chemokines, namely Ccl19 and Ccl21.[161] While Ccl19 and Ccl21 both interact with, bind with and regulate the same chemokine receptor CCR7, they are structurally and functionally quite different. Ccl19 is secreted by activated (otherwise known as mature) DCs, whereas Ccl21 is secreted by afferent lymphatic vessels.[162, 163] However they are both expressed by the stromal cells of lymph nodes and lumen of high endothelial venules (HEVs). Ccl19 has also been suggested to be 10-100 times more potent than Ccl21 in inducing migration of DCs.[162 163] Hence, it could also be determined if migration was Ccl19 or Ccl21 specific, or if either chemokine showed increased migration compared to the other.

Migratory ability of BMDC were analysed specifically from the four mouse groups following LPS and CSE exposure. While there were some significant changes in certain graphs regarding migrated DCs and subsets of DC, one variable that remained relatively consistent was the donor mouse groups. While it was originally thought that BMDCs derived from various mouse genotypes may have some inherent differences, as neutrophils from A1AT deficiency have shown this, there was insufficient evidence of this in this study with BMDCs. While there is still a possibility that this occurs, the evidence from this study suggests any changes may be more nuanced, or may involve processes not explored in this thesis. While there were some increases in DC in some CS samples, this change is not consistent across treatment or chemokine and therefore no concrete conclusions can be made. However, of particular interest were the no chemokine samples (Figure 6.7), as there was significant variance attributed to mouse group most likely attributed to the increased migration in cells of smoke mice exposed to LPS compared to air mice exposed to LPS. LPS is a known stimulant in activation of DC, and this pathway and process has been studied. CS has been shown both in the literature and in this study, to lead to increased DCs in the lung. While this increase in DCs may initially seem beneficial, it has been shown in the literature that the DCs produced are often dysfunctional and are inflammatory DCs, meaning they contribute to the inflammatory environment. While this has been shown in the literature, this had not been investigated in cases of A1AT deficiency.

The effects of A1AT or A1AT deficiency on DCs is a topic that requires further study. While the importance of A1AT has been highlighted in autoimmune disease such as rheumatoid arthritis and lupus, there are still significant gaps in research. What is known from the literature however, is the importance of A1AT in reducing inflammatory response. Specifically, for DC this is either by A1AT inhibiting DC activation and function, or by reducing inflammatory response by altering inflammatory gene expressions in DC. This is in addition to the typical immune system regulating properties of DCs.

There were significant changes observed in migration in BMDCs as a result of treatment, in particular from LPS, as well as due to chemokine. DCs were significantly increased in response to LPS, evident in Figure 6.7 D, E and F where LPS samples were increased independent of migratory stimulus i.e. no chemokine, Ccl19, and Ccl21 respectively. Additionally, the variance from treatment had statistical significance of greater than 50% of total variation in the data.

Variation due to chemokine was also observed, however, in samples where Ccl19 was used to induce migration to the lower chamber, there was significantly less migration compared to Ccl21 and no chemokine. (Figure 6.8 A-C). Thus, Ccl21 may be preferred or is specific to this finding. Unfortunately, as Ccl21 is not significantly different to no chemokine, there is a reluctance to draw conclusions based on chemokine specific findings. However, this does still show a particularly interesting story regarding migration, particularly when linked with the increased CD103+ ‘migratory’ DCs present in the lungs of A1AT KO CS mice. There was a significant increase in migratory cDC1 in response to CS, migratory cDC1 in response to A1AT KO genotype, and an increase in cDC2 in A1AT KO CS mice compared to A1AT KO air (Figure 6.4 E, F, I and J). This could suggest a mechanism regarding cDC migration that is A1AT specific. While there were no significant changes to cytotoxic T cells (which are heavily implicated in cDC1) it is believed that there should be further investigation into the relationship between A1AT, cDC1, NK cells and cytotoxic T cells.

To summarise DC migration was increased in vivo in A1AT KO CS and the quantity of migrated cells from BMDC were sometimes increased in CS groups, however this may change upon examination of specific subsets of DC e.g. migratory cDC1 vs migratory cDC2. An interesting counterpoint however is that the literature has previously suggested that DC migration is not inhibited by A1AT. However, this does not necessarily mean the opposite is true and the absence of A1AT does not affect DCs, especially considering the role of A1AT on inflammation and the role of DCs in immune response.

BMDCs showed increased inflammatory markers in response to LPS

Inflammatory cytokines were measured to determine if BMDCs were activated. There was an increase in TNF, IL1β, KC, and IL6 due to LPS (Figure 6.9). This however is due to a combination of activated DCs and activated macrophages. There were also changes in mouse group, notably an increase in TNF in LPS CS mice, particularly in A1AT KO which was significantly higher than WT.

Future directions should focus on DC activation, most likely through DC activation markers. As A1AT has been reported to affect DC activation specifically to inhibits DC activation (in a mouse model of lupus).[93] Thus, it would be critical to explore these findings in combination.

Pro-inflammatory cytokines such as IL-1β, IL-6, and TNF are produced by DCs via TLR4. LPS treatments were hence particularly useful as LPS is an agonist to TLR4. As mentioned human A1AT inhibits cDC maturation, however human A1AT also significantly decreased IL-1β and TNF secretion from DCs, as well as inhibits IFN-I production from DCs. Thus, it is expected that mice with circulating A1AT protein i.e. WT mice, have decreased IL-1β and TNF relative to the A1AT KO mice which have no circulating A1AT. While previously observed (Chapter 4, Aim 2), increased IL-1β in A1AT KO mice (significant at 2 and 8 weeks CS), it must be acknowledged that DCs are not the only cells that produce IL-1β. Similarly, in BMDCs there is also the presence

of macrophages (BMDMs – bone marrow derived macrophages), which also produce IL-1β and TNF. [93]

DC maturation/activation – limitations and future directions

While many facets of DCs and CS/COPD were investigated, notably DC accumulation and circulation in vivo, differentiation, mortality, and migration, DC activation was not investigated. This would therefore be a very useful next step for this study, however there are a limited number of studies in the literature that have investigated DC activation pertaining to CS or to A1AT deficiency.

Regarding A1AT it has previously been discussed that human A1AT treatment inhibited cDC activation and cytokine production.[93] However, there is also an impact of CS. DC have been reported to be increased in CS and COPD. This has been compounded in CS induced damage as CS has been shown to differentially modulate dendritic cell maturation and function. CSE was shown to stimulate activation of DCs as well as increased pro-inflammatory cytokines. Both of which would contribute to increased inflammation and further damage.[158] Hence, it is pivotal to investigate DC and specifically cDC activation as they seem to play a key role in CS exacerbated A1AT deficient related pathogenesis.

Given the effects of A1AT and CS separately, it would be beneficial to study this finding in this mice/model where the combined effects of genotype and CS exposure on DC activation can be investigated. One potential avenue that could be explored experimentally, that also looks into DC differentiation, is by exposing BMDCs during differentiation to CS and to A1AT. While it has been explored in literature that A1AT inhibits maturation and CSE drives maturation, this does not mean that the absence of A1AT will also drive DCs towards maturation, however this is heavily suggested. Additionally, the quantity or presence of A1AT in WT BMDCs was not measured, hence the presence or quantity of A1AT also requires exploration. Finally, as mentioned earlier BM differentiation to DCs should also be explored with stimulation/treatment during the differentiation stage.

Conclusion

While the involvement of DCs pertaining to CS and A1AT specifically is quite understudied and inconclusive, a start has been made to explore avenues to elucidate potential differences in A1AT KO mice (A1AT deficiency). Specifically, to characterise changes in DC quantities in circulation, lung and BALF, as well as changes in differentiation, mortality and migration.

No change in BMDC differentiation due to mouse group, and no change in the amount of circulating DCs (blood) in vivo was observed. There was however an accumulation of DCs in the lung upon CS. There was also increased cDC1 in response to CS, which was significantly amplified in A1AT KO CS compared to WT CS, thus, increased cDC1 accumulation in A1AT KO CS mice. As there was no increase in circulating DCs, this finding is quite interesting and concludes there is an increased accumulation in the lung.

There appears to be an interesting mechanism regarding A1AT, however, the findings on DC migration were somewhat inconclusive. There was increased inflammation in CS and particularly in A1AT KO CS evident by increased cDC1 migratory cells in A1AT KO CS (compared to A1AT KO air and WT CS) and even increased cDC2 in A1AT KO compared to air, in vivo, as well as some increases in migration with CS.

DCs play a pivotal role in activating a number of inflammatory and immune cells, that have been shown to increase in A1AT deficiency and COPD, and hence further investigation into these concepts could elucidate key information in A1AT deficiency disease progression.

Chapter 7: Thesis Summary, concluding statements and future directions.

This work examined the impact of CS on A1AT deficiency. Specifically, in Chapter 3, gene and protein expression of A1AT were assessed in an experimental model of CS-induced COPD in WT mice, and was discovered that CS caused fluctuating increases in A1AT protein in the lung; most likely a protective response due to CS.

The mechanisms of A1AT deficiency in CS induced COPD with A1AT KO mice were investigated in Chapter 4. Results showed increased inflammation in these mice as early as 2 weeks with inflammation predominantly driven by neutrophils and also possibly by IL1β and CXCL15. There was also increased alveolar destruction (after 8 weeks) in A1AT KO CS compared to WT CS mice, highlighting exacerbated lung damage in the absence of A1AT. This model, particularly the 8 week timepoint, was also determined to be suitable for testing future treatments and therapies.

Upon investigating the Z mutation, (Chapter 5), functional, structural and inflammatory changes were observed in PiZ mice, however these were attributed to CS and were not significantly different to WT mice. Although increased alveolar destruction was attributed to Z toxicity, further experimentation is required to elucidate the mechanism(s) of action.

Finally, investigation of dendric cells (DC) (Chapter 2) suggests there may be A1AT specific mechanisms involved in the behaviour and biology of DCs. Further investigation (Chapter 4) showed that conventional DCs specifically accumulated in the lungs of A1AT KO CS mice with increased migration in A1AT KO compared to WT.

These studies have demonstrated novel potential findings contributing to the field of A1AT deficiency and COPD. This thesis highlights the impact of A1AT, not only as an antiprotease but as a modulator of inflammation, specifically neutrophils, cDCs and certain cytokines. Additionally, an improved model of A1AT deficiency and COPD was established to evaluate future therapies.

I would like to continue to research DCs and the impact of A1AT and CS. Specifically, to elucidate the mechanisms of action and investigate the activation of DCs particularly cDCs, using the mouse models established in this thesis.
Additionally, DCs and A1AT deficiency in COPD are severely understudied both in mice and humans. It would be very useful to see if these findings are also consistent in human patients. An interesting next step would be to stain (e.g., with OPAL staining) lung histology sections from human patients. Tissue samples for both smoke and A1AT deficient patients are located at St Vincents hospital, and I was in the process of obtaining and staining these human samples with a DC panel. This may support and confirm my DC findings and also show if this is applicable and reproducible in human patients, which is the main goal of this mouse work.

This thesis has highlighted the importance and detriment of chronic inflammation in alveolar damage. In these mouse models specifically, the absence of A1AT (A1AT KO) showed a stronger impact on inflammation evident by increased inflammatory cells and inflammasomes, than the protease-antiprotease balance. This was somewhat unexpected as the protease-antiprotease imbalance is often highlighted as the main cause of A1AT related damage. This research highlights both the complexity and significance of inflammation and inflammatory cells in disease progression. In studies focusing on the contribution of CS in causing COPD, the influence of increased immune cells in particular increased alveolar macrophage cellularity is considered a significant cause and contributor, both directly and indirectly in disease progression and worsened COPD. This increased cellularity is typically attributed to chemotactic factors generated in the lung. [151] In A1AT the inflammatory profile is frequently overlooked, in lieu of the simpler protease-antiprotease imbalance as the main cause for disease progression. By investigating both the role of A1AT and CS smoke concurrently in this thesis, through the use of WT air, WT CS, A1AT KO air, A1AT KO CS mice, not only has the influence of A1AT been assessed on disease progression, but also we have established a clear story of inflammation over time and the effect of this in the overall story of A1AT deficiency and COPD. We have highlighted the importance of A1AT as a key immunomodulator against inflammation, and the importance of investigating and treating inflammation in A1AT deficiency. We have explored the role of immune cells with particular emphasis to neutrophils, macrophages, and in Chapter 6 in particular the role of DCs, which were greatly

understudied in A1AT and even more so in A1AT and COPD combined. We discovered that there was increased inflammation in CS mice and in particularly in A1AT KO CS mice, evident by increased cDC1 migratory cells in A1AT KO CS (compared to A1AT KO air and WT CS mice) and even increased cDC2 in A1AT KO compared to air, in vivo, as well as some increases in migration with CS.
On this note, the greatest potential to treat A1AT and COPD may lie in anti-inflammatory/immunomodulatory treatments either alone or in combination with the standard transient A1AT augmentation IV therapy used to increase A1AT.

This model is hence particularly useful in probing the immunomodulatory effects of A1AT. Utilising this model, future treatments based on A1AT deficient, and inflammation led mechanisms could be explored. Other promising treatments that could be explored in the future include novel genomic editing, such as exploiting lentiviral, plasmid and liposomal vectors to target and induce permanent expression of A1AT.

References

(1) Quaderi, S. A.; Hurst, J. R. The unmet global burden of COPD. *Glob Health Epidemiol Genom* **2018**, *3*, e4-e4. DOI: 10.1017/gheg.2018.1 PubMed. Lozano, R. P.; Naghavi, M. P.; Lim, S. P.; Aboyans, V. P.; Abraham, J. M. P. H.; Adair, T. P.; Ahn, S. Y. M. P. H.; AlMazroa, M. A. M. D.; Anderson, H. R. P.; Anderson, L. M. P.; et al. Global and regional mortality from 235 causes of death for 20 age groups in 1990 and 2010: a systematic analysis for the Global Burden of Disease Study 2010. *The Lancet (British edition)* **2012**, *380* (9859), 2095-2128. DOI: 10.1016/S0140-6736(12)61728-0. *Chronic obstructive pulmonary disease (COPD)*. https://www.who.int/news-room/fact-sheets/detail/chronic-obstructive-pulmonary-disease-(copd) (accessed 2021 28th October 2021).
(2) Prevalence and attributable health burden of chronic respiratory diseases, 1990-2017: a systematic analysis for the Global Burden of Disease Study 2017. *Lancet Respir Med* **2020**, *8* (6), 585-596. DOI: 10.1016/s2213-2600(20)30105-3 From NLM.
(3) Zhou, Y.; Ampon, M. R.; Abramson, M. J.; James, A. L.; Maguire, G. P.; Wood-Baker, R.; Johns, D. P.; Marks, G. B.; Reddel, H. K.; Toelle, B. G. Respiratory Symptoms, Disease Burden, and Quality of Life in Australian Adults According to GOLD Spirometry Grades: Data from the BOLD Australia Study. *Int J Chron Obstruct Pulmon Dis* **2023**, *18*, 2839-2847. DOI: 10.2147/copd.S425202 From NLM.
(4) Welfare, A. I. o. H. a. *Chronic respiratory conditions: Chronic obstructive pulmonary disease*. Australian Government: Australian Institute of Health and Welfare, https://www.aihw.gov.au/reports/chronic-respiratory-conditions/copd (accessed.
(5) Innovation, N. G. A. f. C. *Chronic obstructive pulmonary disease*. NSW Government Agency for Clinical Innovation, https://aci.health.nsw.gov.au/statewide-programs/lbvc/chronic-obstructive-pulmonary-disease (accessed.
(6) Chen, S.; Kuhn, M.; Prettner, K.; Yu, F.; Yang, T.; Bärnighausen, T.; Bloom, D. E.; Wang, C. The global economic burden of chronic obstructive pulmonary disease for 204 countries and territories in 2020-50: a health-augmented macroeconomic modelling study. *Lancet Glob Health* **2023**, *11* (8), e1183-e1193. DOI: 10.1016/s2214-109x(23)00217-6 From NLM.
(7) Bowerman, K. L.; Rehman, S. F.; Vaughan, A.; Lachner, N.; Budden, K. F.; Kim, R. Y.; Wood, D. L. A.; Gellatly, S. L.; Shukla, S. D.; Wood, L. G.; et al. Disease-associated gut microbiome and metabolome changes in patients with chronic obstructive pulmonary disease. *Nature communications* **2020**, *11* (1), 5886-5886. DOI: 10.1038/s41467-020-19701-0.
(8) Salvi, S. S.; Barnes, P. J. Chronic obstructive pulmonary disease in non-smokers. *Lancet* **2009**, *374* (9691), 733-743. DOI: 10.1016/s0140-6736(09)61303-9 From NLM. Sana, A.; Somda, S. M. A.; Meda, N.; Bouland, C. Chronic obstructive pulmonary disease associated with biomass fuel use in women: a systematic review and meta-analysis. *BMJ Open Respir Res* **2018**, *5* (1), e000246. DOI: 10.1136/bmjresp-2017-000246 From NLM. Zheng, X. Y.; Li, Z. L.; Li, C.; Guan, W. J.; Li, L. X.; Xu, Y. J. Effects of cigarette smoking and biomass fuel on lung function and respiratory symptoms in middle-aged adults and the elderly in Guangdong province, China: A cross-sectional study. *Indoor Air* **2020**, *30* (5), 860-871. DOI: 10.1111/ina.12671 From NLM.

(9) Zhou, J. J.; Cho, M. H.; Castaldi, P. J.; Hersh, C. P.; Silverman, E. K.; Laird, N. M. Heritability of chronic obstructive pulmonary disease and related phenotypes in smokers. *Am J Respir Crit Care Med* **2013**, *188* (8), 941-947. DOI: 10.1164/rccm.201302-0263OC From NLM.
(10) Stolz, D.; Mkorombindo, T.; Schumann, D. M.; Agusti, A.; Ash, S. Y.; Bafadhel, M.; Bai, C.; Chalmers, J. D.; Criner, G. J.; Dharmage, S. C.; et al. Towards the elimination of chronic obstructive pulmonary disease: a Lancet Commission. *Lancet* **2022**, *400* (10356), 921-972. DOI: 10.1016/s0140-6736(22)01273-9 From NLM.
(11) Adeloye, D.; Song, P.; Zhu, Y.; Campbell, H.; Sheikh, A.; Rudan, I. Global, regional, and national prevalence of, and risk factors for, chronic obstructive pulmonary disease (COPD) in 2019: a systematic review and modelling analysis. *Lancet Respir Med* **2022**, *10* (5), 447-458. DOI: 10.1016/s2213-2600(21)00511-7 From NLM.
(12) Yang, I. A.; Jenkins, C. R.; Salvi, S. S. Chronic obstructive pulmonary disease in never-smokers: risk factors, pathogenesis, and implications for prevention and treatment. *Lancet Respir Med* **2022**, *10* (5), 497-511. DOI: 10.1016/s2213-2600(21)00506-3 From NLM.
(13) Perret, J. L.; Lodge, C. J.; Lowe, A. J.; Johns, D. P.; Thompson, B. R.; Bui, D. S.; Gurrin, L. C.; Matheson, M. C.; McDonald, C. F.; Wood-Baker, R.; et al. Childhood pneumonia, pleurisy and lung function: a cohort study from the first to sixth decade of life. *Thorax* **2020**, *75* (1), 28-37. DOI: 10.1136/thoraxjnl-2019-213389 From NLM. Menezes, A. M.; Hallal, P. C.; Perez-Padilla, R.; Jardim, J. R.; Muiño, A.; Lopez, M. V.; Valdivia, G.; Montes de Oca, M.; Talamo, C.; Pertuze, J.; et al. Tuberculosis and airflow obstruction: evidence from the PLATINO study in Latin America. *Eur Respir J* **2007**, *30* (6), 1180-1185. DOI: 10.1183/09031936.00083507 From NLM. Gingo, M. R.; Nouraie, M.; Kessinger, C. J.; Greenblatt, R. M.; Huang, L.; Kleerup, E. C.; Kingsley, L.; McMahon, D. K.; Morris, A. Decreased Lung Function and All-Cause Mortality in HIV-infected Individuals. *Ann Am Thorac Soc* **2018**, *15* (2), 192-199. DOI: 10.1513/AnnalsATS.201606-492OC From NLM.
(14) Bui, D. S.; Walters, H. E.; Burgess, J. A.; Perret, J. L.; Bui, M. Q.; Bowatte, G.; Lowe, A. J.; Russell, M. A.; Thompson, B. R.; Hamilton, G. S.; et al. Childhood Respiratory Risk Factor Profiles and Middle-Age Lung Function: A Prospective Cohort Study from the First to Sixth Decade. *Ann Am Thorac Soc* **2018**, *15* (9), 1057-1066. DOI: 10.1513/AnnalsATS.201806-374OC From NLM.
(15) Wang, Y.; Xu, J.; Meng, Y.; Adcock, I. M.; Yao, X. Role of inflammatory cells in airway remodeling in COPD. *Int J Chron Obstruct Pulmon Dis* **2018**, *13*, 3341-3348. DOI: 10.2147/copd.S176122 From NLM.
(16) Wu, J.; Zhao, X.; Xiao, C.; Xiong, G.; Ye, X.; Li, L.; Fang, Y.; Chen, H.; Yang, W.; Du, X. The role of lung macrophages in chronic obstructive pulmonary disease. *Respiratory Medicine* **2022**, *205*, 107035. DOI: https://doi.org/10.1016/j.rmed.2022.107035.
(17) MacNee, W. Pathology, pathogenesis, and pathophysiology. (0959-8138 (Print)). From 2006 May 20.
(18) Liu, T.; Zhang, L.; Joo, D.; Sun, S.-C. NF-κB signaling in inflammation. *Signal Transduction and Targeted Therapy* **2017**, *2* (1), 17023. DOI: 10.1038/sigtrans.2017.23.
(19) Nayak, A. P.; Deshpande, D. A.; Penn, R. B. New targets for resolution of airway remodeling in obstructive lung diseases. *F1000Res* **2018**, *7*. DOI: 10.12688/f1000research.14581.1 From NLM.

(20) Thurlbeck, W. M. The pathobiology and epidemiology of human emphysema. *J Toxicol Environ Health* **1984**, *13* (2-3), 323-343. DOI: 10.1080/15287398409530501 From NLM.
(21) Pahal P, A. A., Afzal M. *Emphysema*. StatPearls Publishing, https://www.ncbi.nlm.nih.gov/books/NBK482217/?utm_source=chatgpt.com (accessed.
(22) JS, L.; EM, W.; RG., T. *Screening for Chronic Obstructive Pulmonary Disease: A Targeted Evidence Update for the U.S. Preventive Services Task Force*; 2022.
(23) Bailey, K. L. The importance of the assessment of pulmonary function in COPD. *Med Clin North Am* **2012**, *96* (4), 745-752. DOI: 10.1016/j.mcna.2012.04.011 From NLM.
(24) Agarwal AK, R. A., Brown BD. *Chronic Obstructive Pulmonary Disease*. StatPearls Publishing, https://www.ncbi.nlm.nih.gov/books/NBK559281/ (accessed.
(25) Shaker, S. B.; Dirksen, A.; Bach, K. S.; Mortensen, J. Imaging in chronic obstructive pulmonary disease. *Copd* **2007**, *4* (2), 143-161. DOI: 10.1080/15412550701341277 From NLM.
(26) Dransfield, M. T.; Kunisaki, K. M.; Strand, M. J.; Anzueto, A.; Bhatt, S. P.; Bowler, R. P.; Criner, G. J.; Curtis, J. L.; Hanania, N. A.; Nath, H.; et al. Acute Exacerbations and Lung Function Loss in Smokers with and without Chronic Obstructive Pulmonary Disease. *Am J Respir Crit Care Med* **2017**, *195* (3), 324-330. DOI: 10.1164/rccm.201605-1014OC From NLM.
(27) Fricker, M.; Deane, A.; Hansbro, P. M. Animal models of chronic obstructive pulmonary disease. *Expert opinion on drug discovery* **2014**, *9* (6), 629-645. DOI: 10.1517/17460441.2014.909805. Qureshi, H.; Sharafkhaneh, A.; Hanania, N. A. Chronic obstructive pulmonary disease exacerbations: latest evidence and clinical implications. *Ther Adv Chronic Dis* **2014**, *5* (5), 212-227. DOI: 10.1177/2040622314532862 PubMed. Haw, T. J.; Starkey, M. R.; Nair, P. M.; Pavlidis, S.; Liu, G.; Nguyen, D. H.; Hsu, A. C.; Hanish, I.; Kim, R. Y.; Collison, A. M.; et al. A pathogenic role for tumor necrosis factor-related apoptosis-inducing ligand in chronic obstructive pulmonary disease. *Mucosal immunology* **2016**, *9* (4), 859-872. DOI: 10.1038/mi.2015.111.
(28) Dau, T.; Sarker, R. S. J.; Yildirim, A. O.; Eickelberg, O.; Jenne, D. E. Autoprocessing of neutrophil elastase near its active site reduces the efficiency of natural and synthetic elastase inhibitors. *Nature Communications* **2015**, *6* (1), 6722. DOI: 10.1038/ncomms7722.
(29) McCarthy, C.; Reeves, E. P.; McElvaney, N. G. The Role of Neutrophils in Alpha-1 Antitrypsin Deficiency. *Ann Am Thorac Soc* **2016**, *13 Suppl 4*, S297-304. DOI: 10.1513/AnnalsATS.201509-634KV From NLM.
(30) Sapey, E. Neutrophil Modulation in Alpha-1 Antitrypsin Deficiency. *Chronic Obstr Pulm Dis* **2020**, *7* (3), 247-259. DOI: 10.15326/jcopdf.7.3.2019.0164 From NLM.
(31) Finicelli, M.; Digilio, F. A.; Galderisi, U.; Peluso, G. The Emerging Role of Macrophages in Chronic Obstructive Pulmonary Disease: The Potential Impact of Oxidative Stress and Extracellular Vesicle on Macrophage Polarization and Function. *Antioxidants (Basel)* **2022**, *11* (3). DOI: 10.3390/antiox11030464 From NLM.
(32) Belchamber, K. B. R.; Walker, E. M.; Stockley, R. A.; Sapey, E. Monocytes and Macrophages in Alpha-1 Antitrypsin Deficiency. *Int J Chron Obstruct Pulmon Dis* **2020**, *15*, 3183-3192. DOI: 10.2147/copd.S276792 From NLM.

(33) Colarusso, C.; Terlizzi, M.; Molino, A.; Pinto, A.; Sorrentino, R. Role of the inflammasome in chronic obstructive pulmonary disease (COPD). *Oncotarget* **2017**, *8* (47), 81813-81824. DOI: 10.18632/oncotarget.17850 From NLM.
(34) Takiguchi, H.; Yang, C. X.; Yang, C. W. T.; Sahin, B.; Whalen, B. A.; Milne, S.; Akata, K.; Yamasaki, K.; Yang, J. S. W.; Cheung, C. Y.; et al. Macrophages with reduced expressions of classical M1 and M2 surface markers in human bronchoalveolar lavage fluid exhibit pro-inflammatory gene signatures. *Sci Rep* **2021**, *11* (1), 8282. DOI: 10.1038/s41598-021-87720-y From NLM.
(35) Sauler, M.; McDonough, J. E.; Adams, T. S.; Kothapalli, N.; Barnthaler, T.; Werder, R. B.; Schupp, J. C.; Nouws, J.; Robertson, M. J.; Coarfa, C.; et al. Characterization of the COPD alveolar niche using single-cell RNA sequencing. *Nature Communications* **2022**, *13* (1), 494. DOI: 10.1038/s41467-022-28062-9.
(36) Kim, G. D.; Lim, E. Y.; Shin, H. S. Macrophage Polarization and Functions in Pathogenesis of Chronic Obstructive Pulmonary Disease. *Int J Mol Sci* **2024**, *25* (11). DOI: 10.3390/ijms25115631 From NLM.
(37) Barnes, P. J. Inflammatory mechanisms in patients with chronic obstructive pulmonary disease. *J Allergy Clin Immunol* **2016**, *138* (1), 16-27. DOI: 10.1016/j.jaci.2016.05.011 From NLM.
(38) Fazleen, A.; Wilkinson, T. The emerging role of proteases in α(1)-antitrypsin deficiency and beyond. *ERJ Open Res* **2021**, *7* (4). DOI: 10.1183/23120541.00494-2021 From NLM.
(39) Demkow, U.; van Overveld, F. J. Role of elastases in the pathogenesis of chronic obstructive pulmonary disease: implications for treatment. *Eur J Med Res* **2010**, *15 Suppl 2* (Suppl 2), 27-35. DOI: 10.1186/2047-783x-15-s2-27 From NLM.
(40) Gramegna, A.; Amati, F.; Terranova, L.; Sotgiu, G.; Tarsia, P.; Miglietta, D.; Calderazzo, M. A.; Aliberti, S.; Blasi, F. Neutrophil elastase in bronchiectasis. *Respiratory Research* **2017**, *18* (1), 211. DOI: 10.1186/s12931-017-0691-x.
(41) Jasper, A. E.; McIver, W. J.; Sapey, E.; Walton, G. M. Understanding the role of neutrophils in chronic inflammatory airway disease. *F1000Res* **2019**, *8*. DOI: 10.12688/f1000research.18411.1 From NLM.
(42) Thorley, A. J.; Tetley, T. D. Pulmonary epithelium, cigarette smoke, and chronic obstructive pulmonary disease. *Int J Chron Obstruct Pulmon Dis* **2007**, *2* (4), 409-428. From NLM.
(43) Xu, J.; Zeng, Q.; Li, S.; Su, Q.; Fan, H. Inflammation mechanism and research progress of COPD. *Front Immunol* **2024**, *15*, 1404615. DOI: 10.3389/fimmu.2024.1404615 From NLM.
(44) Barnes, P. J.; Cosio, M. G. Characterization of T lymphocytes in chronic obstructive pulmonary disease. *PLoS Med* **2004**, *1* (1), e20. DOI: 10.1371/journal.pmed.0010020 From NLM.
(45) Polverino, F.; Cosio, B. G.; Pons, J.; Laucho-Contreras, M.; Tejera, P.; Iglesias, A.; Rios, A.; Jahn, A.; Sauleda, J.; Divo, M.; et al. B Cell-Activating Factor. An Orchestrator of Lymphoid Follicles in Severe Chronic Obstructive Pulmonary Disease. *Am J Respir Crit Care Med* **2015**, *192* (6), 695-705. DOI: 10.1164/rccm.201501-0107OC From NLM.
Polverino, F.; Seys, L. J.; Bracke, K. R.; Owen, C. A. B cells in chronic obstructive pulmonary disease: moving to center stage. *Am J Physiol Lung Cell Mol Physiol* **2016**, *311* (4), L687-l695. DOI: 10.1152/ajplung.00304.2016 From NLM.

(46) Chung, K. F. Inflammatory mediators in chronic obstructive pulmonary disease. *Curr Drug Targets Inflamm Allergy* **2005**, *4* (6), 619-625. DOI: 10.2174/156801005774912806 From NLM.
(47) Henrot, P.; Prevel, R.; Berger, P.; Dupin, I. Chemokines in COPD: From Implication to Therapeutic Use. *Int J Mol Sci* **2019**, *20* (11). DOI: 10.3390/ijms20112785 From NLM.
(48) Hughes, C. E.; Nibbs, R. J. B. A guide to chemokines and their receptors. *Febs j* **2018**, *285* (16), 2944-2971. DOI: 10.1111/febs.14466 From NLM.
(49) Rovina, N.; Koutsoukou, A.; Koulouris, N. G. Inflammation and immune response in COPD: where do we stand? *Mediators Inflamm* **2013**, *2013*, 413735. DOI: 10.1155/2013/413735 From NLM.
(50) Bergin, D. A.; Reeves, E. P.; Meleady, P.; Henry, M.; McElvaney, O. J.; Carroll, T. P.; Condron, C.; Chotirmall, S. H.; Clynes, M.; O'Neill, S. J.; et al. α-1 Antitrypsin regulates human neutrophil chemotaxis induced by soluble immune complexes and IL-8. *J Clin Invest* **2010**, *120* (12), 4236-4250. DOI: 10.1172/jci41196 From NLM.
(51) Karakioulaki, M.; Papakonstantinou, E.; Stolz, D. Extracellular matrix remodelling in COPD. *Eur Respir Rev* **2020**, *29* (158). DOI: 10.1183/16000617.0124-2019 From NLM.
(52) Kular, J. K.; Basu, S.; Sharma, R. I. The extracellular matrix: Structure, composition, age-related differences, tools for analysis and applications for tissue engineering. *J Tissue Eng* **2014**, *5*, 2041731414557112. DOI: 10.1177/2041731414557112 From NLM.
(53) Tanino, Y. Roles of extracellular matrix in lung diseases. *Fukushima J Med Sci* **2024**, *70* (1), 1-9. DOI: 10.5387/fms.2023-07 From NLM.
(54) Polverino, E.; Rosales-Mayor, E.; Dale, G. E.; Dembowsky, K.; Torres, A. The Role of Neutrophil Elastase Inhibitors in Lung Diseases. *Chest* **2017**, *152* (2), 249-262. DOI: 10.1016/j.chest.2017.03.056.
(55) Pandey, K. C.; De, S.; Mishra, P. K. Role of Proteases in Chronic Obstructive Pulmonary Disease. *Frontiers in pharmacology* **2017**, *8*, 512-512. DOI: 10.3389/fphar.2017.00512 PubMed.
(56) Liu, G.; Cooley, M. A.; Jarnicki, A. G.; Borghuis, T.; Nair, P. M.; Tjin, G.; Hsu, A. C.; Haw, T. J.; Fricker, M.; Harrison, C. L.; et al. Fibulin-1c regulates transforming growth factor–β activation in pulmonary tissue fibrosis. *JCI Insight* **2019**, *4* (16). DOI: 10.1172/jci.insight.124529.
(57) Joglekar, M. M.; Bekker, N. J.; Ngassie, M. L. K.; Vonk, J. M.; Borghuis, T.; Reinders-Luinge, M. A.; Bakker, J.; Woldhuis, R. R.; Pouwels, S. D.; Melgert, B. N.; et al. The lung extracellular matrix protein landscape in severe early-onset and moderate chronic obstructive pulmonary disease. 1.1 ed.; Cold Spring Harbor Laboratory: 2023.
(58) Dekkers, B. G. J.; Saad, S. I.; van Spelde, L. J.; Burgess, J. K. Basement membranes in obstructive pulmonary diseases. *Matrix Biology Plus* **2021**, *12*, 100092. DOI: https://doi.org/10.1016/j.mbplus.2021.100092.
(59) Schumann, D. M.; Leeming, D.; Papakonstantinou, E.; Blasi, F.; Kostikas, K.; Boersma, W.; Louis, R.; Milenkovic, B.; Aerts, J.; Sand, J. M. B.; et al. Collagen Degradation and Formation Are Elevated in Exacerbated COPD Compared With Stable Disease. *Chest* **2018**, *154* (4), 798-807. DOI: https://doi.org/10.1016/j.chest.2018.06.028.
(60) Rønnow, S. R.; Sand, J. M. B.; Langholm, L. L.; Manon-Jensen, T.; Karsdal, M. A.; Tal-Singer, R.; Miller, B. E.; Vestbo, J.; Leeming, D. J. Type IV collagen turnover is predictive of mortality in COPD: a comparison to fibrinogen in a prospective analysis of the ECLIPSE cohort. *Respir Res* **2019**, *20* (1), 63. DOI: 10.1186/s12931-019-1026-x From NLM.

(61) Stolz, D.; Leeming, D. J.; Kristensen, J. H. E.; Karsdal, M. A.; Boersma, W.; Louis, R.; Milenkovic, B.; Kostikas, K.; Blasi, F.; Aerts, J.; et al. Systemic Biomarkers of Collagen and Elastin Turnover Are Associated With Clinically Relevant Outcomes in COPD. *Chest* **2017**, *151* (1), 47-59. DOI: 10.1016/j.chest.2016.08.1440 From NLM.
(62) McElvaney, O. F.; Murphy, M. P.; Reeves, E. P.; McElvaney, N. G. Anti-cytokines as a Strategy in Alpha-1 Antitrypsin Deficiency. *Chronic Obstr Pulm Dis* **2020**, *7* (3), 203-213. DOI: 10.15326/jcopdf.7.3.2019.0171 From NLM. Strange, C. Anti-Proteases and Alpha-1 Antitrypsin Augmentation Therapy. *Respir Care* **2018**, *63* (6), 690-698. DOI: 10.4187/respcare.05933 From NLM. Guyot, N.; Butler, M. W.; McNally, P.; Weldon, S.; Greene, C. M.; Levine, R. L.; O'Neill, S. J.; Taggart, C. C.; McElvaney, N. G. Elafin, an elastase-specific inhibitor, is cleaved by its cognate enzyme neutrophil elastase in sputum from individuals with cystic fibrosis. *J Biol Chem* **2008**, *283* (47), 32377-32385. DOI: 10.1074/jbc.M803707200 From NLM. Twigg, M. S.; Brockbank, S.; Lowry, P.; FitzGerald, S. P.; Taggart, C.; Weldon, S. The Role of Serine Proteases and Antiproteases in the Cystic Fibrosis Lung. *Mediators of inflammation* **2015**, *2015*, 293053-293053. DOI: 10.1155/2015/293053 PubMed.
(63) Paulissen, G.; Rocks, N.; Gueders, M. M.; Crahay, C.; Quesada-Calvo, F.; Bekaert, S.; Hacha, J.; El Hour, M.; Foidart, J.-M.; Noel, A.; et al. Role of ADAM and ADAMTS metalloproteinases in airway diseases. *Respiratory Research* **2009**, *10* (1), 127. DOI: 10.1186/1465-9921-10-127.
(64) Greene, C. M.; McElvaney, N. G. Proteases and antiproteases in chronic neutrophilic lung disease - relevance to drug discovery. *Br J Pharmacol* **2009**, *158* (4), 1048-1058. DOI: 10.1111/j.1476-5381.2009.00448.x From NLM.
(65) Health, S. V. s. H. L. *Alpha -1 Antitrypsin Deficiency*. St Vincent's Hospital Lung Health, (accessed.
(66) Dummer, J.; Dobler, C. C.; Holmes, M.; Chambers, D.; Yang, I. A.; Parkin, L.; Smith, S.; Wark, P.; Dev, A.; Hodge, S.; et al. Diagnosis and treatment of lung disease associated with alpha one-antitrypsin deficiency: A position statement from the Thoracic Society of Australia and New Zealand. *Respirology* **2020**, *25* (3), 321-335. DOI: 10.1111/resp.13774 From NLM.
(67) Nakanishi, T.; Forgetta, V.; Handa, T.; Hirai, T.; Mooser, V.; Lathrop, G. M.; Cookson, W. O. C. M.; Richards, J. B. The undiagnosed disease burden associated with alpha-1 antitrypsin deficiency genotypes. *European Respiratory Journal* **2020**, *56* (6), 2001441. DOI: 10.1183/13993003.01441-2020.
(68) van Steenbergen, W. Alpha 1-antitrypsin deficiency: an overview. *Acta Clin Belg* **1993**, *48* (3), 171-189. From NLM.
(69) Brode, S. K.; Ling, S. C.; Chapman, K. R. Alpha-1 antitrypsin deficiency: a commonly overlooked cause of lung disease. *CMAJ : Canadian Medical Association journal = journal de l'Association medicale canadienne* **2012**, *184* (12), 1365-1371. DOI: 10.1503/cmaj.111749 PubMed.
(70) Alam, S.; Li, Z.; Atkinson, C.; Jonigk, D.; Janciauskiene, S.; Mahadeva, R. Z α1-antitrypsin confers a proinflammatory phenotype that contributes to chronic obstructive pulmonary disease. *American journal of respiratory and critical care medicine* **2014**, *189* (8), 909-931. DOI: 10.1164/rccm.201308-1458OC PubMed.
(71) Janciauskiene, S. M.; Bals, R.; Koczulla, R.; Vogelmeier, C.; Köhnlein, T.; Welte, T. The discovery of α1-antitrypsin and its role in health and disease. *Respiratory Medicine* **2011**, *105* (8), 1129-1139. DOI: https://doi.org/10.1016/j.rmed.2011.02.002.

(72) Kalsheker, N.; Morley, S.; Morgan, K. Gene regulation of the serine proteinase inhibitors alpha1-antitrypsin and alpha1-antichymotrypsin. *Biochem Soc Trans* **2002**, *30* (2), 93-98. From NLM.
(73) Seixas, S.; Marques, P. I. Known Mutations at the Cause of Alpha-1 Antitrypsin Deficiency an Updated Overview of SERPINA1 Variation Spectrum. *Application of clinical genetics* **2021**, *14*, 173-194. DOI: 10.2147/TACG.S257511.
(74) Sinden, N. J.; Baker, M. J.; Smith, D. J.; Kreft, J.-U.; Dafforn, T. R.; Stockley, R. A. α-1-antitrypsin variants and the proteinase/antiproteinase imbalance in chronic obstructive pulmonary disease. *American journal of physiology. Lung cellular and molecular physiology* **2015**, *308* (2), L179-L190. DOI: 10.1152/ajplung.00179.2014.
(75) Petrache, I.; Hajjar, J.; Campos, M. Safety and efficacy of alpha-1-antitrypsin augmentation therapy in the treatment of patients with alpha-1-antitrypsin deficiency. *Biologics : targets & therapy* **2009**, *3*, 193-204. DOI: 10.2147/btt.2009.3088 PubMed.
(76) Senn, O.; Russi, E. W.; Imboden, M.; Probst-Hensch, N. M. α1-Antitrypsin deficiency and lung disease: risk modification by occupational and environmental inhalants. *European Respiratory Journal* **2005**, *26* (5), 909-917. DOI: 10.1183/09031936.05.00021605.
(77) Al Ashry, H. S.; Strange, C. COPD in individuals with the PiMZ alpha-1 antitrypsin genotype. *European respiratory review* **2017**, *26* (146), 170068. DOI: 10.1183/16000617.0068-2017.
(78) Stoller, J. K.; Aboussouan, L. S. α1-antitrypsin deficiency. *The Lancet (British edition)* **2005**, *365* (9478), 2225-2236. DOI: 10.1016/S0140-6736(05)66781-5.
(79) McNulty, M. J.; Silberstein, D. Z.; Kuhn, B. T.; Padgett, H. S.; Nandi, S.; McDonald, K. A.; Cross, C. E. Alpha-1 antitrypsin deficiency and recombinant protein sources with focus on plant sources: Updates, challenges and perspectives. *Free Radical Biology and Medicine* **2021**, *163*, 10-30. DOI: https://doi.org/10.1016/j.freeradbiomed.2020.11.030.
(80) Chiuchiolo, M. J.; Crystal, R. G. Gene Therapy for Alpha-1 Antitrypsin Deficiency Lung Disease. *Annals of the American Thoracic Society* **2016**, *13 Suppl 4* (Suppl 4), S352-S369. DOI: 10.1513/AnnalsATS.201506-344KV PubMed.
(81) Gómez-Mariano, G.; Matamala, N.; Martínez, S.; Justo, I.; Marcacuzco, A.; Jimenez, C.; Monzón, S.; Cuesta, I.; Garfia, C.; Martínez, M. T.; et al. Liver organoids reproduce alpha-1 antitrypsin deficiency-related liver disease. *Hepatology International* **2020**, *14* (1), 127-137. DOI: 10.1007/s12072-019-10007-y.
(82) Carlson, J. A.; Barton, B.; Sifers, R. N.; Finegold, M. J.; Clift, S. M.; De Mayo, F. J.; Bullock, D. W.; Woo, S. L. C. Accumulation of PiZ α1-antitrypsin causes liver damage in transgenic mice. *The Journal of clinical investigation* **1989**, *83* (4), 1183-1190.
(83) Janciauskiene, S.; Welte, T. Well-Known and Less Well-Known Functions of Alpha-1 Antitrypsin. Its Role in Chronic Obstructive Pulmonary Disease and Other Disease Developments. *Annals of the American Thoracic Society* **2016**, *13 Suppl 4* (Supplement_4), S280-S288. DOI: 10.1513/AnnalsATS.201507-468KV.
(84) Wang, D.; Wang, W.; Dawkins, P.; Paterson, T.; Kalsheker, N.; Sallenave, J.-M.; McGarry Houghton, A. Deletion of serpina1a, a murine α1-antitrypsin ortholog, results in embryonic lethality. *Experimental lung research* **2011**, *37* (5), 291-300. DOI: 10.3109/01902148.2011.554599.
(85) Franciosi, A. N.; Hobbs, B. D.; McElvaney, O. J.; Molloy, K.; Hersh, C.; Clarke, L.; Gunaratnam, C.; Silverman, E. K.; Carroll, T. P.; McElvaney, N. G. Clarifying the Risk of

Lung Disease in SZ Alpha-1 Antitrypsin Deficiency. *Am J Respir Crit Care Med* **2020**, *202* (1), 73-82. DOI: 10.1164/rccm.202002-0262OC From NLM. Hiller, A. M.; Piitulainen, E.; Tanash, H. The Clinical Course of Severe Alpha-1-Antitrypsin Deficiency in Patients Identified by Screening. *Int J Chron Obstruct Pulmon Dis* **2022**, *17*, 43-52. DOI: 10.2147/copd.S340241 From NLM.
(86) Thun, G. A.; Ferrarotti, I.; Imboden, M.; Rochat, T.; Gerbase, M.; Kronenberg, F.; Bridevaux, P. O.; Zemp, E.; Zorzetto, M.; Ottaviani, S.; et al. SERPINA1 PiZ and PiS heterozygotes and lung function decline in the SAPALDIA cohort. *PLoS One* **2012**, *7* (8), e42728. DOI: 10.1371/journal.pone.0042728 From NLM.
(87) Smith, D. J.; Ellis, P. R.; Turner, A. M. Exacerbations of Lung Disease in Alpha-1 Antitrypsin Deficiency. *Chronic obstructive pulmonary diseases* **2021**, *8* (1), 162-176. DOI: 10.15326/JCOPDF.2020.0173.
(88) Huang, D. Q.; Chan, K. E.; Tan, C.; Zeng, R. W.; Koh, B.; Ong, E. Y. H.; Ong, C. C. H.; Ong, C. E. Y.; Tan, D. J. H.; Lim, W. H.; et al. Meta-analysis: Prevalence of significant or advanced fibrosis in adults with alpha-1-antitrypsin deficiency. *Aliment Pharmacol Ther* **2023**, *58* (2), 152-158. DOI: 10.1111/apt.17516 From NLM.
(89) Afonso, M.; Silva, C.; Pinho, I.; Vale, A.; Fernandes, A. A rare mutation on alpha-1 antitrypsin deficit and lung fibrosis: case report. *Sarcoidosis Vasc Diffuse Lung Dis* **2020**, *37* (4), e2020019. DOI: 10.36141/svdld.v37i4.9877 From NLM.
(90) M, M.; A, S.; M, A. *Alpha-1 Antitrypsin Deficiency*; StatPearls Publishing, 2024.
(91) Bai, X.; Schountz, T.; Buckle, A. M.; Talbert, J. L.; Sandhaus, R. A.; Chan, E. D. Alpha-1-antitrypsin antagonizes COVID-19: a review of the epidemiology, molecular mechanisms, and clinical evidence. *Biochem Soc Trans* **2023**, *51* (3), 1361-1375. DOI: 10.1042/bst20230078 From NLM.
(92) Song, S. Alpha-1 Antitrypsin Therapy for Autoimmune Disorders. *Chronic obstructive pulmonary diseases* **2018**, *5* (4), 289-301. DOI: 10.15326/jcopdf.5.4.2018.0131.
(93) Elshikha, A. S.; Lu, Y.; Chen, M. J.; Akbar, M.; Zeumer, L.; Ritter, A.; Elghamry, H.; Mahdi, M. A.; Morel, L.; Song, S. Alpha 1 Antitrypsin Inhibits Dendritic Cell Activation and Attenuates Nephritis in a Mouse Model of Lupus. *PLoS One* **2016**, *11* (5), e0156583. DOI: 10.1371/journal.pone.0156583 From NLM.
(94) Pini, L.; Paoletti, G.; Heffler, E.; Tantucci, C.; Puggioni, F. Alpha1-antitrypsin deficiency and asthma. *Curr Opin Allergy Clin Immunol* **2021**, *21* (1), 46-51. DOI: 10.1097/aci.0000000000000711 From NLM.
(95) Tubío-Pérez, R. A.; Torres-Durán, M.; Fernández-Villar, A.; Ruano-Raviña, A. Alpha-1 antitrypsin deficiency and risk of lung cancer: A systematic review. *Transl Oncol* **2021**, *14* (1), 100914. DOI: 10.1016/j.tranon.2020.100914 From NLM.
(96) Thomas, C. E.; Ehrhardt, A.; Kay, M. A. Progress and problems with the use of viral vectors for gene therapy. *Nature Reviews Genetics* **2003**, *4* (5), 346-358. DOI: 10.1038/nrg1066.
(97) Hill, R. E.; Shaw, P. H.; Boyd, P. A.; Baumann, H.; Hastie, N. D. Plasma protease inhibitors in mouse and man: divergence within the reactive centre regions. *Nature (London)* **1984**, *311* (5982), 175-177. DOI: 10.1038/311175a0. Barbour, K. W.; Wei, F.; Brannan, C.; Flotte, T. R.; Baumann, H.; Berger, F. G. The murine alpha(1)-proteinase inhibitor gene family: polymorphism, chromosomal location, and structure. *Genomics (San Diego, Calif.)* **2002**, *80* (5), 515-522. DOI: 10.1016/S0888-7543(02)96864-3.

(98) Borel, F.; Sun, H.; Zieger, M.; Cox, A.; Cardozo, B.; Li, W.; Oliveira, G.; Davis, A.; Gruntman, A.; Flotte, T. R.; et al. Editing out five Serpina1 paralogs to create a mouse model of genetic emphysema. *Proceedings of the National Academy of Sciences - PNAS* **2018**, *115* (11), 2788-2793. DOI: 10.1073/pnas.1713689115.
(99) Kuiperij, H. B.; van Pel, M.; de Rooij, K. E.; Hoeben, R. C.; Fibbe, W. E. Serpina1 (α1-AT) is synthesized in the osteoblastic stem cell niche. *Experimental Hematology* **2009**, *37* (5), 641-647. DOI: https://doi.org/10.1016/j.exphem.2009.02.004.
(100) Paterson, T.; Moore, S. The expression and characterization of five recombinant murine alpha 1-protease inhibitor proteins. *Biochem Biophys Res Commun* **1996**, *219* (1), 64-69. DOI: 10.1006/bbrc.1996.0182 From NLM.
(101) Ni, K.; Serban, K. A.; Batra, C.; Petrache, I. Alpha-1 Antitrypsin Investigations Using Animal Models of Emphysema. *Annals of the American Thoracic Society* **2016**, *13 Suppl 4* (Suppl 4), S311-S316. DOI: 10.1513/AnnalsATS.201510-675KV PubMed.
(102) Beckett, E. L. B. B. S.; Stevens, R. L. P.; Jarnicki, A. G. P.; Kim, R. Y. B. B. S.; Hanish, I. B.; Hansbro, N. G. P.; Deane, A. B.; Keely, S. P.; Horvat, J. C. P.; Yang, M. M. D. P.; et al. A new short-term mouse model of chronic obstructive pulmonary disease identifies a role for mast cell tryptase in pathogenesis. *Journal of allergy and clinical immunology* **2013**, *131* (3), 752-762.e757. DOI: 10.1016/j.jaci.2012.11.053.
(103) Jax. 035015 - AAT KO line 31C Strain Details. Laboratory, T. J., Ed.; jax.org: 2022.
(104) Laboratory, T. J. *Protocol 38095 - Serpina1<em3Chmu>*. https://www.jax.org/Protocol?stockNumber=035015&protocolID=38095 (accessed 2022 4.11.22).
(105) Jax. 035411 - PiZ Strain Details. Laboratory, T. J., Ed.; jax.org: 2022.
(106) (JAX), T. J. L. *B6.Cg-Tg(SERPINA1*E342K)Z11.03Slcw/ChmuJ Protocol 22158: QPCR Assay - Tg(SERPINA1*E342K)#Slcw*. https://www.jax.org/Protocol?stockNumber=035411&protocolID=22158 (accessed 7/1/25).
(107) Abcam. *BMDC isolation protocol - mouse*. Abcam, 2023. https://www.abcam.com/en-us/technical-resources/protocols/isolation-of-bone-marrow-dervied-dendritic-cells?srsltid=AfmBOooCWPB6Oe_K7lDxvBLLbZOJ7xYSzgLzVHu-4JLHsN5sNfUjDMnq (accessed 9/12/24).
(108) Sauter, M.; Sauter, R. J.; Nording, H.; Olbrich, M.; Emschermann, F.; Langer, H. F. Protocol to isolate and analyze mouse bone marrow derived dendritic cells (BMDC). *STAR Protoc* **2022**, *3* (3), 101664. DOI: 10.1016/j.xpro.2022.101664 From NLM.
(109) Clemmensen, S. N.; Jacobsen, L. C.; Rørvig, S.; Askaa, B.; Christenson, K.; Iversen, M.; Jørgensen, M. H.; Larsen, M. T.; van Deurs, B.; Ostergaard, O.; et al. Alpha-1-antitrypsin is produced by human neutrophil granulocytes and their precursors and liberated during granule exocytosis. *Eur J Haematol* **2011**, *86* (6), 517-530. DOI: 10.1111/j.1600-0609.2011.01601.x From NLM.
(110) Lockett, A. D.; Kimani, S.; Ddungu, G.; Wrenger, S.; Tuder, R. M.; Janciauskiene, S. M.; Petrache, I. α_1-Antitrypsin modulates lung endothelial cell inflammatory responses to TNF-α. *Am J Respir Cell Mol Biol* **2013**, *49* (1), 143-150. DOI: 10.1165/rcmb.2012-0515OC From NLM.
(111) Aggarwal, N.; Koepke, J.; Matamala, N.; Martinez-Delgado, B.; Martinez, M. T.; Golpon, H.; Stolk, J.; Janciauskiene, S.; Koczulla, R. Alpha-1 Antitrypsin Regulates

Transcriptional Levels of Serine Proteases in Blood Mononuclear Cells. *Am J Respir Crit Care Med* **2016**, *193* (9), 1065-1067. DOI: 10.1164/rccm.201510-2062LE From NLM.
(112) Janciauskiene, S. Conformational properties of serine proteinase inhibitors (serpins) confer multiple pathophysiological roles. *Biochimica et Biophysica Acta (BBA) - Molecular Basis of Disease* **2001**, *1535* (3), 221-235. DOI: https://doi.org/10.1016/S0925-4439(01)00025-4. Bošković, G.; Twining, S. S. Local control of α1-proteinase inhibitor levels: regulation of α1-proteinase inhibitor in the human cornea by growth factors and cytokines. *Biochimica et Biophysica Acta (BBA) - Molecular Cell Research* **1998**, *1403* (1), 37-46. DOI: https://doi.org/10.1016/S0167-4889(98)00018-4.
(113) Perlmutter, D. H.; Punsal, P. I. Distinct and additive effects of elastase and endotoxin on expression of alpha 1 proteinase inhibitor in mononuclear phagocytes. *Journal of Biological Chemistry* **1988**, *263* (31), 16499-16503. DOI: https://doi.org/10.1016/S0021-9258(18)37620-8.
(114) Knoell, D. L.; Ralston, D. R.; Coulter, K. R.; Wewers, M. D. Alpha 1-antitrypsin and protease complexation is induced by lipopolysaccharide, interleukin-1beta, and tumor necrosis factor-alpha in monocytes. *Am J Respir Crit Care Med* **1998**, *157* (1), 246-255. DOI: 10.1164/ajrccm.157.1.9702033 From NLM.
(115) Taggart, C.; Cervantes-Laurean, D.; Kim, G.; McElvaney, N. G.; Wehr, N.; Moss, J.; Levine, R. L. Oxidation of either Methionine 351 or Methionine 358 in α1-Antitrypsin Causes Loss of Anti-neutrophil Elastase Activity*. *Journal of Biological Chemistry* **2000**, *275* (35), 27258-27265. DOI: https://doi.org/10.1016/S0021-9258(19)61505-X.
(116) JK, S.; V, H.; LS., A. *Alpha-1 Antitrypsin Deficiency*; University of Washington, Seattle, 2006.
(117) Lee, J. H.; Brantly, M. Molecular mechanisms of alpha1-antitrypsin null alleles. *Respir Med* **2000**, *94 Suppl C*, S7-11. DOI: 10.1053/rmed.2000.0851 From NLM.
Ferrarotti, I.; Carroll, T. P.; Ottaviani, S.; Fra, A. M.; O'Brien, G.; Molloy, K.; Corda, L.; Medicina, D.; Curran, D. R.; McElvaney, N. G.; et al. Identification and characterisation of eight novel SERPINA1 Null mutations. *Orphanet J Rare Dis* **2014**, *9*, 172. DOI: 10.1186/s13023-014-0172-y From NLM.
(118) Senn, O.; Russi, E. W.; Imboden, M.; Probst-Hensch, N. M. α1-Antitrypsin deficiency and lung disease: risk modification by occupational and environmental inhalants. *European Respiratory Journal* **2005**, *26* (5), 909. DOI: 10.1183/09031936.05.00021605.
(119) Kokturk, N.; Khodayari, N.; Lascano, J.; Riley, E. L.; Brantly, M. L. Lung Inflammation in alpha-1-antitrypsin deficient individuals with normal lung function. *Respiratory Research* **2023**, *24* (1), 40. DOI: 10.1186/s12931-023-02343-3.
(120) Liu, G.; Jarnicki, A. G.; Paudel, K. R.; Lu, W.; Wadhwa, R.; Philp, A. M.; Van Eeckhoutte, H.; Marshall, J. E.; Malyla, V.; Katsifis, A.; et al. Adverse roles of mast cell chymase-1 in chronic obstructive pulmonary disease. *Eur Respir J* **2022**. DOI: 10.1183/13993003.01431-2021 From NLM.
(121) A, A.; TJ., C. *Alpha-1 Antitrypsin Mutation*; StatPearls Publishing, 2022.
(122) Murphy, M. P.; McEnery, T.; McQuillan, K.; McElvaney, O. F.; McElvaney, O. J.; Landers, S.; Coleman, O.; Bussayajirapong, A.; Hawkins, P.; Henry, M.; et al. α(1) Antitrypsin therapy modulates the neutrophil membrane proteome and secretome. *Eur Respir J* **2020**, *55* (4). DOI: 10.1183/13993003.01678-2019 From NLM.

(123) Janciauskiene, S.; Wrenger, S.; Immenschuh, S.; Olejnicka, B.; Greulich, T.; Welte, T.; Chorostowska-Wynimko, J. The Multifaceted Effects of Alpha1-Antitrypsin on Neutrophil Functions. *Front Pharmacol* **2018**, *9*, 341. DOI: 10.3389/fphar.2018.00341 From NLM.
(124) Rabolli, V.; Lison, D.; Huaux, F. The complex cascade of cellular events governing inflammasome activation and IL-1β processing in response to inhaled particles. *Part Fibre Toxicol* **2016**, *13* (1), 40. DOI: 10.1186/s12989-016-0150-8 From NLM.
(125) Edwards, M. R.; Mukaida, N.; Johnson, M.; Johnston, S. L. IL-1β induces IL-8 in bronchial cells via NF-κB and NF-IL6 transcription factors and can be suppressed by glucocorticoids. *Pulmonary Pharmacology & Therapeutics* **2005**, *18* (5), 337-345. DOI: https://doi.org/10.1016/j.pupt.2004.12.015.
(126) King, P. T. Inflammation in chronic obstructive pulmonary disease and its role in cardiovascular disease and lung cancer. *Clin Transl Med* **2015**, *4* (1), 68. DOI: 10.1186/s40169-015-0068-z From NLM.
(127) Kanno, S.; Hirano, S.; Sakamoto, T.; Furuyama, A.; Takase, H.; Kato, H.; Fukuta, M.; Aoki, Y. Scavenger receptor MARCO contributes to cellular internalization of exosomes by dynamin-dependent endocytosis and macropinocytosis. *Scientific Reports* **2020**, *10* (1), 21795. DOI: 10.1038/s41598-020-78464-2.
(128) Freeman, C. M.; Curtis, J. L. Lung Dendritic Cells: Shaping Immune Responses throughout Chronic Obstructive Pulmonary Disease Progression. *Am J Respir Cell Mol Biol* **2017**, *56* (2), 152-159. DOI: 10.1165/rcmb.2016-0272TR From NLM.
(129) Bosteels, V.; Janssens, S. Striking a balance: new perspectives on homeostatic dendritic cell maturation. *Nat Rev Immunol* **2025**, *25* (2), 125-140. DOI: 10.1038/s41577-024-01079-5 From NLM.
(130) Marciscano, A. E.; Anandasabapathy, N. The role of dendritic cells in cancer and anti-tumor immunity. *Semin Immunol* **2021**, *52*, 101481. DOI: 10.1016/j.smim.2021.101481 From NLM. Backer, R. A.; Probst, H. C.; Clausen, B. E. Classical DC2 subsets and monocyte-derived DC: Delineating the developmental and functional relationship. *European journal of immunology* **2023**, *53* (3), e2149548-n/a. DOI: 10.1002/eji.202149548.
(131) Fazleen, A.; Wilkinson, T. The emerging role of proteases in α₁-antitrypsin deficiency and beyond. *ERJ Open Research* **2021**, *7* (4), 00494-02021. DOI: 10.1183/23120541.00494-2021.
(132) Atkinson, J. J.; Senior, R. M. Matrix metalloproteinase-9 in lung remodeling. *Am J Respir Cell Mol Biol* **2003**, *28* (1), 12-24. DOI: 10.1165/rcmb.2002-0166TR From NLM.
(133) Dahl, M.; Tybjaerg-Hansen, A.; Lange, P.; Vestbo, J.; Nordestgaard, B. G. Change in lung function and morbidity from chronic obstructive pulmonary disease in alpha1-antitrypsin MZ heterozygotes: A longitudinal study of the general population. *Ann Intern Med* **2002**, *136* (4), 270-279. DOI: 10.7326/0003-4819-136-4-200202190-00006 From NLM.
(134) Sørheim, I. C.; Bakke, P.; Gulsvik, A.; Pillai, S. G.; Johannessen, A.; Gaarder, P. I.; Campbell, E. J.; Agustí, A.; Calverley, P. M.; Donner, C. F.; et al. α_1-Antitrypsin protease inhibitor MZ heterozygosity is associated with airflow obstruction in two large cohorts. *Chest* **2010**, *138* (5), 1125-1132. DOI: 10.1378/chest.10-0746 From NLM.
(135) Packer, M. S.; Chowdhary, V.; Lung, G.; Cheng, L.-I.; Aratyn-Schaus, Y.; Leboeuf, D.; Smith, S.; Shah, A.; Chen, D.; Zieger, M.; et al. Evaluation of cytosine base editing and adenine base editing as a potential treatment for alpha-1 antitrypsin deficiency.

Molecular Therapy **2022**, *30* (4), 1396-1406. DOI: https://doi.org/10.1016/j.ymthe.2022.01.040.
(136) Hidvegi, T.; Stolz, D. B.; Alcorn, J. F.; Yousem, S. A.; Wang, J.; Leme, A. S.; Houghton, A. M.; Hale, P.; Ewing, M.; Cai, H.; et al. Enhancing Autophagy with Drugs or Lung-directed Gene Therapy Reverses the Pathological Effects of Respiratory Epithelial Cell Proteinopathy *. *Journal of Biological Chemistry* **2015**, *290* (50), 29742-29757. DOI: 10.1074/jbc.M115.691253 (acccessed 2025/01/11).
(137) Hurley, K.; Lacey, N.; O'Dwyer, C. A.; Bergin, D. A.; McElvaney, O. J.; O'Brien, M. E.; McElvaney, O. F.; Reeves, E. P.; McElvaney, N. G. Alpha-1 antitrypsin augmentation therapy corrects accelerated neutrophil apoptosis in deficient individuals. *J Immunol* **2014**, *193* (8), 3978-3991. DOI: 10.4049/jimmunol.1400132 From NLM.
(138) Carroll, T. P.; Greene, C. M.; O'Connor, C. A.; Nolan, A. M.; O'Neill, S. J.; McElvaney, N. G. Evidence for unfolded protein response activation in monocytes from individuals with alpha-1 antitrypsin deficiency. *J Immunol* **2010**, *184* (8), 4538-4546. DOI: 10.4049/jimmunol.0802864 From NLM.
(139) Bazzan, E.; Tinè, M.; Biondini, D.; Benetti, R.; Baraldo, S.; Turato, G.; Fagiuoli, S.; Sonzogni, A.; Rigobello, C.; Rea, F.; et al. α(1)-Antitrypsin Polymerizes in Alveolar Macrophages of Smokers With and Without α(1)-Antitrypsin Deficiency. *Chest* **2018**, *154* (3), 607-616. DOI: 10.1016/j.chest.2018.04.039 From NLM. Mulgrew, A. T.; Taggart, C. C.; Lawless, M. W.; Greene, C. M.; Brantly, M. L.; O'Neill, S. J.; McElvaney, N. G. Z alpha1-antitrypsin polymerizes in the lung and acts as a neutrophil chemoattractant. *Chest* **2004**, *125* (5), 1952-1957. DOI: 10.1378/chest.125.5.1952 From NLM.
(140) Lee, J.; Mohammad, N.; Lu, Y.; Kang, K.; Han, K.; Brantly, M. Alu RNA induces NLRP3 expression through TLR7 activation in α-1-antitrypsin–deficient macrophages. *JCI Insight* **2022**, *7* (12). DOI: 10.1172/jci.insight.158791.
(141) Janoff, A.; Carp, H.; Lee, D. K.; Drew, R. T. Cigarette smoke inhalation decreases alpha 1-antitrypsin activity in rat lung. *Science* **1979**, *206* (4424), 1313-1314. DOI: 10.1126/science.316187 From NLM.
(142) Alam, S.; Li, Z.; Janciauskiene, S.; Mahadeva, R. Oxidation of Z α1-antitrypsin by cigarette smoke induces polymerization: a novel mechanism of early-onset emphysema. *Am J Respir Cell Mol Biol* **2011**, *45* (2), 261-269. DOI: 10.1165/rcmb.2010-0328OC From NLM.
(143) Brusselle, G. G.; Joos, G. F.; Bracke, K. R. New insights into the immunology of chronic obstructive pulmonary disease. *Lancet* **2011**, *378* (9795), 1015-1026. DOI: 10.1016/s0140-6736(11)60988-4 From NLM.
(144) Song, L.; Dong, G.; Guo, L.; Graves, D. T. The function of dendritic cells in modulating the host response. *Mol Oral Microbiol* **2018**, *33* (1), 13-21. DOI: 10.1111/omi.12195 From NLM.
(145) Guilliams, M.; Dutertre, C. A.; Scott, C. L.; McGovern, N.; Sichien, D.; Chakarov, S.; Van Gassen, S.; Chen, J.; Poidinger, M.; De Prijck, S.; et al. Unsupervised High-Dimensional Analysis Aligns Dendritic Cells across Tissues and Species. *Immunity* **2016**, *45* (3), 669-684. DOI: 10.1016/j.immuni.2016.08.015 From NLM.
(146) Pallazola, A. M.; Rao, J. X.; Mengistu, D. T.; Morcos, M. S.; Toma, M. S.; Stolberg, V. R.; Tretyakova, A.; McCloskey, L.; Curtis, J. L.; Freeman, C. M. Human lung cDC1 drive increased perforin-mediated NK cytotoxicity in chronic obstructive pulmonary disease. *Am J Physiol Lung Cell Mol Physiol* **2021**, *321* (6), L1183-l1193. DOI: 10.1152/ajplung.00322.2020 From NLM.

(147) Bosteels, C.; Neyt, K.; Vanheerswynghels, M.; van Helden, M. J.; Sichien, D.; Debeuf, N.; De Prijck, S.; Bosteels, V.; Vandamme, N.; Martens, L.; et al. Inflammatory Type 2 cDCs Acquire Features of cDC1s and Macrophages to Orchestrate Immunity to Respiratory Virus Infection. *Immunity* **2020**, *52* (6), 1039-1056.e1039. DOI: 10.1016/j.immuni.2020.04.005 From NLM.
(148) Swiecki, M.; Colonna, M. The multifaceted biology of plasmacytoid dendritic cells. *Nat Rev Immunol* **2015**, *15* (8), 471-485. DOI: 10.1038/nri3865 From NLM.
(149) Segura, E. Human dendritic cell subsets: An updated view of their ontogeny and functional specialization. *Eur J Immunol* **2022**, *52* (11), 1759-1767. DOI: 10.1002/eji.202149632 From NLM. Liu, Z.; Wang, H.; Li, Z.; Dress, R. J.; Zhu, Y.; Zhang, S.; De Feo, D.; Kong, W. T.; Cai, P.; Shin, A.; et al. Dendritic cell type 3 arises from Ly6C(+) monocyte-dendritic cell progenitors. *Immunity* **2023**, *56* (8), 1761-1777.e1766. DOI: 10.1016/j.immuni.2023.07.001 From NLM.
(150) Zieger, M.; Borel, F.; Greer, C.; Gernoux, G.; Blackwood, M.; Flotte, T. R.; Mueller, C. Liver-directed SERPINA1 gene therapy attenuates progression of spontaneous and tobacco smoke-induced emphysema in α1-antitrypsin null mice. *Mol Ther Methods Clin Dev* **2022**, *25*, 425-438. DOI: 10.1016/j.omtm.2022.04.003 From NLM.
(151) Lugg, S. T.; Scott, A.; Parekh, D.; Naidu, B.; Thickett, D. R. Cigarette smoke exposure and alveolar macrophages: mechanisms for lung disease. *Thorax* **2022**, *77* (1), 94-101. DOI: 10.1136/thoraxjnl-2020-216296 From NLM.
(152) Liu, X.; Shin, S. Viewing Legionella pneumophila Pathogenesis through an Immunological Lens. *J Mol Biol* **2019**, *431* (21), 4321-4344. DOI: 10.1016/j.jmb.2019.07.028 From NLM.
(153) Vlahos, R.; Bozinovski, S. Role of alveolar macrophages in chronic obstructive pulmonary disease. *Front Immunol* **2014**, *5*, 435. DOI: 10.3389/fimmu.2014.00435 From NLM.
(154) Misharin, A. V.; Morales-Nebreda, L.; Mutlu, G. M.; Budinger, G. R.; Perlman, H. Flow cytometric analysis of macrophages and dendritic cell subsets in the mouse lung. *Am J Respir Cell Mol Biol* **2013**, *49* (4), 503-510. DOI: 10.1165/rcmb.2013-0086MA From NLM.
(155) Xue, W.; Ma, J.; Li, Y.; Xie, C. Role of CD(4) (+) T and CD(8) (+) T Lymphocytes-Mediated Cellular Immunity in Pathogenesis of Chronic Obstructive Pulmonary Disease. *J Immunol Res* **2022**, *2022*, 1429213. DOI: 10.1155/2022/1429213 From NLM. Williams, M.; Todd, I.; Fairclough, L. C. The role of CD8 + T lymphocytes in chronic obstructive pulmonary disease: a systematic review. *Inflamm Res* **2021**, *70* (1), 11-18. DOI: 10.1007/s00011-020-01408-z From NLM. Olloquequi, J.; Ferrer, J.; Montes, J. F.; Rodríguez, E.; Montero, M. A.; García-Valero, J. Differential lymphocyte infiltration in small airways and lung parenchyma in COPD patients. *Respir Med* **2010**, *104* (9), 1310-1318. DOI: 10.1016/j.rmed.2010.03.002 From NLM.
(156) Pianigiani, T.; Paggi, I.; Cooper, G. E.; Staples, K. J.; McDonnell, M.; Bergantini, L. Natural killer cells in the lung: novel insight and future challenge in the airway diseases. *ERJ Open Res* **2025**, *11* (2). DOI: 10.1183/23120541.00683-2024 From NLM.
(157) Nakano, H.; Burgents, J. E.; Nakano, K.; Whitehead, G. S.; Cheong, C.; Bortner, C. D.; Cook, D. N. Migratory properties of pulmonary dendritic cells are determined by their developmental lineage. *Mucosal Immunol* **2013**, *6* (4), 678-691. DOI: 10.1038/mi.2012.106 From NLM.

(158) Givi, M. E.; Folkerts, G.; Wagenaar, G. T.; Redegeld, F. A.; Mortaz, E. Cigarette smoke differentially modulates dendritic cell maturation and function in time. *Respir Res* **2015**, *16*, 131. DOI: 10.1186/s12931-015-0291-6 From NLM.
(159) Chen, T.; Ehnert, S.; Tendulkar, G.; Zhu, S.; Arnscheidt, C.; Aspera-Werz, R. H.; Nussler, A. K. Primary Human Chondrocytes Affected by Cigarette Smoke-Therapeutic Challenges. *Int J Mol Sci* **2020**, *21* (5). DOI: 10.3390/ijms21051901 From NLM.
Schamberger, A. C.; Staab-Weijnitz, C. A.; Mise-Racek, N.; Eickelberg, O. Cigarette smoke alters primary human bronchial epithelial cell differentiation at the air-liquid interface. *Sci Rep* **2015**, *5*, 8163. DOI: 10.1038/srep08163 From NLM.
(160) Ruez, R.; Dubrot, J.; Zoso, A.; Bacchetta, M.; Molica, F.; Hugues, S.; Kwak, B. R.; Chanson, M. Dendritic Cell Migration Toward CCL21 Gradient Requires Functional Cx43. *Front Physiol* **2018**, *9*, 288. DOI: 10.3389/fphys.2018.00288 From NLM. Rhee, I.; Zhong, M. C.; Reizis, B.; Cheong, C.; Veillette, A. Control of dendritic cell migration, T cell-dependent immunity, and autoimmunity by protein tyrosine phosphatase PTPN12 expressed in dendritic cells. *Mol Cell Biol* **2014**, *34* (5), 888-899. DOI: 10.1128/mcb.01369-13 From NLM.
(161) Tiberio, L.; Del Prete, A.; Schioppa, T.; Sozio, F.; Bosisio, D.; Sozzani, S. Chemokine and chemotactic signals in dendritic cell migration. *Cell Mol Immunol* **2018**, *15* (4), 346-352. DOI: 10.1038/s41423-018-0005-3 From NLM.
(162) Hjortø, G. M.; Larsen, O.; Steen, A.; Daugvilaite, V.; Berg, C.; Fares, S.; Hansen, M.; Ali, S.; Rosenkilde, M. M. Differential CCR7 Targeting in Dendritic Cells by Three Naturally Occurring CC-Chemokines. *Front Immunol* **2016**, *7*, 568. DOI: 10.3389/fimmu.2016.00568 From NLM.
(163) Brandum, E. P.; Jørgensen, A. S.; Rosenkilde, M. M.; Hjortø, G. M. Dendritic Cells and CCR7 Expression: An Important Factor for Autoimmune Diseases, Chronic Inflammation, and Cancer. *Int J Mol Sci* **2021**, *22* (15). DOI: 10.3390/ijms22158340 From NLM.